



WPI



E.&J. Gallo Winery.

Bottling Line Splitter Design

A Major Qualifying Project Report

Submitted to the Faculty of the

WORCESTER POLYTECHNIC INSTITUTE

in partial fulfillment of the requirements for the

Degree of Bachelor of Science

in Mechanical Engineering

By

William Robinson Caruso

James Saunders

Date: March 3rd, 2007

Approved:

Prof. Holly K. Ault

Keywords:

1. Bottling
2. Machine Design
3. Beverage Production

Acknowledgements

Special thanks to those persons without whom this project would not have been possible.

Worcester Polytechnic Institute

Professor Holly K. Ault
Professor Henry Nowick
James Phelan
IGSD
Professor Robert L. Norton

E & J Gallo Wineries

Mike Delikowski
Laura Hoffman
David Booth
Loel Peters
Brandon Abell
Shawn Burns
Jim Bellins
Tim Phillipsen
Juan Nevarez

Others

RPDG San Diego
Rexell-Norcal Modesto

Abstract

E&J Gallo Winery in Modesto, CA has numerous high speed bottling lines where it is necessary to split a single line of bottles into two lines. The current lane splitting mechanism uses multiple pneumatic actuators that require costly maintenance and cause excessive line downtime. A prototype mechanism utilizing a unique three-dimensional camoid design and single servo motion control was designed, fabricated using rapid prototyping methods, and tested. Preliminary tests results proved acceptable functionality. Shape optimization and long-term tests for reliability were recommended.

ACKNOWLEDGEMENTS.....	I
ABSTRACT	II
LIST OF FIGURES.....	VIII
LIST OF TABLES.....	X
LIST OF EQUATIONS	XI
CHAPTER 1.0 - INTRODUCTION	1
CHAPTER 2.0 - GOAL STATEMENT	3
CHAPTER 3.0 - TASK SPECIFICATIONS	4
3.1 - ASSUMPTIONS.....	4
3.2 - PERFORMANCE SPECIFICATIONS.....	4
3.3 - DESIGN SPECIFICATIONS	4
3.4 - IDEAL CASES.....	5
CHAPTER 4.0 - BACKGROUND.....	6
4.1 - GALLO'S HIGH SPEED BOTTLING OPERATIONS.....	6
4.2 - E&J GALLO LINE 2 OVERVIEW	6
4.3 - HEUFT REJECTION SYSTEM	7
4.3.1 - OVERVIEW	7
4.3.2 - MECHANISM COMPONENTS	8
4.3.3 - CONTROLS	10
4.4 - PLANT TOURS.....	13
4.4.1 - WACHUSETT MICRO-BREWERY	13
4.4.2 - NORTHEASTERN REGIONAL ANHEUSER-BUSCH BREWERY	14
4.5 - OTHER HIGH SPEED LINE SPLIT SOLUTIONS	15
4.5.1 - PATENT RESEARCH.....	15
4.5.2 - OEM PRODUCTS.....	15
4.6 - RAPID PROTOTYPING.....	19
4.7 - SERVO MOTORS	19
CHAPTER 5.0 - CAMOID DESIGN CONCEPTION.....	20
5.1 - CAMOID GEOMETRY.....	22
5.1.1 - CAMOID CONCEPT	22
5.1.2 - CAMOID INSPIRATION.....	22

5.1.3 - CAMOID DESIGN	23
5.2 - ACTUATION DESIGN.....	29
5.2.1 - WHY USE A SERVO?.....	29
5.2.2 - CHOOSING A SERVO.....	30
5.2.3 - SIZING A SERVO	30
5.2.4 - CONTROLLING THE SERVO	31
5.2.5 - ACTUATION DESIGN CONCLUSIONS	32
5.3 - DESIGN CONCEPT SUMMARY	32

CHAPTER 6.0 - METHODOLOGY **33**

6.1 - ASSUMPTIONS	33
6.1.1 - LINE 2 PROPERTIES	33
6.1.2 - HEUFT LANER.....	33
6.2 - DATA COLLECTION AND ANALYSIS	34
6.2.1 - HEUFT ANALYSIS	34
6.2.2 - CONTOUR DESIGN AND ANALYSIS	34
6.2.3 - CHOOSING CONTOUR.....	35
6.3 - CAMOID GEOMETRY DESIGN	36
6.3.1 - MANUFACTURE.....	36
6.4 - ACTUATION DESIGN.....	38
6.4.1 - SIZING A SERVO	38
6.5.2 - CONTROLLING THE SERVO	39
6.5.3 - STRESS ANALYSIS.....	41
6.5.4 - FATIGUE STRESS ANALYSIS	41
6.6 - PART GATHERING	41
6.7 - CHASSIS DESIGN.....	41
6.7.1 - MATERIAL	42
6.7.2 - COMPONENT LAYOUT.....	42
6.7.3 - IMPLEMENTATION ON LINE	43
6.7.4 - MANUFACTURABILITY	44
6.8 - DRIVE SYSTEM	44
6.9 - MECHANISM ASSEMBLY	45
6.10 - IMPLEMENTATION.....	45
6.11 - TESTING	46

CHAPTER 7.0 - CAMOID LANER DETAILED DESIGN **47**

7.1 - CAMOID GEOMETRY DESIGN	47
7.1.1 - ITERATIVE DESIGN	47
7.1.2 - GEOMETRY FINAL VALUES	52
7.1.3 - GEOMETRY CONSTRUCTION.....	52
7.2 - CAMOID PROTOTYPE	52
7.3 - ACTUATION DESIGN.....	53
7.3.1 - SERVO SIZING	53
7.3.2 - SERVO SYSTEM.....	53
7.3.3 - CONTROL LOGIC CONCEPT.....	57
7.3.4 - DRIVE TRAIN SPECS	57
7.3.5 - TIMING.....	57

7.4 - MOTION ANALYSIS.....	60
7.4.1 - CAM EXTENSION.....	60
7.5 - CHASSIS DESIGN DETAILS	60
7.5.1 - MATERIAL CHOICE	62
7.5.2 - LAYOUT	62
7.5.3 - TOLERANCES	63
7.5.4 - FASTENERS	64
7.5.5 - BEARINGS	64
7.6 - DRIVE DESIGN DETAILS	64
7.6.1 - RECOMMENDATION	66
7.6.2 - CLAIMED BENEFITS	66
7.6.3 - CHASSIS LAYOUT	66
7.6.4 - DRIVE RATIO	66
7.6.5 - AVAILABILITY	66
7.6.6 - BELT TENSIONER.....	66
7.7 - FULL ASSEMBLY.....	68
7.8 - MECHANISM ASSEMBLY	69
7.8.1 - CAMOID POSITION ON SHAFT	69
7.8.2 - CAMOID SHAFT ALIGNMENT	69
7.8.3 - SERVO INSTALLATION	70
7.8.4 - SPROCKET POSITION.....	70
7.8.5 - BELT TENSIONING	70
7.8.6 - INITIAL MOTION TEST	71
7.9 - IMPLEMENTATION.....	71
<u>CHAPTER 8.0 - DATA COLLECTION AND ANALYSIS</u>	<u>72</u>
8.1 - BOTTLE DYNAMIC ANALYSIS.....	72
8.1.1 - FRICTION TEST	72
8.1.2 - CENTER OF GRAVITY TEST.....	72
8.1.3 - NECK STRENGTH TEST	73
8.2 - CAM PROFILE DESIGN AND ANALYSIS	73
8.2.1 - CONSTRAINTS	74
8.2.2 - KINEMATIC ANALYSIS.....	75
8.2.3 - FORCE ANALYSIS.....	80
8.2.4 - MOMENT ANALYSIS	82
8.3 - TRAJECTORY TEST	83
8.4 - CHOOSING A CONTOUR	84
8.4.1 - ACCEPTABLE FINAL VELOCITY	84
8.4.2 - MINIMIZING MAXIMUM ACCELERATION	84
8.4.3 - MINIMIZING JERK	84
8.4.4 - MINIMIZING FORCE	84
8.4.5 - MINIMIZING MOMENT	84
8.5 - TORQUE REQUIREMENTS	84
8.5.1 - OPERATING ROTATIONAL VELOCITY	84
8.5.2 - ANGULAR ACCELERATION	85
8.5.3 - TORQUE REQUIRED.....	86
8.6 - STRESS ANALYSIS.....	87
8.7 - FATIGUE STRESS ANALYSIS	89

CHAPTER 9.0 - PROTOTYPE TESTING..... 91

9.1 - MATERIALS..... 91
9.2 - OBJECTIVE..... 91
9.3 - VARIABLES 91
9.4 - SETUP SAFETY PRECAUTION..... 91
9.5 - SETUP 92
9.5.1 - BOTTLE TEST BATCHES..... 92
9.5.2 - TEST LOOP SPEED..... 93
9.5.3 - PHOTOEYE PLACEMENT..... 93
9.5.4 - ELECTRONIC ATTACHMENT 93
9.6 - PROCEDURE SAFETY PRECAUTION..... 94
9.7 - PROCEDURE..... 94
9.7.1 - DATA RECORDING 94

CHAPTER 10.0 - TEST RESULTS..... 95

10.1 - TESTING LIMITATIONS 95
10.1.1 - LINE ENCODER 96
10.1.2 - VARIABLE LINE SPEED 96
10.1.3 - CONVEYOR CONDITION 96
10.1.4 - LINE SPEED 96
10.2 - PRELIMINARY TESTING 96
10.3 - RESULTS TABLE 98
10.3.1 - MINIMUM BOTTLE SPACING: EXTENSION 99
10.3.2 - MINIMUM BOTTLE SPACING: RETRACTION 99
10.3.3 - MAGNITUDE OF DISPLACEMENT 99
10.3.4 - PHOTOEYE PLACEMENT 99
10.4 - MECHANISM OBSERVATIONS 100
10.5 - TEST RESULTS CONCLUSIONS..... 100

CHAPTER 11.0 - COST COMPARISON..... 101

CHAPTER 12.0 - RECOMMENDATIONS 102

12.1 - LINE SPEED TESTING 102
12.2 - BOTTLE TESTING 102
12.3 - ENDURANCE TESTING 102
12.4 - PART ACQUISITION 102
12.5 - PROGRAM OPTIMIZATION..... 102
12.6 - GEOMETRY OPTIMIZATION 102

CHAPTER 13.0 - CONCLUSIONS..... 103

REFERENCES 104

APPENDICES 105

APPENDIX A - RELEVANT PATENTS	106
APPENDIX B - RAPID PROTOTYPING QUOTES.....	113
APPENDIX C - BILL OF MATERIALS	114
APPENDIX D - MOTION ANALYZER INPUT VALUES.....	118
APPENDIX E - SERVO DETAILS.....	120
APPENDIX F - SERVO DRIVER DETAILS.....	122
APPENDIX G - CHASSIS DRAWINGS.....	125
APPENDIX H - GOODYEAR EAGLE PD POWER TRANSMISSION	133
APPENDIX I - BOTTLE TESTS.....	141
I.1 - CENTER OF GRAVITY TEST	141
I.2 - COEFFICIENT OF STATIC FRICTION TEST	145
I.3 - BOTTLE NECK FAILURE TEST	147
I.3 - BOTTLE NECK FAILURE TEST	148
APPENDIX J - RAPID PROTOTYPING METHODS	150
J.1 - STEREOLITHOGRAPHY (SLA).....	150
J.2 - FUSED DEPOSITION MODELING (FDM)	150
J.2 - FUSED DEPOSITION MODELING (FDM)	151
J.3 - SELECTIVE LASER SINTERING (SLS)	151
J.4 - ELECTRON BEAM MELTING (EBM).....	151
APPENDIX K – TEST DATA TABLE	152
APPENDIX M - DETAILED MATHEMATICS.....	153

List of Figures

Figure 1: Patent 4,369,873 Concept.....	8
Figure 2 (left): Line 2 Heuft Delta-FW On Position.....	8
Figure 3 (right): Line 2 Heuft Delta-FW Off Position.....	8
Figure 4: Cylinder Layout (top view).....	9
Figure 5 (left): Segments in Off Position (top view).....	9
Figure 6 (right): Contour in On Position.....	9
Figure 7: Segment Depth and Bristles.....	10
Figure 8: Segment Close-up (top view). Note bristles on end of each segment.....	10
Figure 9: Heuft operation off to on switch.....	12
Figure 10: Wachusett Lane Splitter.....	14
Figure 11: Heuft Delta-K Unit.....	16
Figure 12: Heuft Flip Rejecter.....	17
Figure 14: KHS Waveform.....	18
Figure 15: Top view of KHS Waveform.....	18
Figure 17: Camoid Laner.....	20
Figure 18: Camoid Extension.....	21
Figure 19: Heuft Delta-K Bottle Rejecter.....	22
Figure 20: Camoid Laner Shape.....	23
Figure 21: Geometry Terminology.....	24
Figure 22: Cam Segment Construction.....	25
Figure 23: Segmented Camoid.....	26
Figure 24: Cam segment phase shifting.....	28
Figure 25: Sections of Continuous Contour.....	28
Figure 26: Heuft Contour and Equation.....	34
Figure 27: Component Layout.....	43
Figure 28: Heuft Attachment to Line.....	44
Figure 29: Test Loop.....	46
Figure 30: Geometric Elements.....	48
Figure 38: Model vs. Rapid prototype.....	53
Figure 39: Servo Control Schematic.....	54
Figure 40: Servo Motor.....	55
Figure 41: Timing Diagram Example.....	58
Figure 42: Top View of Cam Extension.....	60
Figure 43: Chassis Assembly View.....	61
Figure 44: Chassis Exploded View.....	62
Figure 45: Important Toleranced Dimensions.....	64
Figure 46: Goodyear Eagle Pd Power Transmission.....	65
Figure 47: Lovejoy Belt Tensioner with smooth idler pulley.....	67
Figure 48: Full CAD Assembly.....	68
Figure 49: Full Assembly.....	69
Figure 50: Tensioning Diagram.....	70
Figure 54: Contour of Each Cam Program.....	76
Figure 55: Displacement Difference, Heuft vs. Cam Programs.....	77
Figure 56: Bottle Transverse Velocity.....	78

Figure 57: Bottle Transverse Acceleration	78
Figure 58: Bottle Transverse Jerk	79
Figure 59: Bottle Free Body Diagram	80
Figure 60: Force on Bottle	81
Figure 61: Induced Moment on Bottles	82
Figure 62: Bottle Trajectories	83
Figure 63: Spin-up time vs. Buffer Angle	85
Figure 64: Acceleration vs. Spin-Up Time	86
Figure 65: Servo Torque Required vs. Spin-Up Time	87
Figure 66: Test loop	92
Figure 67: Electronics Board	93
Figure 68: Final Mechanism Cycle Sequence	95
Figure 69: Photoeye Placement	99
Figure 70: Patent 4,986,407	106
Figure 71: Patent 4,643,291	107
Figure 72: Patent 4,321,994	108
Figure 73: Patent 4,369,873	109
Figure 74: Patent 6588575	110
Figure 75: Patent 6,822,181	111
Figure 76: Patent 3,791,518	112
Figure 77: Servo Overview	120
Figure 78: Driver Details and Benefits	122
Figure 79: Driver Specifications	123
Figure 80: Driver Specifications	124
Figure 81: Belt Nomenclature	133
Figure 82: Eagle Pd Belt Product Numbers	134
Figure 83: Sprocket Nomenclature	135
Figure 84: Eagle Pd White Sprockets	136
Figure 85: Belt Nomenclature	137
Figure 86: Eagle Pd Belt Product Numbers	138
Figure 87: Sprocket Nomenclature	139
Figure 88: Eagle Pd White Sprockets	140
Figure 89: Center of Gravity Experiment	142
Figure 90: Free Body Diagram	143
Figure 91: Free Body Diagram	Error! Bookmark not defined.
Figure 93: Coefficient of Static Friction Experiment	145
Figure 94: Free Body Diagram	146
Figure 97: Bottle Neck Failure Experiment	148
Figure 98: Free Body Diagram	149

List of Tables

Table 1: Manufacturing Method Comparison.....	37
Table 2: Rapid Prototyping Method Comparison.....	37
Table 3: Material Comparison	42
Table 4: Camoid Geometry Final Values	52
Table 5: Servo Motor and Gearbox Overview Specs	56
Table 6: Driver Overview Specs.....	56
Table 7: Tolerance Reasons.....	63
Table 8: Belt Used	65
Table 9: Sprockets Used	65
Table 10: Cam Program Constraints.....	75
Table 11: Graphic Color Scheme.....	76
Table 12: Maximum Kinematic Values.....	80
Table 13: Maximum Force Analysis Values	83
Table 14: Time Data	85
Table 15: Keyway Stress Analysis	88
Table 16: Shaft Stress Analysis	89
Table 17: Shaft Fatigue Analysis.....	89
Table 18: Keyway Stress Concentration Analysis.....	90
Table 19: Test Results.....	98
Table 20: Cost Comparison	101
Table 21: Full Bill of Materials	115
Table 22: Bill of Materials with Piggy Backed Electronics	117
Table 23: Axis Setup Tab	118
Table 24: Cycle Profile Tab.....	118
Table 25: Mechanism Tab	119
Table 26: Transmission Stages Tab	119
Table 27: Data Recording Table.....	152

List of Equations

Equation 1: Bottle and Laner Contact Time	85
Equation 2: Operational Rotational Velocity.....	85
Equation 3: Worst Case Scenario Time Between Two Bottles	85
Equation 4: Acceleration Function	86
Equation 5: Torque Function	86
Equation 6: Shear Force at Key	88
Equation 7: Keyway Average Shear Stress	88
Equation 8: Safety Factor.....	88
Equation 9: Area of Key	88
Equation 10: Required Torque.....	88
Equation 11: Shaft Torsional Deflection	89
Equation 12: Shaft Shear Stress due to Torsion.....	89
Equation 13: Shaft Polar Moment of Inertia.....	89
Equation 14: Corrected Fatigue Function	89
Equation 15: Safety Factor.....	89
Equation 16: Fatigue Stress Concentration Factor.....	90
Equation 17: Shear Stress Concentration due to Torsion	90
Equation 18: Safety Factor.....	90

Chapter 1.0 - Introduction

E&J Gallo Winery is one of the largest winemaking operations in the world. Founded in 1933 by Ernest and Julio Gallo, the Gallo Winery is still a family business and since has expanded to the global market. Currently, Gallo Winery employs over 4600 people and retails wines throughout the United States and over 90 foreign countries. Grapes used are from vineyards spanning California's most important wine-producing regions and Gallo runs operations in sites across Sonoma County including Modesto, Monterey and Napa Valley. The diverse product line of Gallo Winery ranges from fine table and sparkling wines, to distilled wine-based spirits and beverages (E&J Gallo, 2003).

This project is conducted in E&J Gallo's Modesto site and focuses on 750mL bottled wine production, specifically on Line 2. At full production Line 2 fills and packages at up to 400 bottles per minute, running 16 hour shifts, seven days per week. The limiting factor in the production speed of the line is the packaging process. In attempt to maximize the efficiency of the line, Gallo employs two parallel packaging lines resulting in the need for a lane split from single file to two independent lanes between the bottle filler and the packing equipment.

Gallo is experiencing expensive maintenance issues with the mechanism which splits the lanes. The current system is manufactured by Heuft. The manufacturer's recommendation for the mechanism states its function to be a single bottle rejecter. However, in Line 2 the Heuft rejecter functions as a high speed lane splitter. The difference is in the number of cycles per unit time. As a rejecter, the mechanism might actuate several dozen times per shift, but as a dedicated lane splitter, it fires several thousand times per shift. This results in a significant deterioration of performance in a relatively short period of time, and thus requires maintenance or replacement often enough to cause concern. Furthermore, as performance degrades, the chance of bottle damage or bottle tipping increases which can cause costly delays in production.

In order to reduce the maintenance cost and production delays associated with the Heuft laning mechanism, Gallo proposed a redesign of the system. Within the proposal, Gallo specified certain criteria that the redesign must follow. The new system must reduce maintenance costs, must fit within the existing footprint, and not damage bottles. The new system must not be a safety hazard. And the system must ideally be replicable on other lines with different size and shape bottles.

This project focuses specifically on the redesign of the Line 2 Heuft system. Through problem identification, research, ideation, analysis, modeling, prototypes and implementation, this project will propose a solution to the problems experienced with the current system. The following report will explain the details of design, implementation, experimentation and results of a unique prototype lane splitting mechanism.

The chapters present information in parallel structures with each successive chapter's investigation driving progressively deeper in detail. After discussing relevant background information, the design process is explained in detail over chapters 5-7. Chapter 5 introduces the idea explaining terminology and design basics. Chapter 6 describes the methodology used to create that design. Chapter 7 describes the detailed design process and gives all values in the final design. Chapter 8 details all important calculations conducted. Chapters 9 and 10 describe the experimental process; procedure

and results. Chapter 11 concludes the project with a cost analysis. Conclusions and recommendations are discussed in the final chapters. This structure will tend to a variety of audiences and allow quicker reference for those familiar with the project and detailed step-by-step explanation for those who are not.

Chapter 2.0 - Goal Statement

The aim of this project is to design a means of splitting one high-speed single-file line of bottles into two independent single-file lines. Alternatively, the existing mechanism may be improved to reduce maintenance costs and upkeep.

Chapter 3.0 - Task Specifications

This chapter outlines the design specifications that must be met in order to claim a successful solution.

3.1 - Assumptions

This specification list was compiled assuming 750mL bottles traveling at 400 bottles/min with a space of one bottle diameter between each bottle. We assume a worst case operation of 16 hours/day, 365 days/year, and a lane switching frequency of 10 bottles per lane. A full cycle requires the mechanism to transition from 'off' to 'on' and back to 'off', allowing 20 bottles to pass. This adds up to nearly 7 million cycles per year.

3.2 - Performance Specifications

The Laning Mechanism Must:

- NOT cost more than \$20,000 in parts, or more than \$10,000 in installation.
- Reduce maintenance costs from the current \$10,000/year.
- NOT damage or scuff bottles or labels.
- Allow for either packer lane to be utilized independently.
 - This would require the mechanism to remain in either the 'on' or 'off' position for extended time if necessary.
- Accommodate for variable line speeds.
- Be frequency adjustable. This refers to the number of bottles to pass per cycle.
- Follow food handling guidelines and regulations.
- Be actuated without interfering with bottles.
 - This means that any mechanism should be able to switch from 'on' to 'off' without a bottle being influenced in this transition. The likely way to accomplish this is to have the actuation take place in the space *between* bottles as they pass. Our estimate of this time is 0.064 seconds.
- Be able to redirect bottles moving with a kinetic energy of 0.5-1.0 Joules.
- Be sustainable with routine maintenance.
- Fit in the existing system's footprint.
- NOT cause downed bottles.
- NOT present a safety hazard to employees during operation or maintenance.

3.3 - Design Specifications

- The frequency adjustability should be done by counting bottles (as opposed to a timed action).
- Routine maintenance should be accommodated in the design. Special tools or parts should not be necessary to service and maintain the mechanism.
- Tipping must be controlled, both induced (through the mechanism's workings) and accidental.

3.4 - Ideal Cases

- The design is applicable in various lines with various bottle types.
- The design has a lifespan of 5 years (35 million cycles).

Chapter 4.0 - Background

Maintenance issues with a high speed lane splitter system on line 2 are causing unneeded expenditures. This background chapter will offer insight into several of the base issues that underlie a high speed lane splitting mechanism. Additional background information regarding various components utilized in the design is also presented. The topics of discussion will be:

- High speed bottling process
- Overview of Gallo's line 2 bottle laning section
- Examples of other bottling facilities
- Heuft Bottle Rejection system
- Rapid Prototyping
- Servo Motors
- Commercially Available High Speed Lane Splitters
- Patent Research

4.1 - Gallo's High Speed Bottling Operations

Gallo is one of the largest wineries in the world selling over 67 million cases of wine annually, 1/3 of which is shipped to international markets. Most of Gallo's bottling operations are handled in the Modesto bottling plant.

The Modesto bottling plant is supplied by millions of gallons of stored wine which is fed to 17 bottling lines. Each of the lines is designed to accommodate a certain type of container. Gallo's container lineup includes Bag-in-Box; 5L and 3L jugs; 1.5L, 750mL, 375mL and 187mL bottles. A variety of different products could fill any of the bottles including table wine, sparkling wine, wine cooler beverages and ciders. The lines run at different speeds depending on bottle size varying from 100 bottles per minute for jugs to up to 1000 bottles per minute for the wine beverages.

The bottling lines are almost completely automated, with a small team of operators, inspectors and mechanics for each line. Occasional problems can occur such as broken or tipped bottles, filling mistakes, labeling mistakes, or misfeeds on caps or corks. The line incorporates a series of inspection and rejection systems to discard any problematic bottles; however operators are still present to ensure smooth operation.

The rejection systems can be found on almost every line. These rejection systems use the same mechanism as the lane splitters, which also can be found on most of the lines. The rejection systems and lane splitters are essential to the company to maintain production quality and speed.

4.2 - E&J Gallo Line 2 Overview

Line two at E&J Gallo is a bottling line dedicated to handling 750mL bottles that can be filled with a variety of product; from white to red table wines. Operating at a maximum of 400 bottles per minute, line 2 is one of the fastest 750mL lines at Gallo. The Heuft rejection system is the topic of interest for this project, however to understand the reasons for the interest, we must explore the nature of the line.

Most lines at Gallo follow a similar procedure to fill and package bottles:

1. Empty bottles arrive up-side-down in cases that are stacked on pallets
2. The rows of cases are stripped from the pallet and fed single file on a conveyor
3. The cases are tipped up-side-down to remove empty bottles
4. Cases and bottles are separated
5. Bottles are rinsed
6. Bottles are filled and corked
7. Bottles are x-ray inspected
8. Bottles are dried
9. Bottles are capped
10. Bottles are labeled
11. Bottles are cased and packaged
12. Cases are palletized and stored

The point of interest is after step 7, which is where rejection and lane splitting occurs. The reason for the lane split is because the packaging machine is not capable of the line speed of the filler. In order to compensate for the slower packaging machine, Gallo employs two machines.

The method by which the bottles are divided into separate lanes is the Heuft Rejection system. This system is designed to be used as a single bottle rejection system, however is used on many of the Gallo lines as a dedicated lane splitter. The system causes a significant amount of maintenance costs because of the number of cycles it must endure. A rejecter may actuate several dozen times per day, while a dedicated laner actuates thousands of times per day. The system is not designed for this high number of cycles and thus experiences malfunctions and wear in a relatively short period of time.

4.3 - Heuft Rejection System

4.3.1 - Overview

The Heuft Rejection System is based on a design invented by Bernhard Heuft and is currently manufactured and distributed by Heuft Systemtechnik GmbH of Germany. Founded in 1979, the company has based its business on innovation and unusual ideas that have since become industry standards. Today Heuft is represented all over the world with 20 subsidiary company locations on 5 continents (Heuft, 2007).

The Heuft rejecter initial concept was filed by Bernhard Heuft for U.S. patent number 4,369,873 filed January 10, 1979 under the title Apparatus for Laterally Deflecting Articles. This concept was later improved upon in patent number 4,321,994 on April 21, 1980 under the title Means for Laterally Deflecting Articles from a Path of Travel. Since conception, the system has undergone minor changes to accommodate for modern production speeds, but the system has remained largely the same as the original concept. This patent is documented in Appendix A.

The Heuft rejecter system used by Gallo Winery is named Heuft Delta-FW 16 and is boasted by the Heuft Company as a “robust, all around system for speed of up to 150,000 containers per hour [2500 containers/min]” (Heuft, 2007). While its primary purpose is to single out a container for rejection, Heuft states it can also be used for the “removal of fallen containers and foreign objects” (Heuft, 2007).

4.3.2 - Mechanism Components

The system is comprised of 16 segments that are linearly actuated transversely across the conveyor in front of the containers' path of travel. Figure 1 shows a top view of the mechanism. Notice the segments' independently controlled actuation and how only a single bottle is diverted while the others are not manipulated. The concept behind the design ensures that the bottles are diverted in a gradual manner to reduce the risk of tipping.

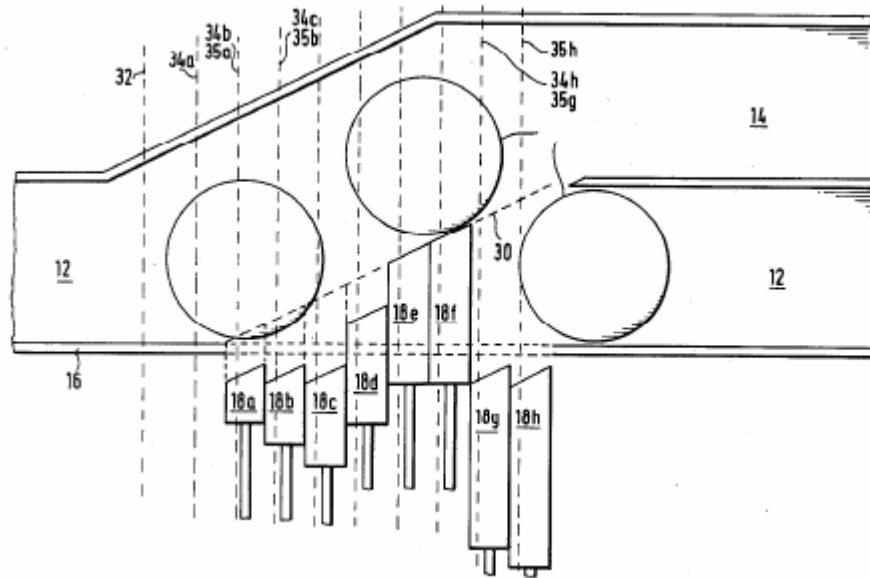


Figure 1: Patent 4,369,873 Concept¹



Figure 2 (left): Line 2 Heuft Delta-FW On Position

Figure 3 (right): Line 2 Heuft Delta-FW Off Position

The Heuft Delta-FW 16 is actuated by a means of 16 pneumatic cylinders ranging in cylinder body size and has adjustable stroke lengths. Each of the 16 cylinders is

¹ Free Patents Online. [Patent Analytics and Patent Searching](http://www.freepatentsonline.com). Retrieved January 8th, 2007. from www.freepatentsonline.com.

controlled individually by an electronic solenoid valve. Note that Gallo uses only 12 of the 16 cylinders (Figure 2).

The 16 cylinders range from 45mm to 155mm in length and have an adjustable stroke length via a threaded piston rod and stopper nut. The strokes are adjustable using ordinary hexagonal sockets. The piston rod includes a rubber shock absorber between the cylinder and the stopper nut to decrease noise as well as wear and fatigue during actuation.



Figure 4: Cylinder Layout (top view)

Attached to each piston rod is a plastic segment by which the bottles are diverted as seen in Figure 2. Each segment is approximately the same width. When all pistons are in the fully “off” position, the bottles are not diverted and continue on a neutral default path (Figure 2 and Figure 5). When the all pistons are actuated in the fully “on” position, the segments are arranged in a curved contour. The contour of each segment is linear, as shown in Figure 8. However the stroke lengths of each piston are such that the array forms the non-linear contour seen in

Figure 6. Also each segment is progressively longer than the previous segment to aid in the horizontal translation.



Figure 5 (left): Segments in Off Position (top view)



Figure 6 (right): Contour in On Position

The segments are approximately 4 inches deep and have a row of bristles that act as a cushion for the bottle to limit impact and bottle scuffing (Figure 7). The bristles are

approximately ¼ inch in length. In addition to bottle cushioning, the bristles also act as a buffer for any irregularities in segment spacing or piston actuation length.



Figure 7: Segment Depth and Bristles



Figure 8: Segment Close-up (top view). Note bristles on end of each segment.

4.3.3 - Controls

The timing of the system is the most crucial element for the successful operation of the system. To completely avoid the chance of tipped bottles, the basic concept of the

design is centered on single point guidance of a bottle. In essence, the timing of the firing sequence is such that the contour is laid out in front of a single container so that the bottle directly in front of the target bottle is not diverted and every bottle after the target *is* diverted. For single bottle diversion, the segments are retracted immediately after the target bottle has passed.

4.3.3.1 - Data Input

In order to start the firing sequence correctly, the position of the bottles on the line must be recorded. This is accomplished by an electronic counting device directly before the rejecter. In order to fire the pistons at the correct time interval after the initial piston, the line speed must be recorded. Coupled to the rejecter's control system is an encoder on the conveyor which records the line speed and bottle position. With these data known, the firing sequence can be timed correctly to avoid bottle tipping (Heuft USA, Inc.).

4.3.3.2 - "Off" to "On" Switch

The first piston (shortest stroke) is always the first piston to fire. This must occur between the target bottle and the bottle directly in front of the target. Depending on the line speed, the pistons will continue to fire between these same two bottles. This insures that the diversion of the bottle is caused by a passive contour, i.e. the bottle will not be "punched" or pushed by an actuating piston. If a punch occurs, the bottle could accelerate laterally into the opposite side and cause an unwanted impact or tip. Once the pistons are all actuated, they remain in this position for a predetermined number of bottles to pass.

Figure 9 shows the firing sequence of the Heuft's pistons. The bottles are highlighted for visualization. Note that the direction of travel is downward. The rejection system is on the right side of each photo.

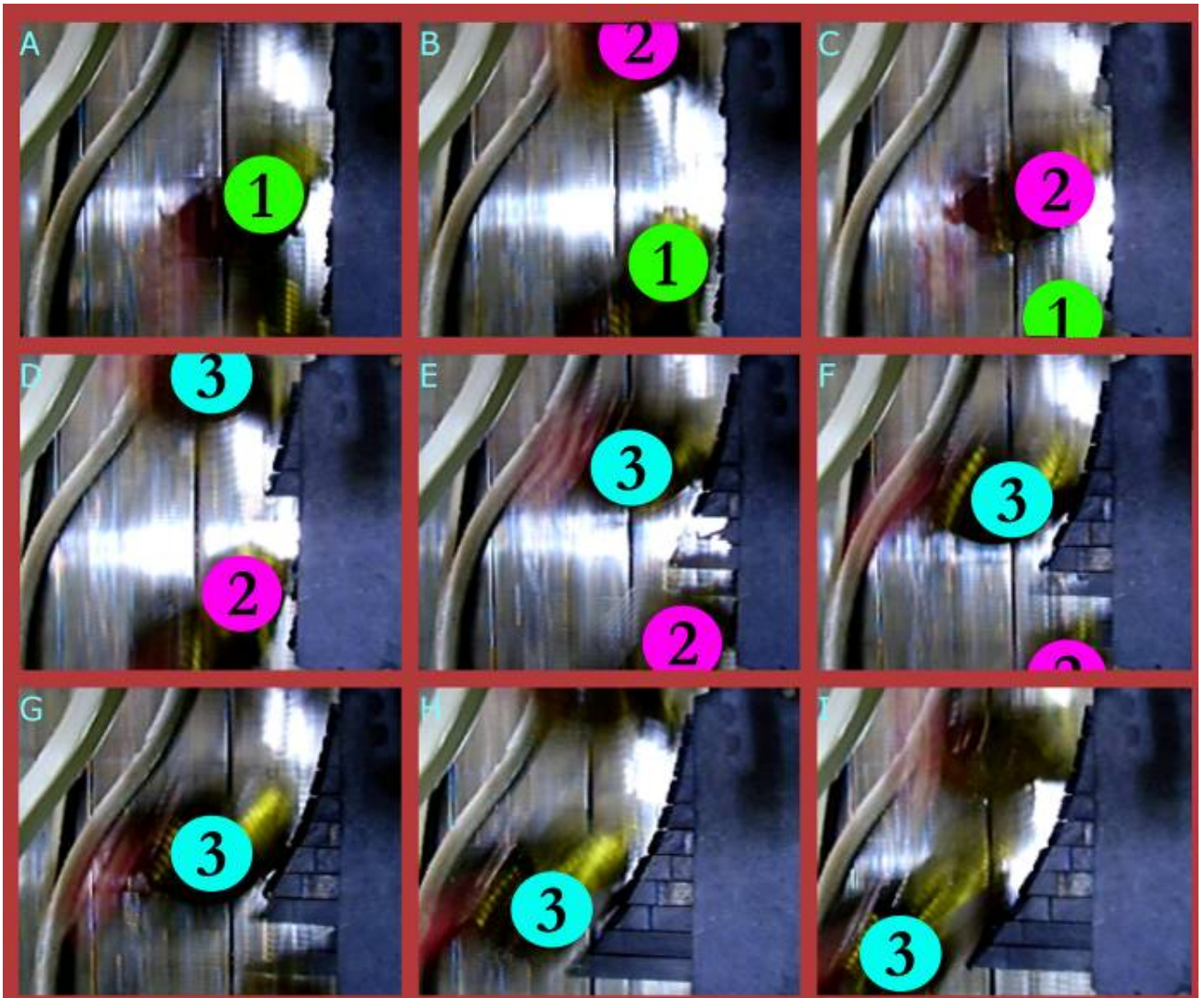


Figure 9: Heuft operation off to on switch

- A. Bottle 1 passes by the off segments. Bottle 2 approaches.
- B. Both Bottle 1 and Bottle 2 are passing the off segments.
- C. Bottle 1 continues to Lane 1. Bottle 2 is still passing the off segments.
- D-F. The segments begin to fire. Bottle 3 enters the beginning of the splitter. Bottle 3 is riding the on segments while Bottle 2 is riding the off segments simultaneously.
- G. Bottle 2 continues to Lane 1. Bottle 3 is riding the on segments.
- H-I. Bottle 3 continues to Lane 2.

4.3.3.3 - “On” to “Off” Switch

Again, the first piston is the first to fire and occurs between the target bottle and bottle directly in front of the target bottle. The sequence firing is the same as the “off” to “on” switch; however the bottle in front of the target bottle follows the contour, while the target bottle follows the default neutral path.

The system is designed to be able to single out one bottle from a stream without disrupting the rest of the stream by laying out a path in front of a single target bottle.

Malfunctions associated with the Heuft system occur most often with the pneumatic actuators. The seals wear and the actuation becomes sluggish over time, which causes timing problems. The timing problems become a liability when working at high speeds, causing tipped bottles and broken bottles. These situations can cause the line to slow down or shut down.

4.4 - Plant Tours

4.4.1 - Wachusett Micro-Brewery

Operations at Wachusett Brewery may not be directly applicable to the production lines at Gallo. There is a vast difference in the volume of production between the two companies. We felt, however, that a visit could offer valuable insight into glass bottle handling in general.

The entire bottling system is contained in one room, with one continuous line. The process begins as the pallet of empty bottles is unloaded to a holding table, which then takes the 440 bottles per tray and feeds them single file into the twist washer. The twist washer spins each bottle several times to clean it inside and out.

As the bottles leave the twist washer they get injected with a spray of liquid nitrogen. The nitrogen evacuates the air from the bottle as it evaporates. The bottles are then fed into the filler, which then passes the bottles to the capper, and then a washer. From here the bottles are split to be fed to two labeling machines; the splitter simply a thin rigid divider that holds several bottles at a time (Figure 10). Once the bottles fill the primary lane, the remaining bottles are deflected down-line to the second labeler. At full speed the two lanes alternate each bottle.



Figure 10: Wachusett Lane Splitter

The labeled bottles continue down the line to an accumulation table where they fill four lanes and are drop packed into their cases, boxed, palletted and either stored onsite or shipped immediately.

Witnessing the manipulation of bottles in person did help us gain some understanding into the problem. It was particularly interesting to hear the plant workers explain how they would separate bottles into two lines, as they have much more experience than us dealing with bottles.

While Wachusett Brewery is orders of magnitude smaller than Gallo in production quantities, the basic principles of dealing with glass bottles are largely the same. The visit to Wachusett gave us a better understanding of these principles, and demonstrated some well established methods of manipulating bottles.

4.4.2 - Northeastern Regional Anheuser-Busch Brewery

Trip Date: Wednesday, November 29th, 2006

With a bottling line rate of approximately 1400 bottles/minute, and an aluminum can line with a rate of around 2000 cans/minute, this facility gives a lot of applicable information to the wine bottle line we are dealing with.

Anheuser runs its main bottling line at 1400 bottles/minute, 24 hours a day, 365 days a year. Production from this brewery is remarkably well engineered and streamlined.

There is one lane split per bottling line that occurs after the bottle filler before the entering the labeling machine. At this point in the process, the full, unlabeled bottles are in single file and moving at maximum velocity. The bottles enter an accumulation zone, the final result of which is 8-10 bottles filed across. This significantly lowers the forward velocity (and thus momentum) such that the lane split is achieved by a passive wedge.

This Anheuser-Busch plant does not use any form of a high speed lane splitting mechanism.

4.5 - Other High Speed Line Split Solutions

Research was conducted on high speed lane split solutions through patent searches and commercially available products.

4.5.1 - Patent Research

There are currently several different patent ideas on how to conduct a high speed lane shift of a container on a conveyor. Many of these ideas are for single container rejection, not for dedicated high speed lane shifters. The abstracts of each patent can be found in Appendix A. All patents research was gathered from www.freepatentsonline.com.

4.5.2 - OEM Products

As stated before there are several products on the market that have the ability for a high speed lane shift, however, most of the products serve as rejection systems, not dedicated lane splitters. Listed below are several companies that manufacture mechanism to cause a diversion of a container from one path to another.

4.5.2.1 - Heuft

Heuft offers several different solutions to the lane diversion/rejection system, most of which are patented by the founder of the company. The following list is Heuft's current line-up of commercially available products for lane splitting.

4.5.2.1.1 - Heuft Delta-K



Figure 11: Heuft Delta-K Unit²

The Heuft Delta-K unit, shown in Figure 11, is similar to the Heuft Delta-FW system, except instead of linearly actuating segments, the Delta-K employs rotating segments that fan down in a similar timing that the Delta-FW follows.

² Heuft USA, Inc. [Container Rejection Systems](http://www.heuft.com). Retrieved January 10th, 2007, from www.heuft.com.

4.5.2.1.2 - Heuft Flip Rejecter



Figure 12: Heuft Flip Rejecter³

The Heuft flip rejecter shown in Figure 12 is a single arm actuator that simply pushes a single container transversely across the conveyor. It is a simple robust option for single container rejection.

Figure 12 is a single arm actuator that simply

4.5.2.1.3 - Heuft XY

The Heuft XY is a multi-segmented linear actuation system shown in Figure 13⁴ capable of multi-lane sorting of containers. It is ideal for sorting as it can divide containers into up to four lanes. This system is most suitable for low speed applications



Figure 13: Heuft XY⁴

4.5.2.2 - KHS

KHS is a respected company in the production industry.

³ Heuft USA

⁴ Heuft USA

KHS does not offer any dedicated lane splitters, however, they offer a unique system that double-files a single file line of bottles. This system could potentially be used in conjunction with a passive wedge lane divider. An example photo is shown in Figure 14.



Figure 14: KHS Waveform⁵

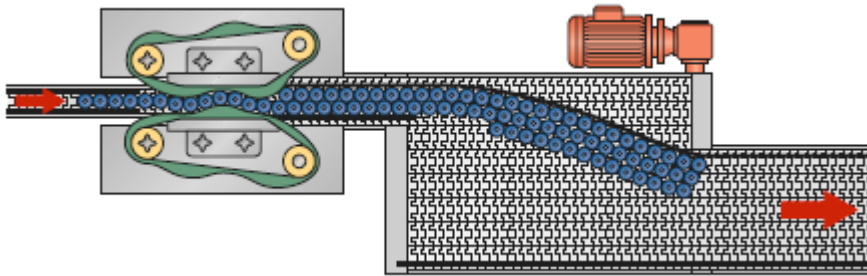


Figure 15: Top view of KHS Waveform⁶

This system is interesting as it uses two spinning belts with complementary waveforms such that as bottles are fed through, they are laned in a staggered double file line. This system could function as a unique laning system if the double file line was then split with a passive wedge.

⁵ KHS. [Container Conveying Solutions](http://www.kisters.com/img/pool/1111_Container%20Conveying%20Systems.pdf). Retrieved November 19, 2007 from www.kisters.com/img/pool/1111_Container%20Conveying%20Systems.pdf.

⁶ KHS

4.6 - Rapid Prototyping

Rapid prototyping is the modern production method of forming solid parts from a CAD model without the use of traditional fabrication techniques. Complex geometries can be formed more quickly for less initial investment than other methods. There is no need for a mold, and typically no secondary operations are necessary. Part accuracy is generally quite good, depending on the process and materials used.

The general concept behind rapid prototyping is to divide the CAD model into many cross sections, and then to build a physical part by accumulating these sections one on the other. There are numerous means of accomplishing this, using stock material in the form of sheets, powder, liquid, resin or wire. The process allows the fabrication of otherwise non-machinable geometries, as seen in Figure 16⁷. More detailed information on rapid prototyping techniques can be found in Appendix J.



Figure 16: Complex Geometry Realized Through Fused Deposition Modeling

4.7 - Servo Motors

Servo motors are, in basic terms, an electric motor with a brain. Servos as described by Robert Norton in Design of Machinery, are “fast-response, closed loop controlled motors capable of providing a programmed function of acceleration or velocity, providing position control, and of holding a fixed position against a load”⁸. The control is based on the closed loop system, which means that sensors on the servo feed back information on the motor’s position and velocity to the controller. The controllers are called drivers, which is a computer that responds to the information and adjusts the current flow to drive the motor. The drivers can be programmed to control the servo motor dynamically to adjust for changes in load and commands. The commands can be input in real time through user interface or can be imbedded in a cycle program.

Servos can be configured in both AC and DC, have high torque capability and perform well in instances needing rapid acceleration and deceleration. They are capable of providing tight toleranced constant velocities, even under dynamic loading.

Servos are gaining rapid acceptance at Gallo, making complicated operations easier to automate. In the last five years, servos have found their way to several of the bottling lines and continue to be implemented.

⁷ Figure retrieved from <http://www.cs.berkeley.edu/~sequin/SCULPTS/SnowSculpt02/maquettes.html>

⁸ Norton, Robert L. Design of Machinery. New York: McGraw Hill, 2004, page 70.

Chapter 5.0 - Camoid Design Conception

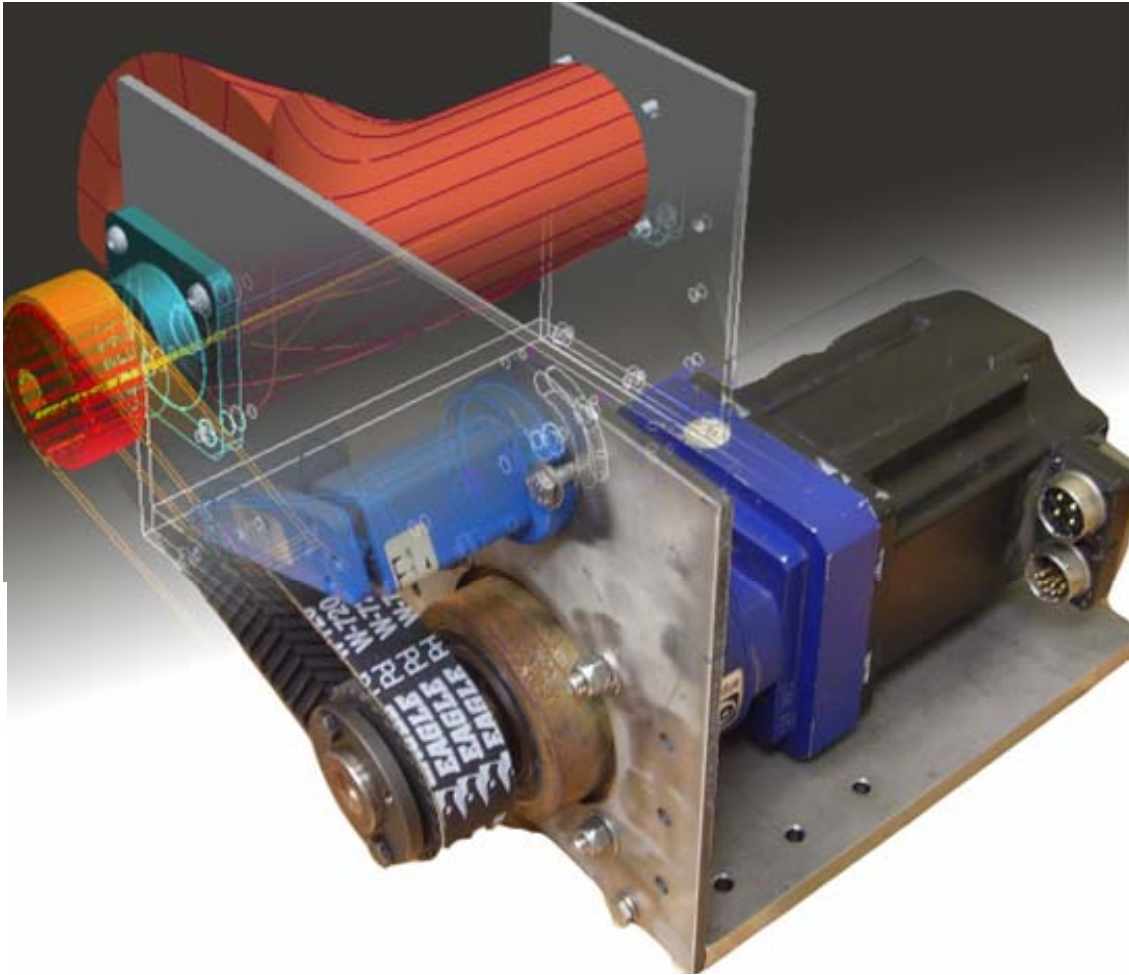


Figure 17: Camoid Laner

The camoid laner concept proposes to replace the Heuft Delta FW 16 segmented rejecter system with a single rotary servo driven, three-dimensional geometric shape. The driving force behind the concept is the need to simplify the actuation system of the process. The Heuft system incorporates 16 independent pneumatic cylinders, which as previously noted can cause maintenance and timing issues. The camoid laner incorporates a single actuator which has the potential to greatly reduce the complexity and increase the reliability of the system.

The operation of the camoid system follows the same logic as the Heuft Delta FW; a binary system in which a contour is laid out in between two bottles such that there is no active translation of bottles. The bottles simply follow a new static contour that diverts them to a new lane. An overhead view of the system in operation is shown in the photo sequence in Figure 18 and the operation sequence is guided in a step by step manner.

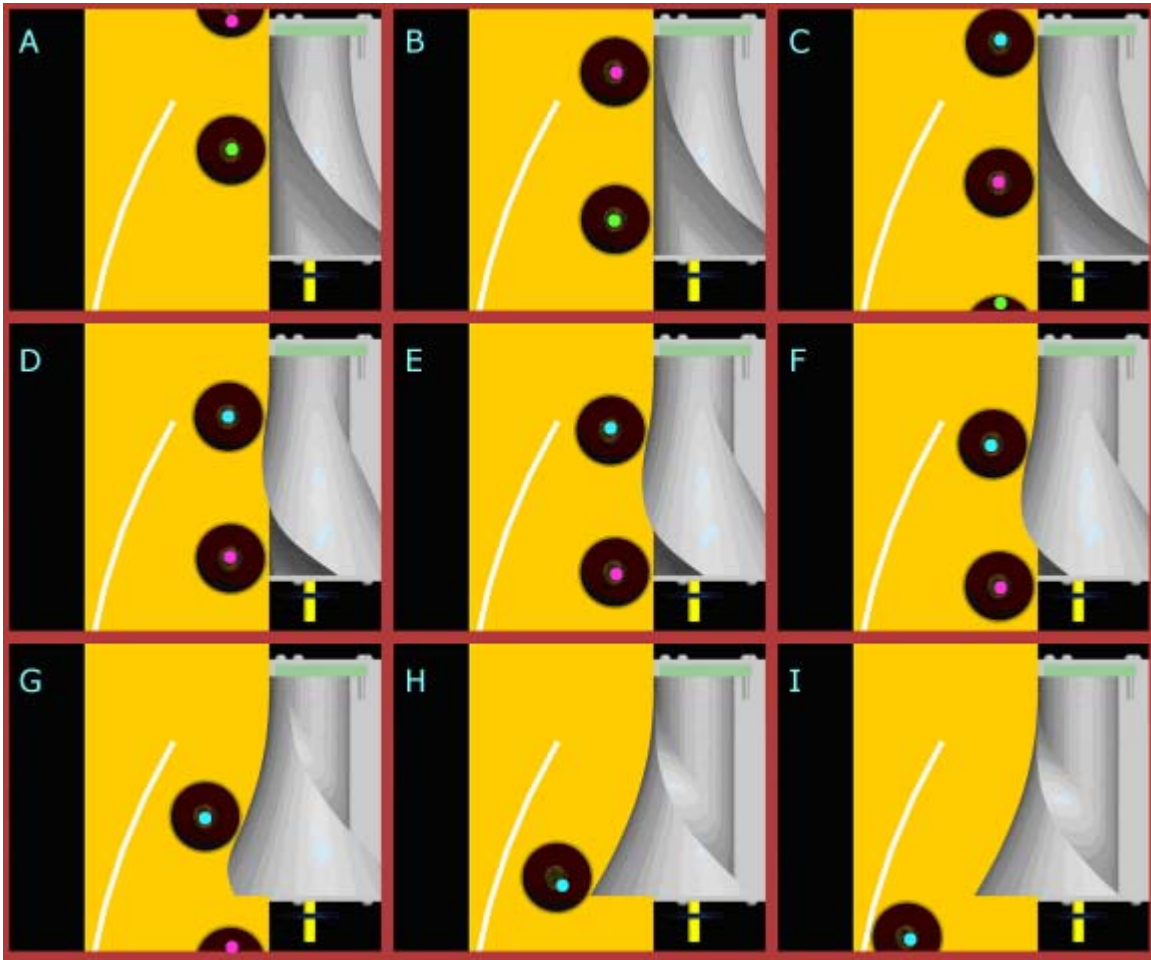


Figure 18: Camoid Extension

- A. Bottle 1 passes by the camoid. Bottle 2 approaches.
- B. Both Bottle 1 and Bottle 2 are passing the camoid.
- C. Bottle 1 continues to Lane 1. Bottle 2 is still in contact with the Low Dwell of the camoid. Bottle 3 enters the beginning of the camoid.
- D-F. The cam rotates, with Bottle 3 riding the High Dwell while Bottle 2 is riding the Low Dwell simultaneously.
- G. Bottle 2 continues to Lane 1. Bottle 3 is riding the High Dwell of the camoid.
- H-I. Bottle 3 continues to Lane 2.

Once the contour is laid out, the camoid will remain in the diverting (on) position until a given number of bottles passes, and then the camoid will begin to spin and the camoid will return to the off position. The camoid will remain in the off position for a given number of bottles, then repeat the process described above.

The operation is very similar to the Heuft Delta FW, but the design offers improvements that will positively affect the reliability of the system. In this chapter the camoid laner mechanism will be explained in a manner to give a basic understanding of the concept and introduce some terminology before detailed investigation into the design process ensues in the proceeding chapters.

5.1 - Camoid Geometry

5.1.1 - Camoid Concept

The heart of the camoid laner is the camoid geometric shape. By definition a camoid is a two degree-of-freedom, three-dimensional cam. Two degrees of freedom means that the shape can cause motion in two directions. Putting this into perspective for a bottle laner, the two degrees of freedom can be described as follows:

- First degree of freedom: The bottles traveling down-line on the conveyor, *x-direction*
- Second degree-of-freedom: The bottles being diverted across the conveyor, *y-direction*

5.1.2 - Camoid Inspiration

Heuft currently has several rejecters on the market as explained in the background section (Chapter 2), and one of which sparked the idea to use a camoid for the laner design. The Heuft Delta K shown in Figure 19 is similar to the Heuft Delta FW 16 system used on the lines currently; however, instead of linearly translating segments, this system uses rotating fingers. The timing would be similar to the Heuft Delta FW; just the actuation motion would be changed.



Figure 19: Heuft Delta-K Bottle Rejecter⁹

As stated before, the driving force of the idea is to reduce the number of actuators. The camoid design stems from the concept of the Heuft segments and timing wrapped about a single axis, effectively controlling timing, translation and contour in a single geometry provided rotation can be controlled accurately.

⁹ Figure retrieved from Heuft USA

5.1.3 - Camoid Design

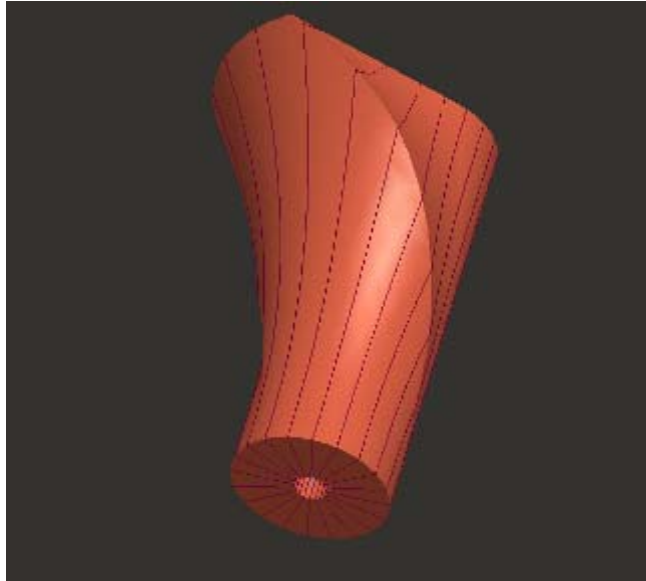


Figure 20: Camoid Laner Shape

The camoid laning geometry is basically the Heuft segments physical nature and actuation control logic wrapped about a single axis. This is easier to understand by examining the Heuft geometry and timing in detail. In the following sections, the process for generating the complex geometric shape shown in Figure 20 will be explained in basic terms providing the necessary background and terminology for understanding of the more detailed analyses in the proceeding chapters.

Figure 21 shown below is an explanation of the terminology used in this section.

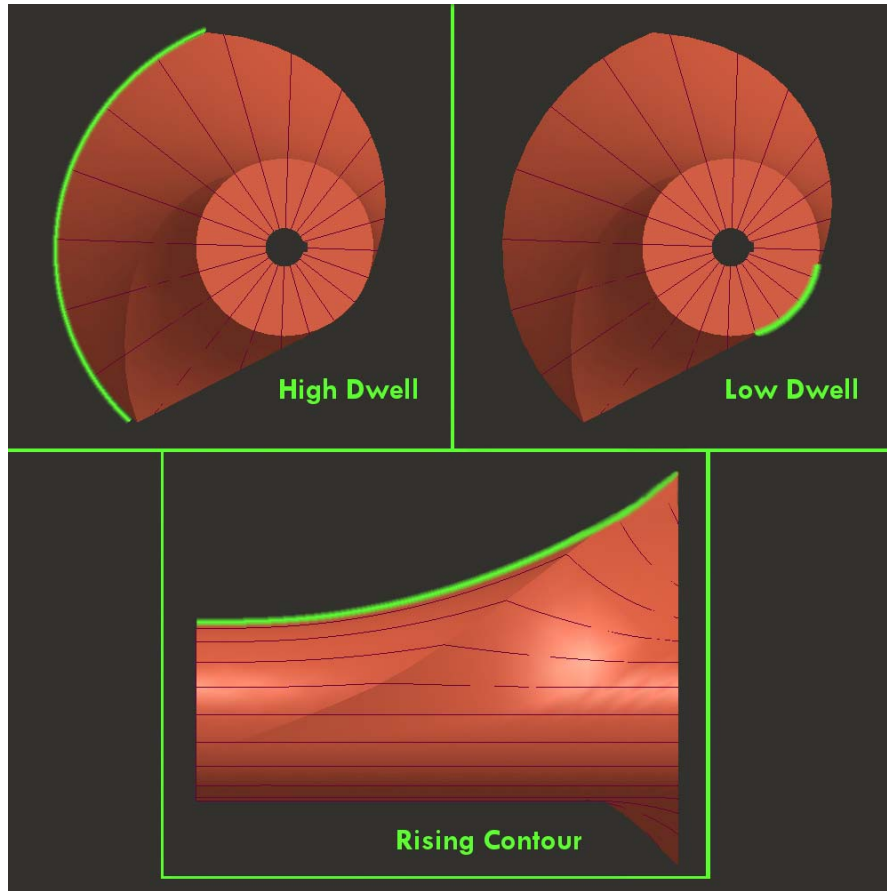


Figure 21: Geometry Terminology

5.1.3.1 - Wrapping Segments Around an Axis

It's easiest to understand the shape if it is explained as a series of cross sections acting like cams with a common rotational axis (camshaft). Each segment of the Heuft Delta FW system can be modeled as a double dwell two-dimensional cam with the cam's high dwell to be equal to the segment displacement and low dwell to be equal to the base circle. This is easiest to explain with the cam segment graphic shown in Figure 22.

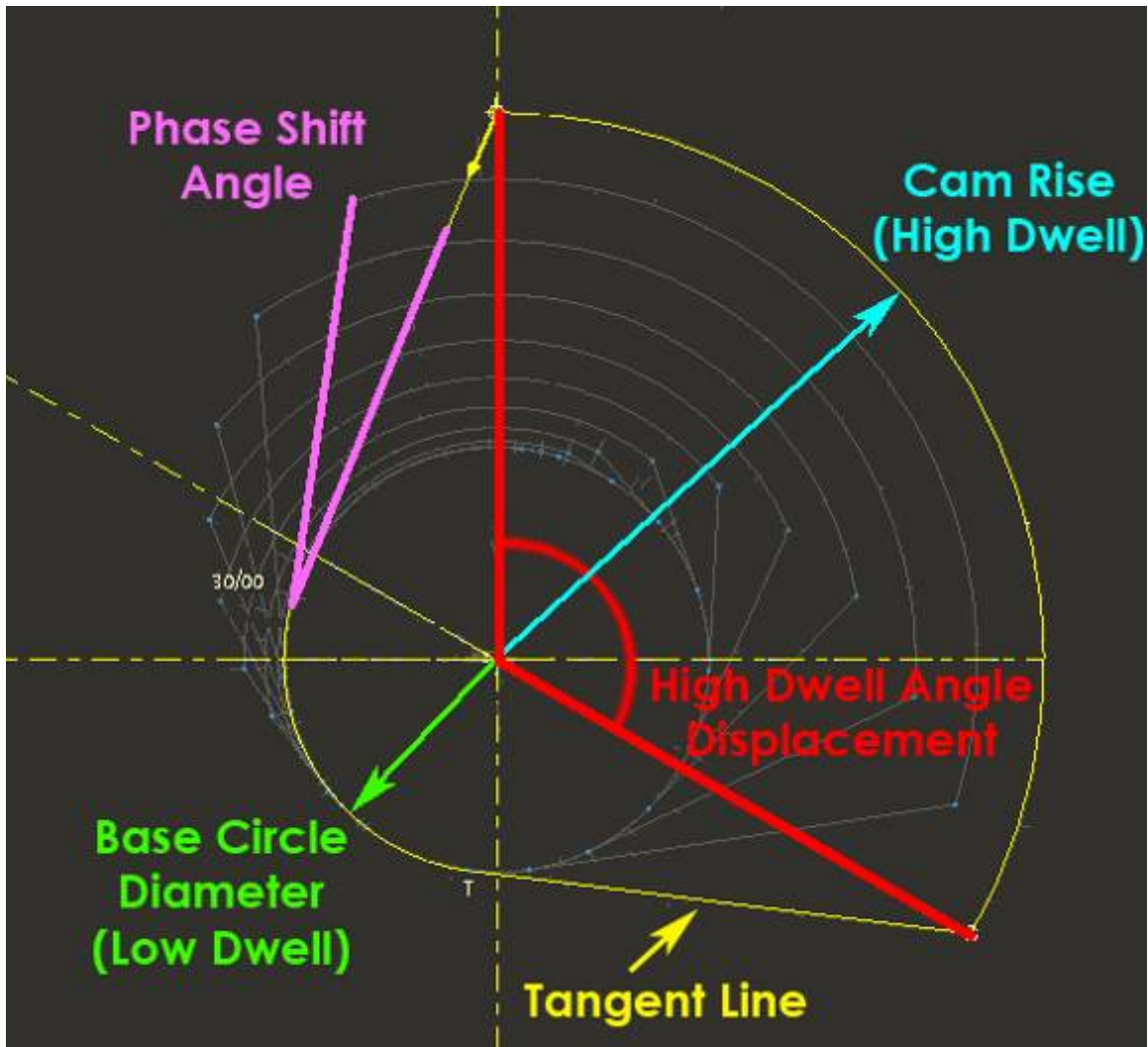


Figure 22: Cam Segment Construction

The cam segment construction is actually quite simple. It consists of two concentric circles, the base circle and cam rise circle. The base circle is representative of the Heuft off position, i.e. all segments not actuated. The cam rise circle is representative of the Heuft on position, its radius equal to the Heuft segment length. The cam rise circle whose chordal length is related to a high dwell angular displacement. The importance of this value will be discussed later in the report in Chapter 7. A tangent line, labeled in Figure 22, is extended from the base circle to either extreme of the cam rise circle section.

If all 16 cams are stacked along the shaft, the resultant shape long drum cam with each successive cam rise making the contour of the Heuft segments. To do this, the base circle of each cam segment remains constant, while the cam rise circle of each cam section represents the length of the corresponding Heuft segment. If we were to spin this, the contour would rise and fall; however each cam's rise would occur simultaneously. From researching the Heuft timing in the previous chapter, we know that the segments fire in sequence between two bottles, they do *not actuate simultaneously*. The next step with the camoid laner geometry is to sequence the rise such that it resembles the Heuft sequence and allow each cam's successive rise to occur between two bottles.

5.1.3.2 - Sequencing the Cam Rise

The main goal is to cause the rise of each successive cam segment to occur between two bottles. If the bottles were not moving parallel to the axis of rotation, the cams could rise simultaneously and remain rising between the two stationary bottles. As we know, this is not the case. In order to cause the cams to rise in succession, each successive cam is out of phase to the previous cam some angle *in the direction opposite to the rotation direction of the camshaft*. This phase shift is shown in Figure 22. This causes each successive cam to delay its rise during rotation of the camshaft, provided the cam shaft is spinning at *constant rotational velocity*. Figure 23 is a representation of what the shape would look like at this point in the explanation. Notice that the cam segments rise wraps around the cam shaft axis in a helical manner. It is this helical shape that allows the cam segments to sequentially rise between two moving bottles during constant cam shaft rotation.

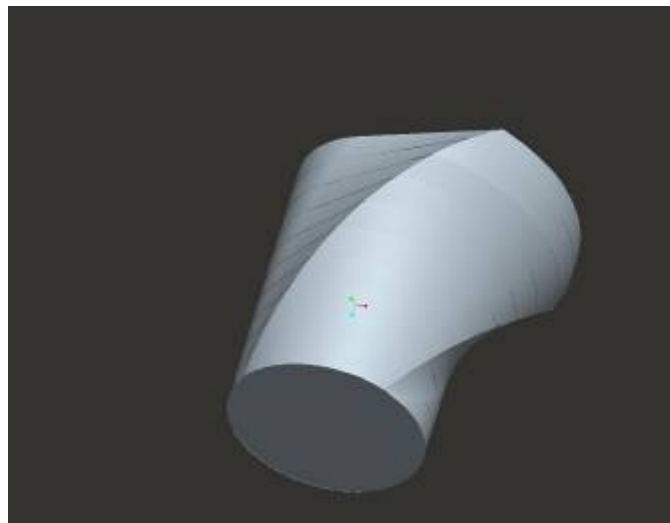


Figure 23: Segmented Camoid

Before the explanation goes further it is important to note that the rise profile (tangent lines connecting high and low dwells) of the *cam segments* is in no way involved in manipulating bottles. The bottles are only in contact with the cam segments high and low dwell surfaces. It is the succession of rising cam segments which creates the profile by which the bottles are diverted.

5.1.3.3 - Smooth Diversion

Both the basic shape of the camoid and basic functionality behind the shape have been described thus far. However, the resolution of the contour is poor with sixteen segments, especially if the segments are not blended together, as they are shown in Figure 23. This resolution is crucial as the bottles will be in contact with this section of the cam and an unblended surface could cause damage to bottles. There are two criteria that must be met in order to create a smoothly rising contour:

- a) The thickness of each cam segment must approach zero
- b) The successive cam segments must rise according to a function that provides satisfactory results in the output bottle motion (acceleration, velocity, etc.)

As the cam segment thickness approaches zero, the resolution of the contour increases, creating a smoothly blended surface that would resemble the shape shown in Figure 20.

The rise succession of the Heuft Delta FW segments does not provide the resolution needed for the contour design; therefore it is necessary to provide a function that governs the successive rises of the cam segments. Since the bottles will be being diverted by this contour, it is important to make sure that the contour will not cause any unwanted or dangerous forces on the bottle as it is being diverted. One method to mathematically ensure an effective contour is to use cam program design.

5.1.3.4 - Contour Design

If we treat the bottle as a follower and the contour as a cam rise profile, we can use cam design methodology to ensure that the displacement, velocity, acceleration, jerk and force caused by the contour are all satisfactory. For a baseline of comparison, the Heuft contour was reversed engineered and then compared to several different cam programs to find the most effective contour. The cam design is explained in more detail in the following sections.

5.1.3.5 - Broad Details of Segment Phase Shifts

The segment rises are controlled in a manner such that the bottles are gently diverted, it is crucial to time the segment rise sequence effectively. This sequential introduction of cam segment rises is caused by the angular offset, or phase shift, of each segment to one another. There are several things to remember when interpreting the phase shift of the cam segments:

- a) The phase shift must be large enough such that the contour rises only between two bottles
- b) It must be large enough to provide a point in camshaft rotation at which all segments are at high dwell, i.e. a continuous strip of contour for bottle diversion (this will be explained in the next section, Controlling the Servo).
- c) It must not be too large to allow the contour to fall between two bottles.

There are only 360 degrees to work within for the phase shift that will allow both a cam segment rise and fall within one rotation. Notice in Figure 24 the phase shifting can be clearly seen by the curve dotted in green. Note that if there were no phase shifting, the dots would make a straight line along the camoid axis, not a curve.

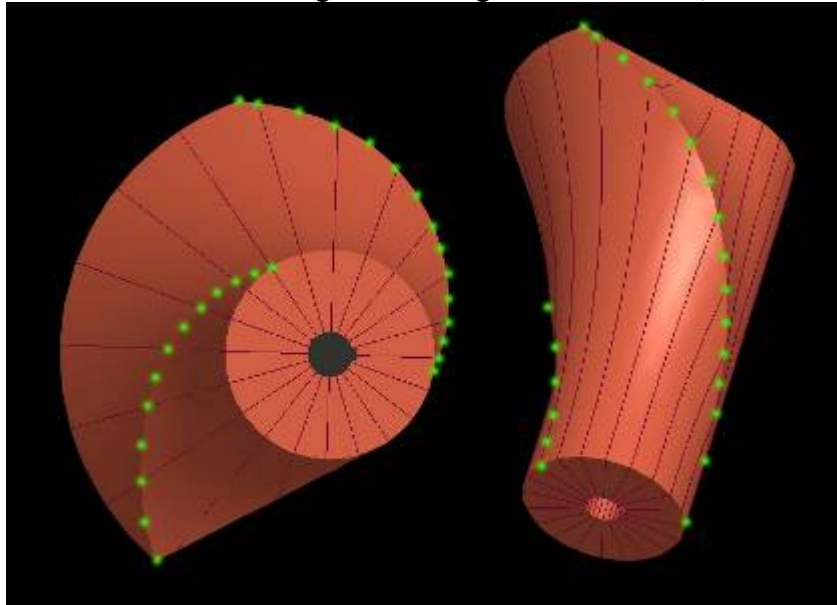


Figure 24: Cam segment phase shifting

5.1.3.6 - Bottle Contact Strip

An important criterion constraining the phase shifting is the necessity of a period in cam rotation at which all cam segments are in high dwell. The reasoning behind this can be explained by the nature of the concept. The system must be binary and the camoid must remain in one position while a given number of bottles are being diverted. This requires a section of the camoid to offer a continuous section of contour at a point in its rotation. An example of the strip is shown in Figure 25. Notice that there is a strip on both the low dwell and the high dwell of the camoid, representing no diversion on the low dwell and positive diversion on the high dwell of the bottle respectively.

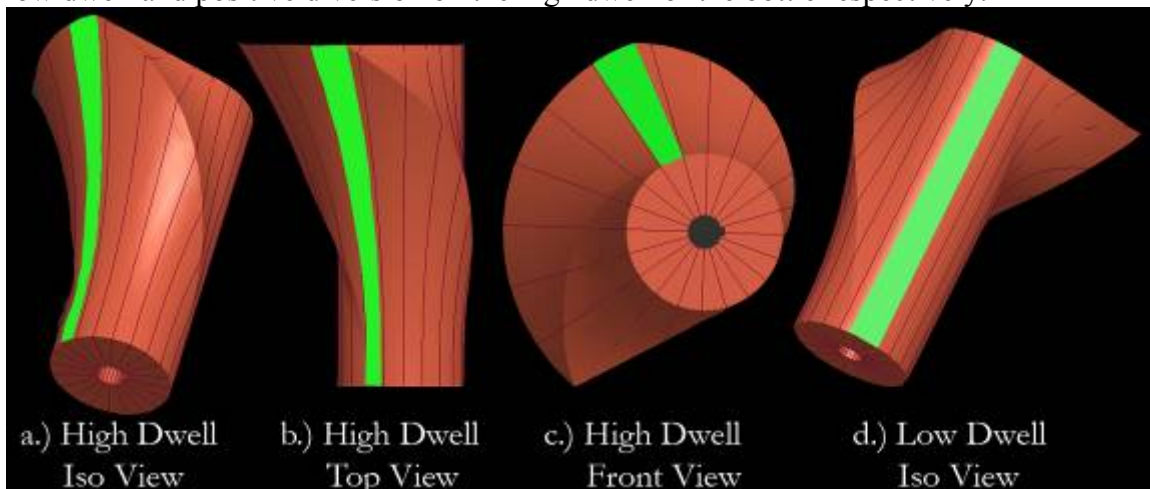


Figure 25: Sections of Continuous Contour

Correctly designing the phase shifts will result in a contour strip of satisfactory width. However, it is a delicate process as different parts of the camoid geometry can be drastically altered with a small change in phase shift. These variations will be discussed in detail later in the report as there are actually several geometric variables that can be adjusted to create a satisfactory contour strip. For the purposes of this section we will not discuss these details.

This strip actually serves two purposes, one of which is offering the continuous contour. In the following section we will see how the contour strip plays a significant role in the timing of the rotational actuation.

5.2 - Actuation Design

If the camoid geometric shape is the heart of the camoid laner mechanism, then the actuation system is the brain. As stated previously, the actuation of the camoid laner is accomplished by a servo motor. There are several key reasons as to why the servo motor was chosen over other actuation methods and in the following subsections of this chapter, these reasons will be introduced. Again, greater detail and analysis behind these decisions can be found in later chapters; however it is necessary to have a basic overview understanding of the actuation system and terminology before any detailed explanation could be interpreted. Topics of investigation of the actuation system in this chapter include:

- Why use a servo?
- Choosing the servo
- Sizing the servo
- Controlling the servo

5.2.1 - Why use a Servo?

As discussed earlier in the chapter, the nature of the camoid operation calls for several required actions during operation:

- The actuation of the system is rotation
- During laning process, the rotational velocity of the camoid must be constant
- The camoid must remain at both high and low dwell (no rotation) for a given number of bottles to pass

There are also several task specifications that must be adhered to:

- The mechanism must be able remain in either on or off position (high or low dwell) for extended periods of time
- The mechanism must accommodate for variable line speeds
- The mechanism must be frequency adjustable, i.e. change the number of bottles to pass

From these constraints we can also deduce further requirements of the actuation system:

- The system must accelerate to a full rotational operating velocity between two bottles
- The system must decelerate as quickly as possible

- The system must be adaptable for actuation start times based on a number of inputs including
 - Bottle velocity
 - Bottle position
- The operational rotational velocity must be a function of the line speed, since the mechanism must adapt to different line speeds in real time
- The system must offer high torque outputs due to high acceleration requirements

Based on the requirements of the actuation system, it is apparent that the actuation must be under careful control. From the discussion about servo motors in the previous chapter we can see how a servo can fulfill the requirements of this application. Recall that servo motors offer:

- Fast response time
- Position control
- Capability to hold a fixed position
- Velocity and acceleration program control
- Rapid acceleration and deceleration capability
- Tight toleranced constant velocity even under dynamic loading
- High torque capability

To achieve the level of control needed by a single rotational actuator, the servo is an excellent candidate.

5.2.2 - Choosing a Servo

Gallo currently is installing an increasing number of servo motors as more precise automation, higher quality and easier production operation is demanded by the company. For this reason, Gallo works closely with a well known and trusted servo automation company, Rockwell Automation. Rockwell provides all the necessary hardware and software to power and control the Allen-Bradley servo motors that Rockwell distributes. Choosing a servo brand to use in this case was dependent on the sponsor company preference.

5.2.3 - Sizing a Servo

Choosing an appropriately sized servo is an important task and care must be taken in doing so. In this case of high accelerations, a servo motor with sufficient torque is necessary. Choosing a servo with insufficient torque will result in the mechanism not accelerating in time, potentially causing damaged bottles. Over-sizing the servo is expensive and unnecessary. A large servo may also not have the acceleration necessary because of high motor inertia.

In order to aid in the process of sizing a servo, Rockwell Automation offers software that will provide a range of servos that would be applicable based on a number of user defined constraints and timing criteria. This will be explained in greater detail in later chapters.

5.2.4 - Controlling the Servo

The servo is controlled through a series of components that compose a closed loop communication system. Information regarding all aspects of the motion is relayed in real-time to adjust the output to accomplish the exact task demanded by the user. Designing a control program for a servo requires attention to detail. After choosing the correct servo and driver components, the general constraints on the motion of the servo are:

- Position
- Operating Velocity
- Acceleration
- Start Time
- Dwell Time

5.2.4.1 - Position

In the case of the camoid laner, the exact position of the servo is essential information to provide the control logic as it is crucial in the successful operation of the system. To accomplish this, the servo motor is equipped with a shaft encoder that feeds back its position data to the control system.

5.2.4.2 - Operating Rotational Velocity

The contour must be laid out between two bottles, thus the rate at which the contour rises is equal to the bottle velocity. This velocity is essential to successful operation and must match the bottle velocity at all times, thus is denoted as the operating velocity. The operating rotational velocity is calculated based on the linear velocity of the bottles on the line.

5.2.4.3 - Acceleration

The servo needs time and distance to accelerate and decelerate the camoid up to/down from the operating velocity. In order to accomplish this, both the geometry of the camoid and the timing of the actuation must be adjusted. Recall that in order for successful diversion of the bottles, the camoid geometry must incorporate a continuous strip of contour running its entire length. Not only does this strip act to provide a continuous contour, but also provides the buffer distance for servo acceleration and deceleration.

5.2.4.4 - Actuation Start and Dwell Times

The start of the actuation and the camoid dwell time are both matters that require sensing bottle positions. The actuation must initiate between two bottles. The camoid must dwell for an amount of time that is dependent on the number of bottles that it diverts. In order to accomplish these tasks, the servo controller must be aware of the bottle positions and how many bottles have passed the laner. To do so, a photoeye is placed on the line that reads when a bottle goes past it. Alone the photoeye is capable of counting bottles as they pass. When coupled with the shaft encoder, the two instruments are capable of sensing a bottle's position as it moves down the line. With this information

input to the servo controller, the actuation initiation and the dwell timing are able to be controlled.

5.2.5 - Actuation Design Conclusions

The properties of a servo make it an ideal candidate for the motion application of the camoid laner. With the servo, all aspects of the motion can be controlled in detail and adjusted in real-time to accommodate a wide range of scenarios that could be experienced out on the line.

5.3 - Design concept summary

Coupling geometric design with proper motion control, the camoid laner is able to accomplish with one actuator what the Heuft Delta FW does with sixteen actuators. Not only is the number of actuators fractioned, but the reliability of the actuation method is increased as well. This chapter was intended to give an overview of the concept behind the design and to introduce some of the terminology that can be expected in the following sections. In the next chapters the camoid design will be explained in detail with mathematical analysis to support the decisions made in the design. Each section will include a brief introduction to the specific aspect of design to be explained; however, if there is any confusion before reading the analysis, this chapter should be referenced.

Chapter 6.0 - Methodology

This chapter outlines the steps that were taken throughout the design process and present the process in a logical order that could be replicated. The actual methodology involved simultaneity and iteration.

6.1 - Assumptions

A number of assumptions were made throughout the design phase of this project. Such assumptions are necessary to prioritize different elements in both the problem definition and the derived solution. Some of the most relevant assumptions are briefly discussed here, along with any verification that the assumptions were valid.

6.1.1 - Line 2 Properties

The process of splitting bottles is heavily dependent upon an accurate kinematic model of a stream of bottles, including their relative positions, velocities, and accelerations. The relation between bottle and conveyor is also of great importance. Considering this, an average set of conditions was taken as the design baseline, with all analyses and decisions made in reference to these conditions. The design should allow for a safe range of conditions around the average.

Line 2 runs at a rate of 400 bottles per minute when operating correctly. This equates to a conveyor roughly 1 meter per second. Based on accounts from Gallo employees and video footage, it was determined that wine bottles on Line 2 were in static friction with the conveyor at the point of the lane split. An assumed minimum bottle spacing (the distance between two adjacent bottles) of one bottle diameter was agreed upon, again through the advice of Gallo engineers. These conditions describe bottles with no relative velocity, neither to each other nor to the conveyor, and with velocity equal to the line speed relative to the stationary splitter.

6.1.2 - Heuft Laner

The direction of the redesign was largely defined upon making one assumption in particular; the laning system currently used by Gallo is successful at its function of diverting bottles, but fails to achieve the desired lifetime. Prior to making this assumption, the design team had looked at alternative methods of achieving a laning diversion. With this assumption, however, the focus shifted to finding alternative means of *driving* the existing system to improve lifetime.

The shift in focus was significant. It made analyses on tipping or breaking bottles less important; if the Heuft Laner did not damage bottles with its current means of actuation (pneumatic cylinders), it follows that the bottles would remain undamaged if the actuation was replaced, but mimicked closely enough.

6.2 - Data Collection and Analysis

6.2.1 - Heuft Analysis

The design requirements of this project are to improve upon the existing design for high speed lane splitting. In order for this to be accomplished, the existing system must be analyzed and understood. The first step taken was to understand key aspects of the operation of the Heuft laning system. The method by which the mechanism functions is explained in the background chapter of this report.

The next step in understanding the Heuft laning system was to analyze the contour by which the bottles are diverted. An understanding of the function of the contour is needed as a baseline of comparison for other contours.

The Heuft contour was measured and a best fit polynomial equation was fit to the points measured. The contour can be understood mathematically allowing kinematic and dynamic analyses can be conducted.

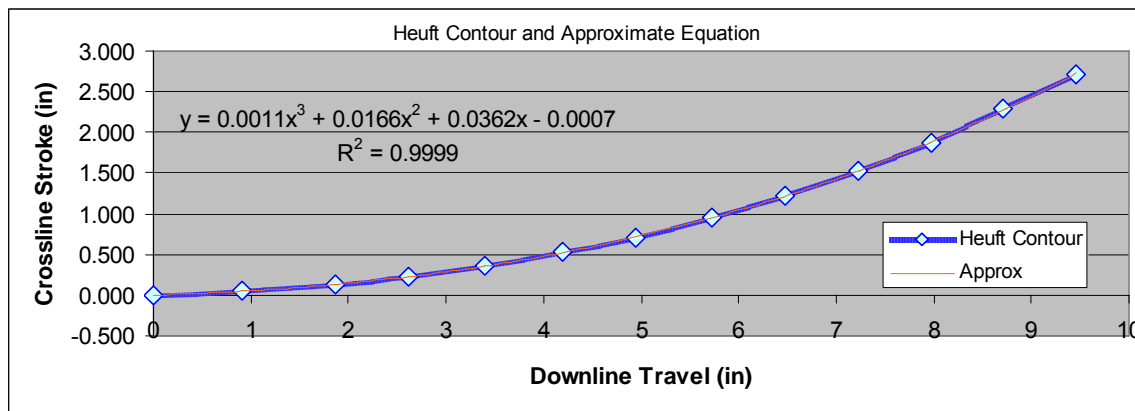


Figure 26: Heuft Contour and Equation

6.2.2 - Contour Design and Analysis

The most important aspect of the design is that no bottles are tipped or damaged during the laning process. In order to improve on the existing system, cam program design is used to develop several contours with controlled acceleration profiles. Based on standard cam design methodology¹⁰, we chose three different cam programs to use as a base for optimization of the existing system. The three cam programs of interest are as follows:

- Simple Harmonic Displacement
- Modified Trapezoid Acceleration
- 4-5-6-7 Polynomial Function Displacement

Each of the programs is designed following some basic criteria that require specific aspects to be constrained.

¹⁰ Norton, Robert L. Design of Machinery. New York: McGraw Hill, 2004.

6.2.2.1 - Simple Harmonic Displacement Constraints

Constraints are set on the final value of displacement.

6.2.2.2 - Modified Trapezoidal Acceleration Constraints

Assumptions are made of the maximum allowable acceleration.

6.2.2.3 - Polynomial 4-5-6-7 Function Displacement Constraints

By adjusting the values of the 8 constants, constraints can be set on the initial and final position, velocity, acceleration and jerk (boundary conditions). Polynomial cam contours offer accurate control of the dynamic conditions at the selected positions, however the displacement function is governed by the boundary conditions and is often difficult to control maximum values.

After specific contours are designed and plotted, they are compared against the existing system, and analysis is conducted on each contour.

6.2.2.4 - Kinematic Analysis

Kinematic analysis includes comparison and discussion on each of the cam displacement, velocity, acceleration and jerk profiles. The three proposed profiles are directly compared with the current Heuft system and are also compared with each other. Topics of investigation include:

- Difference compared to Heuft
- Abnormal peaks
- Maximum values
- Minimum values

6.2.2.5 - Force Analysis

Force analysis was conducted with the same criteria listed above in kinematic analysis except analyzes the force and moment induced by the contour on the moving bottle. In addition, the force and moment were compared to the friction force between the bottle and conveyor making sure that the contour will induce enough force to overcome static friction fast enough to minimize tipping potential.

6.2.3 - Choosing Contour

The most suitable contour is chosen based on several important criteria:

- Acceptable Final Velocity
- Minimizing Maximum Acceleration
- Minimizing Jerk
- Maximum Force
- Maximum Induced Moment on Bottle

The last two criteria are most important as both are involved directly with damaging and tipping bottles. Taking each of these criteria into consideration, a contour is chosen that best suits high speed bottle laning.

6.3 - Camoid Geometry Design

The design of the camoid geometry is an iterative process. There are several elements of the camoid that are manipulated to generate the complex geometry. The elements are interdependent; changing one element affects the others, which in turn affects the entire geometry of the camoid. The elements of the geometry that are manipulated are:

- Profile Rise Contour
- Cam Phase Angles
- High Dwell Angle Displacement
- Low Dwell Angle Displacement
- Buffer Angle
- Base Circle Radius
- Overall Length of Laner

This detailed design process can be found in detail in Chapter 7 of this report.

6.3.1 - Manufacture

It was agreed early that the material of the camoid will be some sort of plastic for its characteristics in:

- Wear resistance
- Oxidation resistance
- High strength to weight ratio
- Low weight
- Forgiveness for bottles during impact (relative to metal)
- Manufacturing flexibility
- Low cost

The geometry of the camoid is complex and could prove to be difficult to manufacture for conventional methods of machining. Furthermore, the geometry must be relatively accurate as there are tight tolerances of certain elements. There are few options available for manufacturing complex geometries:

- CNC Machining
- Rapid Prototyping
- Injection Molding

Each method offers advantages and disadvantages shown in Table 1.

CNC		Rapid Prototyping		Injection Molding	
Adv.	Disadv.	Adv.	Disadv.	Adv.	Disadv.
Inexpensive (relative to other methods)	Limits of geometric complexity due to tooling and nature of process	Complex Geometries	Expensive	Inexpensive for large quantity orders	Expensive for single part order
Large Material Variety		Fast turnover	Material Limitations	Large Material Variety	Limits of geometric complexity (mold still must be machined)
Many companies			Availability Issues		

Table 1: Manufacturing Method Comparison

Due to the complex geometry of the design, the most logical choice for manufacturing was rapid prototyping. However, there are several different methods for rapid prototyping that offer a set of advantages and disadvantages. The rapid prototyping comparison can be seen in Table 2.

Stereolithography (SLA)		Fused Deposition Modeling (FDM)		Selective Laser Sintering (SLS)		Electron Beam Melting (EBM)	
Adv.	Disadv.	Adv.	Disadv.	Adv.	Disadv.	Adv.	Disadv.
Most commonly used	Slower than other RP methods	Produces robust parts	Less accuracy than SLA	Material Variety	Less accuracy than SLA	Material variety (same as SLS)	Immature Technology
Accurate	Parts not as robust as other	Material variety	Secondary curing needed	Secondary curing unneeded	Porous parts	Non porous, homogenous, robust parts (titanium)	Expensive
	Secondary curing needed					Faster and more efficient than SLS	
	Support structure may be needed during production process		Support structure may be needed during production process			Accurate	

Table 2: Rapid Prototyping Method Comparison

After researching the methods of the rapid prototyping the search was narrowed down. For the purpose of the camoid laner, SLS is not appropriate because the part cannot be porous due to the moist environment and the part must be smooth. EBM is too expensive and a titanium part is unnecessary. This leaves SLA and FDM to choose from.

Stereolithography was the method of choice for several reasons:

- Adequate material strength

- Accuracy is needed on several sections of the camoid, especially a keyway
- Best price offer
- Best turnover time

See Appendix B for a full list of prices and companies that were considered.

6.4 - Actuation Design

The timing and geometry criteria must be strictly adhered to for the successful operation of this laner. Once this information is known, analysis can be conducted on the rotational velocity, accelerations, and torques required to achieve successful timing.

6.4.1 - Sizing a Servo

Accurate sizing of the servo is important because of the precision needed in this application. An undersized servo will not create the accelerations needed to reach operating velocity in the buffer angle given. An oversized servo is more difficult to tune and is more expensive to purchase and operate.

Allen-Bradley motors are Gallo's trusted motor company and currently offer free software¹¹ to aid in the sizing of A-B servo motors to fit specific applications. The Rockwell Motion Analyzer software is used to accurately size the servo to this camoid application.

The software accurately sizes a servo based on several input values including:

- Voltage Supply type and nominal value
- Velocity-Time cycle profile (timing diagram)
- Mechanism data
 - Inertia Values
 - Starting angle
- Transmission data
 - Type (belt, spur, etc.)
 - Ratio
 - Efficiency
 - Friction

Once these values are input, the software searches an internal database of the A-B servo product line and produces a range of motors that fit the criteria entered. Motor data accompanies the motor models including, but not limited to:

- Peak velocity
- Peak and RMS torque
- Current Draw
- Gearbox ratio
- Relative Cost (to motors in search results)
- Relative Performance (to motors in search results)

¹¹ Rockwell Automation. [Motion Analyzer Software](http://www.ab.com/motion/software/motion_analyzer.html). Retrieved February 11, 2007 from www.ab.com/motion/software/motion_analyzer.html

The motor list can be arranged according to the user's desire. The software also runs graphical torque analysis comparing the torque-speed diagram to the user required torque.

The software offers a detailed, motor model specific comparison allowing accuracy and confidence when attempting to size the servo to the application.

6.5.2 - Controlling the Servo

Along with camoid geometry, the control logic of the servo is the most important part of successful operation of the camoid laner mechanism. There are several pieces of hardware and software required to get from the control logic concept to the output motion of the servo. These elements are:

1. Control Logic Software
2. CPU Interface Module
3. Servo Driver
4. Servo

Together these elements make a closed loop information chain to create and adjust the servo motion exactly to specifications and real-time data feeds. These elements will be explained in greater detail in Chapter 7

It should be noted that the control logic is designed in specific software offered by Rockwell Automation. The logistics of the software and the programming protocol¹² will not be explained in this report as Gallo employs specifically trained engineers for servo controls. However, the servo actuation sequence will be explained and how it is directly related to the camoid geometry.

The specifications for the servo control program was written by the camoid design engineers as it is important to follow the correct criteria that Gallo demands for servo motion control. There are several safety issues concerning servo operation and must be included. For this reason, the actual servo control program writing was outsourced to David Booth of Gallo's Controls department.

6.5.2.1 - Assumptions

- The camoid must begin spinning such that the contour rises and remains rising between two bottles.
- The camoid must be accelerated to operating rotational speed as fast as possible.
- Operating speed is directly proportional to the line speed and is such that the camoid must complete its rotation cycle in the time that one bottle travels the camoid length.
- The cam must decelerate as fast as possible.

6.5.2.2 - Timing

1. From rest (0°) position spin to high dwell at operating speed
2. Remain at high dwell for a bottle count (10 bottles)

¹² Information regarding this program logic can be found at www.rockwellautomation.com/rockwellsoftware/design

3. Spin from high dwell to position 360° at operating speed
4. Remain at low dwell for a bottle count (10 bottles)

There are several aspects to keep in mind during this timing sequence:

- a) The servo needs time and distance (angular distance) to accelerate the camoid up to operating velocity
- b) The servo needs time and distance to decelerate the camoid from operating velocity
- c) The operating velocity is directly proportional to the line speed (which may change at any time)
- d) The amount of time the camoid remains in dwell is dependent on a number of bottles (which may be non-uniformly spaced)

Each of these aspects are worthy for investigation in this section to provide baseline understanding of the program details explained in the following chapters.

6.5.2.3 - Operating Velocity

As stated before, the successful operation of the camoid laner relies on the camoid being rotated at a constant velocity. The velocity at which it rotates is directly related to the line speed, as the contour must rise in between two bottles on the line. However, because the bottling line is subject to frequent shut downs and decreases in speed, the operating velocity of the camoid laner must be able to accommodate such instances.

In order to accomplish this task, the servo controller must always be 'aware' of the line speed. To do so, a shaft encoder attached to the conveyor line feeds line speed information to the servo controller. The operating rotational velocity of the camoid is directly related to the line speed by a mathematical function. Once input into the controller, the servo output velocity can be adjusted in real-time to accommodate the dynamic conditions of the bottling line.

6.5.2.4 - Servo Acceleration and Deceleration

The servo needs time and distance to accelerate and decelerate the camoid up to/down from the operating velocity. In order to accomplish this, both the geometry of the camoid and the timing of the actuation must be adjusted.

Allowing a buffer distance for the servo to accelerate and decelerate is a matter that concerns the camoid geometry. Recall that in order for successful diversion of the bottles, the camoid geometry must incorporate a continuous strip of contour running its entire length. Not only does this strip act to provide a continuous contour, but also provides the buffer distance for servo acceleration and deceleration.

The strip acts as a buffer because of the fact that the camoid neither rises or falls, i.e. there is no bottle diversion. This means that the camoid can rotate a certain angle amount, the buffer angle for explicative purposes, without a bottle being manipulated. This becomes necessary as the servo can use this buffer angle to accelerate and decelerate after it has completed its operating cycle.

Adjusting the timing to allow for servo acceleration and deceleration is a matter of starting the actuation somewhere within the buffer angle. The buffer angle will allow

the servo to accelerate up to the necessary operating velocity without any bottle manipulation.

6.5.2.5 - Torque

Based on the acceleration necessary and the geometry of the cam, the necessary torque to achieve the desired effects is calculated. The cam mass moment of inertia must be known for this calculation and is obtained using 3D modeling software due to the complex camoid geometry.

6.5.2.6 - Actuation Start and Dwell Times

The start of the actuation and the camoid dwell time are both matters that require reading bottle positions. The actuation must initiate between two bottles. The camoid must dwell for an amount of time that is dependent on the number of bottles that it diverts. In order to accomplish these tasks, the servo controller must be aware of the bottle positions and how many bottles have passed. To do so, a photoeye is placed on the line that reads when a bottle goes past it. Alone the photoeye is capable of counting bottles as they pass. When coupled with the shaft encoder, the two instruments are capable of knowing a bottle's position as it moves down the line. With this information input to the servo controller, the actuation information and dwell timing are able to be controlled.

6.5.3 - Stress Analysis

An important consideration in the camoid analysis is stress induced from the torque. Since the torque must be transmitted to the camoid, the method used will be a key and keyway. Several different stress analyses are conducted:

- Shaft Shear Stress
- Torsional Deflection
- Keyway Stress Concentration
- Safety Factors with different materials

6.5.4 - Fatigue Stress Analysis

The nature of the splitting operation is such that the camoid is subject to cyclic application of torque to accelerate and decelerate to and from operating velocity. Thus, it is important to conduct fatigue stress analysis. The fatigue strength of the shaft is calculated to ensure adequate lifetime.

6.6 - Part Gathering

An important part in this design process was finding the correct parts needed to build the prototype. A full bill of materials can be found in appendix C

6.7 - Chassis Design

The last step in the process is to design the frame, or chassis, that will house the system. There are several points of interest of the design that warrant discussion:

- Material

- General layout of components
- Implementation on bottling line
- Manufacturability

6.7.1 - Material

There are several criteria that the material must meet:

- It must not oxidize
- It must not be toxic
- It must be structurally sound

The most common structural materials used in Gallo’s bottling lines are steel, stainless steel and aluminum. Each material offers advantages and disadvantages which are shown in Table 3.

Steel		Stainless Steel		Aluminum	
Adv.	Disadv.	Adv.	Disadv.	Adv.	Disadv.
Inexpensive	Oxidizes	Resists Oxidation	Expensive	Resists Oxidation	Expensive
Strong	Requires Surface Finishing (paint)	Widely accepted for food handling	Availability Issues		Less Strength and Toughness (relative to steel)
Tough		Strong			
High Availability		Tough			

Table 3: Material Comparison

An important issue to keep in mind is that the chassis will be in a section of the bottling line in which there are open containers of product. The environment is wet from spilt product, line lubrication, and cleaning activities. It should be noted that Gallo requires all steel parts to be painted with a specific grade paint to resist oxidation of the steel and chipping.

6.7.2 - Component Layout

The layout of the components is important as it determines the overall size of the mechanism as well as the layout of the transmission for the camoid. The layout for the mechanism can be seen in Figure 27.

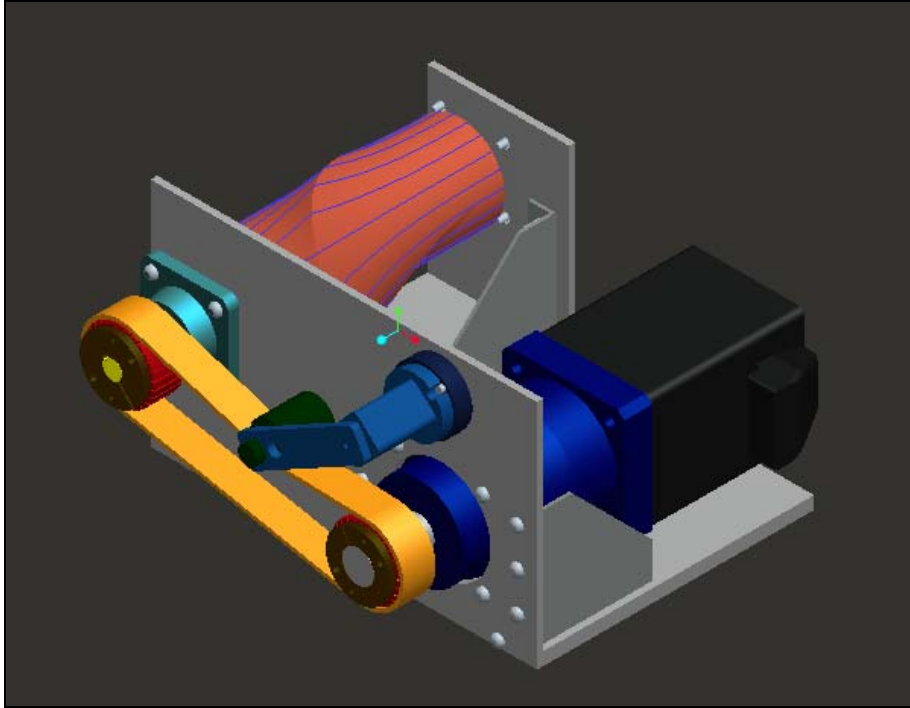


Figure 27: Component Layout

There are several ways to drive the camoid; one idea was to directly couple the camoid shaft with the servo shaft. However, the chosen layout is advantageous for several reasons:

- Minimizes overall length of the system
- Fits within the footprint of the Heuft Delta W 16 system
- Keeps motor away from conveyor line
- Allows easy motor access for maintenance/replacement

6.7.3 - Implementation on Line

The chassis design must be designed such that the implementation on the bottling line is accomplished easily. The nature of the design is such that it is a direct replacement of the Heuft system. It will utilize the same method for attachment that the Heuft currently uses. Figure 28 shows the current method by which the Heuft system is attached to the line. Notice that the entire system is independent from the line. It is simply bolted to the side of the conveyor on the front edge and supported in the back by a single leg. The camoid laner chassis will be designed to be implemented on the line in a similar fashion to the Heuft system. This implementation method is advantageous as it allows for easy initial installment and easy replacement if needed.

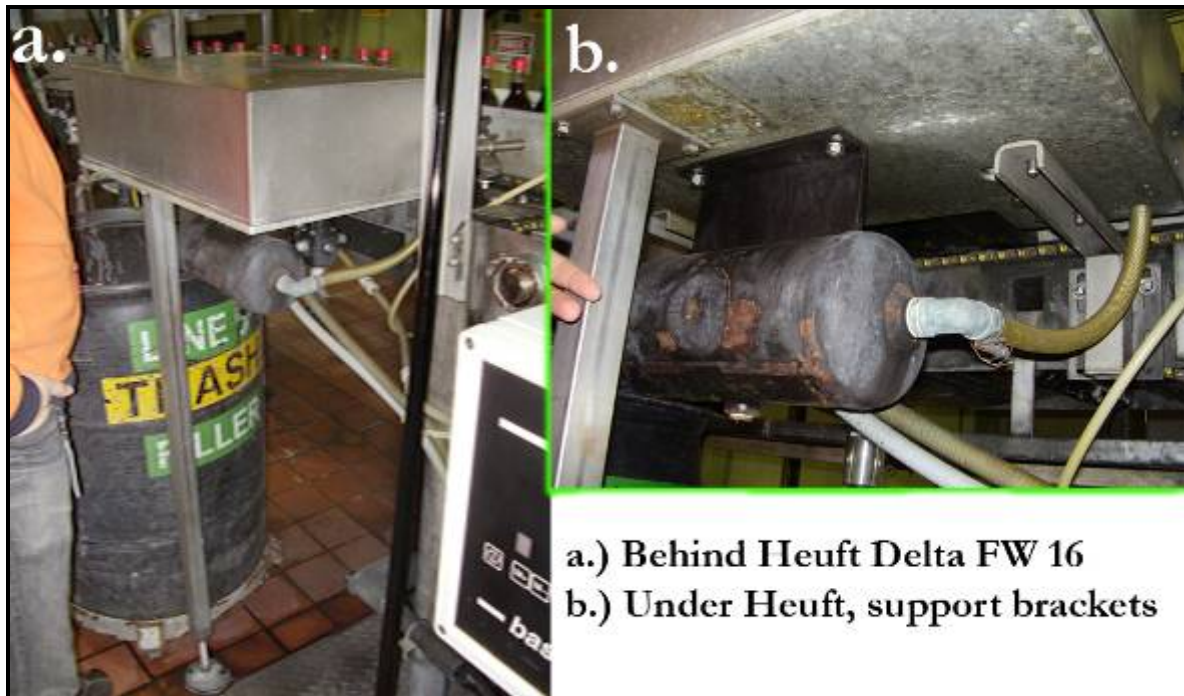


Figure 28: Heuft Attachment to Line

6.7.4 - Manufacturability

The chassis is a simple, easily manufactured design consisting of several plates fastened together with bolts and supported by several brackets (Figure 27). The most difficult part of the manufacturing process will be drilling the bearing mount holes to fit the tolerances needed for the shaft to spin freely. Fully tolerated technical drawings were provided to the machining company.

6.8 - Drive System

There are many different power transmission systems commercially available. In order to narrow down the options, the design of the drive system must be constrained. The power transmission from the servo to the camoid needs to be a robust system that meets several criteria:

- positive transmission
- low backlash
- low friction
- low inertia
- smooth/quiet operation

The easiest method for positive transmission with low backlash is to incorporate teeth into the transmission. Spur gears and chain drives were the first options explored, however either option could present problems and not meet the desired criteria.

The cam shaft and servo shaft are relatively far apart as the distance between must clear the high dwell of the camoid and the servo body. This distance would require two relatively large diameter spur gears, which would increase the inertia. Furthermore, the

spur gears could cause unwanted noise. A chain and sprocket drive could be used; however this could also cause unwanted noise and high inertias.

Gallo employs a large number of transmissions on the bottling lines to drive power from a motor to a conveyor. On newer lines, a specific type of toothed belt and sprocket system is used, similar to an automobile engine timing belt. After consulting Mr. Loel Peters, the benefits of this transmission became apparent; ability to handle high torques, offer low backlash and availability in Gallo's storeroom.

The Goodyear Eagle Pd Belt and sprockets incorporate a double herringbone tooth pattern which prevents both tangential and lateral belt slip (off the side of the sprocket). The system met all criteria set forth, provided immediate availability and was an economic solution. Furthermore, Gallo trusts the system enough to employ it elsewhere in the plant.

6.9 - Mechanism Assembly

The mechanism is fastened with hardware obtained from Gallo's storeroom. Once built, the mechanism was subject to an initial motion test at a simulated 600 bottles per minute for one hour to assure the mechanism was functional. During the test, observations were noted of any abnormalities such as:

- Immediate Wear
- Noise
- Heat due to friction
- Loose parts

Tests proved to be successful and no readjustment was necessary.

6.10 - Implementation

Implementation on the line is under the supervision of Jason Elliot of Aubry Construction Company. The line used to test the laner is a test loop previously installed by Gallo employees. The loop is open to allow for testing of new equipment.



Figure 29: Test Loop

The test loop rails were adjusted to our design specifications. The test loop includes all necessary hardware including photo eye and shaft encoder.

No housing for the electronics was constructed; therefore all electronics must be portable and temporary as Gallo safety rules do not allow uncontained electronics, especially those operating on 480V. The servo driving system was attached to a flat plate and carted to the test loop. It was removed immediately after the testing and never left unsupervised.

David Booth supervised the setup of the electronic systems assuring all safety guidelines are followed.

6.11 - Testing

Testing was conducted following a detailed test protocol found in Chapter 9.

Chapter 7.0 - Camoid Laner Detailed Design

The detailed process of the laner design is discussed in this chapter. All final values are either given or referred to in the appropriate appendix.

7.1 - Camoid Geometry Design

The camoid laner is based on the wrapping the Heuft Delta FW segment lengths and actuating time around a rotating axis. If each segment of the Heuft was represented by a cam, the segment's linear translation would be the cam's rise which would occur by rotating the cam. The series of the cams are attached to a common shaft with progressive rises that follow a contour similar to the Heuft segments. If the phase of each successive cam is shifted it is possible to cause the similar effect of laying the contour in front of the bottle that the Heuft accomplishes by sequentially firing the segments in front of the bottle. Finally, if the thickness of the cams approaches zero, the contour will be a smoothly blended surface.

In order to accomplish this task there are several elements of the geometry that must be designed simultaneously to offer the correct output motion, provided the actuator can be precisely controlled for angular displacement and angular velocity. In the following section the design of the geometry will be explained in detail.

Note that the design process was conducted in PTC ProEngineer Wildfire 2.0.

7.1.1 - Iterative Design

Arguably the most crucial aspect to the successful operation of high speed laning is the timing at which the diversion occurs; timing tolerances can be as tight as several milliseconds. In the case of the Heuft laner, the independent linear pneumatic actuators are fired in sequence governed by the line speed. In the case of the camoid, the timing is based not only on the line speed, but also the rotational actuation and geometry. Since the timing is directly related to the geometry, careful analysis is conducted to assure that the cam behaves properly. This design process is iterative and occurs simultaneously with the rotational timing design (explained in the next section). The elements of the geometry that are manipulated for the design process are:

- Diverting Contour
- Cam Phase Angles
- High Dwell Angle Displacement
- Low Dwell Angle Displacement
- Buffer Angle
- Base Circle Radius
- Overall Length of Laner

These elements are represented below by Figure 30, but will also be individually represented in the following sections.

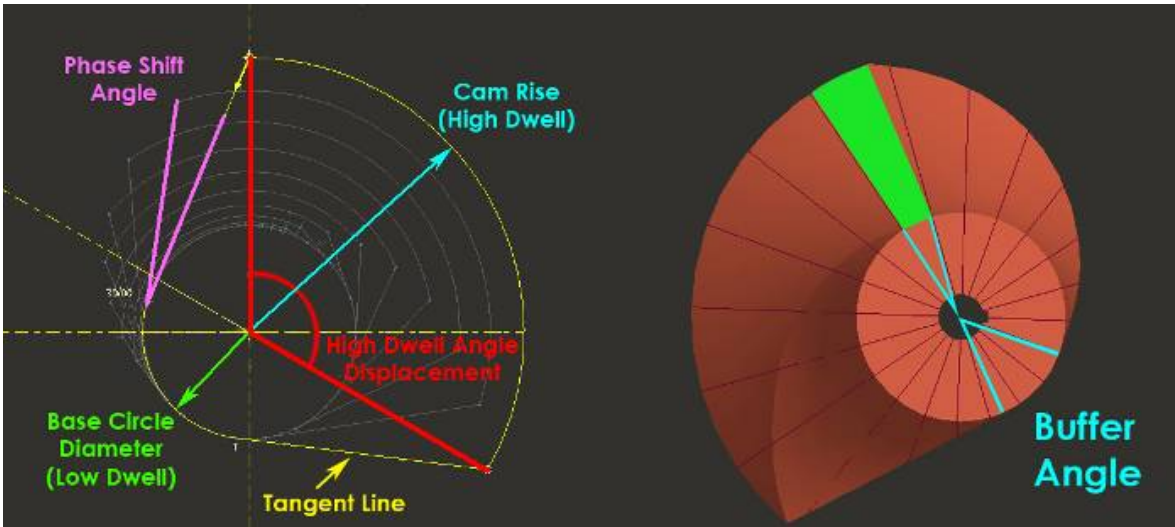


Figure 30: Geometric Elements

Each of these elements is manipulated and affects different aspects of the timing and bottle diversion.

7.1.1.1 - Diverting Contour

The diverting contour is defined by the successive rises of each cam segment. This is the contour by which the bottles are guided. Each cam segment's rise is governed by the cam programs explained in the previous section.

7.1.1.2 - Cam Phase Angles

The cam phase angle is the angle that each cam is offset relative to the previous cam. This controls the rate at which the contour is laid out in addition to rotational velocity. This also affects the value of rotational speed. If the phase angles are larger, the contour will take longer to be laid out, thus requiring a faster rotational velocity.

7.1.1.3 - High Dwell Angular Displacement

The high dwell angular displacement is the angle of each segment over which the high dwell spans. A crucial design criterion for the camoid is that when the *camoid* is fully extended, every segment of the camoid must be in high dwell. Recall from Chapter 3 that this is the contour strip. If the phase angles are larger, and high dwell angular displacement is kept the same, the strip gets thinner until it no longer exists, creating discontinuity in the contour. The high dwell angular displacement is manipulated such that the strip is kept wide enough to properly guide a bottle during camoid dwell.

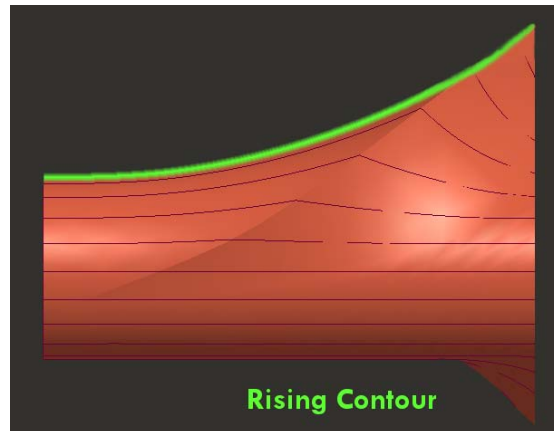


Figure 31: Diverting Contour

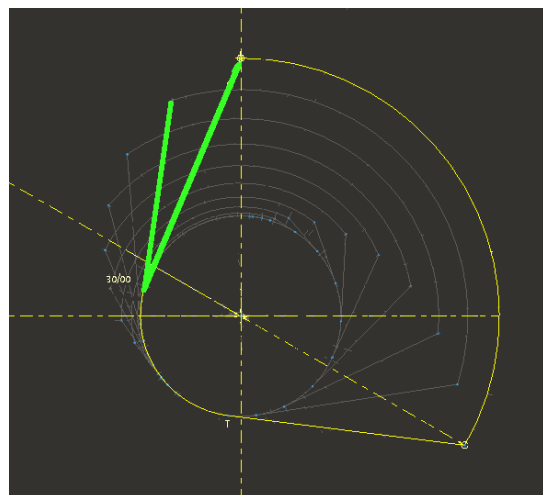


Figure 32: Phase Shift Angle

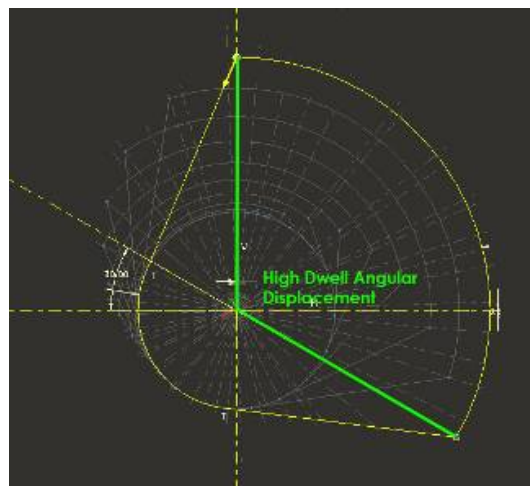


Figure 33: High Dwell Angular Displacement

7.1.1.4 - Low Dwell Angular Displacement

The low dwell angular displacement is similar to the high dwell, except with the low dwell of the segments. When the camoid is fully retracted, the cam segments must be in low dwell. This creates a strip of low dwell flat contour parallel to the camoid's axis of rotation. This value is not manipulated but rather serves as a limit to the value of the high dwell angular displacement.

As high dwell angular displacement increases, low dwell angular displacement decreases. Care is taken to assure that the high dwell angle is small enough to allow adequate low dwell angular displacement.

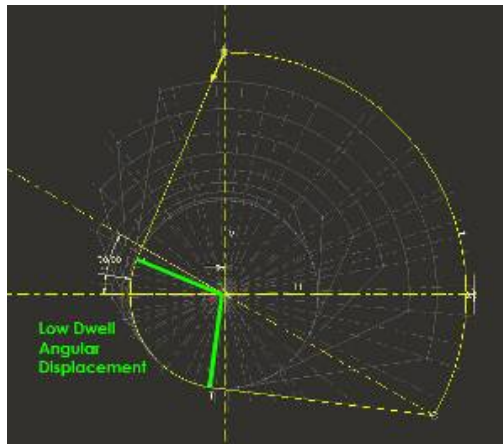


Figure 34: Low Dwell Angular Displacement

7.1.1.5 - Buffer Angle

The buffer angle is directly related to the thickness of the contour strip, it is the angle of rotation over which the strip occupies. Because there are two contour strips, there are two buffer angles. The buffer angle at the high dwell is directly a function of the cam phase angles and the high dwell angular displacement. The buffer angle at the low dwell is a function of cam phase angles, high dwell angular displacement *and* high dwell buffer angle. This is because the low dwell angular displacement is dependent on the high dwell angular displacement.

Care is taken to assure the buffer angle is adequate both for high and low dwell. If the buffer angle is too small, the acceleration needed will be high and require a significant amount of torque, increasing motor size and thus expense.

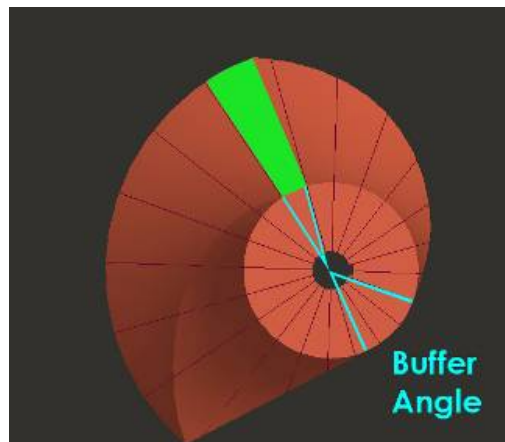


Figure 35: Buffer Angle

7.1.1.6 - Base Circle Radius

The base circle radius affects the width of the low dwell strip. If the base circle is too small, the tangent line of the highest cam segment approaches the tangent line of the lowest dwell segment, effectively eliminating the low dwell. If the base circle is too large, the cam will be too large to fit on the bottling line. Furthermore, if the base circle is too large, the contact point (strip)

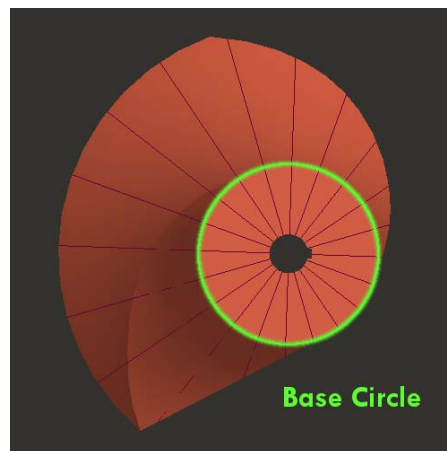


Figure 36: Base Circle

will be too high on the bottle inducing a potentially high tipping force. Lastly, if the base circle is too large, the part will be excessively massive and require higher torques to accelerate.

7.1.1.7 - Length of Camoid

The length of the camoid affects the acceleration and thus force caused by the contour. If the camoid is too short, the working contour will rise abruptly, potentially causing high accelerations and forces. If the camoid is too long, the operating rotational velocity must increase to successfully lay the contour between two streaming bottles. This increase causes rotational accelerations to increase, thus increasing the required torque. With increased torque, motor size and expense increase as well as stress and fatigue on the system.

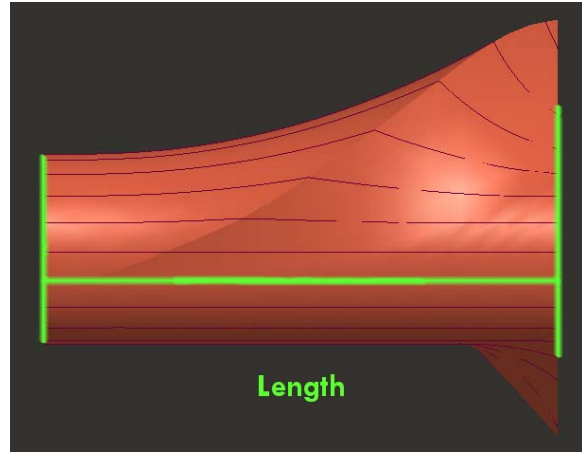


Figure 37: Camoid Length

7.1.2 - Geometry Final Values

The final values of the geometric elements are shown in Table 4. It should be noted that the geometry of the camoid is a smooth blended surface; however it is broken into 11 cross sections for purposes of discussion and computer modeling.

Section Number	Contour Rise (in.)	Phase Shift (deg)	High Dwell Angle (deg)	High Dwell Buffer Angle (deg)	Low Dwell Buffer Angle (deg)	Base Circle Radius (in.)	Camoid Length (in.)
1	0.001	0	145	7.5	32.8	1.75	9.5
2	0.006856	12	140				
3	0.052	12	135				
4	0.159	12	130				
5	0.333	12	130				
6	0.574	14	130				
7	0.883	14	130				
8	1.259	14	130				
9	1.703	15	130				
10	2.21	17.5	125				
11	2.758	17.5	120				

Table 4: Camoid Geometry Final Values

7.1.3 - Geometry Construction

Because of the complexity of the geometry, it is not feasible to machine the part using conventional cutting techniques such as CNC milling or lathe machines. The part is constructed using a Stereo Lithography (SLA) rapid prototyping machine. After research it was apparent that the process offered satisfactory tolerances and material strength. Outsourcing the part for manufacture is a matter of emailing the correct format of the model to the company.

7.2 - Camoid Prototype

Figure 38 is a picture of the comparison of the CAD model and the actual rapid prototyped part.



Figure 38: Model vs. Rapid prototype

7.3 - Actuation Design

The servo system must provide accurate and precise actuation of the camoid through millions of cycles. Attention to detail is important in the design of the servo system. This detail is explained in this section.

7.3.1 - Servo Sizing

The servo is sized using Motion Analyzer software from Rockwell Automation. For detailed tables conveying the values used for the motor sizing for this application see Appendix D.

7.3.2 - Servo System

The servo system is set up to allow for completely automated control of the actuation of the camoid based on line speed and bottle spacing. The system can adjust for varying line speeds that are experienced during line start up and shut down. It can remain in one position for extended periods of time. In order to provide the automated control, there are several important components of the servo control system that warrant discussion.

- Servo Motor
- Driver
- CPU Motion Control Module
- Control Program Logic

The basic setup for the servo control system is shown in Figure 39. The system is adaptable allowing data inputs from a variety of different tools and also can be controlled remotely via Ethernet. Furthermore, the system can be configured to control multiple axes (servos) with a variety of different program profiles. The following explanation outlines one particular setup. Note that this system meets Gallo's standards and operates on 480V 3 Phase AC electrical.

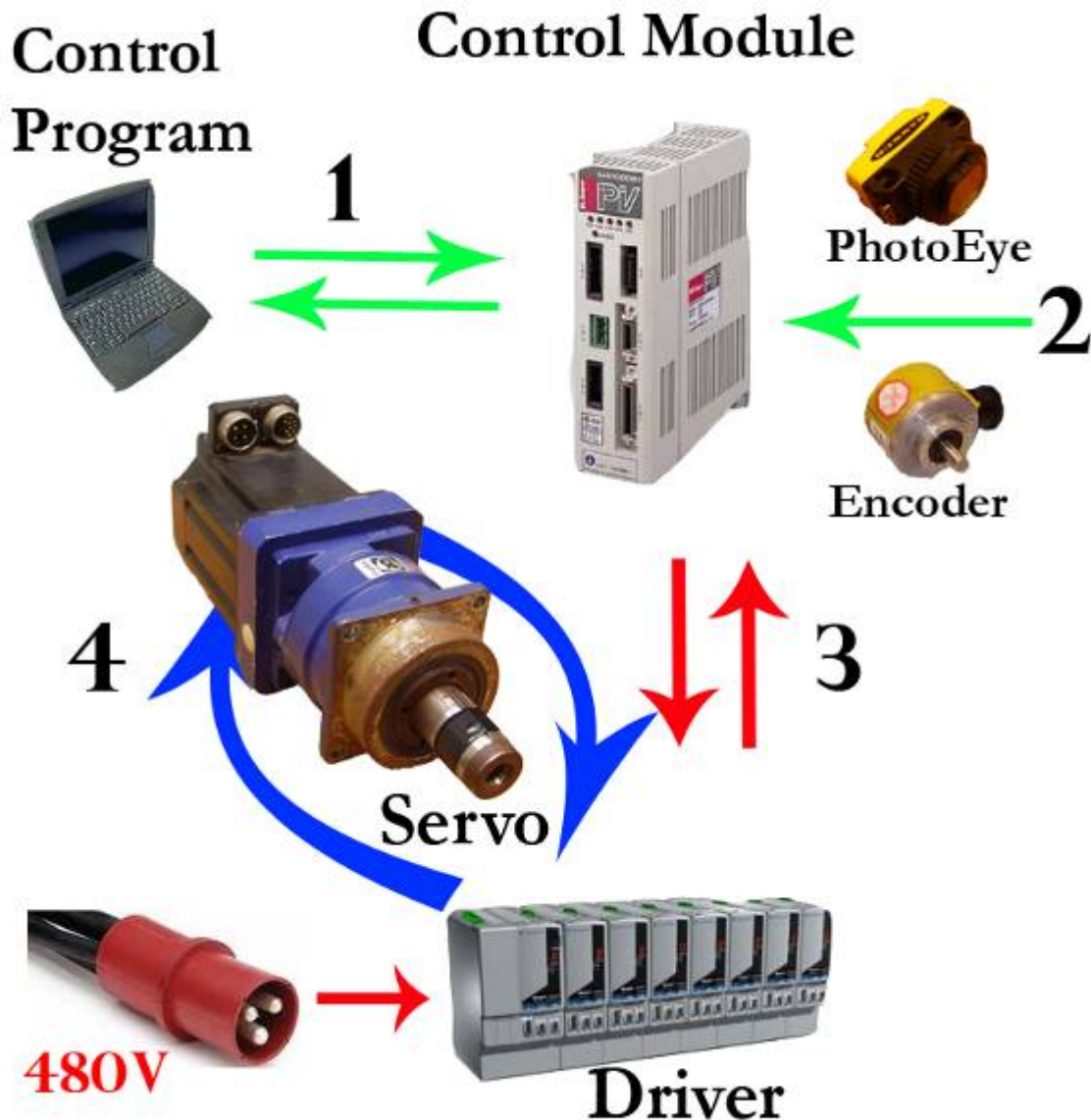


Figure 39: Servo Control Schematic

The following is a step-by-step explanation of the schematic shown in Figure 39. Each of the numbers indicates the part of the control information transfer shown in the figure. Note that there is a continuous loop of information and communication does not necessarily always occur in this sequence explained.

1. Control program software uploads control information to a CPU control module. In this case the program is made with Logix 5000 software. The module simultaneously feeds back information to the computer.
2. In addition to program logic from the software, information from sensors can be input into the control module. In this case, a photoeye and shaft encoder will be used to transmit bottle position and velocity to the module. It should be noted that the control program must have the proper protocol for reading and interpreting the data from these sensors. With this input data, the program can make adjustments that answer to real-time dynamic variations in servo loading and/or timing demands.
3. The CPU control interface interprets the information of the Logix 5000 software and outputs a signal to the driver. The driver simultaneously feeds back information to the module regarding servo statistics.
4. The driver interprets the information from the CPU module and adjusts the output current to the servo motor. The servo's internal encoder feeds back information to the driver regarding position and velocity.

7.3.2.1 - Servo Motor

The servo motor was obtained from Gallo's spare parts shelves along with the necessary power and feedback cables. The servo motor from Gallo falls in the range of applicable motors from the Motion Analyzer software. The motor included an attached gearbox. Table 5 below is a basic overview of the motor and gearbox specifications. For more detailed specifications see Appendix E.



Figure 40: Servo Motor

Manufacturer	Allen-Bradley
Model	MPL – B4520 – MJ22AA
Max Speed	5000 rpm
Continuous Stall Torque	6.1 N-m / 54 in.-lbs.
Power	2.5 kW
Gearbox Manufacturer	Alpha
Gearbox Ratio	10:1

Table 5: Servo Motor and Gearbox Overview Specs

The servo motor includes an input and feedback cable connection. The power to the servo is delivered by the driver. Inside the servo is an encoder that reads and outputs the position of the servo through the feedback cable. The feedback is read by the driver and the power is adjusted to deliver the necessary power to follow user input controls.

7.3.2.2 - Driver

The driver was obtained from Gallo’s control department from a decommissioned servo driven project. The purpose of the driver is to interpret the control logic from the computer and provide the correct electrical current to move the servo motor in the exact manner specified by the computer control logic. The input signal can be either analog or digital depending on the level of control demanded by the user. Analog is adequate for systems with a few axes (less than 6). However, for more complicated systems, digital interfacing is often used to reduce the number of connecting wires needed. Digital systems, however, are significantly more expensive.

Manufacturer	Rockwell Automation
Model	2098-DSD-HV150
Operating Voltage	480V AC 3 Phase
Peak Current (amps)	68
Continuous Current (amps)	34
Continuous Power (kW)	15

Table 6: Driver Overview Specs

7.3.2.3 - CPU Control Module

The CPU interface module is the component that interprets the control logic from the computer software and outputs a readable signal to the driver. The input connection is obtained via Ethernet cable. This connection is extremely versatile enabling remote control changes over the internet. This is beneficial as it becomes possible for the control engineer to manipulate servo controls from any location that enables internet access. The modules used for this system were also obtained from Gallo’s storehouse.

7.3.2.4 - Control Program Logic

The human interface of the servo control is the Logix 5000 software, which can be run on any PC with an Ethernet port (for data transfer). This software allows for the ultimate control of the servo motor. Details such as timing, position, velocity, acceleration, acceleration profiles and torque can all be controlled with fine precision. In

addition to servo controls, any number of safety and system check protocols can be input into the system. For example, the servo can be told to reset itself to zero after a given number of cycles to maintain system accuracy.

7.3.3 - Control Logic Concept

As stated before, the logistics behind creating the control program will not be discussed in this report; however, a motion control outline is described below. There is a detailed set of constraints and assumptions and a timing diagram.

7.3.3.1 - Assumptions

1. The actuation for contour rise must begin between bottles and be at full operational velocity
 - a. The actuator is given a buffer angle, on the cam segments low dwell, in which acceleration can occur.
2. The contour rise must occur at a rate such that it remains between bottles.
3. The actuation must stop and hold within the angle of the aforementioned high contour strip.
4. The actuator must be held at this position for a data input number of bottles.
5. The actuation for contour fall must begin between bottles and be at full operational velocity.
 - a. The actuator is given a buffer angle, on the aforementioned high dwell strip.
6. The contour fall must occur at a rate such that it remains between bottles.
7. The actuation must stop and hold within the aforementioned low dwell contour strip.

These timing criteria are the baselines that must be followed for the successful operation of the camoid laner.

7.3.4 - Drive Train Specs

- Final drive ratio 10:1

7.3.5 - Timing

1. From rest (0°) position spin 164° at operating speed
2. Remain at high dwell for a bottle count (10 bottles)
3. Spin from 164° to position 360° at operating speed
4. Remain at low dwell for a bottle count (10 bottles)

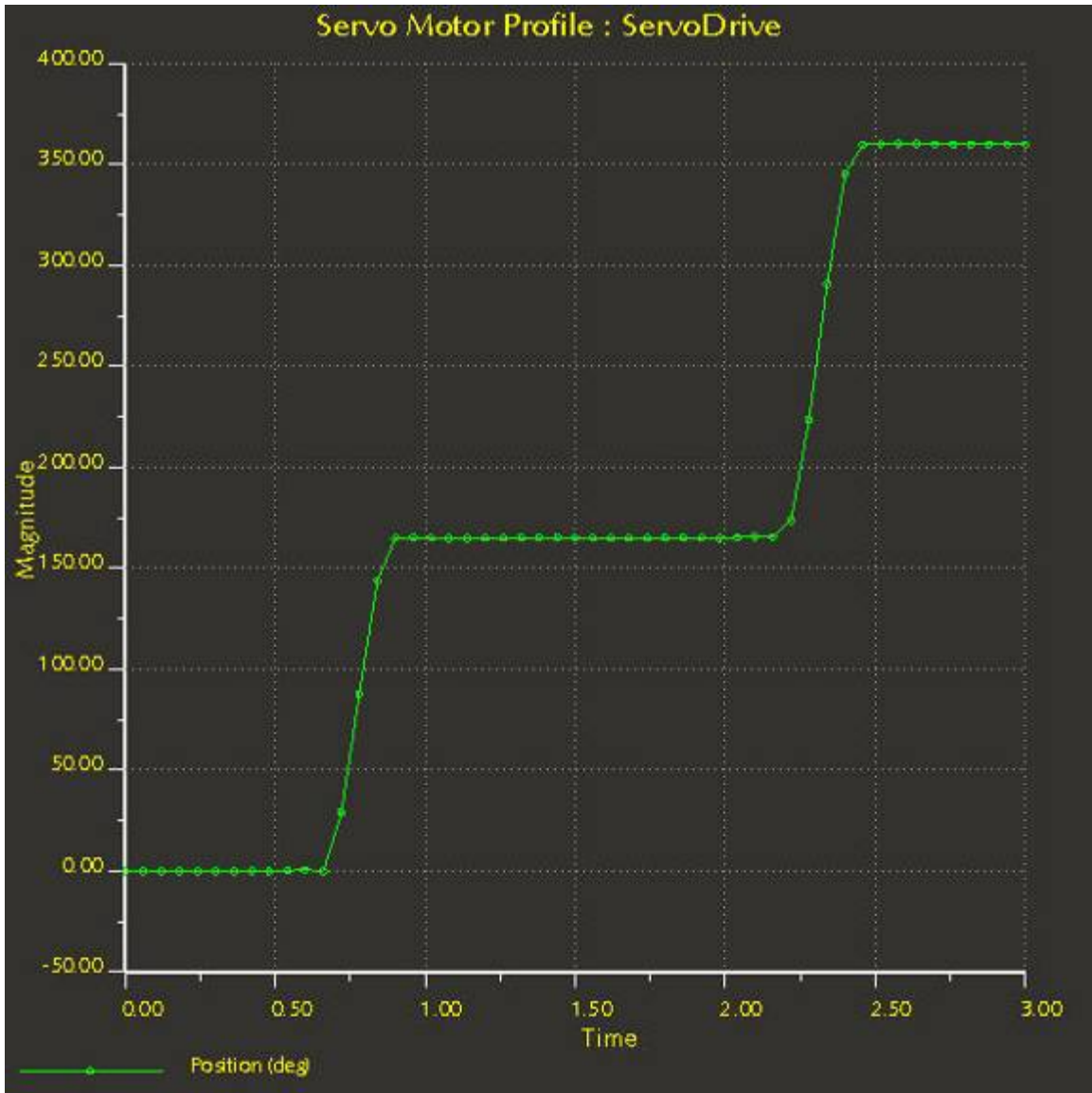


Figure 41: Timing Diagram Example

Because the timing of the motor is constantly adjusted to match the line speed, this timing diagram represents an example of the timing at a particular line speed. There are several important characteristics of the timing diagram that should be noted.

1. The x axis is time in seconds, the y axis is the angular position
2. This diagram represents a full cycle of the camoid laner. A full cycle includes:
 - a. Low camoid dwell, no bottles diverted
 - b. Camoid spins such that the contour rises
 - c. High camoid dwell, all bottles diverted
 - d. Camoid spins such that contour falls
3. The horizontal sections of the curve represent the camoid rotation in a dwell period.

4. The sloped line represents the camoid during it spin
 - a. The constant sloped section represents operating velocity
 - b. Notice the acceleration¹³ up to operating velocity which occurs between the horizontal and sloped linear segments.

The actual dwell and spin times are functions of the line speed and change according to the inputs from the shaft encoder and photoeye.

¹³ In the actual timing diagram, the angle over which this acceleration occurs will be the same magnitude of the buffer angle. This timing diagram is a basic theoretical representation.

7.4 - Motion Analysis

When the actuation design is finished, the camoid will behave as shown in Figure 42.

7.4.1 - Cam Extension

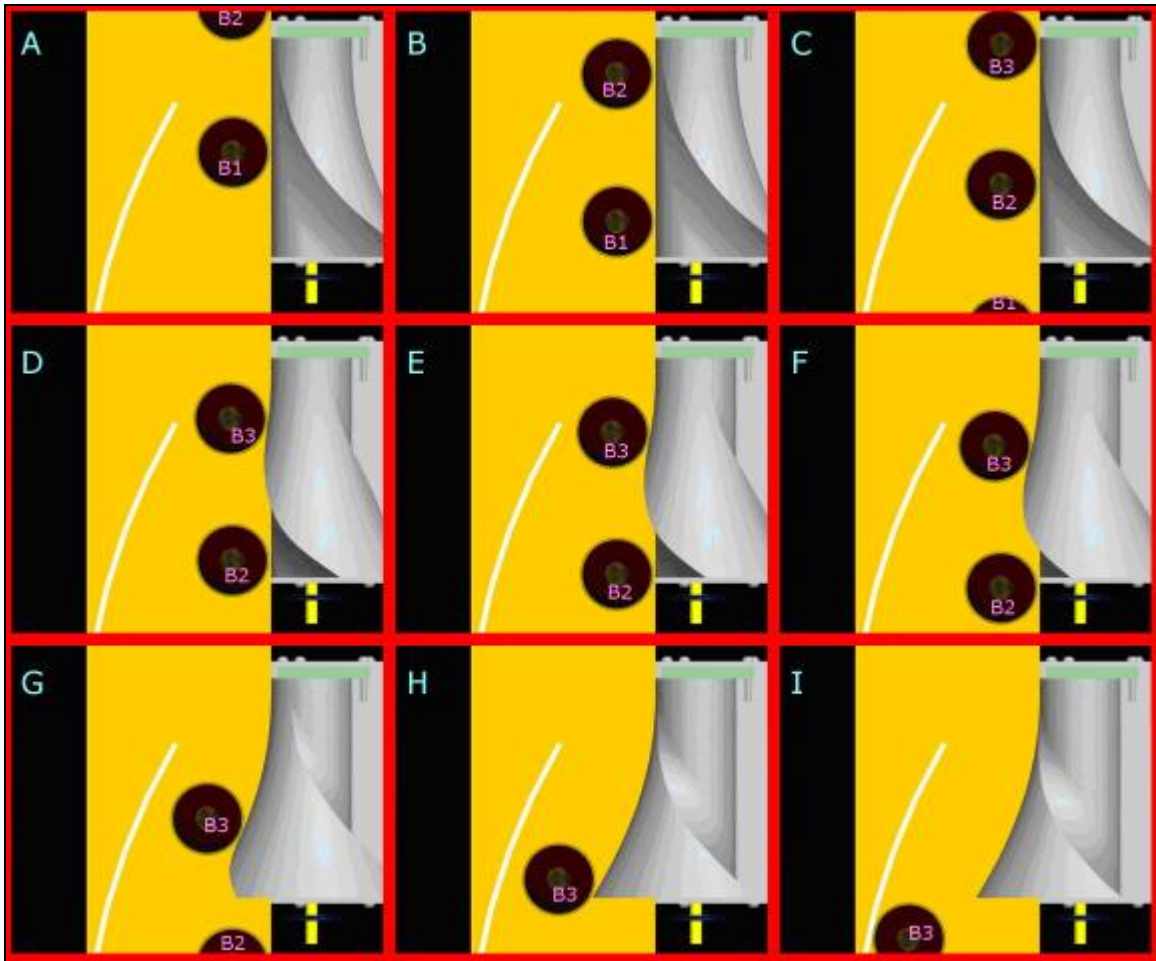


Figure 42: Top View of Cam Extension

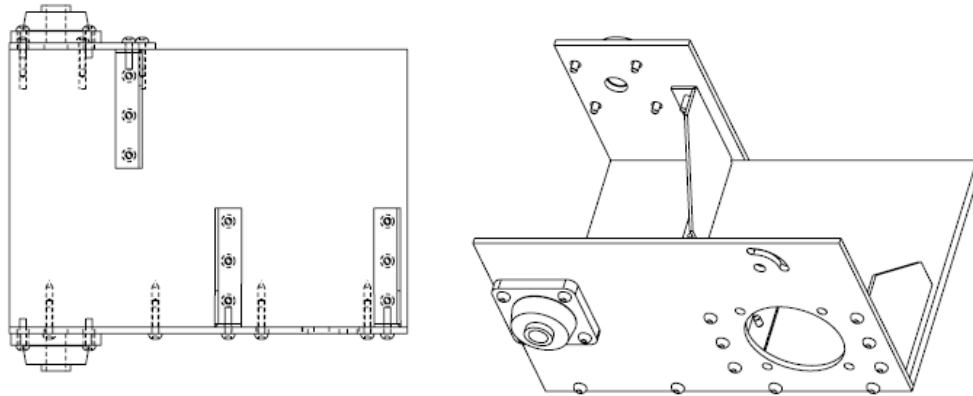
- A. Bottle 1 passes by the splitter. Bottle 2 approaches.
- B. Both Bottle 1 and Bottle 2 are passing the splitter.
- C. Bottle 1 continues to Lane 1. Bottle 2 is still in contact with the Low Dwell of the cam. Bottle 3 enters the beginning of the splitter.
- D-F. The cam rotates, with Bottle 3 riding the High Dwell while Bottle 2 is riding the Low Dwell simultaneously.
- G. Bottle 2 continues to Lane 1. Bottle 3 is riding the High Dwell of the cam.
- H-I. Bottle 3 continues to Lane 2.

7.5 - Chassis Design Details

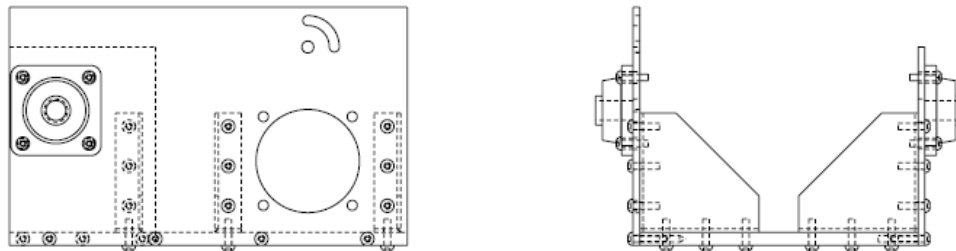
There are specific points of interest that are important to discuss regarding the design of the chassis:

- Material Choice
- Layout
- Tolerances
- Fasteners
- Bearings

The chassis was outsourced for manufacture to Billington Steel as per recommendation by Jim Bellins in Gallo's machine shop. Fully dimensioned technical drawings can be found in Appendix F.



SEE SHEET 2 FOR ASSEMBLY NOTES



Drawn By: James Saunders	February 13, 2007	Part Name: Model Assembly
Tol: 0.01 Unless Noted	Sheet 1 of 2	W.D. #: 600419 W.

Figure 43: Chassis Assembly View

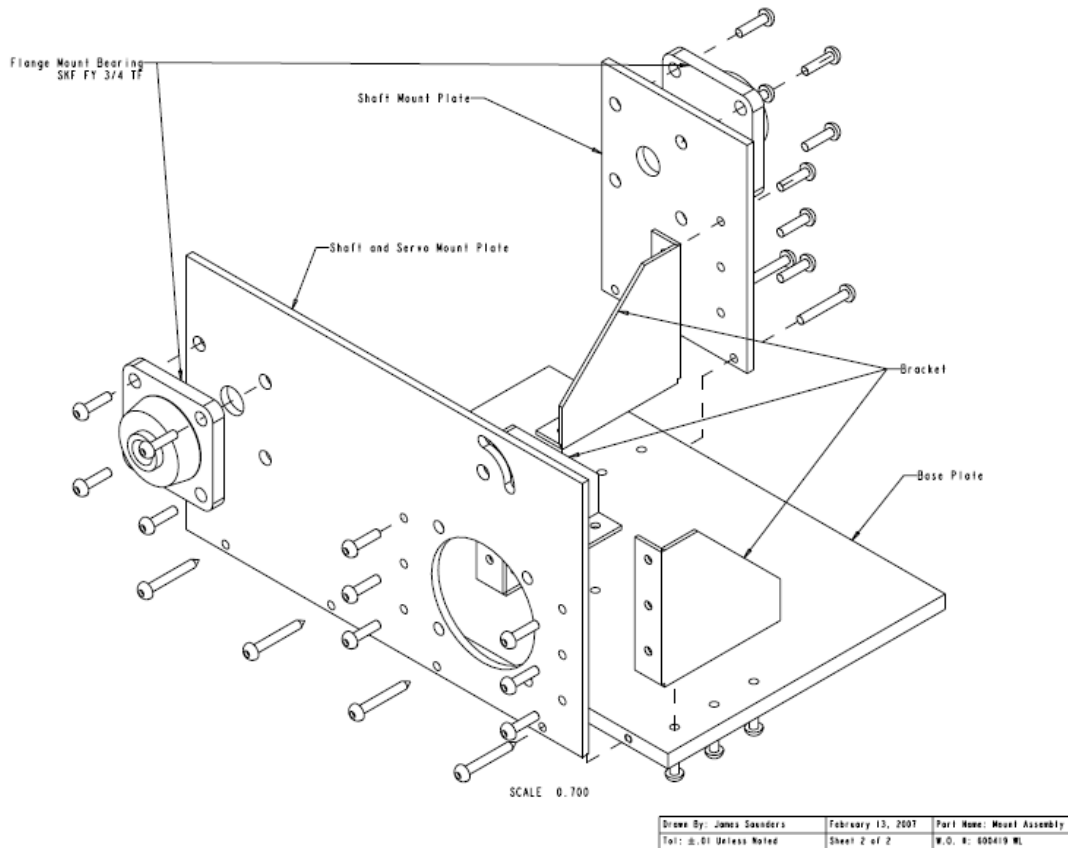


Figure 44: Chassis Exploded View

7.5.1 - Material Choice

The material used in the chassis design is stainless steel plate. The choice follows recommendation from Loel Peters because of the following reasons:

- Provides the strength to support torque and heavy components
- Resists oxidation in moist environments
- Doesn't require any surface finishing
- Widely used on Gallo's bottling lines
- Aesthetically pleasing

Referring to Figure 44, the material thicknesses chosen are as follows:

- Base Plate – 1/2"
- Shaft and Shaft and Servo Mount Plate – 1/4"
- Brackets – 1/8"

The half inch plate will allow for 1/4" tapped holes in the side of the plate for fastening the other plates perpendicularly.

7.5.2 - Layout

The layout of the chassis is designed to minimize the footprint of the system such that it fits within the Heuft's footprint. In order to accomplish this, the servo must be

mounted next to the camoid, as opposed to inline. There are several key points that must be kept in mind during the layout design process. Key layout design points are:

- Servo and cam axis are parallel and offset enough distance to allow clearance during camoid rotation
- The axis offset is such that a nominal size belt can be used for power transmission
- There are mounting holes for a belt tensioner
- The camshaft axis places the camoid low dwell at the conveyor edge
- The camshaft axis places the camoid high enough to clear the bottom of the chassis
- The camshaft axis places the camoid at the correct height for bottle contact
- The chassis can accommodate mounting hardware for implementation on the line
- The chassis can accommodate safety shields over drive transmission

7.5.3 - Tolerances

Because of the spinning camoid shaft and the belt drive transmission, there are several dimensions that must be carefully toleranced to assure smooth operation. The most important dimensions are shown in Table 7 and by Figure 45. The table and figure are color coded for explanation.

	Dimensions	Reason
A	Bearing mount bolt pattern position on both servo and shaft plates	Camshaft alignment
A	Camshaft through holes on servo and shaft plates	Camshaft alignment
B	Servo and shaft plate fastener holes	Camshaft alignment
C	Bearing mount bolt pattern position and servo bolt pattern position	Transmission belt tension
C	Servo through hole position	Transmission belt tension

Table 7: Tolerance Reasons

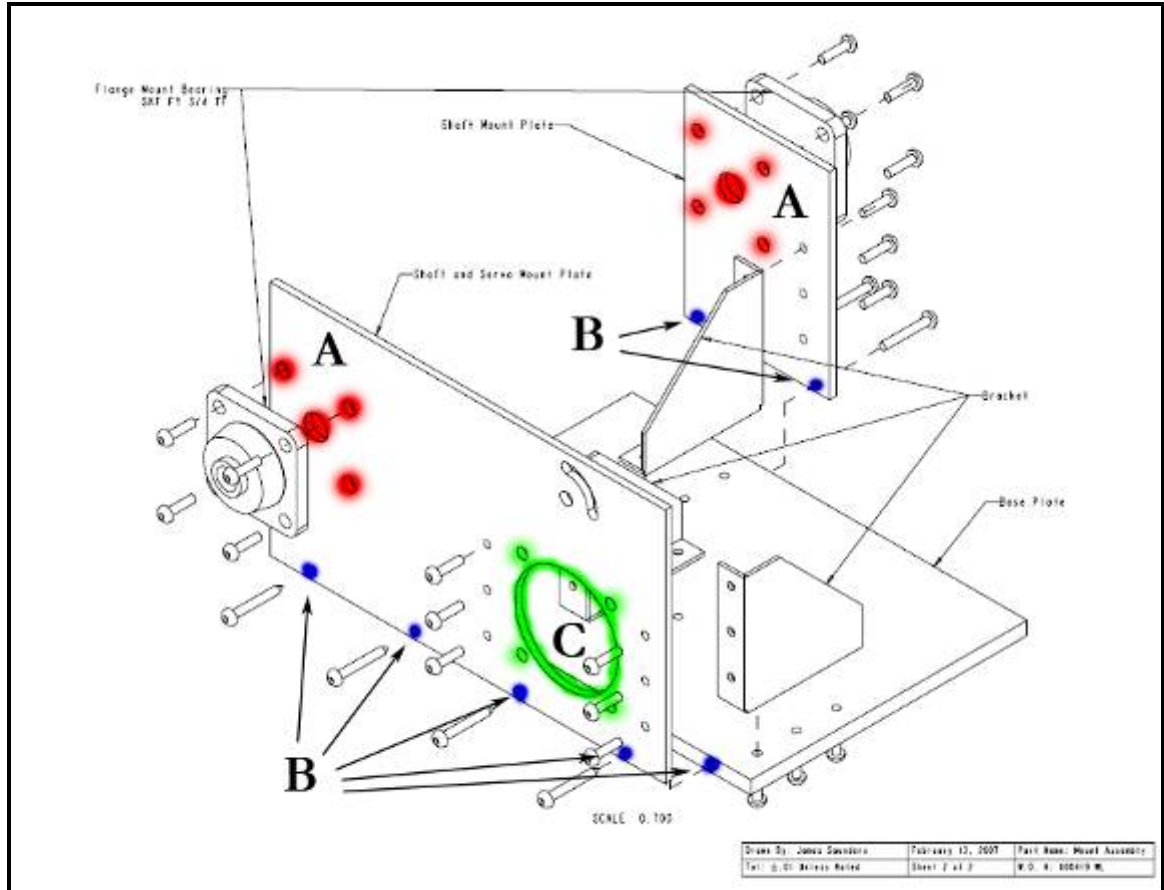


Figure 45: Important Toleranced Dimensions

For actual tolerance values, consult the drawings in Appendix G.

7.5.4 - Fasteners

All plates are fastened together using either 1/4 -20 or 3/8- 16 bolts (see appendix G for bolt types and locations) and locking nuts where nuts are needed. Bolts were chosen over welding as welding could cause unwanted warping of the plates from the heat.

7.5.5 - Bearings

The bearings chosen to use are SKF FY 3/4 TF 4 Bolt Flange Mount Bearings and were purchased from the Gallo storeroom. These are the standard flange mount bearings that Gallo uses and supplies for this specific shaft size.

7.6 - Drive Design Details

The drive transmission chosen is manufactured by Goodyear¹⁴. The system components were readily available in Gallo's part storeroom. See Appendix H for

¹⁴ Refer to Appendix H - Goodyear Eagle Pd Power Transmission for a complete list of Goodyear Eagle Pd power transmission products

complete details on the Goodyear product used. The basic specifications of the belt and sprockets can be seen in Table 8 and Table 9 respectively.



Figure 46: Goodyear Eagle Pd Power Transmission

Manufacturer	Goodyear
Model	Eagle Pd W-720
Length	720mm
Width	32mm
Pitch	8mm

Table 8: Belt Used

Manufacturer	Goodyear
Model	Eagle Pd W-28S-H
No. of Teeth	28
Hub Type	Keyed Quick Disconnect (QD)
Pitch	8mm
Width	33mm

Table 9: Sprockets Used

There were several criteria that outlined the decision to use the Goodyear products:

- Recommendation
- Claimed benefits of the system
- Chassis layout
- Drive ratio
- Availability
- Belt Tensioner

7.6.1 - Recommendation

The Goodyear products were chosen following the recommendation of Loel Peters and Mike Delikowski.

7.6.2 - Claimed Benefits

The company claimed benefits from the website¹⁵:

- Consistent Dimensional Stability
- Low Pre-tension
- Low Noise
- High Abrasion Resistance
- Low Maintenance
- High Flexibility
- High Precision Linear Positioning

Each of these benefits fit the needs of the camoid laner.

7.6.3 - Chassis Layout

The sprocket size was chosen for several reasons:

- a) The sprocket attached to the camoid shaft needed to be small enough such that it would not overhang past the chassis and interfere with bottles on the line, i.e. not be larger than the base circle diameter of the camoid.
- b) Smaller sprockets have smaller inertias.
- c) Smaller sprockets will need a smaller belt length

7.6.4 - Drive Ratio

The drive ratio for the transmission was chosen to be 1:1. The servo already incorporates a satisfactory gearbox ratio of 10:1 and there is no need to adjust beyond that. Furthermore, the parts list is simplified by using two of the same sprockets.

7.6.5 - Availability

The final criterion governing our choice for the drive transmission was the immediate availability of most of the components in the Gallo storeroom.

7.6.6 - Belt Tensioner

In order to provide adequate tension and allow for easy initial installation, a belt tensioner is to be attached to the chassis. Gallo currently uses Eagle Pd power transmissions that are tensioned with a commercial tensioner arm available in the Gallo storeroom. The tensioner is a Lovejoy SE-18 ROSTA Tensioner. It will provide a force on the outside (smooth side) of the belt and thus requires the Lovejoy R-15/18 Roller Idler-SE15/18, which is a non-toothed idler wheel. The orientation of the tensioner can be seen in Figure 48: Full CAD Assembly

¹⁵ Goodyear Industrial. [Eagle Pd Industrial Power Transmissions](http://www.goodyearindustrialproducts.com/powertransmission/products/pdf/eagle_pd_belt.pdf). Retrieved February 10, 2007, from http://www.goodyearindustrialproducts.com/powertransmission/products/pdf/eagle_pd_belt.pdf.



Figure 47: Lovejoy Belt Tensioner with smooth idler pulley

7.7 - Full Assembly

The full assembly is shown below with all components discussed in this chapter in the proper locations.

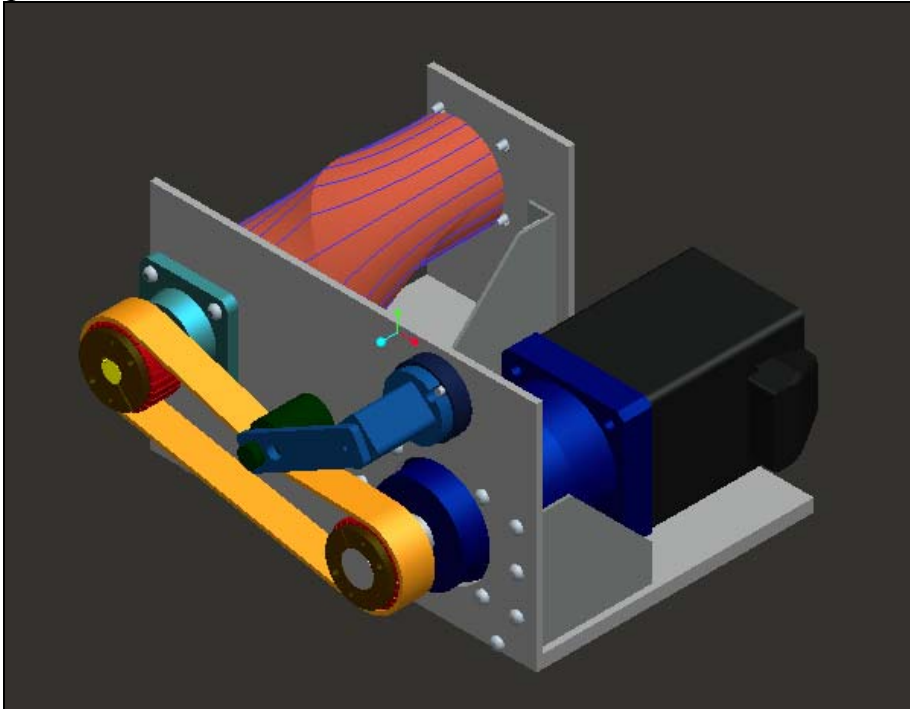


Figure 48: Full CAD Assembly

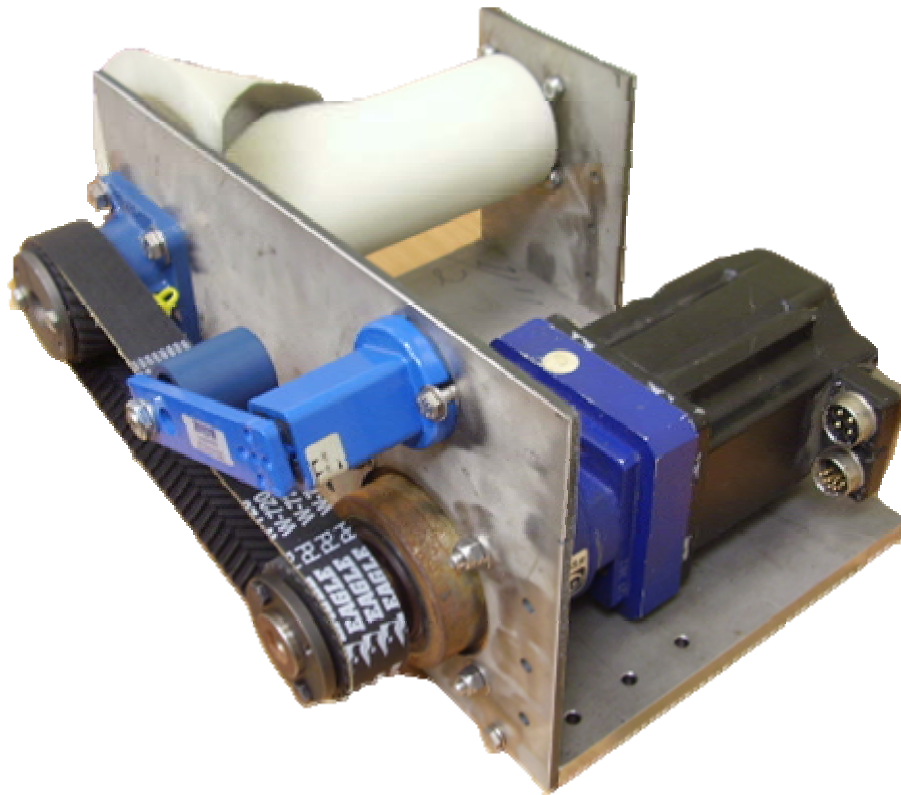


Figure 49: Full Assembly

7.8 - Mechanism Assembly

Several important aspects about mechanism assembly must be noted to assure proper function of the mechanism:

- Camoid position on shaft
- Camoid shaft trueness
- Servo installation
- Sprocket position of camoid and servo shaft
- Belt tensioning

7.8.1 - Camoid Position on Shaft

The edge of the larger side of the camoid should line up directly with the end of the keyway. Shaft collars should be tightened against the camoid to prevent translation along the camoid axis.

7.8.2 - Camoid Shaft Alignment

It is important for the camoid shaft to have a true fit on the bearings, i.e. the bearings should share the same axis. It is possible to adjust this during the installation. Because there are tolerances on the bearing mount bolt pattern in the plate, we do not tightened the bearing bolts until the shaft is installed and trued.

7.8.3 - Servo Installation

It must be assured that the servo mounting bolts are sufficiently tightened as the servo hangs unsupported from the mounting flange.

7.8.4 - Sprocket Position

The sprockets must be positioned simultaneously on the camoid and servo shaft to ensure the belt is centered on each sprocket, especially as the belt is specifically designed to guard against sprocket wander. The sprockets are directional; make sure both sprockets are oriented correctly to accommodate the belt.

7.8.5 - Belt Tensioning

The Lovejoy tensioner must be tensioned in a specific manner. See Figure 50 for visualization.

1. A large wrench is used to apply torque to the square body into the belt
2. The angle of the arm relative to the body must read 20 degrees based on manufacturers specifications
3. The mounting bolt is tightened
4. The safety bolt is tightened

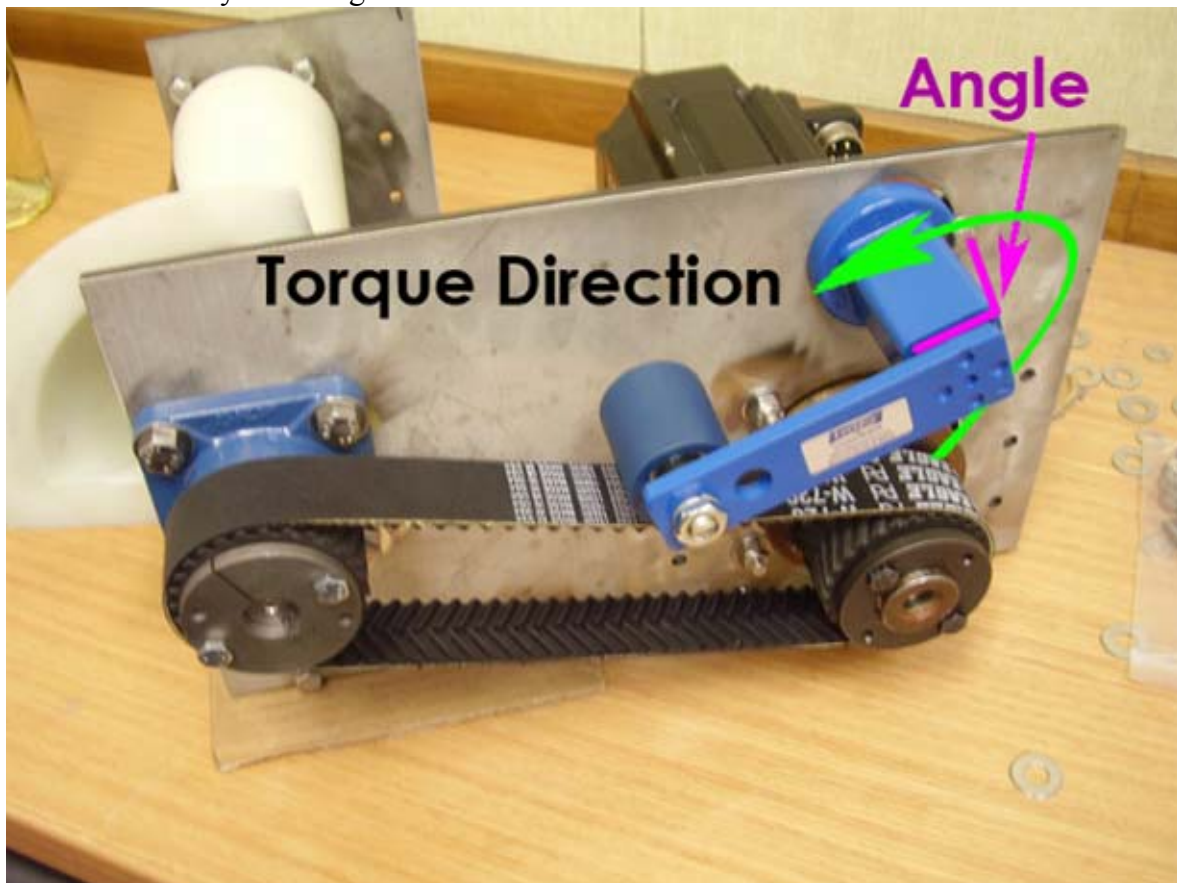


Figure 50: Tensioning Diagram

7.8.6 - Initial Motion Test

The initial motion test was conducted in the controls office. The test was basic and consisted of running the laner mechanism at a simulated speed of 600 bottles per minute. The laner was allowed to run for 30 minutes and observations were made on the mechanism ensuring full functionality. The initial motion testing ran smoothly. There was no need for initial adjustments.

7.9 - Implementation

Implementation on the test loop must meet several criteria:

- Photoeye positioned directly in front of (up-line) from the laner (due to programming protocol)
- Shaft encoder must be properly connected to conveyor shaft
- Test loop rails must be set to accommodate a lane shift of bottles
- Electronics are safely installed and connected

The implementation was completely supervised by Gallo employees to assure proper safety and installation guidelines are followed. Jason Elliot supervised the laner installation and resetting of rails. David Booth supervised electronic installation and connection, including photoeye and shaft encoder.

Chapter 8.0 - Data Collection and Analysis

This chapter outlines the calculations that were conducted throughout the design process. These calculations provide the reasoning behind many of the decisions made in the final design. Calculations conducted include:

- Bottle analysis
- Cam profile analysis
- Bottle trajectory analysis (after leaving laner)
- Torque requirements
- Stress analysis
- Fatigue analysis

8.1 - Bottle Dynamic Analysis

To better understand the behavior of bottles on a conveyor line, several tests are conducted to test bottle physical properties. These tests include a static friction test, center of gravity test and a neck strength test.

8.1.1 - Friction Test

An experiment was conducted to test the coefficient of static friction of a full wine bottle on the two materials commonly used for conveyor systems on the Gallo bottling lines. A section of conveyor links is supported and assured to be level using an inclinometer. The conveyor is lubricated with detergent (glycol based). With the bottle on the conveyor section, the conveyor is inclined until the bottle begins to slide. The angle is measured using the inclinometer.

The friction coefficient is obtained by calculating $\tan(\theta)$ ¹⁶. Two separate tests were conducted with plastic and stainless steel conveyor materials and five trials on each material were conducted.

Plastic	
Angle (degrees)	Coefficient Static Friction
Average	0.125

Figure 52: Plastic Friction Test

Stainless Steel	
Angle (degrees)	Coefficient Static Friction
Average	0.126

Figure 51: Stainless Steel Friction Test

8.1.2 - Center of Gravity Test

An experiment was conducted to test the center of gravity of a full wine bottle. The center of gravity is measured through the use of a pendulum, the full bottle being the mass. The period of a pendulum is a function of the force of gravity and length of the pendulum arm. The relationship is:

¹⁶ see Appendix I - Bottle Tests

$$T = 2\pi\sqrt{\frac{l}{g}}$$

Where T is time of one period, l is the length of pendulum from an objects center of gravity, and g is the acceleration due to gravity. By measuring the time of one period the effective length (from pivot to center of gravity) of the pendulum is obtained by rearranging the above relationship:

$$l = \left[\frac{T}{2\pi} \right]^2 * g$$

Since we know the dimensions of the bottle and length of the rope used for the pendulum test, the location of the center of gravity in relation to the bottle is calculated. Assumptions are also made that the bottle is symmetric about two axes such that the center of gravity is in the center of the bottle at some height on the z axis.

Several tests were conducted with different lengths of rope. The time was recorded for ten periods to pass. Several runs were conducted for each length of rope. The center of gravity is calculated relative to the base of the bottle. Time was recorded with a computer stop clock accurate to 0.05 seconds. Length was measured with a tape measure accurate to 1/8 inch. The results are recorded in Figure 53.

Center of Gravity Pendulum Test		
	Height from Top (in.)	Height from Bottom (in.)
Average	7.9	4.3

Figure 53: Pendulum Test Results

8.1.3 - Neck Strength Test

An experiment was conducted to test the failure load of the bottle neck using a static load acting at an extreme point on the bottle neck. The bottle overhangs off a solid surface with a rope attached to the bottle neck and a means to supply the force.

The results of the test concluded that the bottle neck was sufficiently strong to withstand the static load of at least 30 kg. Failure was not achieved because of the lack of equipment and the obvious dangers associated with broken glass.

8.2 - Cam Profile Design and Analysis

It is important for the bottles to be guided in a manner such that the acceleration across the conveyor is induced gradually and with control. Several different programs were analyzed to compare output kinematic and dynamic analysis. In this case, lower accelerations are desirable as this leads to lower forces that the bottle will experience. The cam programs that were analyzed included simple harmonic, modified trapezoid and a 4-5-6-7 polynomial function. For baseline comparison the contour of the current Heuft system follows the same analysis.

8.2.1 - Constraints

Several different constraints were made on each of the cam programs and are discussed as follows. Detailed calculations can be found in Appendix M - Detailed Mathematics.

8.2.1.1 - Simple Harmonic Displacement Constraints

The maximum final displacement is made to constrain the amplitude of the sine function. The max displacement is based on the current Heuft system.

A second assumption is made based on the fact that the bottles are contacted only on one side. This means that the acceleration is constrained to only being positive, since a wall cannot provide a negative (pulling) force. This constrains the displacement curve to be cut off at the inflection point (where concavity changes, and thus the second derivative changes from negative to positive), meaning the effective contour is $\frac{1}{4}$ of a sine wave.

8.2.1.2 - Modified Trapezoidal Acceleration Constraints

The maximum allowable acceleration is made to set a working value to build the function. The maximum acceleration value primarily is based on an iterative process to provide the necessary displacement (which is solely based on the Heuft system). The iterative process consisted of specifying maximum accelerations and finding the double integral of the function such that the maximum displacement equaled that of the Heuft system.

As stated above, the acceleration profile of the contour must remain positive. The full cycle of a mod trap contour is 50% negative acceleration. Thus, in order to constrain to positive acceleration, the acceleration profile function must be cut in half.

8.2.1.3 - Polynomial Displacement Constraints

Since the initial and final values of displacement, velocity, acceleration and jerk can be controlled, we have many options to adjust the reaction of the bottle. In this particular case, we want the initial values to all be zero, which will assure the bottle reaction is brought on gradually. However, assumptions must be made on the other end of the profile for final displacement, velocity, acceleration and jerk. These values were adjusted to form a reasonable contour and acceleration profile and took some time to find a satisfactory outcome. One method attempted was to input final values of another profile into the polynomial function and observe results. Another method was to use all zero final values.

Table 10 shown below is the initial values input into the calculations to give plot the contours of the cam programs. NS in the table signifies that the value was not specified in the assumption.

Constraints		Simple Harmonic	Mod Trap	4-5-6-7 Poly
Displacement (m)	<i>Initial</i>	0	NS	0
	<i>Final</i>	0.069	0.07 (iterative)	0.069
Velocity (m/s)	<i>Initial</i>	NS	NS	0
	<i>Final</i>	NS	NS	0.6
Acceleration (m/s²)	<i>Initial</i>	NS	0	0
	<i>Final</i>	NS	NS	0
	<i>MAX</i>	NS	3.0	NS
Jerk (m/s³)	<i>Initial</i>	NS	NS	0
	<i>Final</i>	NS	NS	0

Table 10: Cam Program Constraints

With these assumed values and following the standard procedure for design of each cam profile, we were able to obtain the plots of the cam contour and its derivatives. Kinematic analysis of the contour program includes plots of the following qualities: displacement, velocity (across conveyor, y-direction), acceleration and jerk. Also included in the analysis is the trajectory that the bottle follows after it travels past the contour.

Dynamic analysis of the contour program includes forces and moments that the bottle experiences during its translation.

All analyses are conducted with the same line conditions: line speed, length of split, bottle physical properties and friction coefficient.

8.2.2 - Kinematic Analysis

Kinematic analysis is in the form of S-V-A-J diagrams of each of the cam contours. Each analysis is conducted as a comparison of the plots in a single chart. The current (Heuft) system is always used as the baseline as the purpose of this project is for improvement.

In the following graphs, each cam program is always represented by the same color line. Table 11 is the graph color scheme used throughout this section.

Graphic Color Scheme	
Heuft	Solid Red Line
Simple Harmonic (Sinusoidal)	Dotted Blue Line
Modified Trapezoidal Acceleration	Dashed Green Line
4-5-6-7 Polynomial Function	Dot-Dash Pink Line

Table 11: Graphic Color Scheme

When interpreting the following charts, it is essential to know the axis orientation. For the purposes of the displacement curve we assume that the curve exemplifies what would be seen looking directly down at the laner. Thus the x axis is *down line* and the y axis is *across the conveyor*. The velocity, acceleration, jerk and force plots all provide data for what the bottle experiences in the y direction, across the conveyor, which is the direction of interest.

8.2.2.1 - Diverting Contour

The diverting contour for each cam program is shown below in Figure 54. Note that the contours look relatively similar. However, each contour offers very different acceleration profiles. In order to gain better understanding of the displacement profiles, we conduct a comparison of each to the Heuft contour by plotting the difference between the two functions shown in Figure 55.

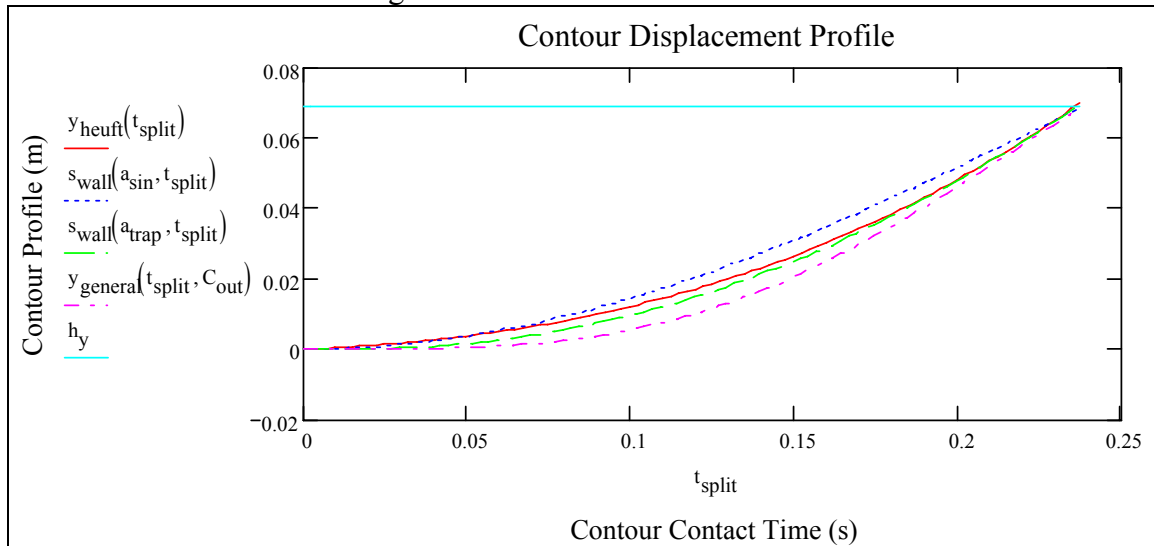


Figure 54: Contour of Each Cam Program

The displacement difference is shown below in Figure 55. Since the standard of the comparison is the Heuft contour, it is not shown in this plot, however the color scheme still holds true. Notice that the modified trapezoid curve is most similar to the Heuft system. The simple harmonic is shallower than that of the Heuft and the polynomial function is a deeper curve.

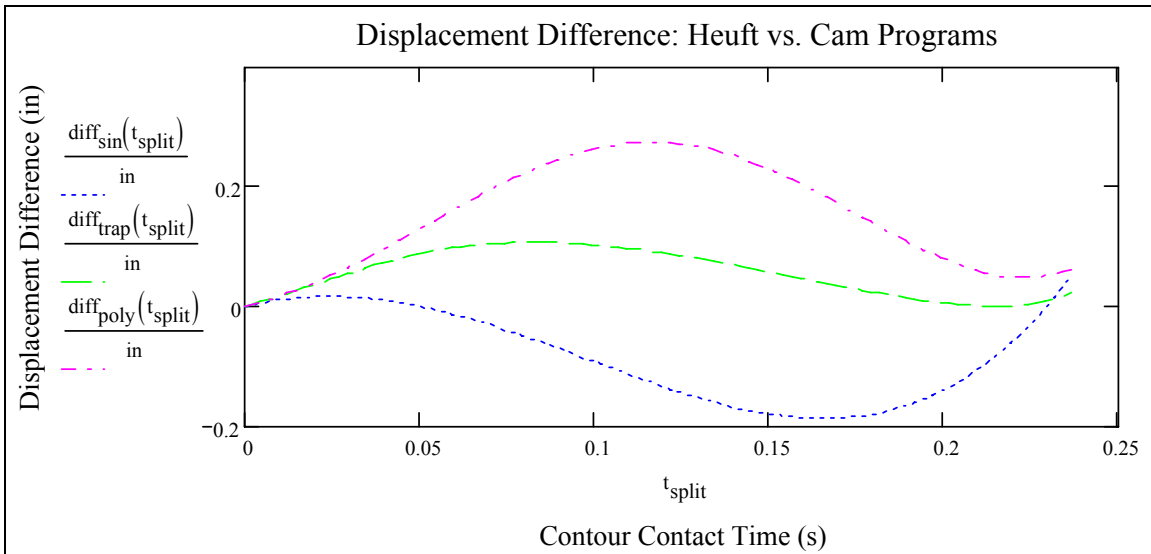


Figure 55: Displacement Difference, Heuft vs. Cam Programs

The shape of the contour gives limited insight into the performance of the contour. In the following sections we will look into the motion dynamics that each contour provides for a bottle traveling at maximum line speed of 400 bottles per minute, which translates to roughly 1 m/s.

8.2.2.2 - Velocity Curve

Shown below in Figure 56 is the velocity of the bottle as it crosses the lane. It is interesting to note that the Heuft system does not start at zero velocity and is always increasing. In general, the four programs offer similar velocity values at each point along the laner. An important note to keep in mind is that the bottles are not guided the entire way across the conveyor. They follow a trajectory after they leave the guide of the contour wall because there is positive transverse velocity. It is important for the bottles to maintain this velocity to clear the division in the conveyor. Note that the simple harmonic profile is significantly lower than the Heuft profile. A good way to accomplish this is to match the velocity of the Heuft system, as it is already known that this system provides a correct final transverse velocity.

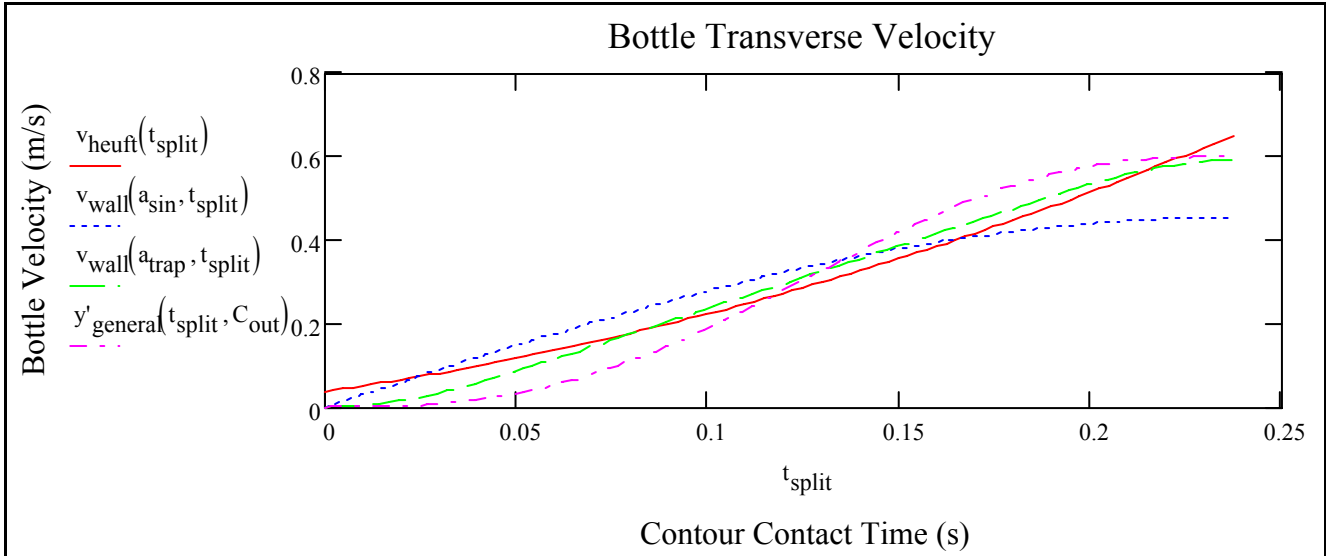


Figure 56: Bottle Transverse Velocity

8.2.2.3 - Acceleration Curve

The acceleration profiles of each contour give the best insight on the behavior of the bottles during the laning. The acceleration profile comparison shown in Figure 57 exemplifies the difference of each cam program. Notice that the Heuft system is a linearly increasing function of acceleration. Both the mod trap and simple harmonic functions have lower maximum accelerations, however the polynomial function has a peak acceleration higher than all compared cam programs.

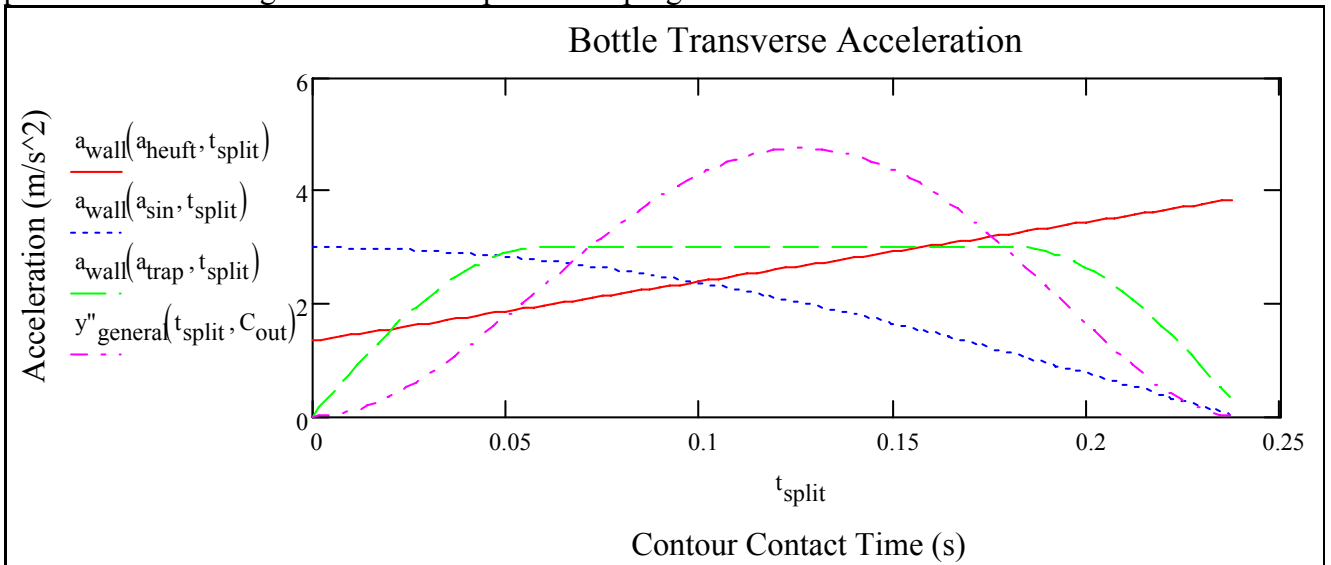


Figure 57: Bottle Transverse Acceleration

8.2.2.4 - Jerk Curve

The jerk plot (shown in Figure 58) gives good indication about the potential for possible impacts. A good indication of impacts is a spike or cusp in the jerk profile. Notice that the mod trap contour induces the highest maximum jerk of the contours. All contours offer smooth jerk curves and none seem to pose any immediate dangers.

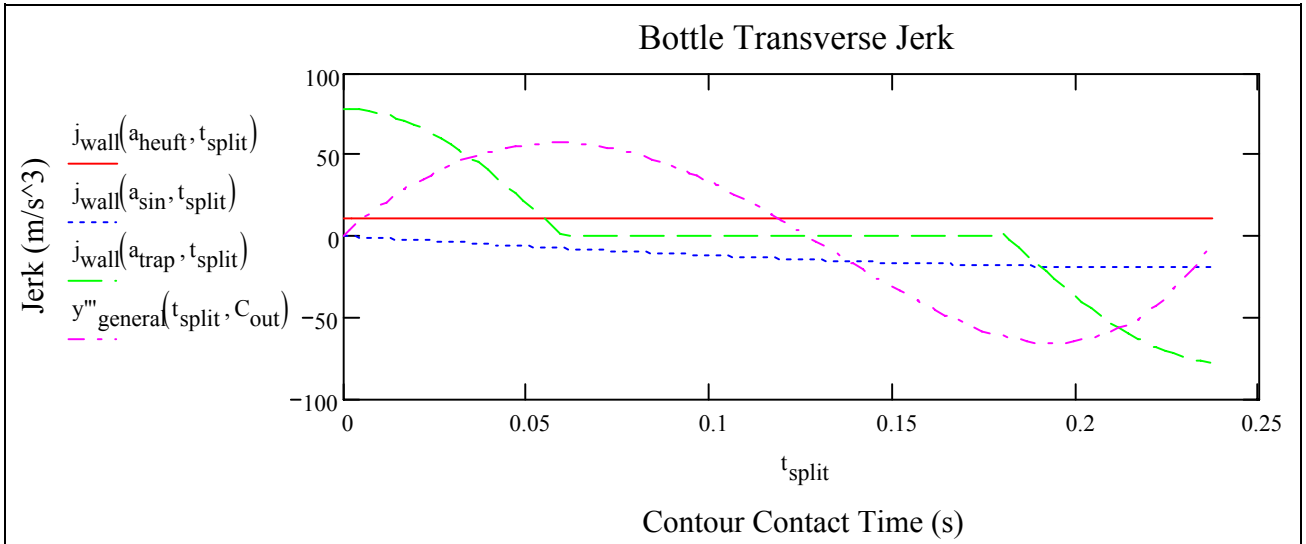


Figure 58: Bottle Transverse Jerk

Table 12 shows the maximum values of the aforementioned plots. The listing order is the same used in the previous plots; Heuft system, simple harmonic, mod trap, 4-5-6-7 polynomial, from top to bottom. Following previously set guidelines, we are looking for the contour to cause minimum amount of acceleration, and thus force. The mod trap and simple harmonic contours seem to have the mildest acceleration. However, the simple harmonic has almost 25% less final velocity than the other contours. For these reasons, the modified trapezoid acceleration profile was chosen for the camoid contour design.

Maximum Kinematic Values		
Maximum Velocity	Maximum Acceleration	Maximum Jerk
$v_{\text{maximum}} = \begin{pmatrix} 0.656 \\ 0.454 \\ 0.592 \\ 0.6 \end{pmatrix} \frac{\text{m}}{\text{s}}$	$a_{\text{maximum}} = \begin{pmatrix} 3.851 \\ 2.987 \\ 3 \\ 4.709 \end{pmatrix} \frac{\text{m}}{\text{s}^2}$	$j_{\text{maximum}} = \begin{pmatrix} 10.54 \\ -19.636 \\ 78.117 \\ 57.263 \end{pmatrix} \frac{\text{m}}{\text{s}^3}$

Table 12: Maximum Kinematic Values

8.2.3 - Force Analysis

Working from the kinematic analysis data, it is possible to conduct analysis on the forces that the bottle will be subject to during the laning process. During the laning process, the bottle is subject to four forces; gravity F_g , normal force from the conveyor F_N , the force of the contour wall F_w and the friction force between the bottle base and conveyor F_f (see Figure 59). Again, the primary concern of the laning device is that no bottles are tipped or damaged. To ensure that this design specification is adhered to, we conduct analysis to test the wall force and overturning moment which occur during the laning process.

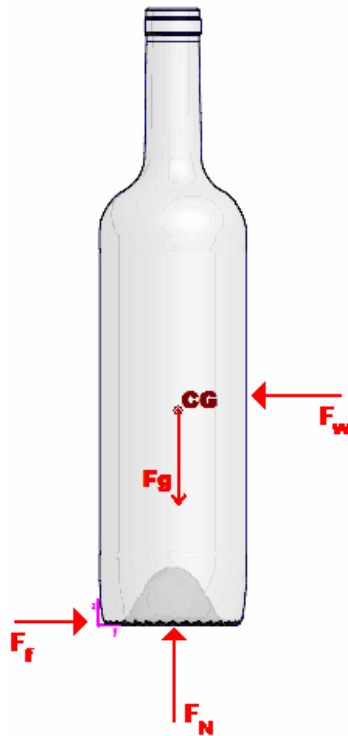


Figure 59: Bottle Free Body Diagram

Using Newton's physical law $F=ma$, we can plot the force that the bottle will see throughout the laning process. Shown below in Figure 60 we can see the plot of force vs. laning time to which the bottle is subject.

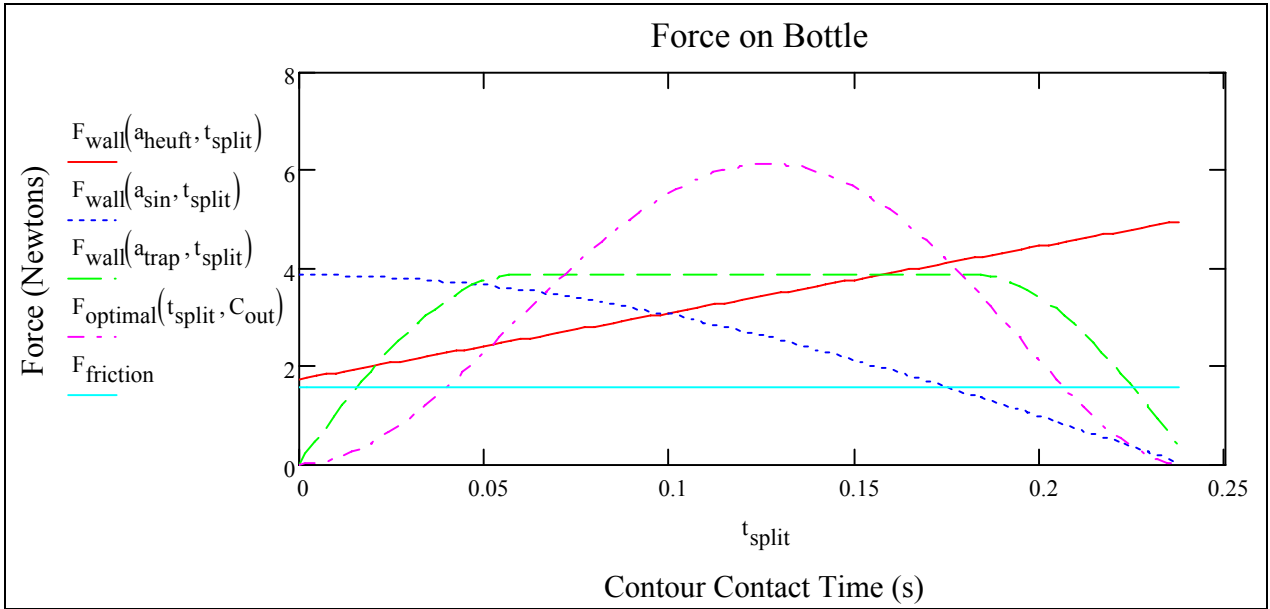


Figure 60: Force on Bottle

Notice that the curves are shaped the same as the acceleration curve because the mass of the bottle is constant in all four cases. Also, notice the solid horizontal cyan force of friction line. This is the force of static friction between the bottle and conveyor (as the bottle is assumed stationary relative to the conveyor, no slip) and represents the point at which static friction switches to kinetic friction. The static friction force is the maximum force that the bottle will experience opposing the force of the wall. The bottle will not begin traversing the conveyor laterally until the force from the wall exceeds the force of static friction. It is desirable to exceed this force as rapidly as possible, as is done in the mod trap profile.

8.2.4 - Moment Analysis

Through the force analysis, the overturning moment can be analyzed, assuming a height at which the contour contacts the bottle. Figure 61 shows the moment plots and again are similar in shape to the acceleration plot.

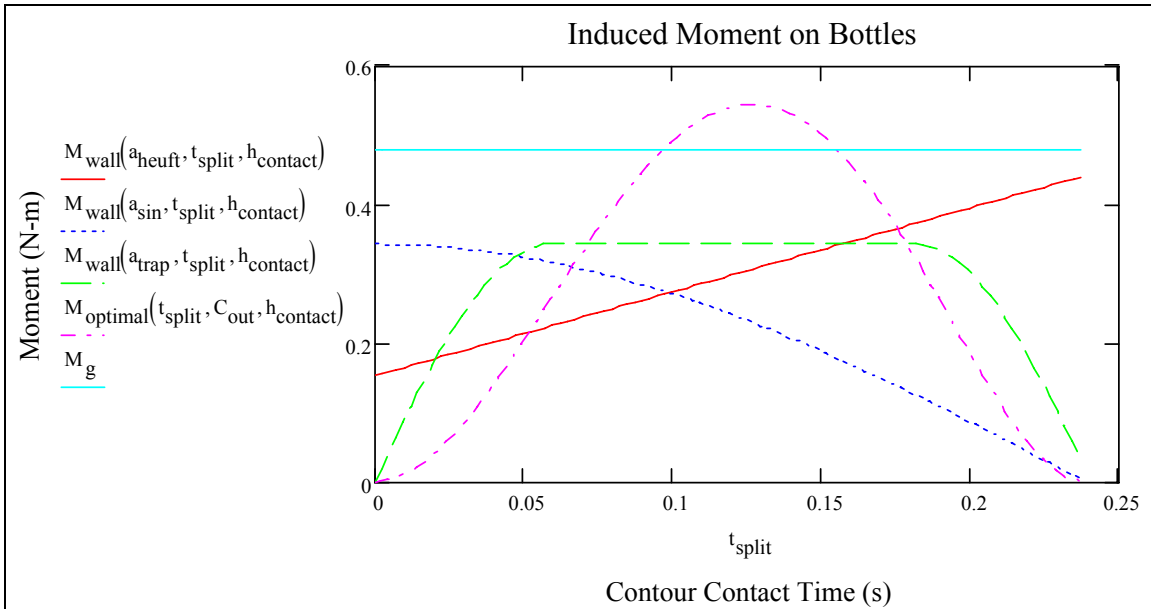


Figure 61: Induced Moment on Bottles

The horizontal cyan line shown in the plot is the moment sufficient to cause the bottle to begin to tip. We can understand this baseline moment calculation by examining Figure 59. Assuming that F_g acts at the center of gravity (CG), this point force induces a moment about the bottom corner of the bottle with the bottle radius as the moment arm. The plots are simply the force of the wall multiplied by the height at which the wall contacts the bottle. If this moment is greater than that caused by gravity, the bottle will begin to tip.

Notice that the polynomial function crosses the tipping mark, meaning this particular contour could have the potential to cause instability in the bottle. The other two contours in question both induce lower maximum moments than the current Heuft system.

Table 13 shows the maximum force and moment of each contour. The order is the same used in all of the plots: Heuft, Simple Harmonic, Mod Trap, and Polynomial. As we can see from the values, the simple harmonic and mod trap yield similar values that are smaller than the other two contours.

Force Analysis	
Maximum Force	Maximum Moment
$F_{\text{maximum}} = \begin{pmatrix} 4.968 \\ 3.853 \\ 3.87 \\ 6.074 \end{pmatrix} \text{ N}$	$M_{\text{maximum}} = \begin{pmatrix} 0.442 \\ 0.343 \\ 0.344 \\ 0.54 \end{pmatrix} \text{ N}\cdot\text{m}$

Table 13: Maximum Force Analysis Values

8.3 - Trajectory Test

The camoid laner is a direct replacement of the Heuft system with no further line or rail manipulation. In order to be certain that the laner will cause the bottles to divert fully into the second lane; the bottle trajectories from the end of the cam contour of the three curves are compared to the Heuft. The trajectories are shown in Figure 62.

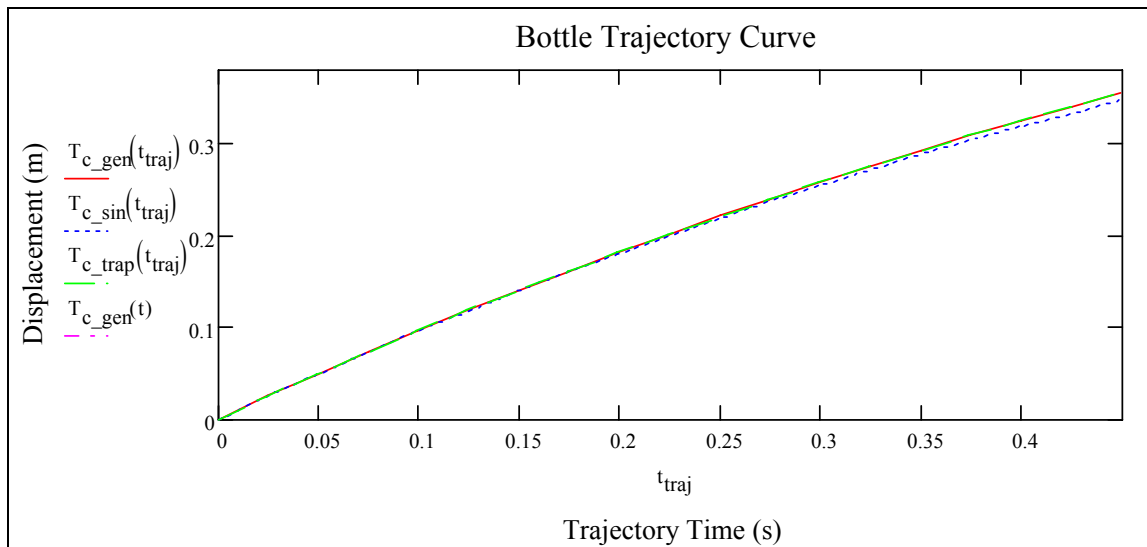


Figure 62: Bottle Trajectories

From the figure we can see that the trajectories are very similar, eliminating any worries about the bottle's following a correct diversion path.

8.4 - Choosing a Contour

After this analysis, it is possible to choose the contour that will most suit the application which we need. For the purposes of the high speed bottle laner, the Modified Trapezoid (mod trap) contour is chosen based on the following explanations.

8.4.1 - Acceptable Final Velocity

The velocity curve of the mod trap closely resembles the current system and provides a similar final velocity, which is essential for the bottle to follow the required trajectory for safe laning.

8.4.2 - Minimizing Maximum Acceleration

While the mod trap does not provide the lowest maximum acceleration, it comes in at a close second to the simple harmonic. However, the simple harmonic curve is not applicable because of an unacceptably low final velocity.

8.4.3 - Minimizing Jerk

The jerk curve of the mod trap is not the best of the group, however still provides continuous and finite values for jerk which are still within the realms of the other analyzed contours. The higher values for jerk are a worthy exception to make for the satisfactory velocity and acceleration profiles.

8.4.4 - Minimizing Force

Examining Table 13, the force induced by the simple harmonic and the mod trap are comparable in magnitude and both significantly lower than the other two contours. Again, because of the mod trap's more acceptable velocity curve, we choose it as the better choice.

8.4.5 - Minimizing Moment

Examining Table 13 again for the moment values, we see a similar trend to the force analysis. The mod trap is chosen over the simple harmonic for the same reasons described above for minimizing force. The polynomial function is not an option as the moment induced by the contour is greater than the tipping moment as seen in Figure 61.

8.5 - Torque Requirements

Once the geometry of the cam has been set, it is possible to begin to design the second part of the mechanism which is the timing of the rotation. This timing relies directly on the geometry

8.5.1 - Operating Rotational Velocity

If the bottle is traveling at line speed, then the time that it takes to travel the length of the cam laner is represented by Equation 1. Equation 2 is the calculation for the operating rotational velocity. Equation 3 shows the worst case scenario time between two bottles with a bottle spacing of one bottle diameter center to center of bottles on conveyor.

Timing Data		
Equation 1: Bottle and Laner Contact Time	$t_{cr} := \frac{L_{split}}{v_{line}}$	$t_{final} = 0.239s$
Equation 2: Operational Rotational Velocity	$\omega_{op} := \frac{140deg}{t_{cr}}$	$\omega_{op} = 97.665rpm$
Equation 3: Worst Case Scenario Time Between Two Bottles	$t_{worst} := \frac{d_{bottle}}{v_{line}}$	$t_{worst} = 0.075s$

Table 14: Time Data

8.5.2 - Angular Acceleration

Recall that the cam must be at full operating velocity before any bottle manipulation can occur. The angular acceleration necessary in the case is based on the spin-up time, the time it takes for the servo to accelerate the camoid up to operating velocity, as well as servo limitations. Recall that the geometry of the cam includes a buffer angle that allows servo acceleration. The allowable spin-up time is directly related to the buffer angle, the smaller the buffer angle the faster the spin-up time required. This relationship is represented by Figure 63.

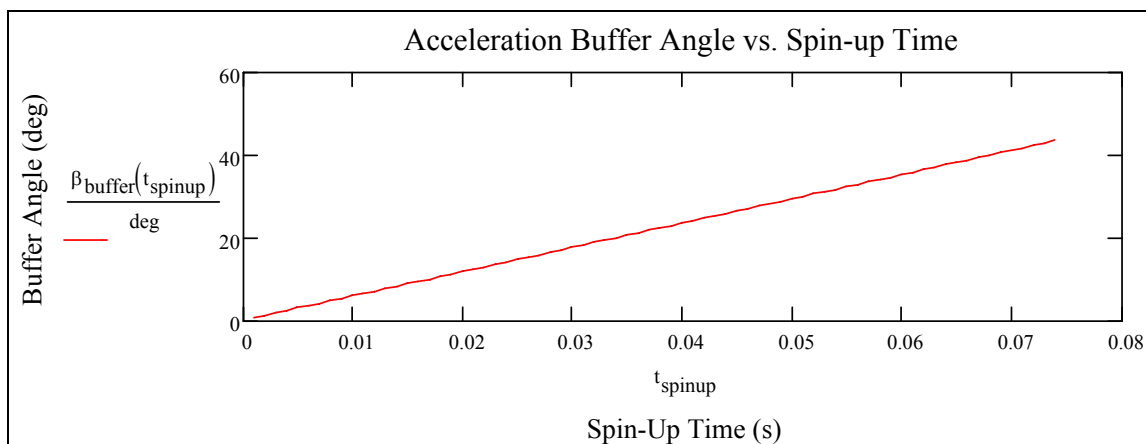


Figure 63: Spin-up time vs. Buffer Angle

Notice that the spin-up time is the independent variable. This is because we can find a lower limit on the spin-up time based on servo characteristics and design the camoid buffer angle from there. There is more flexibility in sizing for servo torque than there is in the design of the buffer angle on the camoid.

The maximum acceleration of a servo is based on its torque, motor inertia and inertia of the cam. For the purposes of graphical representation, we can specify a lower extreme time of 0 seconds for spin-up. The acceleration plot is based on Equation 4.

Equation 4: Acceleration Function	$\alpha(t_{\text{spinup}}) := \frac{\omega_{\text{op}}}{t_{\text{spinup}}}$
--	---

The acceleration plot shown in Figure 64 shows the acceleration necessary to reach operating velocity for a range of spin-up times. The plot follows intuition as the amount of time allowed to reach a certain velocity increases, the acceleration necessary to reach that velocity increases, in this case, asymptotically.

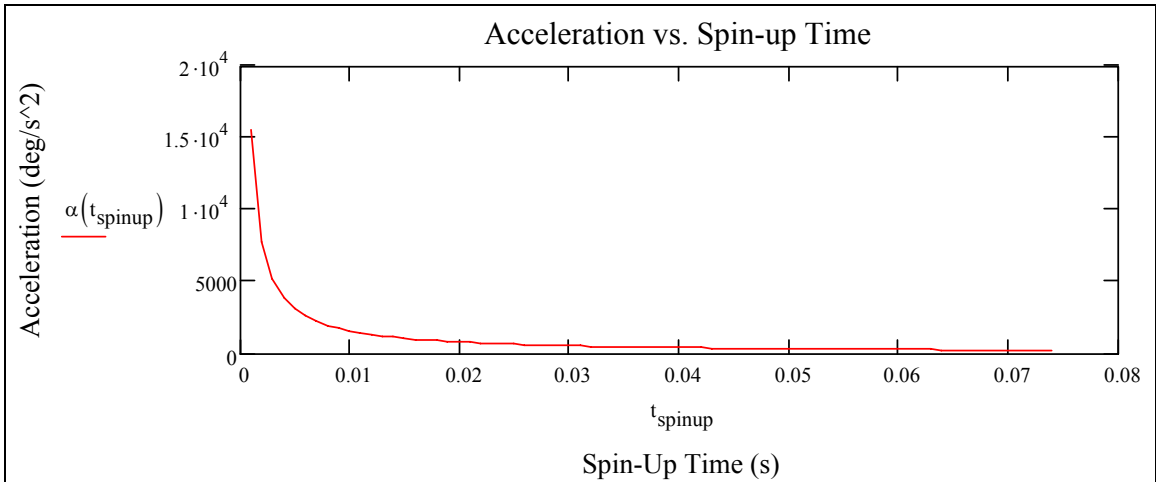


Figure 64: Acceleration vs. Spin-Up Time

8.5.3 - Torque Required

Now that the acceleration profile is plotted, we can specify the torque needed based on the cam and motor mass inertia properties. Equation 5 shows the function used to plot the necessary torque for a desired spin-up time.

Equation 5: Torque Function	$T_{\text{servo}}(t_{\text{spinup}}) := \alpha(t_{\text{spinup}}) \cdot (I_{\text{zz_cam}} + I_{\text{zz_motor}})$	
Where:	$I_{\text{zz_cam}}$	<i>Cam Moment of Inertia About Rotational Axis</i>
	$I_{\text{zz_motor}}$	<i>Motor Moment of Inertia About Rotational Axis</i>

Figure 65 shows the torque vs. spin-up time plot. Notice that it is the same shape as the acceleration curve.

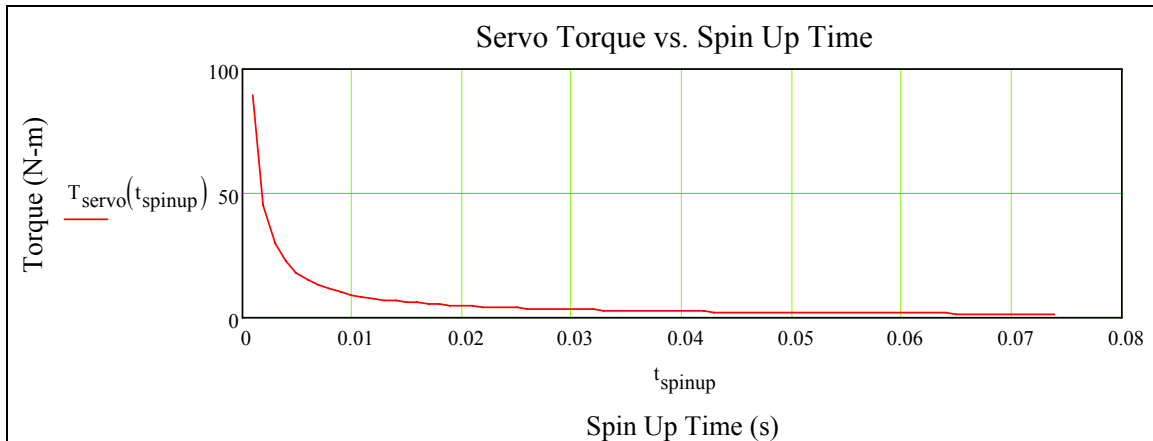


Figure 65: Servo Torque Required vs. Spin-Up Time

This torque graph is rendered for visualization purposes. We will demonstrate in the following section how the motor torque is actually calculated. However, the graph gives a range of what can be expected for the required torques.

8.6 - Stress Analysis

Once the maximum torque that will be transmitted is known, we can begin stress analysis on the parts that will experience the most stress. The servo will drive a camshaft which will transmit torque to the camoid by means of a key and keyway. The keyway stress analysis is shown in Table 15. It should be noted that the required torque is based on a spin-up time obtained from the Motion Analysis software, which is the time to accelerate from 0 to operating velocity in the final buffer angle of 7.5 degrees. This time was then input into Equation 5.

Keyway Stress Analysis		
	<i>Key Width</i> $W_{\text{key}} := \frac{3}{16} \text{ in}$	<i>Key Length</i> $L_{\text{key}} := 1.5 \text{ in}$
		<i>Key Depth</i> $D_{\text{key}} := \frac{3}{32} \text{ in}$
Equation 6: Shear Force at Key	$F_{\text{shear}} := \frac{T_{\text{max}}}{\frac{D_{\text{shaft}}}{2}}$	$F_{\text{shear}} = 684.893 \text{ N}$
Equation 7: Keyway Average Shear Stress	$\tau_{\text{ave}} := \frac{F_{\text{shear}}}{A_{\text{sec}}}$	$\tau_{\text{ave}} = 2.491 \text{ MPa}$
Equation 8: Safety Factor	$\eta_{\text{steel}} := \frac{S_{\text{sys_steel}}}{\tau_{\text{ave}}}$	$\eta_{\text{steel}} = 50.177$
Where		
Equation 9: Area of Key	$A_{\text{sec}} := W_{\text{key}} \cdot L_{\text{key}}$	
Equation 10: Required Torque	$T_{\text{max}} := T_{\text{servo}} (.01367)$	<i>Required Torque based on Motion Analysis Tool and MathCAD Torque Plot</i>
	$S_{\text{sys_steel}} = 125 \text{ MPa}$	<i>Theoretical Yield Strength of Steel</i>

Table 15: Keyway Stress Analysis

Notice that the safety factor of 50 is adequate for this application.

Stress analysis is conducted on the shaft as shown in Table 16. The torsional deflection and shear stress are the main points of interest for the analysis.

Shaft Stress Analysis		
<i>Shaft Diameter</i> $D_{\text{shaft}} := .75\text{in}$	<i>Shaft Length</i> $L_{\text{shaft}} = 16\text{in}$	<i>Material</i> Stainless Steel
Equation 11: Shaft Torsional Deflection	$\delta_{\theta\text{shaft}} := \frac{T_{\text{max}} \cdot L_{\text{shaft}}}{G_{\text{steel}} \cdot J_{\text{shaft}}}$	$\delta_{\theta\text{shaft}} = 0.036\text{deg}$
Equation 12: Shaft Shear Stress due to Torsion	$\tau_{\text{shaft}} := \frac{T_{\text{max}} \cdot \frac{D_{\text{shaft}}}{2}}{J_{\text{shaft}}}$	$\tau_{\text{shaft}} = 3.172\text{MPa}$
Where		
Equation 13: Shaft Polar Moment of Inertia	$J_{\text{shaft}} := \frac{\pi}{2} \cdot \left(\frac{D_{\text{shaft}}}{2} \right)^4$	
	$G_{\text{steel}} := 216\text{GPa}$	<i>Stainless Steel Modulus of Elasticity</i>

Table 16: Shaft Stress Analysis

8.7 - Fatigue Stress Analysis

Because the system will be under cyclic torque loading, it is necessary to conduct fatigue stress analysis which is shown in Table 17. The calculations are conducted for a shaft with a ground surface finish, operating in ambient temperatures, 99% reliability and under non-reversing torsional loading. The corrected fatigue function and safety factor are shown in Equation 14 and Equation 15 respectively.

Shaft Fatigue		
	$S_e' = 200\text{MPa}$	<i>Stainless Steel Uncorrected Endurance Limit</i>
Equation 14: Corrected Fatigue Function	$S_e := C_{\text{load}} \cdot C_{\text{size}} \cdot C_{\text{surface}} \cdot C_{\text{temperature}} \cdot C_{\text{reliability}} \cdot S_e'$	$S_e = 124.049\text{MPa}$
Equation 15: Safety Factor	$\eta_{\text{torsion}} := \frac{S_e}{\tau_{\text{shaft}}}$	$\eta_{\text{torsion}} = 39.109$
See Appendix M - Detailed Mathematics <i>for detailed information on the mathematics of this section</i>		

Table 17: Shaft Fatigue Analysis

Notice that the safety factor of 39 is adequate for this application.

Inevitably, keyways cause stress concentrations due to the sharp radii of the cut. The stress concentration is based on several factors including notch radius, Neuber's Constant, and a notch sensitivity factor. The safety factor is calculated based on the yield strength of the stainless steel.

Keyway Stress Concentration		
$S_{ys_steel} = 125\text{MPa}$		<i>Yield Strength of Stainless Steel</i>
Equation 16: Fatigue Stress Concentration Factor	$K_{fs} := 1 + q \cdot (K_t - 1)$	$K_{fs} = 2.442$
Equation 17: Shear Stress Concentration due to Torsion	$\tau_{concentration} := K_{fs} \cdot \tau_{shaft}$	$\tau_{concentration} = 6.869\text{MPa}$
Equation 18: Safety Factor	$\eta_{keyway} := \frac{S_{ys_steel}}{\tau_{concentration}}$	$\eta_{keyway} = 18.199$

Table 18: Keyway Stress Concentration Analysis

Notice that the safety factor of 18 is adequate for this application.

Chapter 9.0 - Prototype Testing

This chapter discusses in detail the testing protocol followed for proper data collection on the functionality of the camoid laner prototype. This section is meant to provide the necessary information to successfully duplicate the experiment and record all results.

9.1 - Materials

- Test Loop
- Camoid Laner
 - Camoid
 - Allen-Bradley MPL - B4520P – MJ22AA servo motor
 - Alpha SP-100-MF1-10 Gearbox 10:1 ratio
 - Rockwell Automation Kinetix 3000 Servo Driver
 - 2x SKF FY ¾ TF Flange Mount Bearings
 - Lovejoy SE-18 ROSTA Tensioner w/ Hardware
 - Lovejoy R-15/18 Roller Idler-SE15/18
 - Stegmann DG60L WSR 5000 pulse/rev shaft encoder
 - 2x Goodyear W-28S-H White Eagle Pd (QD Bushed) Sprockets
 - Martin H ¾ QD Bushing
 - Martin H 32mm QD Bushing
 - Goodyear Pd W-720 Eagle Belt
 - Custom length ¾” keyed stainless steel shaft
 - Custom chassis design
- 30 test bottles
- Data recording device (computer, pen, paper)

9.2 - Objective

This test is to ensure no bottles are tipped or damaged during operation, and ensure the repeatability.

9.3 - Variables

There are several specific variables that will be tested in order to meet aforementioned objective.

- Bottle Spacing
- Number of Bottles per Cycle

9.4 - Setup Safety Precaution

Safety is of primary concern when dealing with high voltage applications. In this case, 480 volt electrical inputs are required. Only those qualified and experienced to handle high voltage should do so.

Servo motors are very powerful and should be handled with care. DO NOT place any body parts on or near any part of mechanism when power is on. DO NOT stand in path of diverting bottles if servo should malfunction and kick bottles off line.

9.5 - Setup

All testing will be conducted on the specific test loop that Gallo has set up for testing new instruments shown in Figure 66. This test setup assumes the laner has been mounted to the line.



Figure 66: Test loop

A series of tests will be conducted testing the two variables mentioned before. The tests will be set up to find an extreme value at which the mechanism no longer functions correctly. Before the test is conducted, there are several initial parameters of the test that must be discussed.

- Bottle Batches
- Test Loop Speed
- Photoeye Placement
- Electronic Attachment

9.5.1 - Bottle Test Batches

Bottle batches are small so that if any problems arise, there is not a catastrophe with tipped bottles. Batches of six bottles will be used, each bottle labeled 1-6. Also, the bottle spacing can be set easier with smaller batches. Once we know that the settings are correct and tipped bottles are minimized, a stream of bottles can be placed safely on the line.

9.5.2 - Test Loop Speed

The test loop has a maximum speed of 24 inches per second without overloading the test loop system.

9.5.3 - Photoeye Placement

The photoeye is placed directly in front of camoid laner in this case for ease of programming. The camoid is triggered as soon as the target bottle breaks the photoeye beam. Care must be taken to assure the photoeye is triggered *once* per bottle. This becomes an issue when the photoeye reads through the transparent bottle body. It is possible to trigger twice; once on the leading edge and once on the trailing edge of the same bottle. To avoid this, the photoeye is placed either at the bottle neck where there is an opaque cork or at the base where the glass is sufficiently thick to block enough of the beam. This test used the latter method.

9.5.4 - Electronic Attachment

All electronics are attached to their respective power sources by control engineer David Booth. The electronics board is shown in Figure 67.

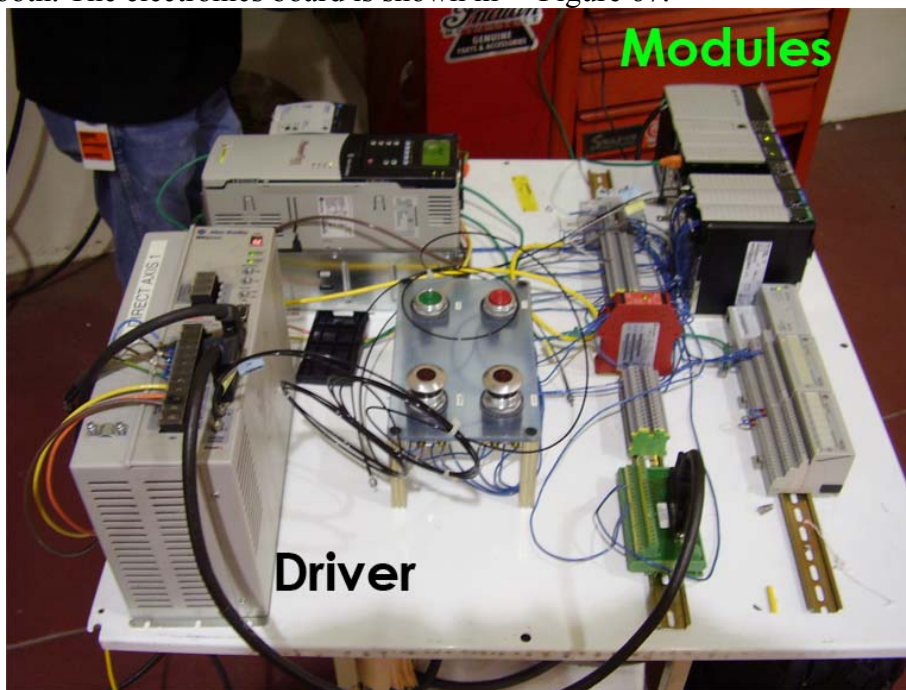


Figure 67: Electronics Board

The setup of the control electronics was conducted by David Booth and Brandon Abell of Gallo's Control engineering department. Information regarding the design of the control schematics and hardware setup will not be discussed in this report. Information this can be researched under the heading motion control.

When attaching electronics to 480V power sources, extra care should be taken.

9.6 - Procedure Safety Precaution

The number of bottles per cycle for the camoid laner should be **NO LESS** than **4 BOTTLES PER CYCLE**. Doing so can result in servo misfiring, potentially kicking bottles off the line at high speed. The first tests conducted with less than four bottles per cycle outlines the steps taken to obtain this safety hazard information.

Again, do not stand in front of the diverting bottles at any time to avoid any potential injury. Any tipped bottles should be removed from the line as fast as possible to avoid misfiring.

9.7 - Procedure

The procedural steps for testing are explained below. These steps are followed only after laner mounted, the servo is programmed, electronics are active, and laner is in its default home position which is in the off position.

1. Set up batch of bottles to be tested with spacing according to test number 1 in the data recording table (shown in Appendix K – Test Data Table) while line is not running
2. Set up program for bottles per cycle according to the test data table.
3. Turn on conveyors
4. Run test five times – bottle batch loops five times – adjust spacing each time
5. Record results
6. Repeat for each test according to test data table

9.7.1 - Data Recording

Any abnormal interactions such as impacts, punches, off timing, diversion due to incorrect geometry, or any other potential problems will be recorded and explained in the test data table. Each bottle is labeled in the batch and if a bottle falls, the number of the bottle is recorded. This will give insight how the actuation and geometry of the camoid are functioning.

In addition to the bottle interaction, a second set of observations is needed to record the functioning of the machine itself and any abnormalities experienced with the mechanics of the cam and actuation.

The test protocol will be set up such that any problems encountered will be followed by a set of recommendations on how to improve and/or solve such problems, if the problems cannot be solved by us in the allotted time.

Chapter 10.0 - Test Results

The results of the testing are discussed in detail in this chapter. Also explained are safety issues and problems experienced during the testing sequence. Conclusions provide a concise explanation of the most important findings. Picture sequence of the testing is shown in Figure 68.

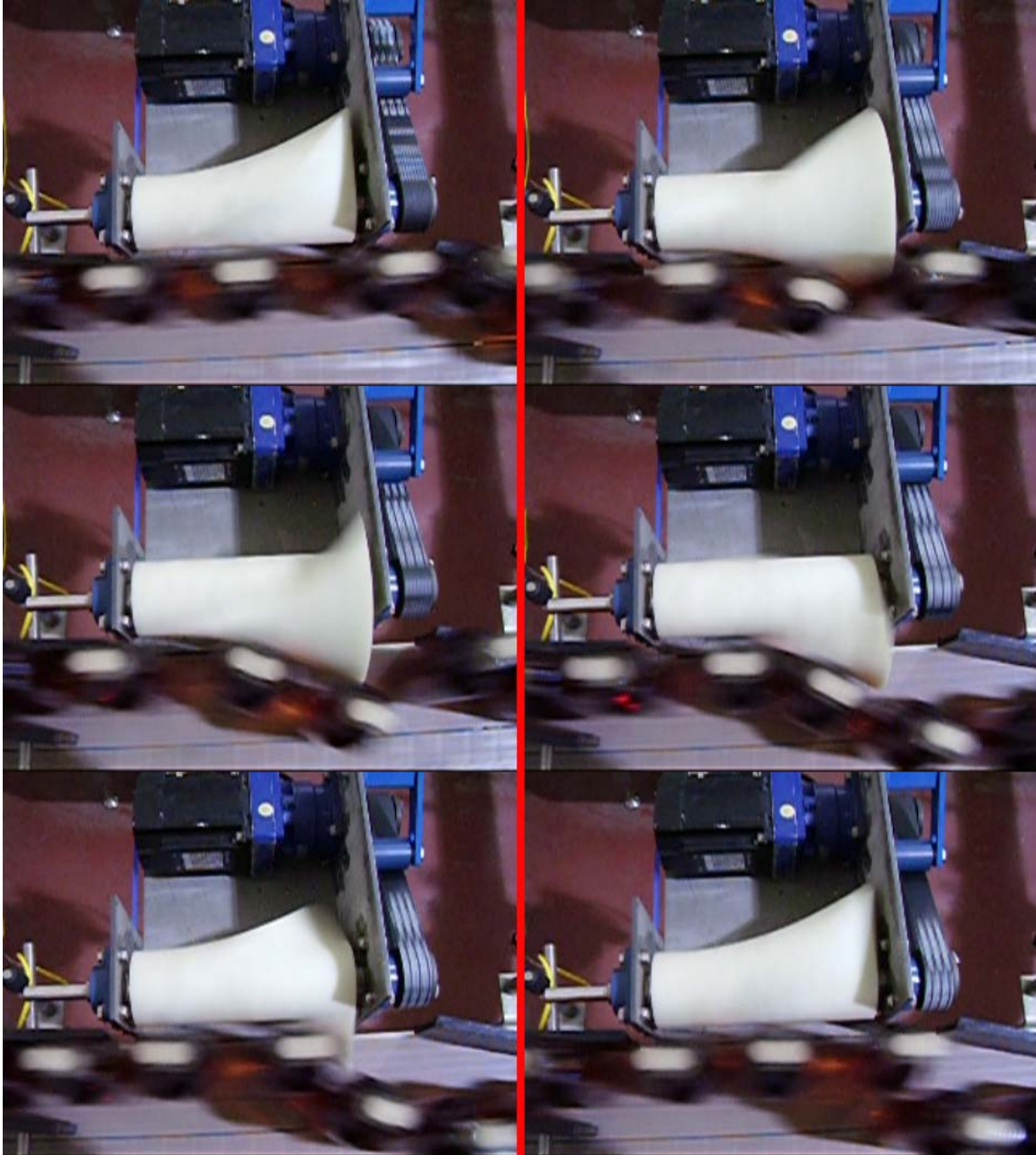


Figure 68: Final Mechanism Cycle Sequence

10.1 - Testing Limitations

There are several limitations experienced with the test loop:

1. No available line encoder

2. No variable line speed
3. Conveyor Condition
4. Not full line speed

10.1.1 - Line Encoder

The test loop did not offer a reliable means to attach a line encoder. This has implications when setting the line speed in the program logic. Since the functionality of the design is reliant on the line speed, outside instruments were used to measure the line speed so that it could be hard coded into the program.

10.1.2 - Variable Line Speed

Because the line speed is hard coded in the control program, the line speed must be held constant. This made testing for variable line speed impossible without shutting the line down and adjusting the program logic.

10.1.3 - Conveyor Condition

The conveyor condition was poor for the purposes of providing a smooth transition across the lines. In several sections of the conveyors, remnants of adhesives caused increased friction as bottles slide across. The test loop also does not include a lubrication system which also results in increased friction. Furthermore, there was a misalignment between two conveyors causing a small lip on which bottles periodically tipped.

10.1.4 - Line Speed

We were not able to set the test loop for full line speed because of the apparent safety hazards that could arise from the poor condition of the conveyors. The line speed was set to 24 inches per second, which translates to roughly 250 bottles per minute.

10.2 - Preliminary Testing

The actual testing of the laner was not conducted until it was certain that the mechanism would function safely. A series of preliminary tests were conducted to ensure safe operation, find the minimum number of bottles per cycle and the placement of the photoeye. Several important results were gathered from the preliminary tests using the current programming logic.

- Minimum number of bottles per cycle is 4
- Photoeye must be placed such that either the base of the bottle or the corked part of the bottles break the beam

The reason for a 4 bottle minimum per cycle lies in the geometry of the camoid and the timing of the actuation. The camoid length is 9.5 inches, which is approximately 3 bottle diameters. If the camoid is set to actuate in 2 or less bottles, the following sequence of events can occur:

1. Bottle 1 triggers actuation
2. Camoid begins rotating

3. Bottle 2 crosses photoeye and begins to be diverted. Camoid is still rotating
4. Bottle 3 crosses photoeye, triggering actuation during camoid rotation

This poses a problem because the second actuation is triggered during the first. Under the current program logic, this caused erratic behavior in the servo. The minimum number of bottles per cycle is set at four to ensure such an event will not occur under any circumstance.

Also under the current program, the photoeye must be placed at the base or neck of the bottle. If it is placed such that its position aligns with the body of the bottle, the beam will be broken twice due to the transparency of some products. This will cause two counts for every one bottle. The current program causes actuation every four counts of the photoeye.

10.3 - Results Table

The results of the test are shown in Table 19.

Camoid Laner Prototype Test: Bottle Interaction								
Test Administered by: William Robinson Caruso, James Freeman Saunders, David Booth, Shawn Burns						Date: February 28, 2007		
Bottle Type: 7305						Time: 9:00-17:00		
Test Number	Line Speed (in/sec)	Bottle Spacing (inches)	Number of Bottles	Bottles per Cycle	Down Bottle #	Motion*	Comments	Recommendations
1	24	0	6	1	all	ext.	Failure due to laning trigger while servo is in rotation. This causes servo to attempt to rotate to position B in the middle of rotating to position A. This behavior is erratic and causes downed bottles.	With current timing program, a minimum of 4 bottles per cycle is required to avoid such an issue. Program optimization could also avoid this issue
2	24	1	6	1	all	ext.		
3	24	2	6	1	all	ext.		
4	24	3	6	1	all	ext.		
5	24	0	6	2	all	ext.		
6	24	1	6	2	all	ext.		
7	24	2	6	2	all	ext.		
8	24	3	6	2	all	ext.		
9	24	0	6	4	3	ext.	The minimum spacing for this laner is approximately 2 inches. If the bottles are tighter, the bottle directly before the target bottle (bottle #3) is adversely affected.	Geometry and controls optimization can be conducted to attempt to cause the camoid to fit between tighter spaced bottles.
10	24	1	6	4	3	ext.		
11	24	2	6	4	none	ext.		
12	24	3	6	4	none	ext.		
13	24	0	6	4	none	ret.	The camoid doesn't have any trouble retracting even at minimum bottle spacing	
14	24	1	6	4	none	ret.		
15	24	2	6	4	none	ret.		
16	24	2	24	4	none	both	All bottles successfully laned. No problems.	

Each test is run 5 times to assure all problems with a batch of 6 bottles looping the test line.
*ext. = extension ret. = retraction

Table 19: Test Results

There are several key points of interest that can be concluded from the results:

- Minimum bottle spacing for reliable camoid extension: 2 inches
- Minimum bottle spacing for reliable camoid retraction: no minimum
- Line speed affects the magnitude of displacement of the bottle
- Photoeye placement

10.3.1 - Minimum Bottle Spacing: Extension

There is a minimum bottle spacing of 2 inches that is required in order for the camoid laner to reliably lane bottles. The potential for tipped bottles increases drastically when the bottles are spaced closer than 2 inches. The bottle that was most often tipped was the last bottle to continue in the default lane, bottle 3 of 6. This occurs because the camoid contacts the bottle during rotation and actively pushed the bottle aside. If the bottles are spaced more than 2 inches, the camoid avoids striking the bottle and rotates successfully between the two bottles.

10.3.2 - Minimum Bottle Spacing: Retraction

There is no minimum for bottle spacing during the retraction of the camoid; the bottles can be directly adjacent to one another. No bottles were tipped or subject to abnormal manipulation at any point during the retraction, regardless of the spacing.

10.3.3 - Magnitude of Displacement

The line speed directly affects the magnitude of displacement. Successful laning of the camoid relies on the trajectory of the bottle after the end of the camoid. The trajectory is dependent on the velocity of the bottle, which is less in slower line speeds. With slower bottle speeds, the bottle tended not to make the full diversion. This lack of displacement is also due to the decreased magnitude of momentum the bottle possesses to overcome frictional forces. The displacement problem could also be linked to the poor conveyor condition and lack of lubrication.

10.3.4 – Photoeye Placement

The servo program is set to trigger as soon as the photoeye is triggered. The best placement for the photoeye for this program proved to be directly on the outside edge of the chassis as close to the conveyor surface as possible. The placement is shown in Figure 69.



Figure 69: Photoeye Placement

10.4 - Mechanism Observations

Observations about the mechanism concluded no visible wear or fatigue. Furthermore, the mechanism operated smoothly and quietly and offered no impacts due to interference of components.

10.5 - Test Results Conclusions

The overall outcome of the testing proved to yield satisfactory results. The original design theory based successful laning on one bottle diameter, or 3 inch, spacing. The test results yield less than the original design concept. Also there is no minimum bottle spacing for the retraction, which also exceeded expectation.

The problem concerning the displacement of the bottles across the line must be addressed. It is expected that under actual line conditions (400 bottles/min, lubricated conveyors) the displacement will act similarly to the Heuft system and fully displace the bottles.

Further testing is essential if the camoid laner is to be implemented for production. However, this test proved that the camoid concept is capable of high speed bottle laning and is candidate for further more rigorous testing.

Chapter 11.0 - Cost Comparison

The final step in analyzing the camoid laner system is performing a cost analysis of all parts that were used in assembling the system. The following table shows the cost of all parts of the camoid laner compared with the Heuft Delta FW system. For detailed cost analysis and bill of materials refer to Appendix C.

Cost Comparison		
Heuft	Camoid	
\$13,000	\$15,532.32	First Unit (all electronics)
	\$9,649.09	Secondary Unit

Table 20: Cost Comparison

The cost of the camoid laner is analyzed for several different scenarios as shown in Table 20. The first unit price includes all electronics used for servo motion control, and at \$15,500 it is more expensive than the Heuft system. However, the servo electronics make up a significant portion of the total cost. As Gallo implements more servos into production, many of the instruments needed are already on the line being used for other motion control purposes. It is possible to piggyback the camoid laner onto the existing control infrastructure. This reduces the cost significantly as shown by the follow-up unit cost, which utilizes key components that are capable of controlling multiple axes.

If the laner were ever to be used in full production, several cost saving strategies could be administered such as:

- In house chassis manufacture
- Camoid price reduction for bulk purchase
- Minimizing servo size
- Piggyback existing motion control infrastructure

If these strategies are used, the original cost could potentially be reduced further.

In addition to reducing the capital cost of the laner, a single actuation servo system offers significant savings in maintenance costs as the number of cycles demanded on the system is within the design specifications of a servo. Also, the camoid system is simple enough to allow easy replacement of components as opposed to the Heuft system which requires replacement of the entire system. For example, if a servo motor required replacement it could be replaced immediately, on the line, provided the part is in stock.

Chapter 12.0 - Recommendations

Prior to implementing the camoid bottle laner in a production setting several tasks must be completed:

12.1 - Line Speed Testing

Experimentation was hindered by the lack of encoder information on the test conveyor. As a result, the laner was not tested under full speed line conditions (400 bottle/minute). It was designed specifically to accommodate full speed, and it is possible that the laner will function *better* at 400 bottle/minute. Additionally, the laner should be further tested reflecting ramping up and ramping down the line speed.

12.2 - Bottle Testing

Only one type of bottle was tested, the 7305 750mL bottle. The 7405 model should theoretically perform worse than the 7305, having a higher, less-stable center of gravity. At the very least, similar tests should be performed on 7405s. Ideally, all bottles that could run on Line 2 would be tested as well.

12.3 - Endurance Testing

The longest single run during testing was 20 minutes. Before production implementation the laner should run constantly for hours. There is no data that suggests that the laner will fail from repetition.

12.4 - Part Acquisition

If additional units are desired, parts can be purchased at much lower cost. New methods for mold fabrication using rapid prototyping now enable small batch injection molding at reasonable cost. A mold could be purchased for future use; subsequent parts would cost significantly less after the investment in a mold. The chassis could also be fabricated in-house, instead of employing an outside contractor. Finally, the servo used in the prototype was recovered from the junk rack, but was significantly larger than necessary. In the future a smaller servo, the MPL-B230P-HJ42AA, could be used, at roughly half the price.

12.5 - Program Optimization

Very little was done with optimization of the servo's controlling logic. Certain safeguards could be added to the logic to prevent misfires. Also, through the use of an encoder and a programmed delay, the photoeye could be positioned elsewhere upstream.

12.6 - Geometry Optimization

The camoid's geometry could be refined with more tests. Because bottles may not impact the laner directly on the rail, the first 1-2 inches of the camoid rise contour are frequently missed entirely. The length could therefore be shortened and the maximum rise could be increased slightly. No geometric alterations are necessary for operation, but could result in a smaller laner footprint.

Chapter 13.0 - Conclusions

Upon completion, the tests demonstrated the camoid laner to be a viable concept, and one that should be investigated further. Several tests have been outlined, to be completed before taking the camoid laner to a production setting. Many of the factors explored in the construction and experimentation of the prototype suggest that it would be a large improvement over the current system. A single-actuated bottle laner could significantly reduce maintenance costs compared to the 12-actuator Heuft Rejecter. Servo driven equipment is more reliable and longer lasting than pneumatic systems. In addition, the camoid laner performs comparably to the Heuft Rejecter under similar conditions.

References

- E&J Gallo Winery. Who We Are. Retrieved January 10th, 2007, from <http://www.ejgallo.com/>
- Engineers Handbook. Rapid Prototyping: Electron Beam Molding. Retrieved January 26, 2007 from <http://www.engineershandbook.com/Rapidprototyping/ebm.htm>.
- Free Patents Online. Patent Analytics and Patent Searching. Retrieved January 8th, 2007. from www.freepatentsonline.com.
- Goodyear Industrial. Eagle Pd Industrial Power Transmissions. Retrieved February 10, 2007, from http://www.goodyearindustrialproducts.com/powertransmission/products/pdf/eagle_pd_belt.pdf.
- Heuft USA, Inc. Container Rejection Systems. Retrieved January 10th, 2007, from www.heuft.com.
- Heuft USA, Inc. Heuft Operator Training. Maintenance Manual. Version 1.0. June 6, 2006. Page 18-21.
- KHS. Container Conveying Solutions. Retrieved November 19, 2007 from www.kisters.com/img/pool/1111_Container%20Conveying%20Systems.pdf.
- Norton, Robert L. Machine Design: An Integrated Approach. Upper Saddle River: Pearson Prentice Hall, 2006.
- Norton, Robert L. Design of Machinery. New York: McGraw Hill, 2004.
- Rockwell Automation. Motion Analyzer Software. Retrieved February 11, 2007 from www.ab.com/motion/software/motion_analyzer.html
- Rockwell Automation. Allen Bradley Servo Motors. Retrieved January 10, 2007 from www.rockwellautomation.com.
- Stratasys. Case Study. Retrieved January 19, 2007 from http://www.stratasys.com/uploadedFiles/North_America/Media/PDF%20Beta%20pulley.pdf
- Toolcraft Plastics Ltd. Explanation Of and Free Help with Stereolithography process. Retrieved January 19, 2007 from http://www.toolcraft.co.uk/help_stereolithography_process_sla_models.htm

Appendices

Appendix A - Relevant Patents

Title: Apparatus for controlling the path of transportation of articles

Document Type and Number: United States Patent 4986407

Link to this Page: <http://www.freepatentsonline.com/4986407.html>

Abstract: An apparatus for controlling the path of transportation of articles comprises a first conveyor belt which delivers the articles to a plurality of second conveyor belt which delivers the articles to a plurality of second conveyor belts arranged in parallel side-by-side relationship which continue the conveyance of the articles. A plurality of deflectors selectively deflect the articles from the first conveyor belt to one of the second conveyor belts. In order to attain an especially compact construction the first conveyor belt extends obliquely over and rests on the second conveyor belts and is a belt of such small thickness that the articles can slide from the first conveyor belt onto one of the second conveyor belts without the risk of toppling over. The deflectors are arranged on the side of the first conveyor belt facing away from the direction of conveyance of the second conveyor belts. The first conveyor belt can be a steel belt having a thickness between 0.1 to 0.5 mm.

Inventors: Heuft, Bernhard

Application Number: 294628

Filing Date: 1988-12-07

Publication Date: 1991-01-22

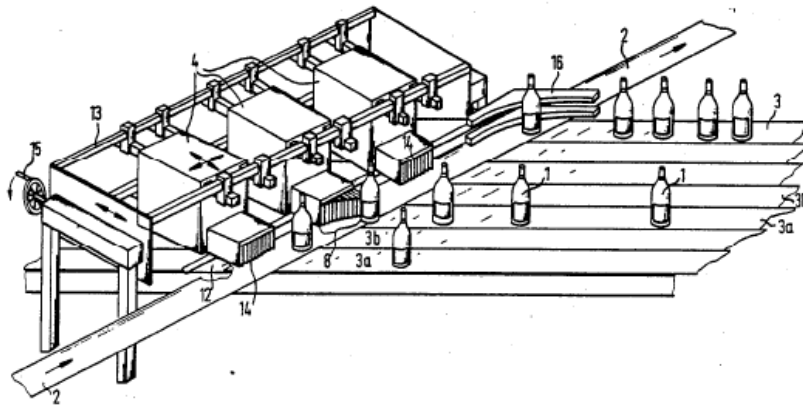


Figure 70: Patent 4,986,407

Title: Linear articulated pusher

Document Type and Number: United States Patent 4643291

Link to this Page: <http://www.freepatentsonline.com/4643291.html>

Abstract: A pusher mechanism supported on a framework for deflecting objects from a conveyor has a retractable pusher which is mounted for linear movement transversely across the conveyor. A paddle is pivotally attached at its midportion to an outer end of the pusher. A movable link is secured between the framework and an end of the paddle. Due to these paddle connections, controlled linear movement of the pusher will cause the paddle to articulate on the pusher from a rest position to an operating position at which an object is deflected from the conveyor and back to the rest position.

Inventors: Counter, Louis F.; Callies, Fritz A.; Lee, Phillip L.;

Application Number: 820855

Filing Date: 1986-01-21

Publication Date: 1987-02-17

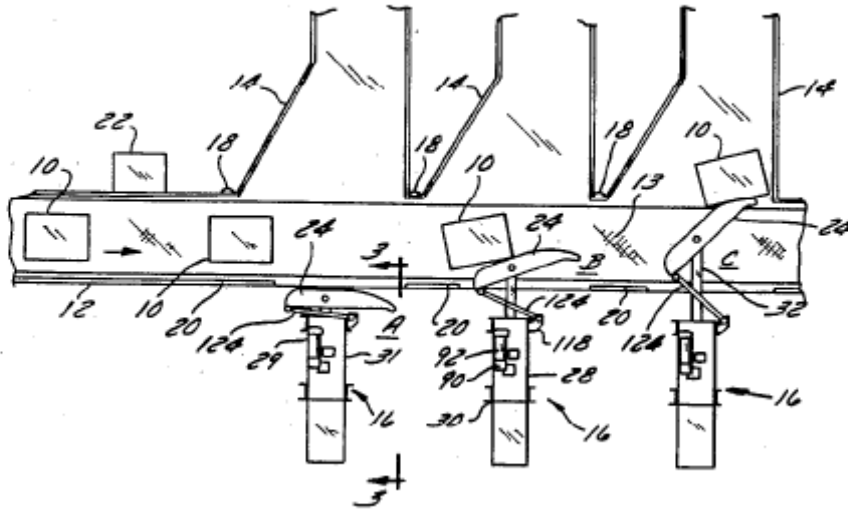


Figure 71: Patent 4,643,291

Title: Means for laterally deflecting articles from a path of travel

Document Type and Number: United States Patent 4321994

Link to this Page: <http://www.freepatentsonline.com/4321994.html>

Abstract: An apparatus for laterally deflecting selected articles from a first conveyor to one or more other conveyors comprises either extensible and retractable deflective segments, or gas nozzles whose intensity is adjustable. The deflective segments have tapered front faces which jointly form a smooth deflecting face whose taper increases in the direction of conveyance. The number of segments used depends on the speed component required, and the segments are extended by only a portion of the lateral distance the articles are to cover, the remainder of the distance being covered by the imparted inertia. Alternative embodiments include a deflecting wedge or flap.

Inventors: Heuft, Bernhard;

Application Number: 141847

Filing Date: 1980-04-21

Publication Date: 1982-03-30

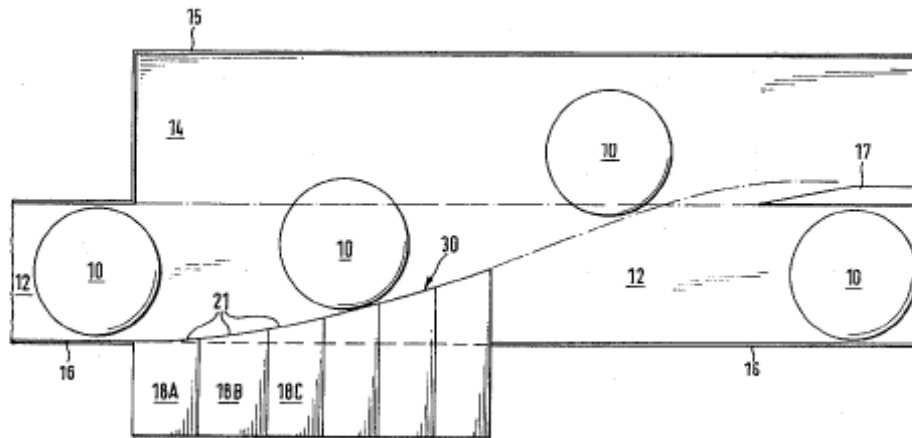


Figure 72: Patent 4,321,994

Title: Apparatus for laterally deflecting articles

Document Type and Number: United States Patent 4369873

Link to this Page: <http://www.freepatentsonline.com/4369873.html>

Abstract: Apparatus for laterally deflecting articles, such as bottles, from the normal path of a series of such articles, on the basis of a predetermined criterion, such as size or shape. The apparatus may be in the form of extensors which operate transversely to the direction of travel of the articles, in such manner that at any given moment only those extensors are extended which contact the article then being deflected.

Inventors: Heuft, Bernhard;

Application Number: 002261

Filing Date: 1979-01-10

Publication Date: 1983-01-25

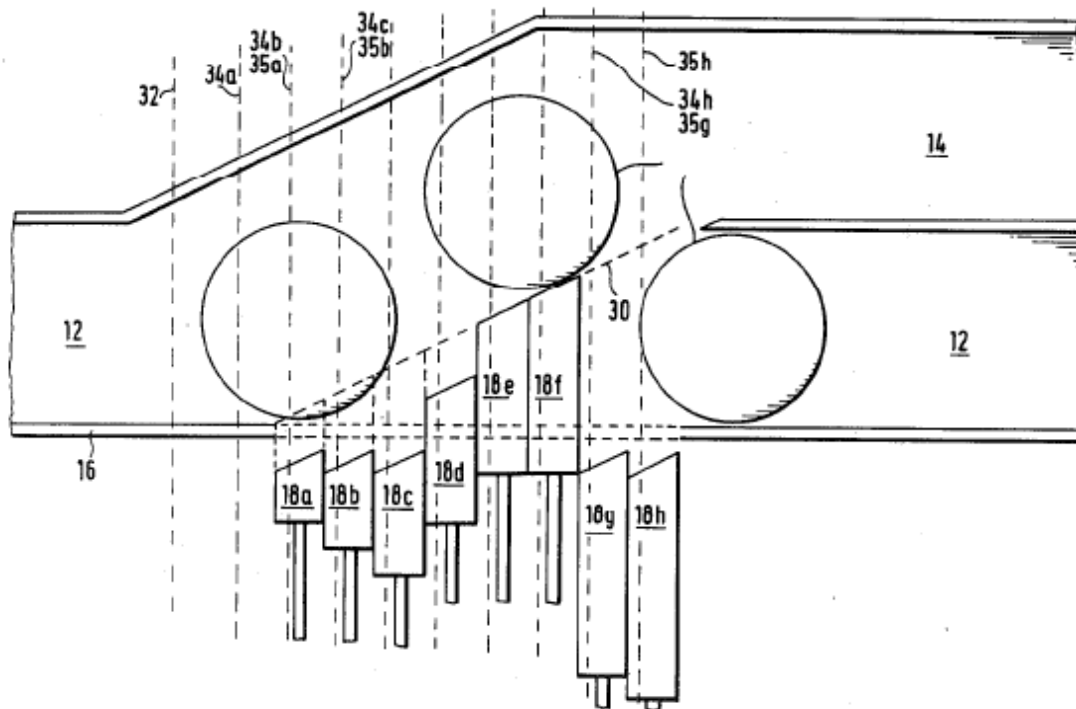


Figure 73: Patent 4,369,873

Title: Device for singling out articles from a flow of such articles

Document Type and Number: United States Patent 6588575

Link to this Page: <http://www.freepatentsonline.com/6588575.html>

Abstract: The device for diverting individual items from a stream of items which are conveyed on a transport apparatus has an extendable and retractable diversion element, which is operated via a gear unit by a drive apparatus moving or swinging to and fro and is precisely time-controllable, in order to impart a cross impulse to items to be diverted so that they slide from the transport apparatus across the direction of transport. The diversion element carries out a complete extension and retraction movement during a single to-or-fro movement or swing of the drive apparatus. The drive apparatus moving to and fro can be a pneumatic cylinder, and the gear unit which transmits the piston movement to the diversion element can be a coulisse link mechanism or a toggle lever.

Inventors: Heuft, Bernhard; Kristandt, Gerd;

Application Number: 030746

Filing Date: 2001-11-01

Publication Date: 2003-07-08

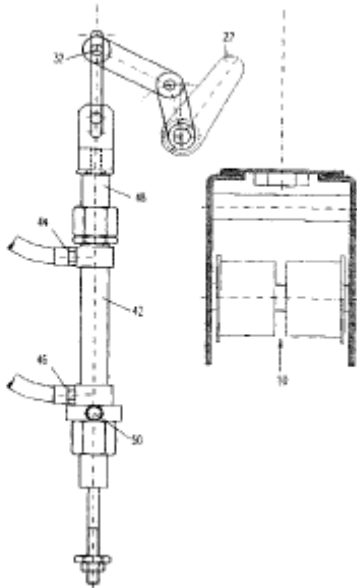


Figure 74: Patent 6588575

Title: Container diverter

Document Type and Number: United States Patent 6822181

Link to this Page: <http://www.freepatentsonline.com/6822181.html>

Abstract: The present invention provides a device and method for selectively removing an article from a stream or line of similar articles travelling in a pathway on a transport system such as a conveyor. The invention utilizes a synchronous electric motor which, in response to a signal to reject a specific article in the stream, rotates an article-contacting member or paddle into the path of the stream of articles travelling along the pathway whereby it contacts and smoothly removes that article from the stream. The use of a synchronous motor to effect the rotation of the paddle is very important to the present invention.

Inventors: Linton, Fredrick L.;

Application Number: 891616

Filing Date: 2001-06-27

Publication Date: 2004-11-23

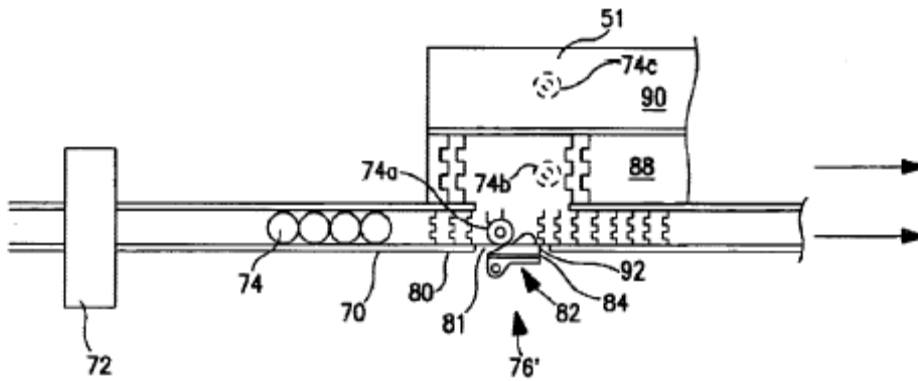


Figure 75: Patent 6,822,181

Title: Side Transfer Sorting Conveyor

Document Type and Number: United States Patent 3791518

Link to this Page: <http://www.freepatentsonline.com/3791518.html>

Abstract: A sorting conveyor having a plurality of movable plaques on one conveyor base arranged to sort merchandise or similar articles carried on another conveyor positioned at one side of the sorting conveyor. The separation of articles may be controlled by some particular property of articles such as weight, size, or color, sensed in a known manner. The plaques on the sorting conveyor are activated to engage the articles carried by the adjoining conveyor and change their relative position so that a series of fences can direct the reoriented articles into predetermined paths

Inventors: Vanderhoof, Frank B.;

Application Number: 355,000

Filing Date: 1973-04-27

Publication Date: 1974-02-12

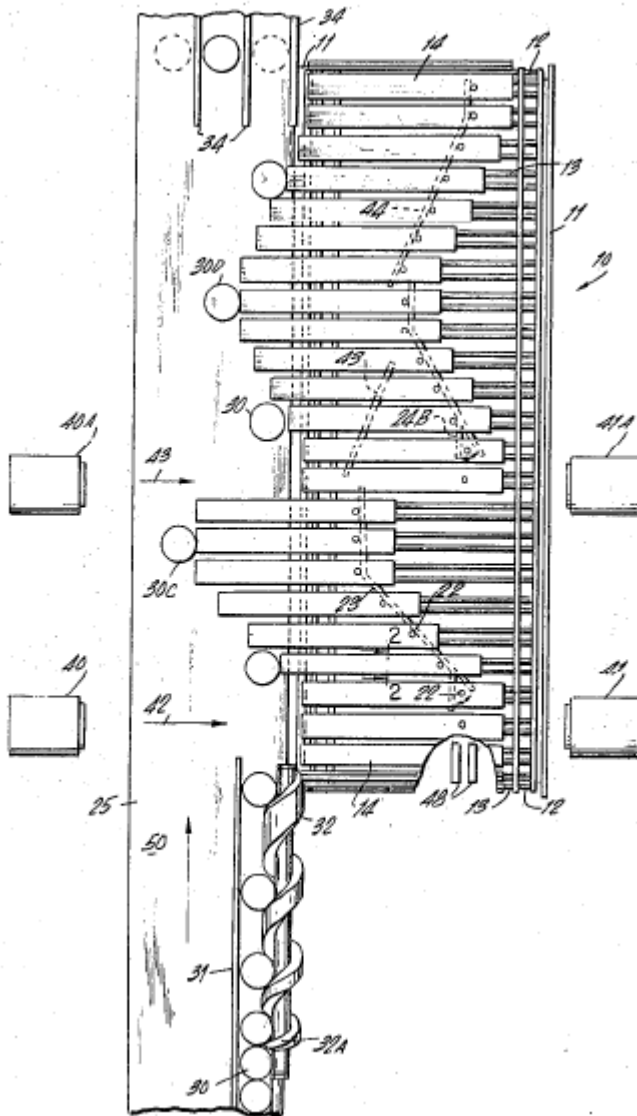


Figure 76: Patent 3,791,518

Appendix B - Rapid Prototyping Quotes

A number of quotes were obtained before ordering the rapid prototyped camoid. A number of different RP techniques and companies were surveyed. The SLA option by RPDG was eventually chosen for the fabrication of the camoid.

Company	Process	Material	Lead Time	Price	Discount	Final \$
RPDG	SLA	ABS-Like	3 days	1219	20	975.2
	SLS	Nylon	5 days	3888	0	3888
	FDM	ABS-Black	3 days	1612	0	1612
	FDM	PC-White	3 days	1612	0	1612
	Objet	ABS-Like	3 days	2232	0	2232
RedEye RPM	FDM	PC-ABS Blend	5 days	1500	10	1350
Realize	SLA	Accura 25	5 days	3550	10	3195

Appendix C - Bill of Materials

Project Budget: Camoid Laner Single Unit Cost						
Item	Description	Part Number	Unit Cost	QTY	Cost	Subtotals
Camoid	SLA Part Cost		\$1,219.00	1	\$1,219.00	\$1,050.56
	20% Discount		-\$244.00	1	-\$244.00	
	Sales Tax		\$75.56	1	\$75.56	
Allen-Bradley Servo	460V 6.1 N-m 2.3 kW Low Inertia Servo	MPL-B4520P-MJ22AA	\$1,352.35	1	\$1,352.35	\$13,022.96
Servo Power Cable	Power	A-B 2090-XXNPMP-14S05 MTR PWR	\$98.00	1	\$98.00	
Servo Feedback Cable	Feedback	A-B 2090-UXNFBMP-S05 MOTOR CAB	\$105.53	1	\$105.53	
Alpha Gearbox	10:1 Planetary Gearbox		\$300.00	1	\$300.00	
PLC Modules					\$0.00	
ControlLogix Chassis	7 Slot ControlLogix Chassis	1756-A7	\$291.28	1	\$291.28	
Ethernet Module	CLX EtherNet/IP 10/100 Bridge Module	1756-ENBT	\$1,159.84	1	\$1,159.84	
DC Input Module	10-31 VDC Input 16 Pts (20 Pin)	1756-OB16E	\$206.27	1	\$206.27	
DC Output Module	10-31 VDC Elec Fused Output 16 Pts (20 Pin)	1756-OB16E	\$332.14	1	\$332.14	
SERCOS Module	3 Axis SERCOS Interface Servo Module	1756-M03SE	\$751.26	1	\$751.26	
Module Power Supply	19.2-32 VDC Power Supply (5V @ 10 Amp)	1756-PB72	\$530.50	1	\$530.50	
ControlLogix Processor	Logix5561 Processor With 2Mbyte Memory	1756-L61	\$3,364.20	1	\$3,364.20	
	Module, Integrated, 400/460V, 6 kW Conv. 9A Inv	2094-BC01-M01	\$1,997.50	1	\$1,997.50	
SERCOS Fi-Os Cable	Fiber Optic Cable		\$81.00	2	\$162.00	
Kinetix Ultra3000 Servo Driver	480V AC 3 Phase	2098-DSD-HV050	\$1,863.20	1	\$1,863.20	
Stegmann Shaft Encoder	5000 pulse/rev 6-30V	DG60L WSR 5000	\$300.00	1	\$300.00	
Stegmann Encoder Cable	12-Pin Cable	DOL-2312-G03MMA3	\$85.00	1	\$85.00	
	Next-Day Shipping		\$40.00	1	\$40.00	
Banner PhotoEye	PE QS18VP6LPQ5	PE QS18VP6LPQ5	\$61.85	1	\$61.85	
	Cable 9m		\$28.23			
	Bracket		\$16.54	1	\$16.54	
	Reflector		\$5.50	1	\$5.50	
Drive Sprocket	Eagle PD 28-Tooth	W-28S-H	\$52.50	2	\$105.00	
Drive Belt	Eagle Pd 720mm Belt	Pd W-720	\$35.19	1	\$35.19	

Sprocket Bushings						
Martin QD Bushing	H-size 3/4 Bore	H 3/4 QD	\$9.44	1	\$9.44	
Martin QD Bushing	H-size 32 mm Bore	H32	\$6.21	1	\$6.21	
	Tax		\$0.46	1	\$0.46	
Lovejoy ROSTA Tensioner	SE18 Tension Arm	SE-18 ROSTA	\$41.10	1	\$41.10	
Lovejoy ROSTA Roller Idler	Smooth Roller Idler	685144-53028	\$34.32	1	\$34.32	
	Tax		\$2.53	1	\$2.53	\$234.25
Chassis	Labor		\$507.50	1	\$507.50	
	Parts		\$576.60	1	\$576.60	
	Tax		\$78.60	1	\$78.60	
SKF Bearing	4-Bolt Flange Mount 3/4 Shaft Bearing	SKF FY 3/4 TF	\$29.21	2	\$58.42	
Hardware	1/4-20x1 hex head bolt		\$0.04	8	\$0.32	
	1/4 split washer		\$0.02	9	\$0.18	
	1/4-20 Nylock nut		\$0.04	1	\$0.04	
	5/16-18x1.25 hex head bolt		\$0.04	4	\$0.16	
	5/16 split washer		\$0.03	8	\$0.24	
	3/8-16x1 hex head bolt		\$0.05	8	\$0.40	
	3/8 washer		\$0.02	8	\$0.16	
	3/8-16 Nylock nut		\$0.04	8	\$0.32	
	3/4 washer		\$0.05	4	\$0.20	
	3/16x3/16x1 key		\$0.02	3	\$0.06	
	3/4 shaft collar		\$2.35	1	\$2.35	\$1,225.55
TOTAL						\$15,533.32

Table 21: Full Bill of Materials

Project Budget: Follow-up Cost

Item	Description	Part Number	Unit Cost	QTY	Cost	Subtotals
Camoid	SLA Part Cost		\$1,219.00	1	\$1,219.00	\$1,050.56
	20% Discount		-\$244.00	1	-\$244.00	
	Sales Tax		\$75.56	1	\$75.56	
Allen-Bradley Servo	460V 6.1 N-m 2.3 kW Low Inertia Servo	MPL-B4520P-MJ22AA	\$1,352.35	1	\$1,352.35	\$7,138.73
Servo Power Cable	Power	A-B 2090-XXNPMP-14S05 MTR PWR	\$98.00	1	\$98.00	
Servo Feedback Cable	Feedback	A-B 2090-UXNFBMP-S05 MOTOR CAB	\$105.53	1	\$105.53	
Alpha Gearbox	10:1 Planetary Gearbox		\$300.00	1	\$300.00	
PLC Modules					\$0.00	
SERCOS Module	3 Axis SERCOS Interface Servo Module	1756-M03SE	\$751.26	1	\$751.26	
	Module, Integrated, 400/460V, 6 kW Conv. 9A Inv	2094-BC01-M01	\$1,997.50	1	\$1,997.50	
SERCOS Fi-Os Cable	Fiber Optic Cable		\$81.00	2	\$162.00	
Kinetix Ultra3000 Servo Driver	480V AC 3 Phase	2098-DSD-HV050	\$1,863.20	1	\$1,863.20	
Stegmann Shaft Encoder	5000 pulse/rev 6-30V	DG60L WSR 5000	\$300.00	1	\$300.00	
Stegmann Encoder Cable	12-Pin Cable	DOL-2312-G03MMA3	\$85.00	1	\$85.00	
	Next-Day Shipping		\$40.00	1	\$40.00	
Banner PhotoEye	PE QS18VP6LPQ5	PE QS18VP6LPQ5	\$61.85	1	\$61.85	
	Cable 9m		\$28.23			
	Bracket		\$16.54	1	\$16.54	
	Reflector		\$5.50	1	\$5.50	
Drive Sprocket	Eagle PD 28-Tooth	W-28S-H	\$52.50	2	\$105.00	\$234.25
Drive Belt	Eagle Pd 720mm Belt	Pd W-720	\$35.19	1	\$35.19	
Sprocket Bushings						
Martin QD Bushing	H-size 3/4 Bore	H ¾ QD	\$9.44	1	\$9.44	
Martin QD Bushing	H-size 32 mm Bore	H32	\$6.21	1	\$6.21	
	Tax		\$0.46	1	\$0.46	
Lovejoy ROSTA Tensioner	SE18 Tension Arm	SE-18 ROSTA	\$41.10	1	\$41.10	
Lovejoy ROSTA Roller Idler	Smooth Roller Idler	685144-53028	\$34.32	1	\$34.32	
	Tax		\$2.53	1	\$2.53	
Chassis	Labor		\$507.50	1	\$507.50	
	Parts		\$576.60	1	\$576.60	
	Tax		\$78.60	1	\$78.60	

SKF Bearing	4-Bolt Flange Mount 3/4 Shaft Bearing	SKF FY 3/4 TF	\$29.21	2	\$58.42	\$1,225.55
Hardware	1/4-20x1 hex head bolt		\$0.04	8	\$0.32	
	1/4 split washer		\$0.02	9	\$0.18	
	1/4-20 Nylock nut		\$0.04	1	\$0.04	
	5/16-18x1.25 hex head bolt		\$0.04	4	\$0.16	
	5/16 split washer		\$0.03	8	\$0.24	
	3/8-16x1 hex head bolt		\$0.05	8	\$0.40	
	3/8 washer		\$0.02	8	\$0.16	
	3/8-16 Nylock nut		\$0.04	8	\$0.32	
	3/4 washer		\$0.05	4	\$0.20	
	3/16x3/16x1 key		\$0.02	3	\$0.06	
	3/4 shaft collar		\$2.35	1	\$2.35	
TOTAL						

Table 22: Bill of Materials with Piggy Backed Electronics

Appendix D - Motion Analyzer Input Values

Each table represents a tab for the motor sizing application. The software can be downloaded for free at www.ab.com/motion/software/motion_analyzer.html.

Axis Setup	
Load Type	Rotary
Motor Type	Rotary
Actuator Type	Non-selected
Voltage Selection	
Supply Type	AC 3-phase
Voltage Type	Single
Nominal Voltage (volts)	480
Tolerances	±10%
Motor Parameters	
Max ambient (°C)	40
Brake	NO

Table 23: Axis Setup Tab

Cycle profile									
Cycle Profile mode:	Multi-segment								
Auto Compile:	ON								
Segment Number	1	2	3	4	5	6	7	8	9
Curve Type (Linear/S-curve)	L	L	L	L	L	L	L	L	L
Initial Velocity (deg/sec)	0	0	878.6	878.6	0	0	1098	1098	1174
Final Velocity (deg/sec)	0	878.6	878.6	0	0	1098	1098	1174	0
Distance (deg)	0	32.8	140	7.5	0	7.5	140	10	65.1
Time (sec)	0.413	0.07466	0.07466	0.01707	1.593	0.01367	0.1276	0.008805	0.1109
Acc/Dec (rpm/sec)	0	1961	1961	-8577	0	13380	0	1448	-1764
Thrust (N-m)	0	0	0	0	0	0	0	0	0
Added Inertia (kg-m ²)	0	0	0	0	0	0	0	0	0
Denotes an entered value									

Table 24: Cycle Profile Tab

Mechanism	
Primary Inertia (kg-m²)	0.0059
Secondary Inertia (kg-m²)	0
Secondary Mass (kg)	0
Losses (N-m)	0
Starting Angle (deg)	220
Axis Separation (mm)	0

Table 25: Mechanism Tab

Transmission Stages	
Transmission	Belt Drive
Ratio	10
Inertia (kg-m²)	0.0005
Efficiency	98%
Friction Torque (N-m)	0

Table 26: Transmission Stages Tab

Appendix E - Servo Details

The following motor descriptions were gathered from Rockwell Automation's web catalog which can be found at http://literature.rockwellautomation.com/idc/groups/literature/documents/pp/mp-pp001_en-p.pdf.

PRODUCT PROFILE

MP-SERIES LOW INERTIA MOTORS

The Allen-Bradley MP-Series Low Inertia, high output brushless servo motors use innovative design characteristics to reduce motor size while delivering significantly higher torque. These compact and highly dynamic brushless servo motors from Rockwell Automation are designed to meet the demanding requirements of high performance motion systems. This series of servo motors is typically used with the Allen-Bradley Kinetix 6000, Kinetix 7000 and Ultra3000 servo drive families. Available in nine frame sizes, these motors provide continuous stall torque from 0.26 to 163 Nm (2.3-1440 lb-in.) and peak torque from 0.77 to 278 Nm (6.8-2460 lb-in.)

MP-SERIES LOW INERTIA MOTORS PROVIDE:

- Innovative winding technology yields up to 40% higher torque per unit size than conventional servo motors
- Improved winding insulation material for enhanced thermal management and heat transfer, resulting in higher performance
- High-energy rare-earth magnets for quicker acceleration
- Low profile, field reversible motor connectors for minimal servo motor impact on machine design
- Integral 24 volt brake option
- Broad torque range - all within one motor family
- Optional Shaft Seal for IP 66 environmental rating
- Standard IEC 72-1 mounting dimensions
- Operating temperature range:
0 - 40° C (32 - 104° F).

BRUSHLESS SERVO MOTORS WITH ABSOLUTE FEEDBACK OPTION



Applications where more power is required in a smaller package will benefit from the use of MP-Series Low Inertia Motors. Typical applications include: packaging, converting, electronics assembly, automotive, metal forming and material handling.

HIGH PERFORMANCE FEEDBACK

MP-Series Low Inertia motors are available with high performance encoders with a choice of Single-turn (-E, -S) or Multi-turn (-V, -M) high resolution feedback.

- Up to 2 million counts per revolution (-M and -S) for smooth performance (MPL-A/B3xx, -A/B4xx, -A/B45xx, -A/B5xx, -B6xx, -B8xx, and -B9xx motors).
- Up to 260 thousand counts per revolution (-E and -V) for smooth performance (MPL-A/B15xx and -A/B2xx motors).
- Single-turn encoder provides high-resolution absolute position feedback within one turn.
- Multi-turn encoder provides high-resolution absolute position feedback with within 4096 turns. The electromechanical design does not require a battery.

Smart Motor Technology

- On-board memory retains motor identity
- RS-485 communication link automatically reports identity to the system upon startup for reduced commissioning time

The MP-Series Low Inertia Motors are UL recognized components to applicable UL and CSA standards and CE marked for all applicable directives.

ALLEN-BRADLEY • ROCKWELL SOFTWARE • DODGE • RELIANCE ELECTRIC **Rockwell Automation**

Figure 77: Servo Overview

460 VOLT MOTOR SPECIFICATIONS

Catalog Number	Rated Speed rpm	Rated Output kW	Rotor Inertia* kg-m ² (lb-in.-s ²)	Continuous Stall Torque Nm (lb-in.)	Peak Stall Torque Nm (lb-in.)	Continuous Stall Current Amperes (0-peak)	Peak Stall Current Amperes (0-peak)	460 volt
MPL-B1510V	8000	0.16	0.000006 (0.000053)	0.26 (2.3)	0.77 (6.8)	0.95	3.1	
MPL-B1520U	7000	0.27	0.000011 (0.000097)	0.49 (4.3)	1.58 (14)	1.80	6.1	
MPL-B1530U	7000	0.39	0.000020 (0.00018)	0.90 (8.0)	2.82 (25)	2.00	7.2	
MPL-B210V	8000	0.37	0.000014 (0.00012)	0.55 (4.9)	1.52 (13.5)	1.75	5.8	
MPL-B220T	6000	0.62	0.000037 (0.00033)	1.61 (14.2)	4.74 (42)	3.30	11.3	
MPL-B230P	5000	0.86	0.000060 (0.00053)	2.10 (18.6)	8.20 (73)	2.60	11.3	
MPL-B310P	5000	0.77	0.000044 (0.00039)	1.58 (14.0)	3.61 (32.0)	2.4	7.1	
MPL-B320P	5000	1.5	0.000078 (0.00069)	3.05 (27.0)	7.91 (70.0)	4.5	14.0	
MPL-B330P	5000	1.8	0.00012 (0.0010)	4.18 (37.0)	11.1 (98.0)	6.1	19.0	
MPL-B420P	5000	1.9	0.00026 (0.0023)	4.74 (42.0)	13.5 (120.0)	6.4	22.0	
MPL-B430P	5000	2.2	0.00038 (0.0033)	6.55 (58.0)	19.8 (175.0)	9.2	32.0	
MPL-B4520P	5000	2.1	0.00028 (0.0024)	5.65 (50.0)	13.5 (120.0)	8.5	24.0	
MPL-B4530F	3000	2.1	0.00040 (0.0036)	8.25 (73.0)	20.3 (180.0)	7.0	21.0	
MPL-B4530K	4000	2.6	0.00040 (0.0036)	8.25 (73.0)	20.3 (180.0)	11.0	31.0	
MPL-B4540F	3000	2.6	0.00052 (0.0046)	10.2 (90.0)	27.1 (240.0)	9.1	29.0	
MPL-B4560F	3000	3.2	0.00078 (0.0067)	14.1 (125.0)	34.4 (305.0)	11.8	36.0	
MPL-B520K	4000	3.5	0.00078 (0.0069)	10.7 (95.0)	23.2 (205.0)	11.5	33.0	
MPL-B540D	2000	3.4	0.00147 (0.013)	19.4 (172.0)	41.0 (362.0)	10.5	23.0	
MPL-B540K	4000	5.4	0.00147 (0.013)	19.4 (172.0)	48.6 (430.0)	20.5	60.0	
MPL-B560F	3000	5.5	0.00213 (0.019)	26.8 (237.0)	67.8 (600.0)	20.6	68.0	
MPL-B580F	3000	7.1	0.00289 (0.023)	34.0 (301.0)	87.0 (770.0)	26.0	94.0	
MPL-B580J	3800	7.9	0.00289 (0.023)	34.0 (301.0)	87.0 (770.0)	32.0	115.0	
MPL-B640F	3000	6.1	0.00400 (0.0354)	36.7 (325.0)	72.3 (640.0)	32.1	65.0	
MPL-B660F	3000	6.15	0.00580 (0.051)	48.0 (425.0)	101.1 (895.0)	38.5	96.0	
MPL-B680D	2000	9.3	0.00775 (0.0685)	62.8 (556.0)	154.2 (1365.0)	34.0	94.0	
MPL-B680F	3000	7.5	0.00775 (0.0685)	60.0 (531.0)	108.5 (960.0)	48.0	96.0	
MPL-B860D	2000	12.5	0.0169 (0.150)	83.0 (735.0)	152.5 (1350.0)	47.5	95.5	
MPL-B880C	1500	12.6	0.0224 (0.198)	110.0 (973.0)	203.0 (1800.0)	47.5	97.5	
MPL-B880D	2000	12.6	0.0224 (0.198)	110.0 (973.0)	147.0 (1300.0)	67.0	96.0	
MPL-B960B	1200	12.7	0.0273 (0.242)	130.0 (1150.0)	231.0 (2050.0)	42.5	94.0	
MPL-B960C	1500	14.8	0.0273 (0.242)	124.3 (1100.0)	226.0 (2000.0)	55.0	125.0	
MPL-B960D	2000	15.0	0.0273 (0.242)	124.3 (1100.0)	226.0 (2000.0)	70.0	125.0	
MPL-B980B	1000	15.2	0.0354 (0.313)	162.7 (1440.0)	278.0 (2460.0)	40.0	94.0	
MPL-B980C	1500	16.8	0.0354 (0.313)	158.2 (1400.0)	271.0 (2400.0)	68.0	140.0	
MPL-B980D	2000	18.6	0.0354 (0.313)	158.2 (1400.0)	260.0 (2300.0)	79.0	140.0	

* Rotor inertia may vary slightly depending upon feedback and brake options.

Appendix F - Servo Driver Details

All information gathered from Rockwell Automation Publication http://www.ab.com/motion/controllers/2098-BR002A-EN-P_1001.pdf

A Global Solution

The Ultra3000 family creates a complete set of servo drive products ranging from simple stand-alone indexing applications to multi-axis integrated motion. These high-performance, digital servo drives meet global voltage requirements and provide flexibility to perform in a variety of machine control architectures. In addition, the Ultra3000 drive is integrated with the ControlLogix platform via SERCOS interface™ for integrated motion. The Ultra3000i digital servo drive with indexing adds basic control capability to the Ultra3000 feature set.

The Ultra3000 family uses the Ultraware software configuration and diagnostic tool set which includes sophisticated digital scope capability, a comprehensive array of diagnostics, and a file management system that helps organize multiple configuration files and motion programs. The Ultra3000 with SERCOS drive is configured through RSLogix 5000 software providing one platform for both motion and machine control.

To complete your system, the entire Ultra3000 family operates a wide variety of Allen-Bradley high-performance rotary servomotors. The Ultra3000 also offers seamless support of high-performance linear motors for your most demanding linear motion applications.



Ultra3000 30 Amp Servo Drive

A Broad Range of Power and Flexibility

- v The Ultra3000 provides simple integration into Allen-Bradley machine control architectures.
- v The Ultra3000 can operate a wide variety of brushless servomotors, including Allen-Bradley MP-, F-, Y-, N- and W-Series and 1326AB motors along with linear and third-party motors.
- v Ultra3000 drives use Smart Motor Technology to provide automatic identification of a specific motor connected to the drive. This reduces commissioning time and safeguards against incorrect motor replacement.
- v The Ultra3000 family accepts high resolution encoder feedback for demanding, high precision applications.
- v The Ultra3000 incorporates application proven designs, tested individually and within overall architectures, to provide world class reliability and increase your machine productivity.
- v The Ultra3000i's built-in indexing capability can eliminate the need for a motion controller or PLC card for point to point positioning moves.
- v To eliminate costly and time consuming machine homing cycles, the Ultra3000 has built-in support for multi-turn absolute encoders or an option to supply external logic power to maintain position during power loss.
- v With Ultraware software the Ultra3000 has a powerful commissioning and diagnostic tool designed to increase your productivity and optimize system performance quickly and easily.
- v When using the Ultra3000 with RSLogix 5000 software as an integrated motion solution programmers can easily configure and add drives and motion axes using wizard-based configuration dialogs.

Ultra3000 Features:

- 100-480V AC options, single and three phase input
- SERCOS or DeviceNet connectivity options
- 7.5A to 150A peak current capability
- Standard high-density D-Shell connectors
- Field programmable flash memory firmware storage
- Seven segment LED for status and error codes
- Eight selectable general purpose inputs
- Four selectable general purpose outputs and relay output
- Serial port for RS-232/RS-485 communications
- CE compliance and UL listed to U.S. and Canadian safety standards



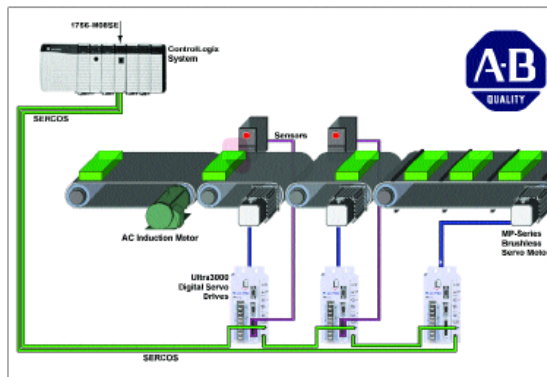
Ultra Family

Figure 78: Driver Details and Benefits

Ultra3000 Digital Servo Drive Specifications

ELECTRICAL CHARACTERISTICS	2098-DSD-005 2098-DSD-010 2098-DSD-020	2098-DSD-030 2098-DSD-075 2098-DSD-150	2098-DSD-HV030 2098-DSD-HV050 2098-DSD-HV100	2098-DSD-HV150 2098-DSD-HV220
Peak Output Current (Amps)	7.5/15/30	30/75/150	14/22/46	68/94
Continuous Output Current (Amps)	2.5/5/10	15/35/65	7/11/23	34/47
Continuous Output Power (kW)	0.5/1/2	3/7.5/15	3/5/10	15/22
INPUT				
Continuous Input Current (Amps RMS)	5/9/18	28/30/46	4/7/14	20/28
Input Voltage	100-240 Volt AC Single-Phase (Three-Phase for -075 and -150)		230-460 Volt AC Three-Phase	
	Optional 5VDC external logic power		12-24 VDC required for Digital I/O	
Input Frequency	47-63 Hz			
OPERATING MODES AND COMMAND SOURCES				
			Ultra3000	
Analog Velocity/Current Mode	+/- 10 Volt input			
Preset Velocity, Current, and Follower Ratios	8 presets, binary selection by digital inputs or serial commands, electronic gearing			
Step and Direction, Step Up/Step Down	2.5 MHz maximum frequency, Differential or single-ended input			
Master Encoder Following	2.5 MHz maximum line frequency, Differential or single-ended input			
Digital Serial Commands	Via serial port and 7-bit ASCII protocol			
Modes	Current, Velocity, Position control			
			Ultra3000i	
Indexing	64 configurable indexes, selectable by digital inputs or serial commands			
Positioning Types	Blended moves at a nonzero velocity, Jogging, Stop Index via digital input or serial command			
Home Routines	Absolute, Incremental, Registration, Jog			
SERCOS	Home-to-sensor, home-to-inaiker, home-to-sensor/marker, or home-to-current-valueg SERCOS interface			
INPUTS/OUTPUTS				
General-Purpose Digital Inputs	8 Optically Isolated 12-24 Volt, Active High Inputs - Assignable to one or more selections			
General-Purpose Digital Outputs	4 Optically Isolated 12-24 volt Outputs, 50 Milliampere Maximum			
General-Purpose Relay Output	1 Normally Open Relay, 30 volts DC Maximum Voltage, 1 Ampere Maximum Current			
Registration Input Capture Response	<100 microseconds			
Analog Command Input	1 14-Bit Analog-to-Digital Converter (+/- 10v, Differential)			
General-Purpose Analog Output	1 8-Bit Digital-to-Analog Converter (+/- 10v, +/- 2ma, single-ended)			
COMMUNICATIONS				
Serial	1 port with RS-232/RS-422/RS-485 at 1200-57,600 baud			
Networking	DeviceNet			
MOTOR FEEDBACK				
Input Modes	Incremental with Index, Sine/cosine High Resolution Absolute (Single and Multi-turn)			
Maximum Input Frequency	2.5 MHz (Encoder Lines), Over 1 million counts/rev (High Resolution)			
Commutation Startup	Hall Sensor			
AUXILIARY FEEDBACK				
Operation	Auxiliary Position Loop Feedback Input			
Input Modes	A quad B			
Input Type	Line Receiver			
Maximum Input Frequency	2.5 MHz (Encoder Lines)			

*HV indicates the 230-460V AC version of the drive
All drives available in indexing non-indexing, SERCOS, DeviceNet or indexing DeviceNet versions*



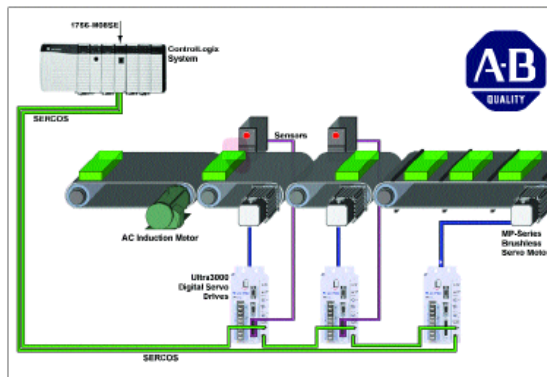
Smart Belt with Ultra3000 Digital Servo Drive and ControlLogix SERCOS interface

Figure 79: Driver Specifications

Ultra3000 Digital Servo Drive Specifications

ELECTRICAL CHARACTERISTICS	2098-DSD-005 2098-DSD-010 2098-DSD-020	2098-DSD-030 2098-DSD-075 2098-DSD-150	2098-DSD-HV030 2098-DSD-HV050 2098-DSD-HV100	2098-DSD-HV150 2098-DSD-HV220
Peak Output Current (Amps)	7.5/15/30	30/75/150	14/22/46	68/94
Continuous Output Current (Amps)	2.5/5/10	15/35/65	7/11/23	34/47
Continuous Output Power (kW)	0.5/1/2	3/7.5/15	3/5/10	15/22
INPUT				
Continuous Input Current (Amps RMS)	5/9/18	28/30/46	4/7/14	20/28
Input Voltage	100-240 Volt AC Single-Phase (Three-Phase for -075 and -150)		230-460 Volt AC Three-Phase	
	Optional 5VDC external logic power		12-24 VDC required for Digital I/O	
Input Frequency	47-63 Hz			
OPERATING MODES AND COMMAND SOURCES				
			Ultra3000	
Analog Velocity/Current Mode	+/- 10 Volt input			
Preset Velocity, Current, and Follower Ratios	8 presets, binary selection by digital inputs or serial commands, electronic gearing			
Step and Direction, Step Up/Step Down	2.5 MHz maximum frequency, Differential or single-ended input			
Master Encoder Following	2.5 MHz maximum line frequency, Differential or single-ended input			
Digital Serial Commands	Via serial port and 7-bit ASCII protocol			
Modes	Current, Velocity, Position control			
			Ultra3000i	
Indexing	64 configurable indexes, selectable by digital inputs or serial commands			
Positioning Types	Blended moves at a nonzero velocity, Jogging, Stop Index via digital input or serial command			
Home Routines	Absolute, Incremental, Registration, Jog			
SERCOS	Home-to-sensor, home-to-inarker, home-to-sensor/marker, or home-to-current-valueg SERCOS interface			
INPUTS/OUTPUTS				
General-Purpose Digital Inputs	8 Optically Isolated 12-24 Volt, Active High Inputs - Assignable to one or more selections			
General-Purpose Digital Outputs	4 Optically Isolated 12-24 volt Outputs, 50 Milliampere Maximum			
General-Purpose Relay Output	1 Normally Open Relay, 30 volts DC Maximum Voltage, 1 Ampere Maximum Current			
Registration Input Capture Response	<100 microseconds			
Analog Command Input	1 14-Bit Analog-to-Digital Converter (+/- 10v, Differential)			
General-Purpose Analog Output	1 8-Bit Digital-to-Analog Converter (+/- 10v, +/- 2ma, single-ended)			
COMMUNICATIONS				
Serial	1 port with RS-232/RS-422/RS-485 at 1200-57,600 baud			
Networking	DeviceNet			
MOTOR FEEDBACK				
Input Modes	Incremental with Index, Sine/cosine High Resolution Absolute (Single and Multi-turn)			
Maximum Input Frequency	2.5 MHz (Encoder Lines), Over 1 million counts/rev (High Resolution)			
Commutation Startup	Hall Sensor			
AUXILIARY FEEDBACK				
Operation	Auxiliary Position Loop Feedback Input			
Input Modes	A quad B			
Input Type	Line Receiver			
Maximum Input Frequency	2.5 MHz (Encoder Lines)			

*HV indicates the 230-460V AC version of the drive
All drives available in indexing non-indexing, SERCOS, DeviceNet or indexing DeviceNet versions*



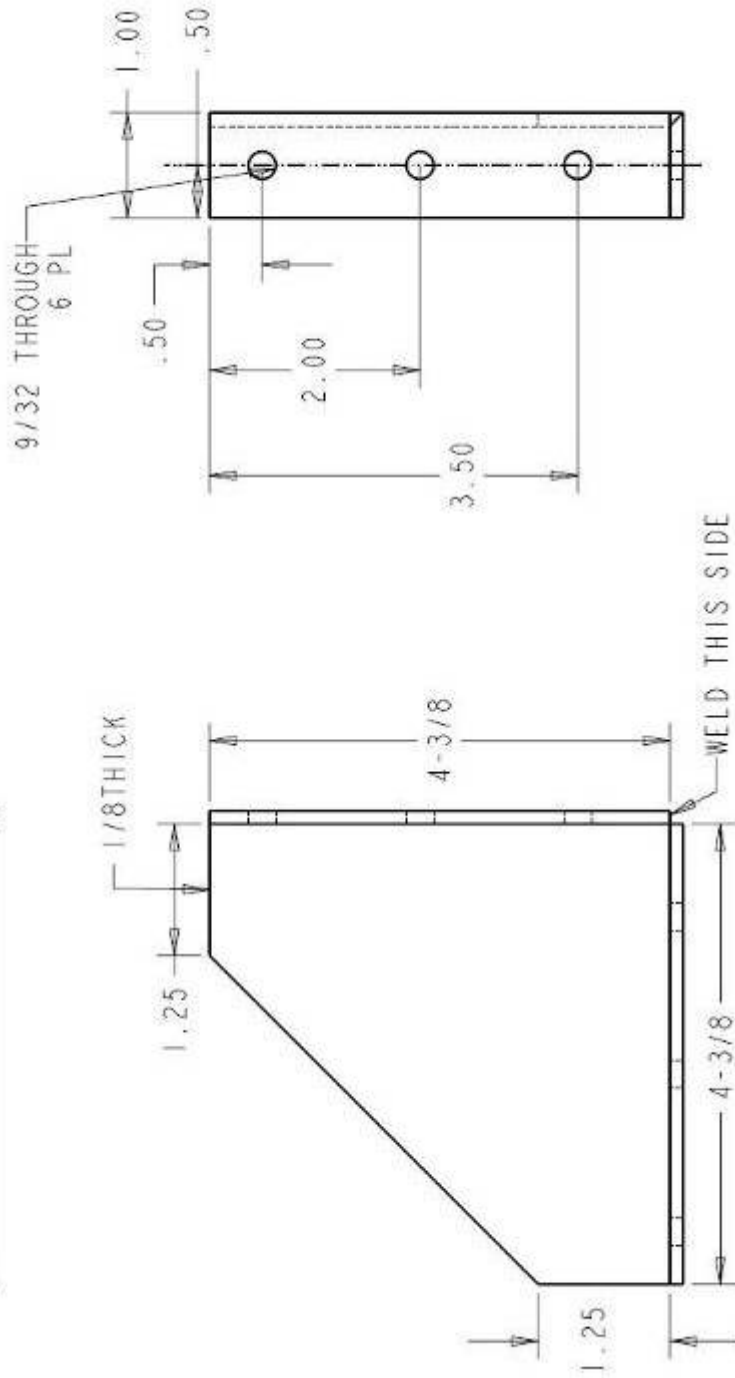
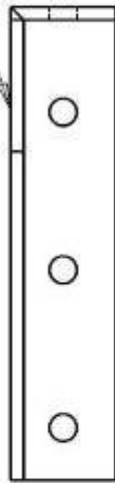
Smart Belt with Ultra3000 Digital Servo Drive and ControlLogix SERCOS interface

Figure 80: Driver Specifications

Appendix G - Chassis Drawings

The following technical drawings were sent to the metalworking contractor. They detail the construction of the chassis components, as well as its assembly. All drawings were made in PTC Pro/ENGINEER Wildfire 2.0. The latest files of each part (PDF, .drw, and .prt files) are included in the electronic version of this report.

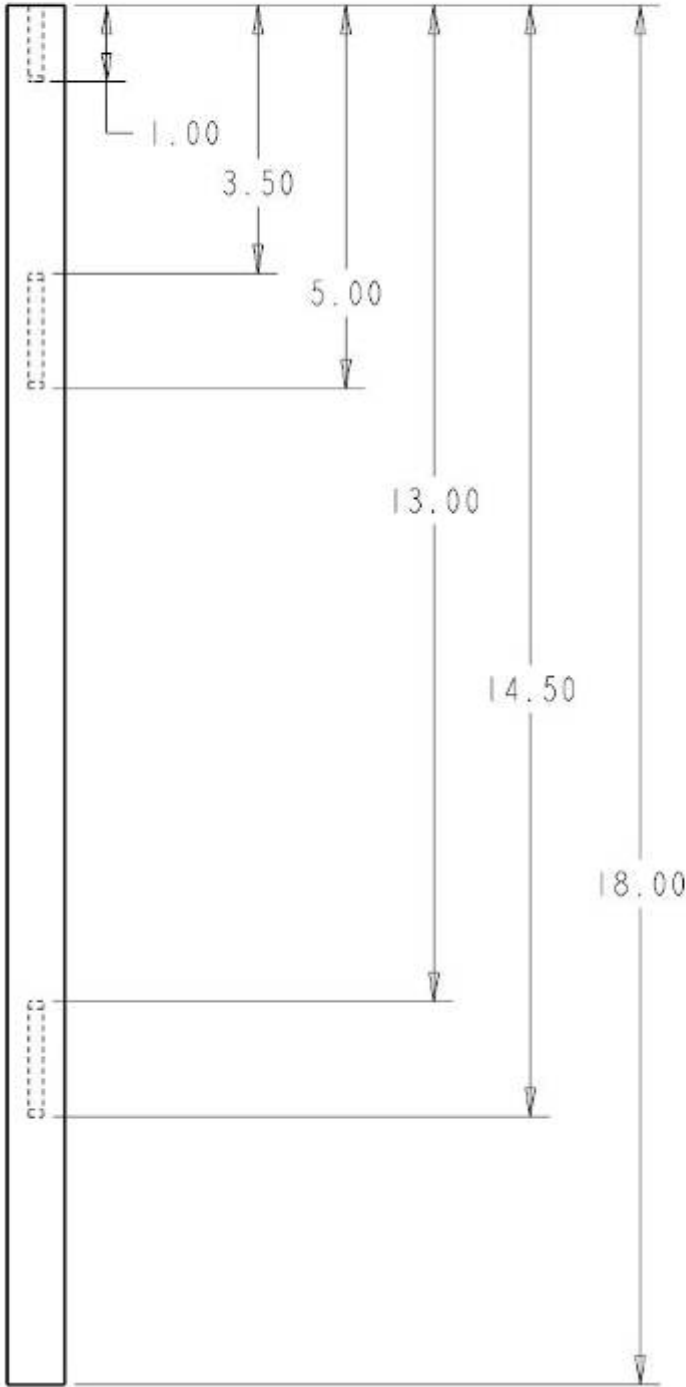
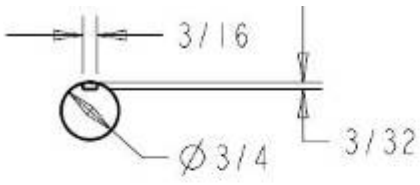
SAME DIMENSIONS AS RIGHT VIEW



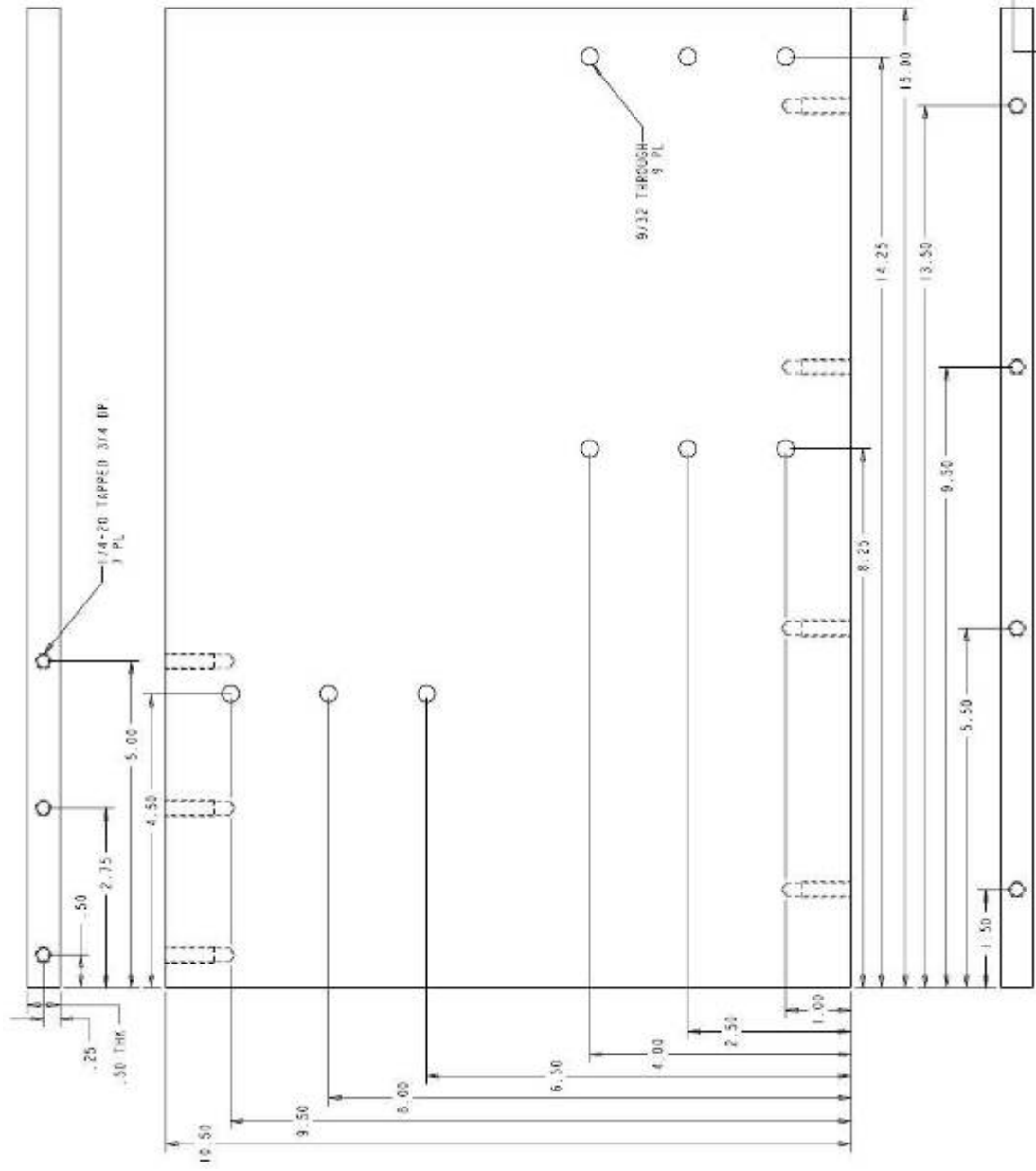
E&J Gallo Winery
600 Yosemite Blvd
Modesto, CA 95354

Drawn By: James Saunders February 12, 2007 Part Name: Bracket

Material: 1/8 Stainless
Tol: ±.01
Unless Noted
W.O. #: 600415 WL

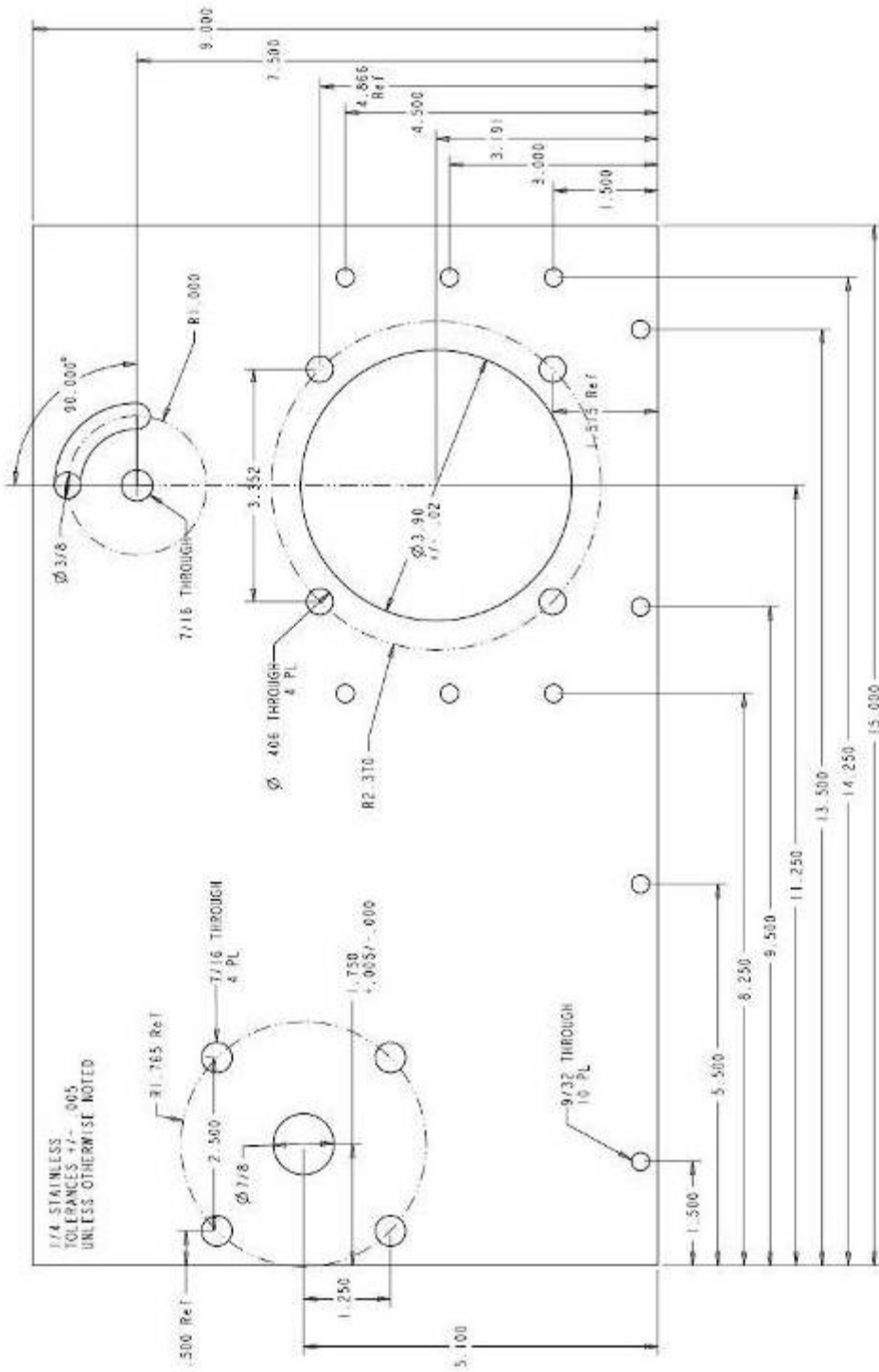


E&J Gallo Winery 600 Yosemite Blvd Modesto, CA 95354		February 13, 2007	Part Name: Cam Shaft
Drawn By: James Saunders	Material: Ø 3/4 Stainless		W.O. #: 600419 WL
		Tol: ±.01	Unless Noted

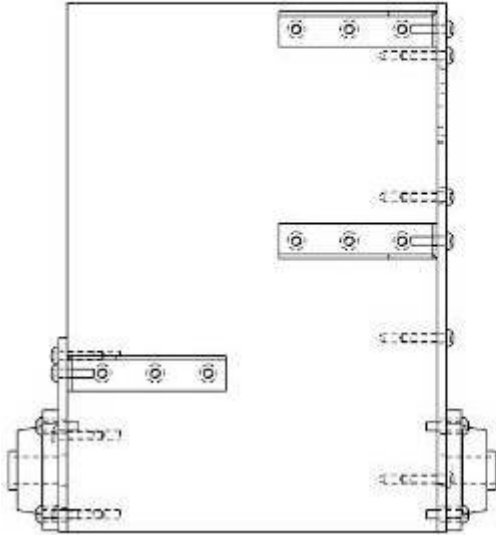
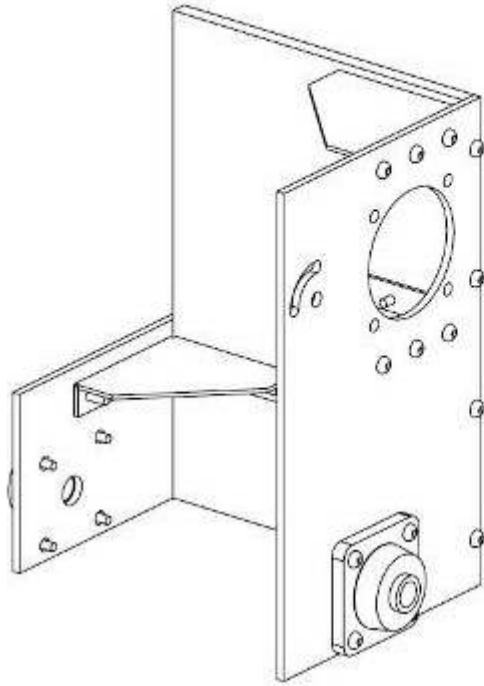


1/2 STAINLESS
+/- .01 TOLERANCE
UNLESS NOTED

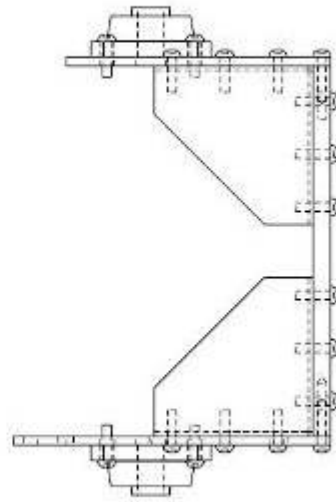
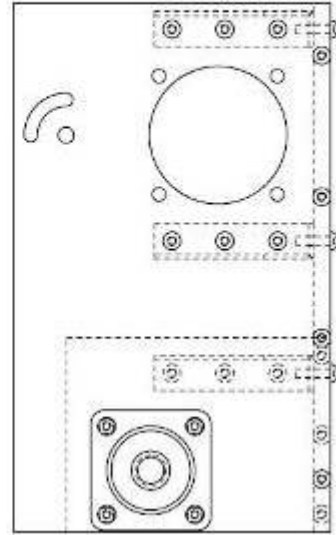
Drawn By: JOHN SHERMAN	Checked By: [Blank]	DATE: 01/11/01	BY: S. BENTON
Ely-Gelle Wirety 10000 S. GARDEN ST. MIRAMONTE, CA 91324		Ely-Gelle Wirety 10000 S. GARDEN ST. MIRAMONTE, CA 91324	



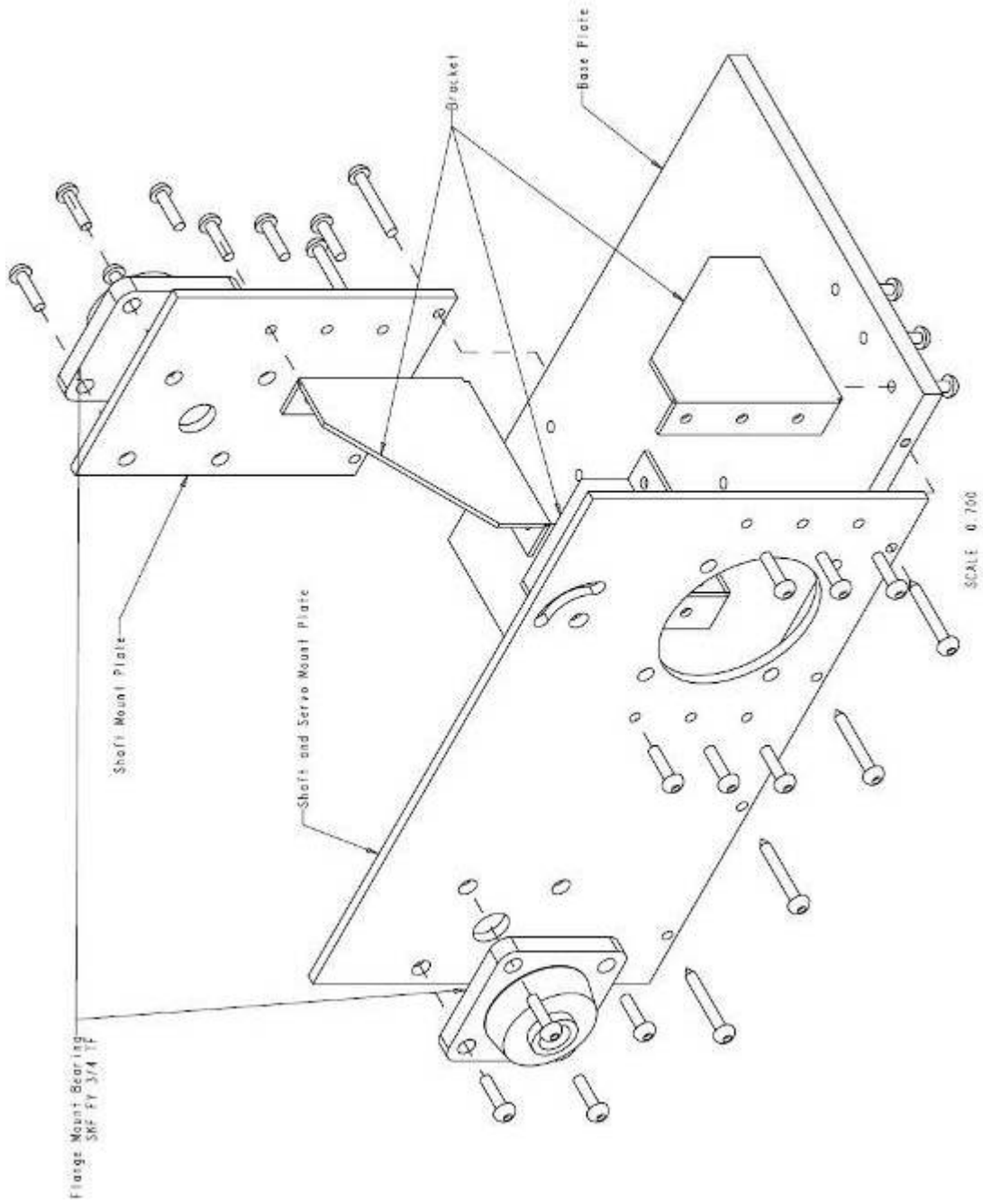
FLJ Gallo Winery	Volume: 17, 2020	Part Name: Wash Parts
600 Yosemite Blvd	Rev: 005	
Model 116, CA 95554	Quantity: 100	Quantity: 100
Drawn By: James Sanchez	Checked By:	



SEE SHEET 2 FOR ASSEMBLY NOTES




Drawn By: James Savadri	February 13, 2007	Port Home Mount Assembly
Tel: 410 6855 8166	Sheet 1 of 2	P.O. #: 608419 NL



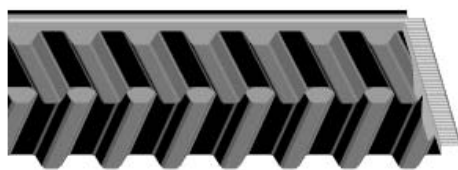

Drawn By: James Swadlow	February 13, 2007	Fort Mums' Mast Assembly
Tel: 407 303-5300	Sheet 2 of 2	P.O. #: 303119-W

Appendix H - Goodyear Eagle Pd Power Transmission

SYNCHRONOUS



EAGLE Pd™ BELT



Part No: B-1750
B Blue = 14 mm Pitch, 35 mm Width
1750 1750 mm Pitch Length

A REVOLUTIONARY BREAKTHROUGH IN SYNCHRONOUS BELT TECHNOLOGY

Much more than an alternative to chain and V-belt drives, Goodyear's Eagle Pd is a total product enhancement that can improve the performance of your drive design.

Eagle's unique HOT (Helical Offset Tooth) design provides a continuous rolling tooth engagement to create a lighter, quieter, reduced vibration, flangeless drive to maximize both the performance and efficiency of your drive system.

Utilizing a concept called "circular arc geometry," Eagle Pd belts and sprockets offer better anti ratcheting resistance, precise movement, increased horsepower ratings, and improved stress distribution allowing the belt's teeth to withstand the shearing action of high torque loads.

LIGHTER, NARROWER DRIVES

The self tracking design of Eagle eliminates the need for sprocket flanges, which reduces face width and weight. The belt is also bidirectional for use in reverse drive applications. And because the belt is comprised of specialized materials, the width of the belt can be reduced without compromising strength. The result is a lighter, narrower, more design-friendly drive option.

BELT MATERIALS COMPOUNDED TO LAST LONGER

Durability starts with the Eagle Pd belt's Hibrex® rubber compound, a cross-linked elastomer formulated to resist tooth deformity and increase tooth rigidity. Hibrex compound is also chemically stable to resist the effects of oils, coolants, heat and ozone.

Eagle's high-strength Flexten® tensile member provides optimal resistance to flex fatigue, elongation and shock loads

APPLICATIONS

Goodyear Eagle Pd belts and sprockets are ideal on a wide variety of applications in all industries.

- Agricultural Equipment
- Packaging Conveyors
- Aggregate Crushers
- Poultry/Meat Grinders
- Wood Debarkers & Saws
- Mining Equipment
- Aluminum/Steel Conveyors
- Paper Presses
- Hog Dehairers
- Chain Drives
- Baking Mixers
- Textile Machines
- Horizontal Drives
- Printing Machines

KEY FEATURES & BENEFITS

- Reduced Noise
- Increased Horsepower
- Higher Efficiency
- Less Bearing Load
- Greater Precision
- Less Vibration
- Less Maintenance
- Compactness
- Self-Tracking
- Bidirectional

while operating at high torque conditions. Eagle's Plioguard® facing also reduces tooth engagement friction while standing up to oil and chemical permeation.

INCREASED EFFICIENCY

Eagle's unique tooth configuration provides continuous tooth engagement and eliminates slippage. With a power efficiency rating of 98%, Eagle Pd can offer you an impressive 5% edge over typical V-belt drives.

Simply stated, with Eagle Pd, you get what you pay for with each energy dollar. This is especially true when the Eagle Pd is applied to high-energy consuming drives that are used 24 hours a day, as well as high horsepower drives that inflate energy consumption during peak periods.

A QUIETER, REDUCED VIBRATION DRIVE

The Helical Offset Tooth design of Eagle Pd belts and sprockets reduces vibration and decreases operating noise by as much as 19 decibels versus other synchronous systems. This can lead to a quieter working environment with improved worker efficiency. Costs associated with monitoring, training and testing to meet OSHA regulations are virtually eliminated with Eagle Pd drives.

LOWER MAINTENANCE COSTS

Unlike chain drives, Eagle Pd belts and sprockets do not require lubrication. There is also no need for retensioning unlike V-belts and chain belts. Install Eagle Pd and watch your maintenance costs drop to practically nothing.

Realize immediate savings with Eagle Pd belts and sprockets. In virtually every measure of comparison, Eagle Pd belts and sprockets are superior.

Figure 81: Belt Nomenclature

EAGLE Pd™ BELT

MATCHING BELT TO SPROCKET HAS NEVER BEEN EASIER

The Eagle Pd Spectrum color system makes it the easiest power transmission drive to sell, purchase and install.

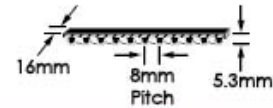
The part numbering system for Eagle Pd centers around a color-coded sizing system for the belts and sprockets. Each belt and sprocket part number includes a letter corresponding to a color and is also branded in that color. The letters Y, W, P, B, G, O, and R indicate the colors Yellow, White, Purple, Blue, Green, Orange, and Red. All Yellow belts are designed to function with all Yellow sprockets, as is the case for the White, Purple, Blue, Green, Orange and Red sizes. An example of the part numbering system nomenclature for belts, sprockets, and bushings follows and also occurs on subsequent pages.

BELT PART NUMBER NOMENCLATURE

- G – 2800
 - G Green Color
 - 2800 2800 mm Pitch Length
- Y – 896
 - Y Yellow Color
 - 896 896 mm Pitch Length

SYNCHRONOUS

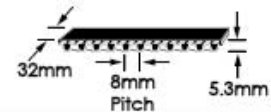
EAGLE Pd™ YELLOW (8 mm Pitch - 16 mm Width)



Part Number	No. of Teeth	Length (in)	Part Number	No. of Teeth	Length (in)
Y-640	80	25.20	Y-1280	160	50.39
Y-720	90	28.35	Y-1440	180	56.69
Y-800	100	31.50	Y-1600	200	62.99
Y-896	112	35.28	Y-1792	224	70.55
Y-1000	125	39.37	Y-2000	250	78.74
Y-1120	140	44.09	Y-2240	280	88.19
Y-1200	150	47.24	Y-2400	300	94.49

The belt length in mm is given in the part number.

EAGLE Pd™ WHITE (8 mm Pitch - 32 mm Width)

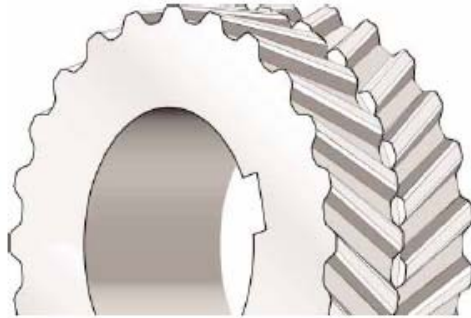


Part Number	No. of Teeth	Length (in)	Part Number	No. of Teeth	Length (in)
W-640	80	25.20	W-1280	160	50.39
W-720	90	28.35	W-1440	180	56.69
W-800	100	31.50	W-1600	200	62.99
W-896	112	35.28	W-1792	224	70.55
W-1000	125	39.37	W-2000	250	78.74
W-1120	140	44.09	W-2240	280	88.19
W-1200	150	47.24	W-2400	300	94.49

The belt length in mm is given in the part number.

Figure 82: Eagle Pd Belt Product Numbers

EAGLE Pd™ SPROCKET



Part No: Y-28S-H
 Y Yellow = 8 mm Pitch, 16 mm Width
 28 28 Teeth
 S Sprocket
 H Hub/Bushing Type

SPROCKET COMBINATIONS TO FIT YOUR DRIVE SYSTEM'S NEEDS

Eagle Pd sprockets have been designed to insure maximum service life and performance. Over 1,000 sprocket combinations are available, making it easier to match the desired design speed. More speed ratio options also means more design flexibility and more compact drives.

Eagle sprockets do not require flanges and are stocked in ductile iron constructions. Other materials such as aluminum, steel and stainless steel are available upon request as made-to-order items.

MATCHING BELT TO SPROCKET HAS NEVER BEEN EASIER

The part numbering system for Eagle Pd centers around a color-coded sizing system for the belts and sprockets. Each belt and sprocket part number includes a letter corresponding to a color and is also branded in that color. The letters Y, W, P, B, G, O, and R indicate the colors Yellow, White, Purple, Blue, Green, Orange, and Red. All Yellow belts are designed to function with all Yellow sprockets, as is the case for the White, Purple, Blue, Green, Orange and Red sizes. An example of the part numbering system nomenclature for sprockets and bushings is given below.

SPROCKET PART NUMBER NOMENCLATURE

Minimum Plain Bore, MPB: O-40S-MPB
 This is an Orange size sprocket with 40 teeth and a Minimum Plain Bore, MPB, style hub. The MPB style sprockets are supplied as is with a minimum bore, typically 1/2" or 1" with H7 tolerances, and will require machining of a keyway and setscrew holes, and possibly boring to a desired bore size.

APPLICATIONS

Goodyear Eagle Pd belts and sprockets are ideal for use on a wide variety of applications in all industries.

KEY FEATURES & BENEFITS

- More design flexibility with more compact drives.
- No flanges.
- Self-tracking design.
- Available in ductile iron, aluminum, steel, or stainless steel.

SYNCHRONOUS

Quick Disconnect, QD:

R-168S-N

This is a Red size sprocket with 168 teeth and a hub machined to fit an 'N' size QD bushing. A bushing is required to install this sprocket on a shaft. Please note that smaller diameter sprockets are not available in the QD style due to space limitations.

Finished Stock Bore, FSB:

G-34S-1 7/8

This is a Green size sprocket with 34 teeth and a Finished Stock Bore, FSB, style hub featuring a bore of 1 7/8". Finished Stock Bore, FSB, sprockets are supplied ready to install with a standard keyway and setscrew holes machined.

Bored To Suit, BTS:

B-28S-BTS-1 13/16

This is a Blue size sprocket with 28 teeth and a hub that has been Bored (BTS) to 1 13/16", per customer specification, and machined for setscrew holes and a keyway. BTS sprockets can be made to almost any bore including metric sizes.

Note: All MPB, QD, and FSB style sprockets are stock items. BTS sprockets are made-to-order and may require longer lead times.

BUSHING PART NUMBER NOMENCLATURE

E 2 1/8: E Bushing Size
 2 1/8 Bushing Bore

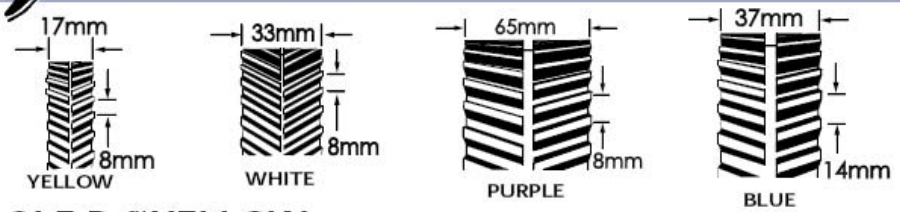
Bushings are supplied with bolts, lock washers, and setscrews. Keys are supplied only if a special shallow key is required. The E 2 1/8" bushing can be used to install any sprocket with an 'E' hub on a 2 1/8" shaft. The QD bushing system is an industry standard, however, to ensure the best match between sprocket and bushing, we recommend using bushings supplied by Goodyear with Eagle Pd sprockets.



Figure 83: Sprocket Nomenclature

EAGLE Pd™ SPROCKET

SYNCHRONOUS



EAGLE Pd™ YELLOW (8 mm Pitch - 17 mm Width)

Part Number	No. of Teeth	Part Number	No. of Teeth	Part Number	No. of Teeth	Part Number	No. of Teeth	Part Number	No. of Teeth
Y-18S-MPB	18	Y-25S-1 1/8	25	Y-34S-H	34	Y-52S-MPB	52	Y-80S-SDS	80
Y-18S-7/8	18	Y-25S-1 3/8	25	Y-36S-MPB	36	Y-56S-MPB	56	Y-90S-MPB	90
Y-20S-MPB	20	Y-26S-MPB	26	Y-36S-SH	36	Y-56S-SDS	56	Y-90S-SK	90
Y-20S-7/8	20	Y-26S-7/8	26	Y-38S-MPB	38	Y-60S-MPB	60	Y-112S-MPB	112
Y-20S-1 1/8	20	Y-26S-1 1/8	26	Y-38S-SH	38	Y-60S-SDS	60	Y-112S-SK	112
Y-22S-MPB	22	Y-26S-1 3/8	26	Y-40S-MPB	40	Y-63S-MPB	63	Y-140S-MPB	140
Y-22S-7/8	22	Y-26S-1 5/8	26	Y-40S-SH	40	Y-63S-SDS	63	Y-140S-SK	140
Y-22S-1 1/8	22	Y-28S-MPB	28	Y-44S-MPB	44	Y-64S-MPB	64	Y-180S-MPB	180
Y-24S-MPB	24	Y-28S-H	28	Y-45S-MPB	45	Y-68S-MPB	68	Y-180S-SF	180
Y-24S-7/8	24	Y-30S-MPB	30	Y-45S-SDS	45	Y-72S-MPB	72	Y-224S-MPB	224
Y-24S-1 1/8	24	Y-30S-H	30	Y-48S-MPB	48	Y-75S-MPB	75	Y-224S-E	224
Y-24S-1 3/8	24	Y-32S-MPB	32	Y-48S-SDS	48	Y-75S-SDS	75		
Y-25S-MPB	25	Y-32S-H	32	Y-50S-MPB	50	Y-76S-MPB	73		
Y-25S-7/8	25	Y-34S-MPB	34	Y-50S-SDS	50	Y-80S-MPB	80		

EAGLE Pd™ WHITE (8 mm Pitch - 33 mm Width)

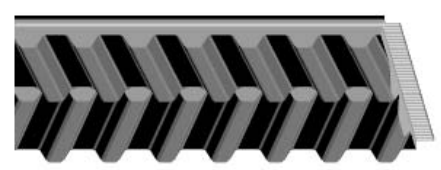
Part Number	No. of Teeth	Part Number	No. of Teeth	Part Number	No. of Teeth	Part Number	No. of Teeth	Part Number	No. of Teeth
W-18S-MPB	18	W-25S-1 1/8	25	W-34S-H	34	W-52S-MPB	52	W-80S-SDS	80
W-18S-7/8	18	W-25S-1 3/8	25	W-36S-MPB	36	W-56S-MPB	56	W-90S-MPB	90
W-20S-MPB	20	W-26S-MPB	26	W-36S-SH	36	W-56S-SDS	56	W-90S-SK	90
W-20S-7/8	20	W-26S-7/8	26	W-38S-MPB	38	W-60S-MPB	60	W-112S-MPB	112
W-20S-1 1/8	20	W-26S-1 1/8	26	W-38S-SH	38	W-60S-SDS	60	W-112S-SK	112
W-22S-MPB	22	W-26S-1 3/8	26	W-40S-MPB	40	W-63S-MPB	63	W-140S-MPB	140
W-22S-7/8	22	W-26S-1 5/8	26	W-40S-SH	40	W-63S-SDS	63	W-140S-SK	140
W-22S-1 1/8	22	W-28S-MPB	28	W-44S-MPB	44	W-64S-MPB	64	W-180S-MPB	180
W-24S-MPB	24	W-28S-H	28	W-45S-MPB	45	W-68S-MPB	68	W-180S-SF	180
W-24S-7/8	24	W-30S-MPB	30	W-45S-SDS	45	W-72S-MPB	72	W-224S-MPB	224
W-24S-1 1/8	24	W-30S-H	30	W-48S-MPB	48	W-75S-MPB	75	W-224S-E	224
W-24S-1 3/8	24	W-32S-MPB	32	W-48S-SDS	48	W-75S-SDS	75		
W-25S-MPB	25	W-32S-H	32	W-50S-MPB	50	W-76S-MPB	76		
W-25S-7/8	25	W-34S-MPB	34	W-50S-SDS	50	W-80S-MPB	80		

Figure 84: Eagle Pd White Sprockets

Screenshots from Goodyear Eagle Pd technical data and product specifications catalog found at:
http://www.goodyearindustrialproducts.com/powertransmission/products/pdf/eagle_pd_belt.pdf

EAGLE Pd™ BELT

SYNCHRONOUS



Part No: B-1750
 B Blue = 14 mm Pitch, 35 mm Width
 1750 1750 mm Pitch Length

A REVOLUTIONARY BREAKTHROUGH IN SYNCHRONOUS BELT TECHNOLOGY

Much more than an alternative to chain and V-belt drives, Goodyear's Eagle Pd is a total product enhancement that can improve the performance of your drive design.

Eagle's unique HOT (Helical Offset Tooth) design provides a continuous rolling tooth engagement to create a lighter, quieter, reduced vibration, flangeless drive to maximize both the performance and efficiency of your drive system.

Utilizing a concept called "circular arc geometry," Eagle Pd belts and sprockets offer better anti ratcheting resistance, precise movement, increased horsepower ratings, and improved stress distribution allowing the belt's teeth to withstand the shearing action of high torque loads.

LIGHTER, NARROWER DRIVES

The self tracking design of Eagle eliminates the need for sprocket flanges, which reduces face width and weight. The belt is also bidirectional for use in reverse drive applications. And because the belt is comprised of specialized materials, the width of the belt can be reduced without compromising strength. The result is a lighter, narrower, more design-friendly drive option.

BELT MATERIALS COMPOUNDED TO LAST LONGER

Durability starts with the Eagle Pd belt's Hibrex® rubber compound, a cross-linked elastomer formulated to resist tooth deformity and increase tooth rigidity. Hibrex compound is also chemically stable to resist the effects of oils, coolants, heat and ozone.

Eagle's high-strength Flexten® tensile member provides optimal resistance to flex fatigue, elongation and shock loads

APPLICATIONS

Goodyear Eagle Pd belts and sprockets are ideal on a wide variety of applications in all industries.

- Agricultural Equipment
- Paper Presses
- Packaging Conveyors
- Hog Dehairers
- Aggregate Crushers
- Chain Drives
- Poultry/Meat Grinders
- Baking Mixers
- Wood Debarkers & Saws
- Textile Machines
- Mining Equipment
- Horizontal Drives
- Aluminum/Steel Conveyors
- Printing Machines

KEY FEATURES & BENEFITS

- Reduced Noise
- Less Vibration
- Increased Horsepower
- Less Maintenance
- Higher Efficiency
- Compactness
- Less Bearing Load
- Self-Tracking
- Greater Precision
- Bidirectional

while operating at high torque conditions. Eagle's Plioguard® facing also reduces tooth engagement friction while standing up to oil and chemical permeation.

INCREASED EFFICIENCY

Eagle's unique tooth configuration provides continuous tooth engagement and eliminates slippage. With a power efficiency rating of 98%, Eagle Pd can offer you an impressive 5% edge over typical V-belt drives.

Simply stated, with Eagle Pd, you get what you pay for with each energy dollar. This is especially true when the Eagle Pd is applied to high-energy consuming drives that are used 24 hours a day, as well as high horsepower drives that inflate energy consumption during peak periods.

A QUIETER, REDUCED VIBRATION DRIVE

The Helical Offset Tooth design of Eagle Pd belts and sprockets reduces vibration and decreases operating noise by as much as 19 decibels versus other synchronous systems. This can lead to a quieter working environment with improved worker efficiency. Costs associated with monitoring, training and testing to meet OSHA regulations are virtually eliminated with Eagle Pd drives.

LOWER MAINTENANCE COSTS

Unlike chain drives, Eagle Pd belts and sprockets do not require lubrication. There is also no need for retensioning unlike V-belts and chain belts. Install Eagle Pd and watch your maintenance costs drop to practically nothing.

Realize immediate savings with Eagle Pd belts and sprockets. In virtually every measure of comparison, Eagle Pd belts and sprockets are superior.



Figure 85: Belt Nomenclature

EAGLE Pd™ BELT

MATCHING BELT TO SPROCKET HAS NEVER BEEN EASIER

The Eagle Pd Spectrum color system makes it the easiest power transmission drive to sell, purchase and install.

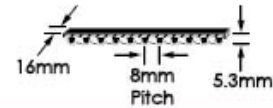
The part numbering system for Eagle Pd centers around a color-coded sizing system for the belts and sprockets. Each belt and sprocket part number includes a letter corresponding to a color and is also branded in that color. The letters Y, W, P, B, G, O, and R indicate the colors Yellow, White, Purple, Blue, Green, Orange, and Red. All Yellow belts are designed to function with all Yellow sprockets, as is the case for the White, Purple, Blue, Green, Orange and Red sizes. An example of the part numbering system nomenclature for belts, sprockets, and bushings follows and also occurs on subsequent pages.

BELT PART NUMBER NOMENCLATURE

- G – 2800
 - G Green Color
 - 2800 2800 mm Pitch Length
- Y – 896
 - Y Yellow Color
 - 896 896 mm Pitch Length

SYNCHRONOUS

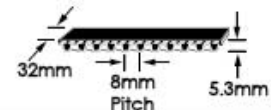
EAGLE Pd™ YELLOW (8 mm Pitch - 16 mm Width)



Part Number	No. of Teeth	Length (in)	Part Number	No. of Teeth	Length (in)
Y-640	80	25.20	Y-1280	160	50.39
Y-720	90	28.35	Y-1440	180	56.69
Y-800	100	31.50	Y-1600	200	62.99
Y-896	112	35.28	Y-1792	224	70.55
Y-1000	125	39.37	Y-2000	250	78.74
Y-1120	140	44.09	Y-2240	280	88.19
Y-1200	150	47.24	Y-2400	300	94.49

The belt length in mm is given in the part number.

EAGLE Pd™ WHITE (8 mm Pitch - 32 mm Width)



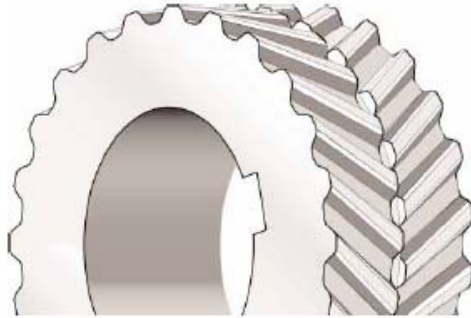
Part Number	No. of Teeth	Length (in)	Part Number	No. of Teeth	Length (in)
W-640	80	25.20	W-1280	160	50.39
W-720	90	28.35	W-1440	180	56.69
W-800	100	31.50	W-1600	200	62.99
W-896	112	35.28	W-1792	224	70.55
W-1000	125	39.37	W-2000	250	78.74
W-1120	140	44.09	W-2240	280	88.19
W-1200	150	47.24	W-2400	300	94.49

The belt length in mm is given in the part number.

Figure 86: Eagle Pd Belt Product Numbers



EAGLE Pd™ SPROCKET



Part No: Y-28S-H
 Y Yellow = 8 mm Pitch, 16 mm Width
 28 28 Teeth
 S Sprocket
 H Hub/Bushing Type

SPROCKET COMBINATIONS TO FIT YOUR DRIVE SYSTEM'S NEEDS

Eagle Pd sprockets have been designed to insure maximum service life and performance. Over 1,000 sprocket combinations are available, making it easier to match the desired design speed. More speed ratio options also means more design flexibility and more compact drives.

Eagle sprockets do not require flanges and are stocked in ductile iron constructions. Other materials such as aluminum, steel and stainless steel are available upon request as made-to-order items.

MATCHING BELT TO SPROCKET HAS NEVER BEEN EASIER

The part numbering system for Eagle Pd centers around a color-coded sizing system for the belts and sprockets. Each belt and sprocket part number includes a letter corresponding to a color and is also branded in that color. The letters Y, W, P, B, G, O, and R indicate the colors Yellow, White, Purple, Blue, Green, Orange, and Red. All Yellow belts are designed to function with all Yellow sprockets, as is the case for the White, Purple, Blue, Green, Orange and Red sizes. An example of the part numbering system nomenclature for sprockets and bushings is given below.

SPROCKET PART NUMBER NOMENCLATURE

Minimum Plain Bore, MPB: O-40S-MPB
 This is an Orange size sprocket with 40 teeth and a Minimum Plain Bore, MPB, style hub. The MPB style sprockets are supplied as is with a minimum bore, typically 1/2" or 1" with H7 tolerances, and will require machining of a keyway and setscrew holes, and possibly boring to a desired bore size.

APPLICATIONS

Goodyear Eagle Pd belts and sprockets are ideal for use on a wide variety of applications in all industries.

KEY FEATURES & BENEFITS

- More design flexibility with more compact drives.
- No flanges.
- Self-tracking design.
- Available in ductile iron, aluminum, steel, or stainless steel.

SYNCHRONOUS

Quick Disconnect, QD:

R-168S-N

This is a Red size sprocket with 168 teeth and a hub machined to fit an 'N' size QD bushing. A bushing is required to install this sprocket on a shaft. Please note that smaller diameter sprockets are not available in the QD style due to space limitations.

Finished Stock Bore, FSB:

G-34S-1 7/8

This is a Green size sprocket with 34 teeth and a Finished Stock Bore, FSB, style hub featuring a bore of 1 7/8". Finished Stock Bore, FSB, sprockets are supplied ready to install with a standard keyway and setscrew holes machined.

Bored To Suit, BTS:

B-28S-BTS-1 13/16

This is a Blue size sprocket with 28 teeth and a hub that has been Bored (BTS) to 1 13/16", per customer specification, and machined for setscrew holes and a keyway. BTS sprockets can be made to almost any bore including metric sizes.

Note: All MPB, QD, and FSB style sprockets are stock items. BTS sprockets are made-to-order and may require longer lead times.

BUSHING PART NUMBER NOMENCLATURE

E 2 1/8: E Bushing Size
 2 1/8 Bushing Bore

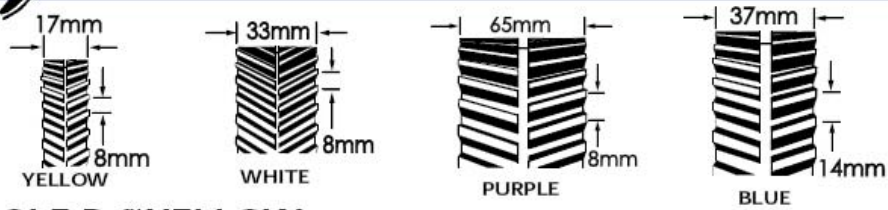
Bushings are supplied with bolts, lock washers, and setscrews. Keys are supplied only if a special shallow key is required. The E 2 1/8" bushing can be used to install any sprocket with an 'E' hub on a 2 1/8" shaft. The QD bushing system is an industry standard, however, to ensure the best match between sprocket and bushing, we recommend using bushings supplied by Goodyear with Eagle Pd sprockets.



Figure 87: Sprocket Nomenclature

EAGLE Pd™ SPROCKET

SYNCHRONOUS



EAGLE Pd™ YELLOW (8 mm Pitch - 17 mm Width)

Part Number	No. of Teeth	Part Number	No. of Teeth	Part Number	No. of Teeth	Part Number	No. of Teeth	Part Number	No. of Teeth
Y-18S-MPB	18	Y-25S-1 1/8	25	Y-34S-H	34	Y-52S-MPB	52	Y-80S-SDS	80
Y-18S-7/8	18	Y-25S-1 3/8	25	Y-36S-MPB	36	Y-56S-MPB	56	Y-90S-MPB	90
Y-20S-MPB	20	Y-26S-MPB	26	Y-36S-SH	36	Y-56S-SDS	56	Y-90S-SK	90
Y-20S-7/8	20	Y-26S-7/8	26	Y-38S-MPB	38	Y-60S-MPB	60	Y-112S-MPB	112
Y-20S-1 1/8	20	Y-26S-1 1/8	26	Y-38S-SH	38	Y-60S-SDS	60	Y-112S-SK	112
Y-22S-MPB	22	Y-26S-1 3/8	26	Y-40S-MPB	40	Y-63S-MPB	63	Y-140S-MPB	140
Y-22S-7/8	22	Y-26S-1 5/8	26	Y-40S-SH	40	Y-63S-SDS	63	Y-140S-SK	140
Y-22S-1 1/8	22	Y-28S-MPB	28	Y-44S-MPB	44	Y-64S-MPB	64	Y-180S-MPB	180
Y-24S-MPB	24	Y-28S-H	28	Y-45S-MPB	45	Y-68S-MPB	68	Y-180S-SF	180
Y-24S-7/8	24	Y-30S-MPB	30	Y-45S-SDS	45	Y-72S-MPB	72	Y-224S-MPB	224
Y-24S-1 1/8	24	Y-30S-H	30	Y-48S-MPB	48	Y-75S-MPB	75	Y-224S-E	224
Y-24S-1 3/8	24	Y-32S-MPB	32	Y-48S-SDS	48	Y-75S-SDS	75		
Y-25S-MPB	25	Y-32S-H	32	Y-50S-MPB	50	Y-76S-MPB	73		
Y-25S-7/8	25	Y-34S-MPB	34	Y-50S-SDS	50	Y-80S-MPB	80		

EAGLE Pd™ WHITE (8 mm Pitch - 33 mm Width)

Part Number	No. of Teeth	Part Number	No. of Teeth	Part Number	No. of Teeth	Part Number	No. of Teeth	Part Number	No. of Teeth
W-18S-MPB	18	W-25S-1 1/8	25	W-34S-H	34	W-52S-MPB	52	W-80S-SDS	80
W-18S-7/8	18	W-25S-1 3/8	25	W-36S-MPB	36	W-56S-MPB	56	W-90S-MPB	90
W-20S-MPB	20	W-26S-MPB	26	W-36S-SH	36	W-56S-SDS	56	W-90S-SK	90
W-20S-7/8	20	W-26S-7/8	26	W-38S-MPB	38	W-60S-MPB	60	W-112S-MPB	112
W-20S-1 1/8	20	W-26S-1 1/8	26	W-38S-SH	38	W-60S-SDS	60	W-112S-SK	112
W-22S-MPB	22	W-26S-1 3/8	26	W-40S-MPB	40	W-63S-MPB	63	W-140S-MPB	140
W-22S-7/8	22	W-26S-1 5/8	26	W-40S-SH	40	W-63S-SDS	63	W-140S-SK	140
W-22S-1 1/8	22	W-28S-MPB	28	W-44S-MPB	44	W-64S-MPB	64	W-180S-MPB	180
W-24S-MPB	24	W-28S-H	28	W-45S-MPB	45	W-68S-MPB	68	W-180S-SF	180
W-24S-7/8	24	W-30S-MPB	30	W-45S-SDS	45	W-72S-MPB	72	W-224S-MPB	224
W-24S-1 1/8	24	W-30S-H	30	W-48S-MPB	48	W-75S-MPB	75	W-224S-E	224
W-24S-1 3/8	24	W-32S-MPB	32	W-48S-SDS	48	W-75S-SDS	75		
W-25S-MPB	25	W-32S-H	32	W-50S-MPB	50	W-76S-MPB	76		
W-25S-7/8	25	W-34S-MPB	34	W-50S-SDS	50	W-80S-MPB	80		

Figure 88: Eagle Pd White Sprockets

Appendix I - Bottle Tests

I.1 - Center of Gravity Test

An experiment was conducted to test the center of gravity of a full wine bottle. Figure 89 demonstrates the experiment set up. The center of gravity is measured through the use of a pendulum. The period of a pendulum is a function of the force of gravity and length of the pendulum arm. The relationship is:

$$T = 2\pi \sqrt{\frac{l}{g}}$$

Where T is time of one period, l is the length of pendulum from an objects center of gravity, and g is the acceleration due to gravity. By measuring the time of one period we are able to obtain the effective length (from pivot to center of gravity) of the pendulum by rearranging the above relationship:

$$l = \left[\frac{T}{2\pi} \right]^2 * g$$

Since we know the dimensions of the bottle and length of the rope we use for the pendulum test, we are able to calculate the location of the center of gravity in relation to the bottle. Assumptions are also made that the bottle is symmetric about two axes such that the center of gravity is in the center of the bottle at some height on the z axis (see Figure 90).



Figure 89: Center of Gravity Experiment



Figure 90: Free Body Diagram

Figure 90 shows the free body diagram of the bottle during the experiment. F_G is the force of gravity acting at the center of gravity. C_G is the center of gravity. L_R is the length of rope used for the experiment. L_{eff} is the effective length of the pendulum acting at the center of gravity. Several tests were conducted with different lengths of rope. The time was recorded for ten periods to pass. Several runs were conducted for each length of rope. The center of gravity is calculated relative to the base of the bottle. Time was recorded with a computer stop clock accurate to 0.05 seconds. Length was measured with a tape measure accurate to 1/8 inch.

Center of Gravity Pendulum Test							
Trial	String Length	Number of Periods	Total Time (s)	Period (s)	Effective Length (in.)	Height from Top (in.)	Height from Bottom (in.)
1	32.6	10	20.3	2.0	40.5	7.9	4.4
2	32.6	10	20.3	2.0	40.5	7.9	4.4
3	32.6	10	20.3	2.0	40.5	7.9	4.4
4	27.3	10	18.8	1.9	34.5	7.2	5.0
5	27.3	10	18.8	1.9	34.5	7.2	5.0
6	16.5	10	15.9	1.6	24.7	8.2	4.0
7	16.5	10	16.0	1.6	25.0	8.5	3.7
8	16.5	10	15.9	1.6	24.7	8.2	4.0
9	42.1	10	22.7	2.3	50.4	8.3	3.9
10	42.1	10	22.6	2.3	50.0	7.8	4.4
Average						7.9	4.3

Figure 91: Pendulum Test Results

I.2 - Coefficient of Static Friction Test

An experiment was conducted to test the coefficient of static friction of a full wine bottle on the two materials commonly used for conveyor systems on the Gallo bottling lines. Figure 92 demonstrates the experiment set up. A section of conveyor links is supported and assured to be level using an inclinometer. The conveyor is lubricated with detergent (glycol based). With the bottle on the conveyor section, the conveyor is inclined until the bottle begins to slide. The angle is measured using the inclinometer.



Figure 92: Coefficient of Static Friction Experiment

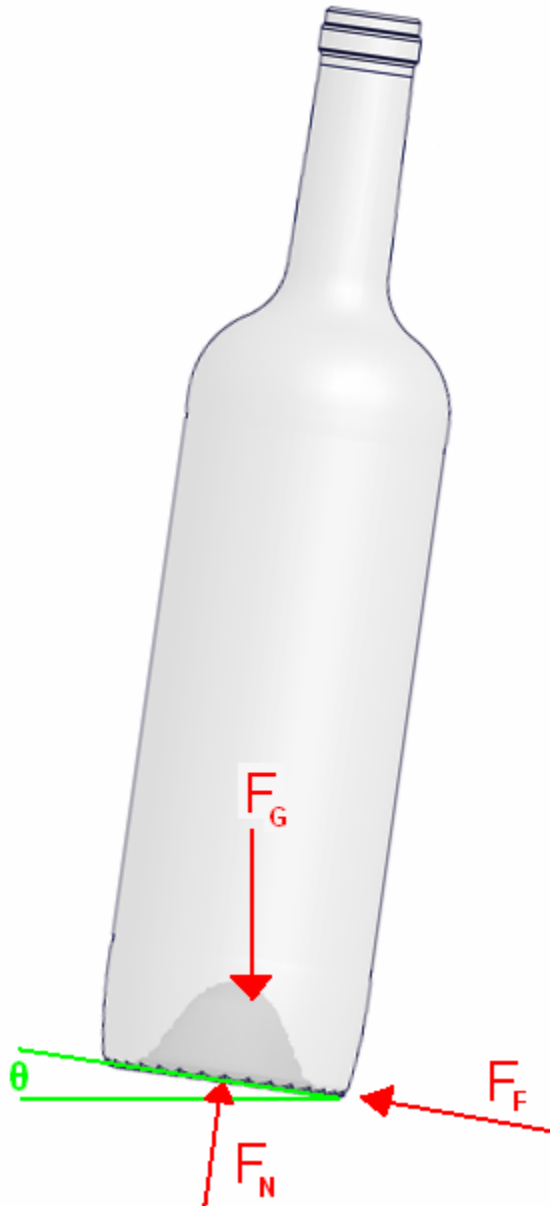


Figure 93: Free Body Diagram

Figure 93 shows the free body diagram of the bottle during the experiment. F_G is the force of gravity acting at the center of gravity. F_N is the normal force of the conveyor. F_F is the friction force of the conveyor. θ is the angle of the tip of the conveyor. The friction coefficient is obtained by calculating $\text{Tan}(\theta)$. Two separate tests were conducted with plastic and stainless steel conveyor materials and five trials on each material were conducted.

Plastic		
Trial	Angle (degrees)	Coefficient Static Friction
1	7	0.122784561
2	7	0.122784561
3	7.5	0.131652497
4	6.5	0.113935608
5	7	0.122784561
Average		0.124721109

Figure 94: Plastic Friction Test

Stainless Steel		
Trial	Angle (degrees)	Coefficient Static Friction
1	7	0.122784561
2	7.5	0.131652497
3	7	0.122784561
4	7	0.122784561
5	7.5	0.131652497
Average		0.126331735

Figure 95: Stainless Steel Friction Test

I.3 - Bottle Neck Failure Test

An experiment was conducted to test the failure load of the bottle neck using a static load acting at an extreme point on the bottle neck. Figure 96 demonstrates the experiment set up. The bottle overhangs off a solid surface with a rope attached to the bottle neck and a means to supply the force.



Figure 96: Bottle Neck Failure Experiment

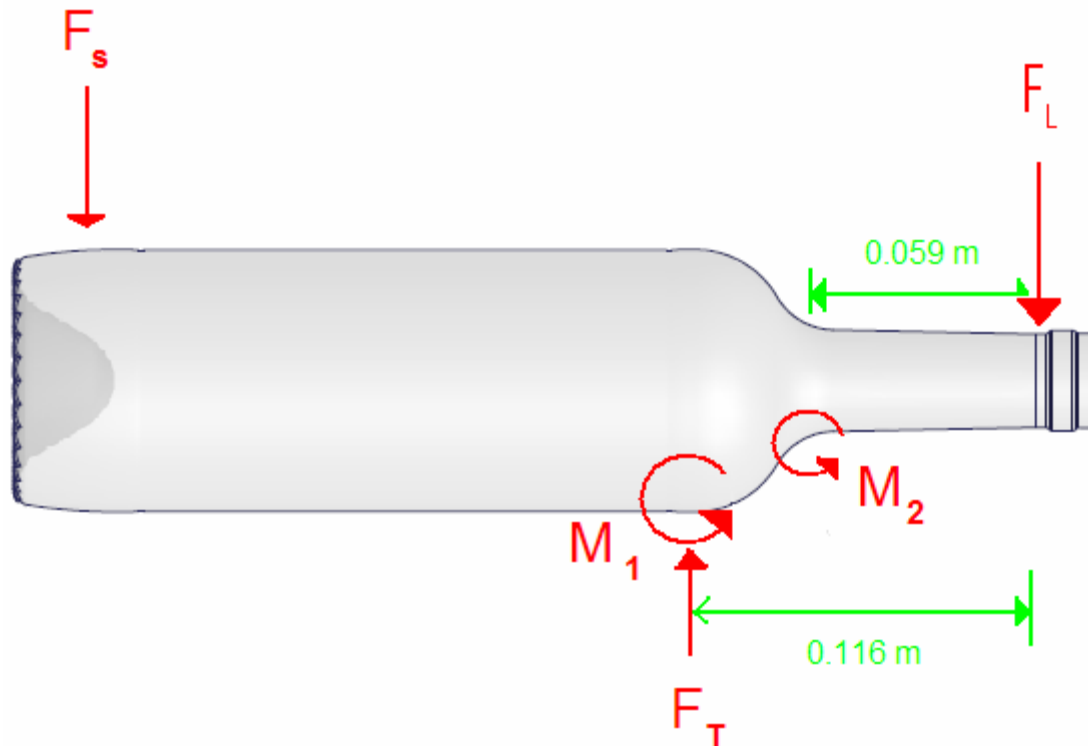


Figure 97: Free Body Diagram

Figure 97 shows the free body diagram of the bottle during the experiment. The force is provided by weights hanging from a rope attached at the point F_L . The bottle is supported by a table at point F_T and rotation is prevented by F_s acting at the base of the bottle. The moment is calculated at two points of interest; the point at M_1 and at the speculated weak point (highest stress concentration factor) at M_2 .

Bottle Neck Test				
Mass (kg)	Force (Newtons) F_L	Moment 1 (N-m)	Moment 2 (N-m)	Failure? (yes/no)
4	39.2	4.6	2.3	NO
8	78.5	9.1	4.6	NO
12	117.7	13.7	6.9	NO
20	196.2	22.8	11.6	NO
30	294.3	34.1	17.4	NO

The results of the test concluded that the bottle neck was sufficiently strong to withstand the static load of at least 30 kg. Failure was not achieved because of the lack of equipment and the obvious dangers associated with broken glass.

Appendix J - Rapid Prototyping Methods

Several different methods of rapid prototyping exist. Each method poses particular benefits and constraints. All use similar basic concepts to construct complex geometry from thin layers. A few available methods are investigated below.

J.1 - Stereolithography (SLA)

Stereolithography is the most commonly used rapid prototyping technique and can produce complex geometries shown in Figure 16. This method uses a screened platform in a reservoir of liquid photopolymer. This liquid hardens when exposed to ultraviolet light. The platform is lowered into the tank of liquid so that only a thin film of the photopolymer (from .125 to .2 mm¹⁷) is above its surface. Then an ultraviolet laser traces the cross section, leaving a hardened layer of plastic. The platform then lowers one layer thickness, where a roller spreads the photopolymer to ensure the correct thickness, and the process is repeated. Once the part is finished, the excess liquid is washed off, and the part typically requires a curing operation to harden the photopolymer completely.

Stereolithography is very accurate, but relatively expensive and somewhat slower than some other RP methods. Parts may need support structures during fabrication. Pieces formed with SLA may only be suitable for limited function, as the material is not the most robust or durable. SLA is offered by 3D Systems.

Figure 98¹⁸ shows a schematic view of the SLA fabrication process. As the platform is lowered into the tank, the SLA model is formed out of the photopolymer liquid resin by the suspended laser, layer by layer. After the forming process the part must still be finished and cured. SLS and EBM (see below) have similar machine setups, but different reservoir material and, in the case of EBM, an electron beam in place of the laser.

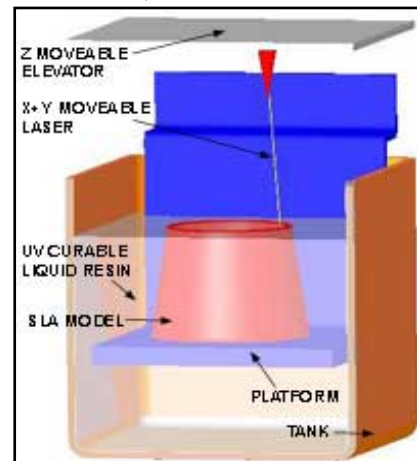


Figure 98: SLA Schematic Diagram

¹⁷ Toolcraft Plastics Ltd. [Explanation Of and Free Help with Stereolithography process](http://www.toolcraft.co.uk/help_stereolithography_process_slamodels.htm). Retrieved January 19, 2007 from http://www.toolcraft.co.uk/help_stereolithography_process_slamodels.htm

¹⁸ Figure retrieved from Toolcraft Plastics Ltd.

J.2 - Fused Deposition Modeling (FDM)

FDM builds a solid part from a plastic wire that is heated and laid in a bead, layer upon layer. FDM suffers slightly less accuracy than stereolithography, but offers greater flexibility in materials. Available materials include polycarbonate and ABS plastic, which are durable enough to be used not only as prototypes, but even in full production settings. One manufacturer replaced a pulley on an industrial belt sander on its production line with an FDM formed part when the aluminum piece failed. The rapid prototyped piece lasted over one month in full production¹⁹. This process is owned by Stratasys, Inc.

J.3 - Selective Laser Sintering (SLS)

SLS uses a bed of powder, which may be plastic, ceramic or metal in a similar manner as stereolithography uses photopolymer liquid. The powder is spread evenly across a piston head and then sintered with a laser to form. The piston lowers and the process is repeated.

SLS pieces are less accurate than those formed with stereolithography, but have no need for support structures or secondary curing. In addition, SLS allows for a great variety of materials to be used. Sintering does result in porous parts, and may require an infiltration process to improve the material properties of the part. Some larger pieces may require up to two days of cooling after the sintering process.

J.4 - Electron Beam Melting (EBM)

A newer development in rapid prototyping is Electron Beam Melting. The process is very similar to SLS, but instead of a laser, an electron beam fully melts the powder. The result is a fully homogenous non-porous part, typically made of titanium. The piece requires no secondary operations, but is suitable for any conventional finish process, including heat treatment. Build layers are quite accurate, having a thickness from 0.05 to 0.2 mm²⁰.

The process is roughly five times faster than SLS and up to ten times as efficient. This is because the laser used in SLS is largely reflected from the powder surface, while the electron beam has much higher absorption. Stratasys offers EBM machines in North America.

¹⁹ Stratasys. Case Study. Retrieved January 19, 2007 from http://www.stratasys.com/uploadedFiles/North_America/Media/PDF%20Beta%20pulley.pdf

²⁰ Engineers Handbook. Rapid Prototyping: Electron Beam Molding. Retrieved January 26, 2007 from <http://www.engineershandbook.com/Rapidprototyping/ebm.htm>.

Appendix K – Test Data Table

Camoid Laner Prototype Test: Bottle Interaction								
Test Administered by:						Date:		
Bottle Type:						Time:		
Test Number	Line Speed (in/sec)	Bottle Spacing (inches)	Number of Bottles	Bottles per Cycle	Down Bottle #	Motion (extend or retract)	Comments	Recommendations
1	24	0	batch	1				
2	24	1	Batch	1				
3	24	2	Batch	1				
4	24	3	Batch	1				
5	24	0	Batch	2				
6	24	1	Batch	2				
7	24	2	Batch	2				
8	24	3	Batch	2				
9	24	0	Batch	X				
10	24	1	Batch	X				
11	24	2	Batch	X				
12	24	3	Batch	X				
13	24	0	Batch	X				
14	24	1	Batch	X				
15	24	2	Batch	X				
16	24	2	stream	x				

Each test is run 5 times to assure all problems with a batch of 6 bottles looping the test line.

Table 27: Data Recording Table

Appendix M - Detailed Mathematics

Summary

This analysis serves several purposes. First of all, we are looking to find an "optimal" contour for the cam of our divider. This requires a look at the accelerations and forces that will arise from shifting this bottle across the lane. Secondly, we want to find the height (z-direction) at which our divider should contact the bottle, in order to prevent tipping. Finally, a look at the forces, stresses, and impacts involved with the splitting motion is necessary to ensure that bottles will not be broken.

There are two approaches to defining the contour of this laner. The first is the Bottom-Up method; describe the y-value (height) of the bottle as it moves downstream, and then to perform acceleration and force analyses to determine if the contour is acceptable. Alternately, with the Top-Down method the acceleration curve can be described first, and the contour follows from there.

We have used both methods in this analysis. For instance, the Simple Harmonic Contour is an example of the Bottom-Up method, while ModTrap is an example of Top-Down.

Problem Definition

Constants:

$$g = 9.807 \frac{\text{m}}{\text{s}^2} \quad \mu := \tan(7 \cdot \text{deg}) \quad \mu = 0.123$$

Bottle Properties:

$m_{\text{bottle}} := 1.29 \cdot \text{kg}$	<i>Bottle Mass</i>	$d_{\text{bottle}} := 2.982 \cdot \text{in}$	<i>Diameter of Bottle</i>
$\text{thickness} := .125 \cdot \text{in}$	<i>Glass Thickness</i>	$F_g := m_{\text{bottle}} \cdot g$	<i>Weight of Bottle</i>
$h_{\text{bottle}} := 12.25 \cdot \text{in}$	<i>Bottle Height</i>	$F_g = 12.651 \text{ N}$	
$h_{\text{cg}} := 4.33 \cdot \text{in}$	<i>Center of Gravity Height</i>		

$$I_{xx} := \frac{m_{\text{bottle}} \cdot \left[3 \cdot \left(\frac{d_{\text{bottle}}}{2} \right)^2 + h_{\text{bottle}}^2 \right]}{12} \quad I_{xx} = 0.011 \text{ kg} \cdot \text{m}^2 \quad I_{yy} := I_{xx}$$

These are very rough estimates, assuming a solid, uniform density cylinder.

$$I_{zz} := m_{\text{bottle}} \cdot \frac{\left(\frac{d_{\text{bottle}}}{2} \right)^2}{2} \quad I_{zz} = 9.251 \times 10^{-4} \text{ kg} \cdot \text{m}^2$$

Line Properties:

$$v_{\text{line}} := 1.01 \cdot \frac{\text{m}}{\text{s}} \quad \text{Conveyor Velocity}$$

Design Parameters

$$v_{\text{line}} = 39.764 \frac{\text{in}}{\text{s}}$$

Laner Properties:

$$h_{\text{contact}} := 3.5 \cdot \text{in}$$

Height at which the laner contacts the bottle

$$\Delta h(Z) := |Z - h_{\text{cg}}|$$

Distance from contact point to center of gravity

$$L_{\text{split}} := 9.5 \cdot \text{in}$$

Total length of the laner track

$$h_y := 2.72 \cdot \text{in}$$

Target "height" (across the conveyor)

Time Calculations:

$$t_{\text{final}} := \frac{L_{\text{split}}}{v_{\text{line}}}$$

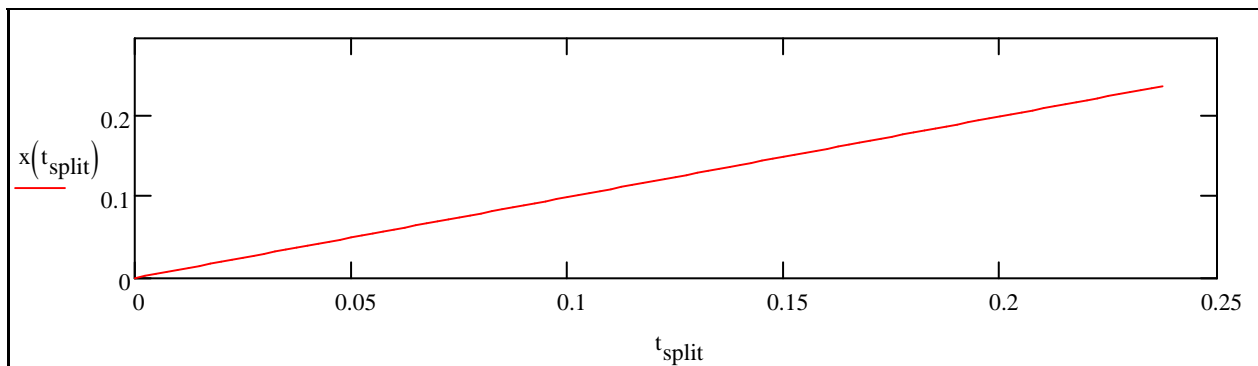
$$t_{\text{final}} = 0.239 \text{ s}$$

Time to lane one bottle (guided by contour)

$$t_{\text{split}} := 0 \cdot \text{s}, 0.0025 \cdot \text{s} \dots t_{\text{final}}$$

X-Direction Travel:

$$x(t) := v_{\text{line}} \cdot t$$

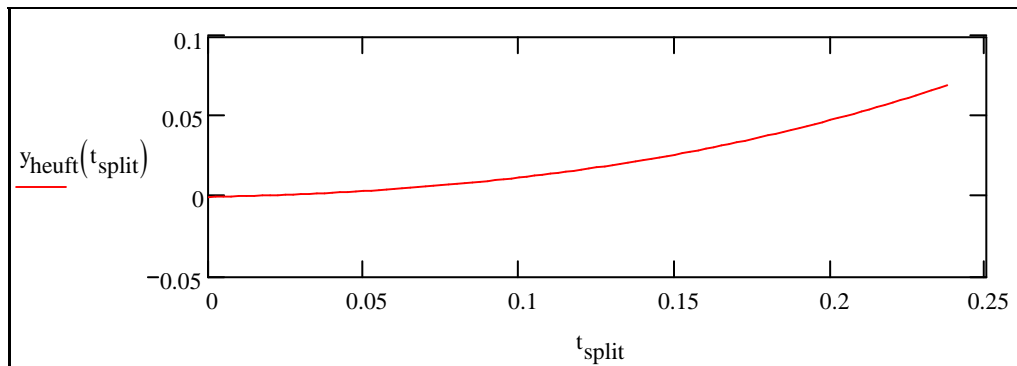


We make the assumption that the bottle speed moving downstream remains essentially constant. The divider will actually slow the bottle, but we argue the loss in speed will be insignificant.

Heuft Laner Acceleration

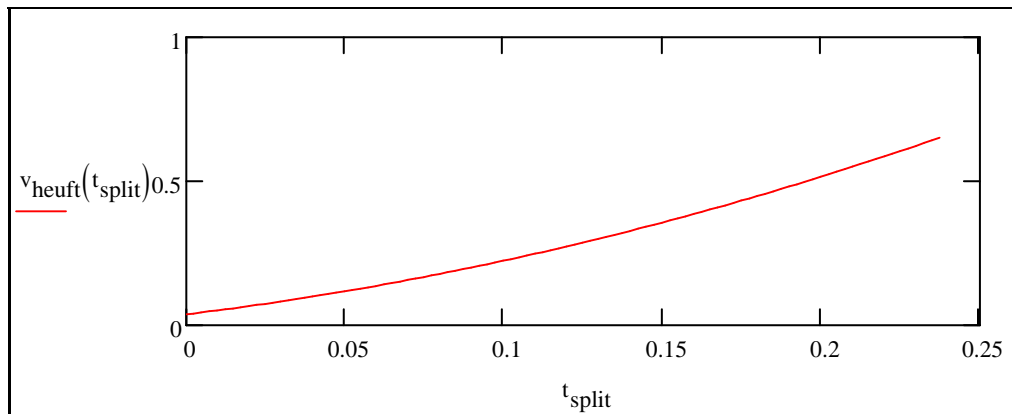
In order to gain a baseline understanding of the accelerations the bottle experiences currently, we will analyze the contour of the Heuft laning system. The analysis is conducted by plotting points along the contour and calculating for the best fit trend line. In this case, a cubic equation was chosen with root mean square value of .9999 (99.99% accuracy).

$$y_{\text{heuft}}(t) := \left[(.0011 \cdot .0254) \cdot \left(\frac{x(t)}{\text{in}} \right)^3 + (.0166 \cdot .0254) \cdot \left(\frac{x(t)}{\text{in}} \right)^2 + (.0362 \cdot .0254) \cdot \frac{x(t)}{\text{in}} - (.0007 \cdot .0254) \right] \cdot \text{m}$$

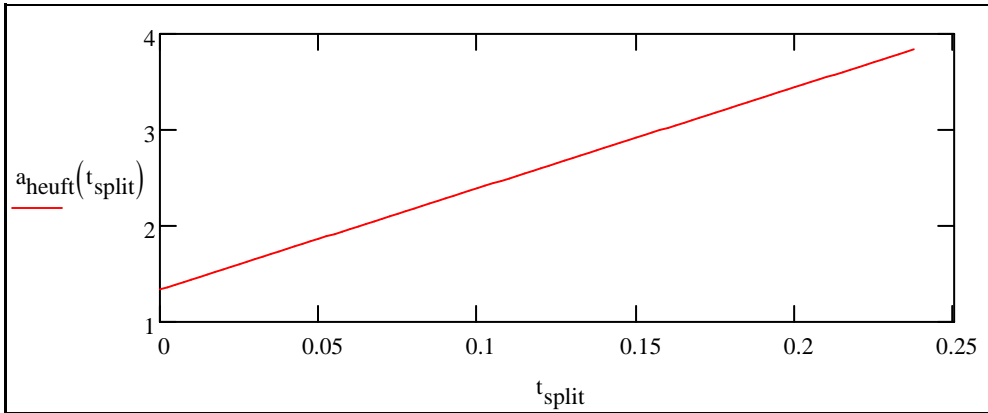


$$y_{\text{heuft}}(t_{\text{final}}) = 2.784 \text{ in}$$

$$v_{\text{heuft}}(t) := \frac{d}{dt} y_{\text{heuft}}(t)$$



$$a_{\text{heuft}}(t) := \frac{d^2}{dt^2} y_{\text{heuft}}(t)$$



Laner Contour:

The contour of our rail can be modeled as a 4-5-6-7 cam polynomial funtion of time with a series of coefficients. We set a series of boundary conditions to solve for the necessary contour.

$$y_{\text{general}}(t, C) := C_0 + C_1 \cdot \frac{t}{s} + C_2 \cdot \left(\frac{t}{s}\right)^2 + C_3 \cdot \left(\frac{t}{s}\right)^3 + C_4 \cdot \left(\frac{t}{s}\right)^4 + C_5 \cdot \left(\frac{t}{s}\right)^5 + C_6 \cdot \left(\frac{t}{s}\right)^6 + C_7 \cdot \left(\frac{t}{s}\right)^7$$

$$y'_{\text{general}}(t, C) := C_1 + 2 \cdot C_2 \cdot \frac{t}{s} + 3 \cdot C_3 \cdot \left(\frac{t}{s}\right)^2 + 4 \cdot C_4 \cdot \left(\frac{t}{s}\right)^3 + 5 \cdot C_5 \cdot \left(\frac{t}{s}\right)^4 + 6 \cdot C_6 \cdot \left(\frac{t}{s}\right)^5 + 7 \cdot C_7 \cdot \left(\frac{t}{s}\right)^6$$

$$y''_{\text{general}}(t, C) := 2 \cdot C_2 + 6 \cdot C_3 \cdot \frac{t}{s} + 12 \cdot C_4 \cdot \left(\frac{t}{s}\right)^2 + 20 \cdot C_5 \cdot \left(\frac{t}{s}\right)^3 + 30 \cdot C_6 \cdot \left(\frac{t}{s}\right)^4 + 42 \cdot C_7 \cdot \left(\frac{t}{s}\right)^5$$

$$y'''_{\text{general}}(t, C) := 6 \cdot C_3 + 24 \cdot C_4 \cdot \frac{t}{s} + 60 \cdot C_5 \cdot \left(\frac{t}{s}\right)^2 + 120 \cdot C_6 \cdot \left(\frac{t}{s}\right)^3 + 210 \cdot C_7 \cdot \left(\frac{t}{s}\right)^4$$

$$C_{\text{general}} := \begin{pmatrix} 1 \\ 1 \\ 1 \\ 1 \\ 1 \\ 1 \\ 1 \\ 1 \end{pmatrix} \cdot h_y$$

This matrix is a series of guess coefficients for the solver to determine our actual coefficients.

Boundary Conditions

Given These conditions are selected to minimize the risk of dangerous dynamics in the lane splitting.

Initial Conditions

$$0 = y_{\text{general}}(0, C_{\text{general}})$$

$$0 = y'_{\text{general}}(0, C_{\text{general}})$$

$$0 = y''_{\text{general}}(0, C_{\text{general}})$$

$$0m = y'''_{\text{general}}(0, C_{\text{general}})$$

$$C_{\text{out}} := \text{Find}(C_{\text{general}})$$

Final Conditions

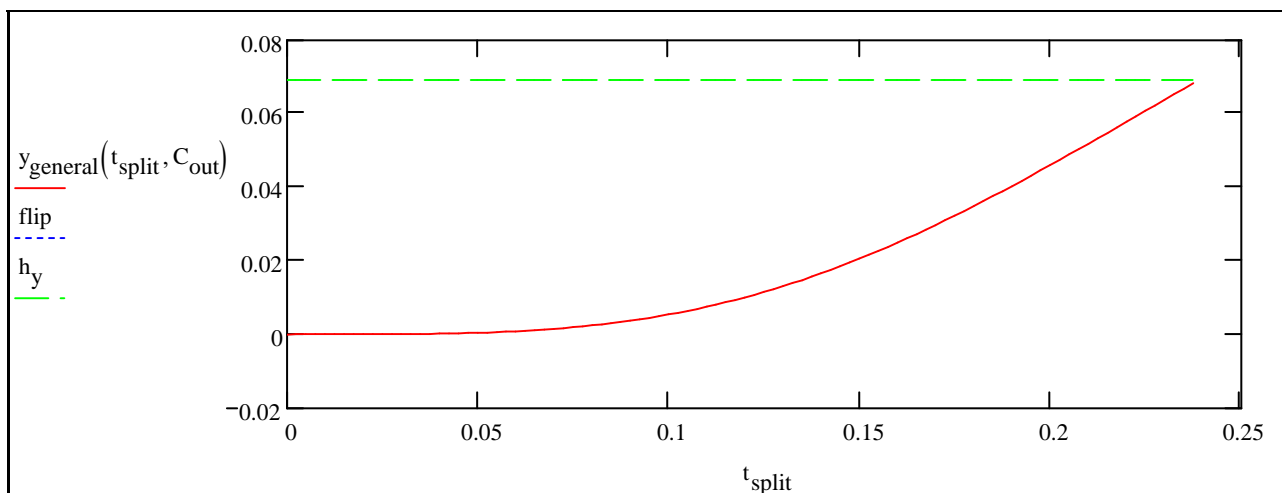
$$h_y = y_{\text{general}}(t_{\text{final}}, C_{\text{general}})$$

$$.6m = y'_{\text{general}}(t_{\text{final}}, C_{\text{general}})$$

$$0 = y''_{\text{general}}(t_{\text{final}}, C_{\text{general}})$$

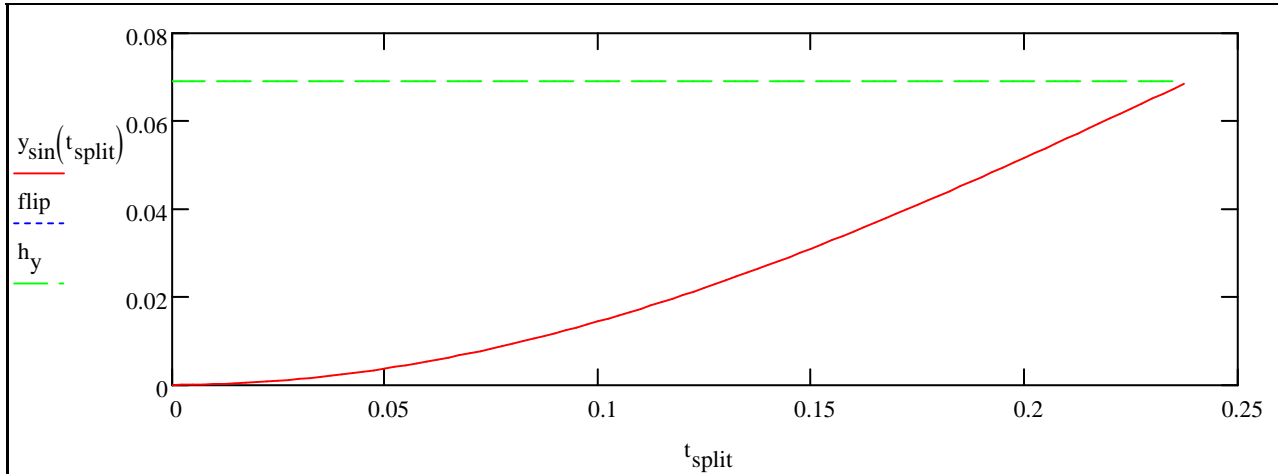
$$0m = y'''_{\text{general}}(t_{\text{final}}, C_{\text{general}})$$

$$C_{\text{out}} = \begin{pmatrix} 0 \\ 0 \\ 0 \\ 0 \\ 3.237 \times 10^3 \\ -1.077 \times 10^4 \\ -7.965 \times 10^3 \\ 4.582 \times 10^4 \end{pmatrix} \text{ in } \text{ This set of coefficients describes our contour as an 8 term polynomial equation. }$$



Simple Harmonic:

$$y_{\sin}(t) := h_y \cdot \left(-\cos\left(\frac{x(t) \cdot \pi}{2L_{\text{split}}}\right) \right) + h_y$$



Analysis

Bottle Considerations:

$$F_{\text{friction}} := \mu \cdot m_{\text{bottle}} \cdot g$$

$$F_{\text{friction}} = 1.553 \text{ N}$$

Friction Force between Bottle and Conveyor

$$a_{\sin}(t) := \frac{d^2}{dt^2} y_{\sin}(t)$$

Mod-Trap Acceleration

$$a_{\max} := 3 \cdot \frac{m}{s^2}$$

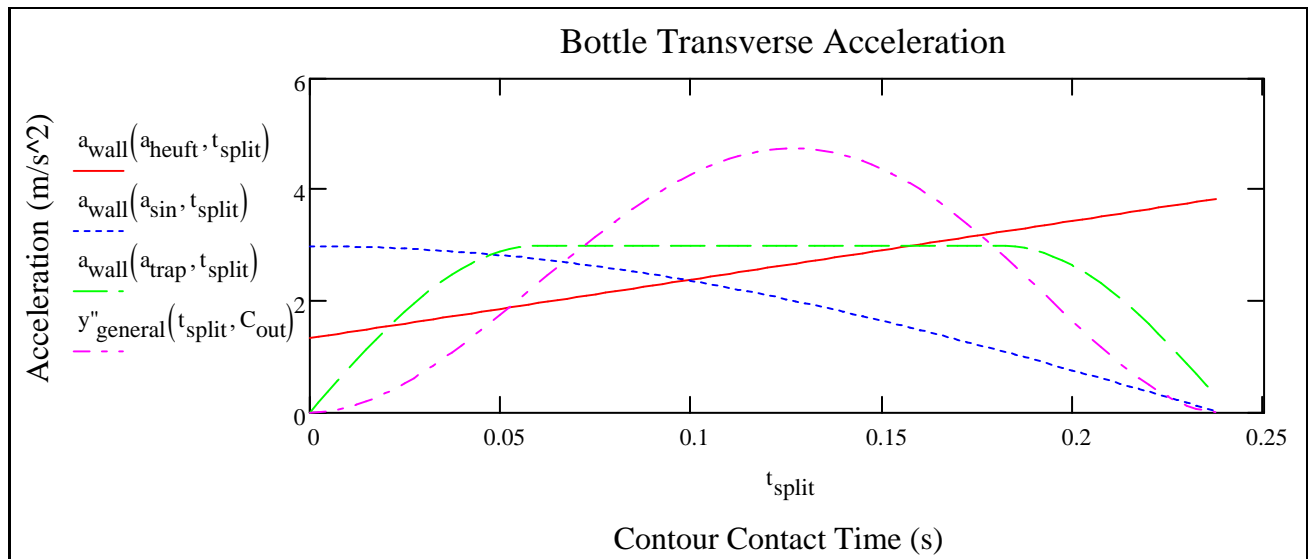
The Modified Trapezoid is a piecewise acceleration curve; partially sinusoidal and partially constant acceleration.

$$a_{\text{trap}}(t) := \begin{cases} a_{\max} \sin\left(\frac{2\pi t \cdot m}{L_{\text{split}} \cdot s}\right) & \text{if } t < \frac{t_{\text{final}}}{4} \\ a_{\max} & \text{if } \frac{t_{\text{final}}}{4} \leq t \leq 3 \cdot \frac{t_{\text{final}}}{4} \\ -a_{\max} \cdot \sin\left(\frac{2\pi t \cdot m}{L_{\text{split}} \cdot s}\right) & \text{if } 3 \cdot \frac{t_{\text{final}}}{4} \leq t \leq \left(t_{\text{final}} + \frac{2t_{\text{final}}}{10}\right) \end{cases}$$

$$a_{\text{trap}}(t_{\text{final}}) = 0.187 \frac{m}{s^2}$$

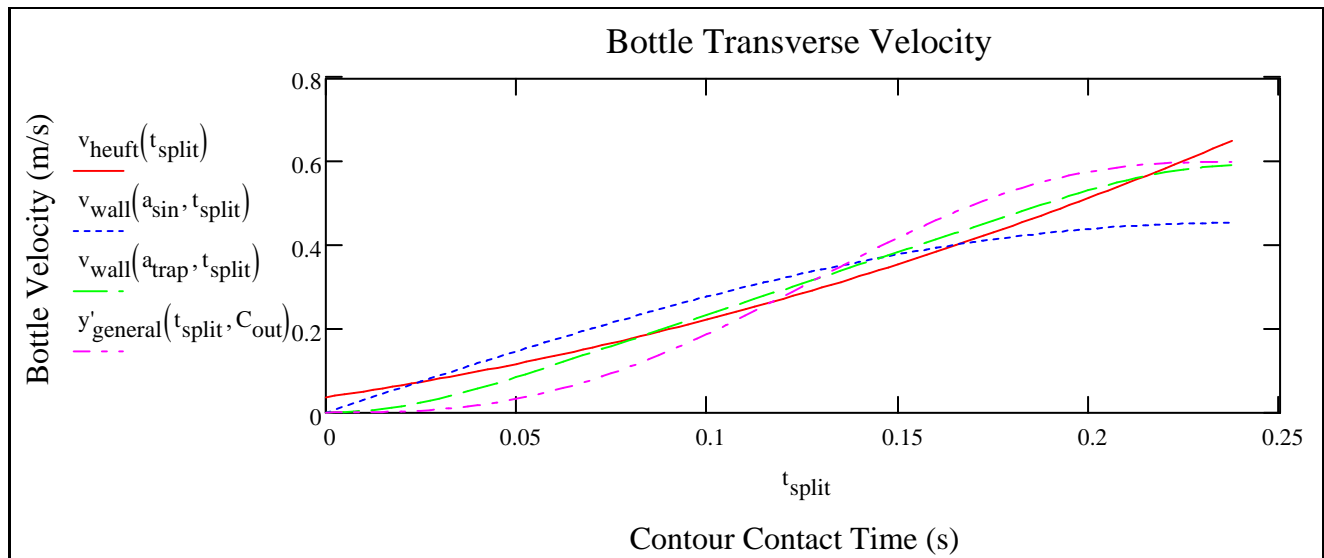
Acceleration Comparison

$$a_{\text{wall}}(a, t) := a(t)$$



Velocity

$$v_{\text{wall}}(a, t) := \int_0^t a(t) dt$$



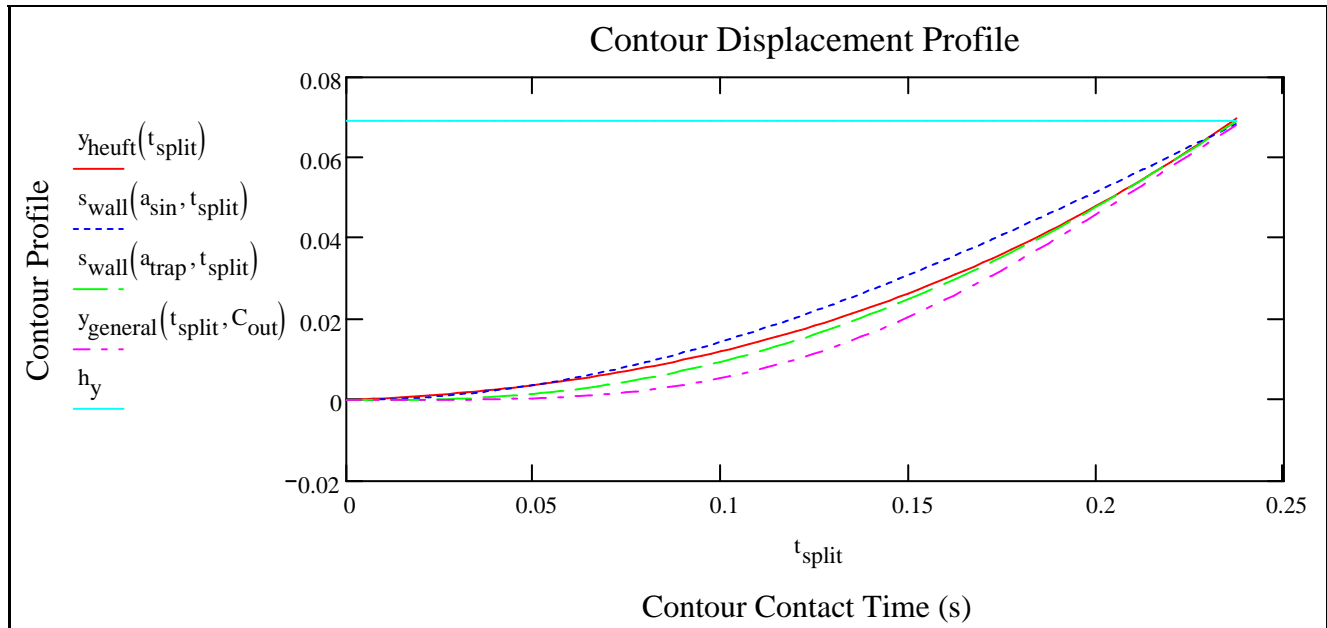
$$v_{\text{final}} := \begin{pmatrix} v_{\text{heuft}}(t_{\text{final}}) \\ v_{\text{wall}}(a_{\text{sin}}, t_{\text{final}}) \\ v_{\text{wall}}(a_{\text{trap}}, t_{\text{final}}) \\ \frac{y'_{\text{general}}(t_{\text{final}}, C_{\text{out}})}{s} \end{pmatrix}$$

$$v_{\text{final}} = \begin{pmatrix} 0.656 \\ 0.454 \\ 0.592 \\ 0.6 \end{pmatrix} \frac{\text{m}}{\text{s}}$$

$$v_{\text{final}} = \begin{pmatrix} 25.824 \\ 17.884 \\ 23.313 \\ 23.622 \end{pmatrix} \frac{\text{in}}{\text{s}}$$

Displacement

$$s_{\text{wall}}(a, t) := \int_0^t \left(\int_0^t a(t) dt \right) dt$$



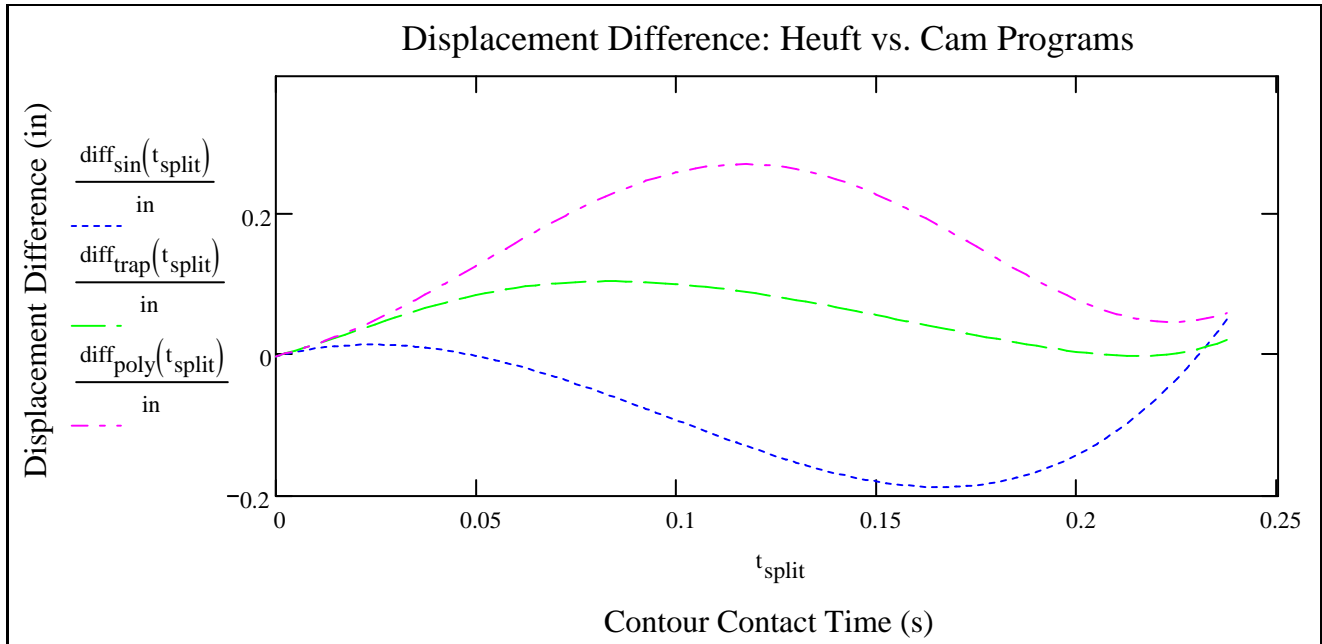
$$s_{\text{final}} := \begin{pmatrix} y_{\text{heuft}}(t_{\text{final}}) \\ s_{\text{wall}}(a_{\text{sin}}, t_{\text{final}}) \\ s_{\text{wall}}(a_{\text{trap}}, t_{\text{final}}) \\ y_{\text{general}}(t_{\text{final}}, C_{\text{out}}) \end{pmatrix} \quad s_{\text{final}} = \begin{pmatrix} 0.071 \\ 0.069 \\ 0.07 \\ 0.069 \end{pmatrix} \text{ m} \quad s_{\text{final}} = \begin{pmatrix} 2.784 \\ 2.72 \\ 2.758 \\ 2.72 \end{pmatrix} \text{ in}$$

Displacement Comparison

$$\text{diff}_{\text{sin}}(t_{\text{split}}) := y_{\text{heuft}}(t_{\text{split}}) - s_{\text{wall}}(a_{\text{sin}}, t_{\text{split}})$$

$$\text{diff}_{\text{trap}}(t_{\text{split}}) := y_{\text{heuft}}(t_{\text{split}}) - s_{\text{wall}}(a_{\text{trap}}, t_{\text{split}})$$

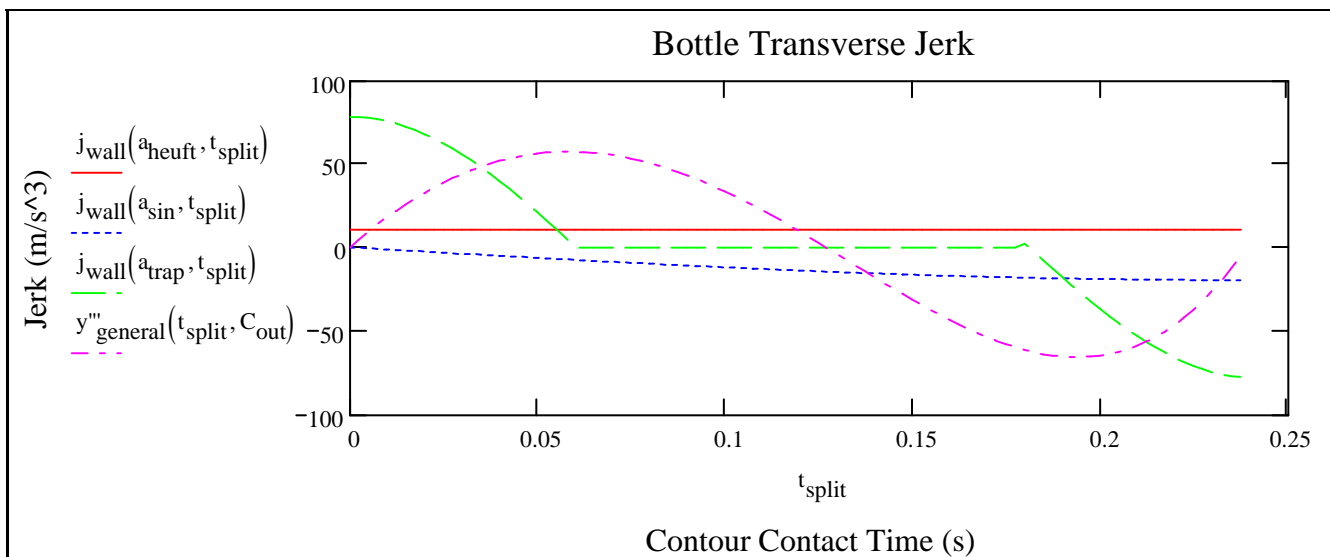
$$\text{diff}_{\text{poly}}(t_{\text{split}}) := y_{\text{heuft}}(t_{\text{split}}) - y_{\text{general}}(t_{\text{split}}, C_{\text{out}})$$



Jerk

In addition to acceleration, velocity, and displacement, we can look at the jerk over the division.

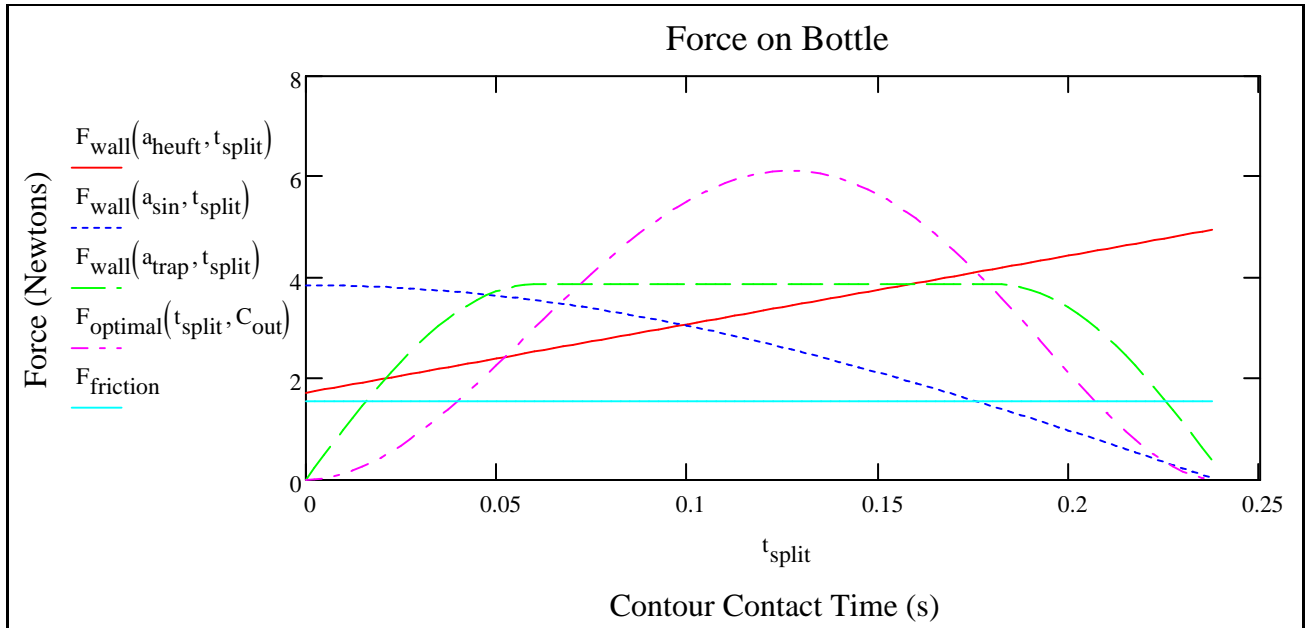
$$j_{\text{wall}}(a, t) := \frac{d}{dt} a(t)$$



Force

$$F_{\text{wall}}(a, t) := a(t) \cdot m_{\text{bottle}}$$

$$F_{\text{optimal}}(t_{\text{split}}, C_{\text{out}}) := y''_{\text{general}}(t_{\text{split}}, C_{\text{out}}) \cdot m_{\text{bottle}}$$



Contour Comparison Table

The following table compares the peak values of velocity, acceleration and jerk of the contour curves. This will influence the decision when choosing the optimal contour for the cam.

Max Velocity

$$v_{\text{maximum}} := \begin{pmatrix} v_{\text{heuft}}(t_{\text{final}}) \\ v_{\text{wall}}(a_{\text{sin}}, t_{\text{final}}) \\ v_{\text{wall}}(a_{\text{trap}}, t_{\text{final}}) \\ \frac{y'_{\text{general}}(t_{\text{final}}, C_{\text{out}})}{s} \end{pmatrix}$$

$$v_{\text{maximum}} = \begin{pmatrix} 0.656 \\ 0.454 \\ 0.592 \\ 0.6 \end{pmatrix} \frac{\text{m}}{\text{s}}$$

$$v_{\text{maximum}} = \begin{pmatrix} 25.824 \\ 17.884 \\ 23.313 \\ 23.622 \end{pmatrix} \frac{\text{in}}{\text{s}}$$

Max Acceleration

$$a_{\text{maximum}} := \begin{pmatrix} a_{\text{heuft}}(t_{\text{final}}) \\ a_{\text{sin}}(0) \\ a_{\text{trap}}(.1\text{s}) \\ \frac{y''_{\text{general}}\left(\frac{t_{\text{final}}}{2}, C_{\text{out}}\right)}{s^2} \end{pmatrix}$$

$$a_{\text{maximum}} = \begin{pmatrix} 3.851 \\ 2.987 \\ 3 \\ 4.709 \end{pmatrix} \frac{\text{m}}{\text{s}^2}$$

$$a_{\text{maximum}} = \begin{pmatrix} 151.633 \\ 117.581 \\ 118.11 \\ 185.389 \end{pmatrix}$$

Max Jerk

$$j_{\text{maximum}} := \begin{pmatrix} j_{\text{wall}}(a_{\text{heuft}}, t_{\text{final}}) \\ j_{\text{wall}}(a_{\text{sin}}, t_{\text{final}}) \\ j_{\text{wall}}(a_{\text{trap}}, 0) \\ \frac{y'''_{\text{general}}\left(\frac{t_{\text{final}}}{4}, C_{\text{out}}\right)}{s^3} \end{pmatrix}$$

$$j_{\text{maximum}} = \begin{pmatrix} 10.54 \\ -19.636 \\ 78.117 \\ 57.263 \end{pmatrix} \frac{\text{m}}{\text{s}^3} \quad j_{\text{maximum}} = \begin{pmatrix} 414.961 \\ -773.073 \\ 3.075 \times 10^3 \\ 2.254 \times 10^3 \end{pmatrix} \frac{\text{in}}{\text{s}^3}$$

Max Force

$$F_{\text{maximum}} := \begin{pmatrix} F_{\text{wall}}(a_{\text{heuft}}, t_{\text{final}}) \\ F_{\text{wall}}(a_{\text{sin}}, 0) \\ F_{\text{wall}}(a_{\text{trap}}, 1\text{s}) \\ \frac{F_{\text{optimal}}\left(\frac{t_{\text{final}}}{2}, C_{\text{out}}\right)}{s^2} \end{pmatrix}$$

$$F_{\text{maximum}} = \begin{pmatrix} 4.968 \\ 3.853 \\ 3.87 \\ 6.074 \end{pmatrix} \text{N} \quad F_{\text{maximum}} = \begin{pmatrix} 1.117 \\ 0.866 \\ 0.87 \\ 1.366 \end{pmatrix} \text{lb}_f$$

Tip Test

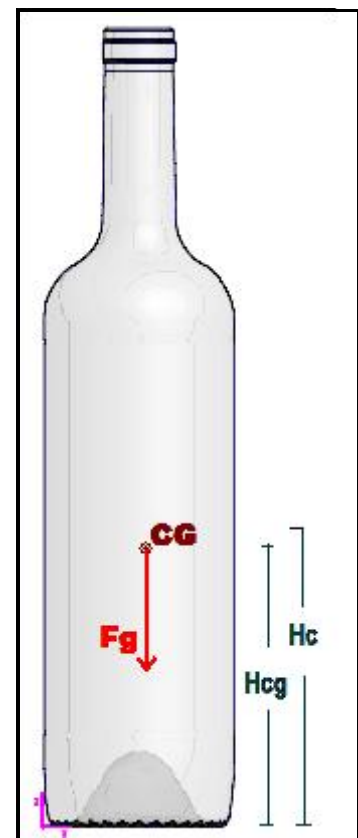
A primary concern in this application is to ensure that no bottles are tipped over. A check is performed here that the force from the divider never creates a moment exceeding the tipping moment of the bottle.

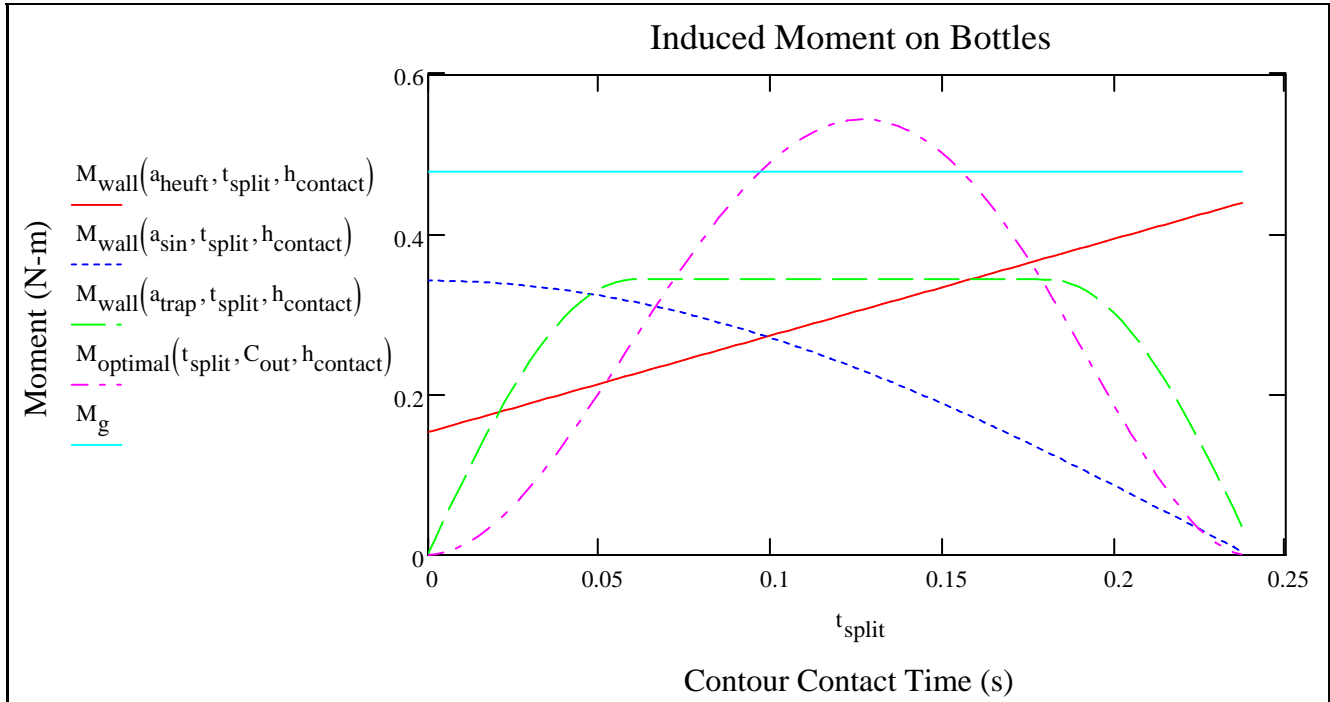
$$M_{\text{wall}}(a, t, h) := F_{\text{wall}}(a, t) \cdot h \quad \text{Moment Induced by Wall}$$

$$M_{\text{g}} := F_{\text{g}} \cdot \left(\frac{d_{\text{bottle}}}{2}\right)$$

$$M_{\text{optimal}}(t, C, h) := F_{\text{optimal}}(t, C) \cdot h$$

Free Body Diagram





Maximum Moment

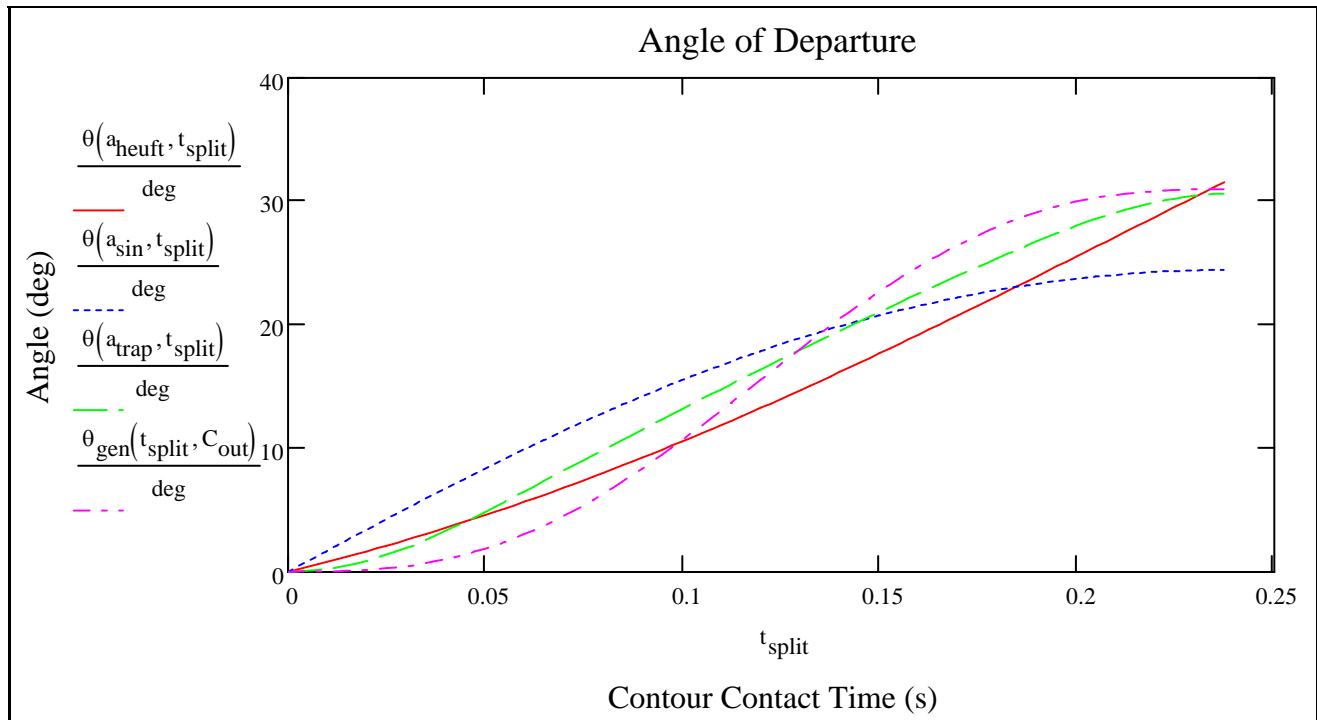
$$M_{\text{maximum}} := \begin{pmatrix} M_{\text{wall}}(a_{\text{heuft}}, t_{\text{final}}, h_{\text{contact}}) \\ M_{\text{wall}}(a_{\text{sin}}, 0, h_{\text{contact}}) \\ M_{\text{wall}}(a_{\text{trap}}, .125\text{s}, h_{\text{contact}}) \\ \frac{M_{\text{optimal}}\left(\frac{t_{\text{final}}}{2}, C_{\text{out}}, h_{\text{contact}}\right)}{\text{s}^2} \end{pmatrix} \quad M_{\text{maximum}} = \begin{pmatrix} 0.442 \\ 0.343 \\ 0.344 \\ 0.54 \end{pmatrix} \text{N}\cdot\text{m} \quad M_{\text{maximum}} = \begin{pmatrix} 3.909 \\ 3.031 \\ 3.045 \\ 4.78 \end{pmatrix} \text{lb}\cdot\text{in}$$

Bottle Trajectory

Since the contour does not guide the bottle the entire distance across the conveyor, a check is performed to ensure the bottle's trajectory will carry the bottle across the division.

Angle of Trajectory

$$\theta(a, t) := \operatorname{atan}\left(\int_0^t a(t) dt \frac{s}{m}\right) \quad \theta_{\text{gen}}(t_{\text{split}}, C_{\text{out}}) := \operatorname{atan}\left(y'_{\text{general}}\left(t_{\text{split}}, \frac{C_{\text{out}}}{m}\right)\right)$$



Final Angle of Departure

$$\theta := \begin{pmatrix} \theta(a_{\text{heuft}}, t_{\text{final}}) \\ \theta(a_{\text{sin}}, t_{\text{final}}) \\ \theta(a_{\text{trap}}, t_{\text{final}}) \\ \theta_{\text{gen}}(t_{\text{final}}, C_{\text{out}}) \end{pmatrix} = \begin{pmatrix} 31.772 \\ 24.43 \\ 30.632 \\ 30.964 \end{pmatrix} \text{deg}$$

Bottle Velocity Components

$$V_x := \begin{pmatrix} v_{\text{line}} \cdot \sin(\theta_0) \\ v_{\text{line}} \cdot \sin(\theta_1) \\ v_{\text{line}} \cdot \sin(\theta_2) \\ v_{\text{line}} \cdot \sin(\theta_3) \end{pmatrix}$$

$$V_x = \begin{pmatrix} 0.532 \\ 0.418 \\ 0.515 \\ 0.52 \end{pmatrix} \frac{\text{m}}{\text{s}}$$

$$V_x = \begin{pmatrix} 20.937 \\ 16.445 \\ 20.26 \\ 20.458 \end{pmatrix} \frac{\text{in}}{\text{s}}$$

$$V_y := \begin{pmatrix} v_{\text{line}} \cdot \cos(\theta_0) \\ v_{\text{line}} \cdot \cos(\theta_1) \\ v_{\text{line}} \cdot \cos(\theta_2) \\ v_{\text{line}} \cdot \cos(\theta_3) \end{pmatrix}$$

$$V_y = \begin{pmatrix} 0.859 \\ 0.92 \\ 0.869 \\ 0.866 \end{pmatrix} \frac{\text{m}}{\text{s}}$$

$$V_y = \begin{pmatrix} 33.805 \\ 36.204 \\ 34.215 \\ 34.097 \end{pmatrix} \frac{\text{in}}{\text{s}}$$

Bottle Friction Deceleration

$$a_{\text{friction}} := \frac{F_{\text{friction}}}{m_{\text{bottle}}}$$

$$a_{\text{friction}} = 1.204 \frac{\text{m}}{\text{s}^2}$$

Acceleration due to Friction

Line Constants

$$L_{\text{glide}} := 18 \text{ in}$$

Length of Unsupported Trajectory

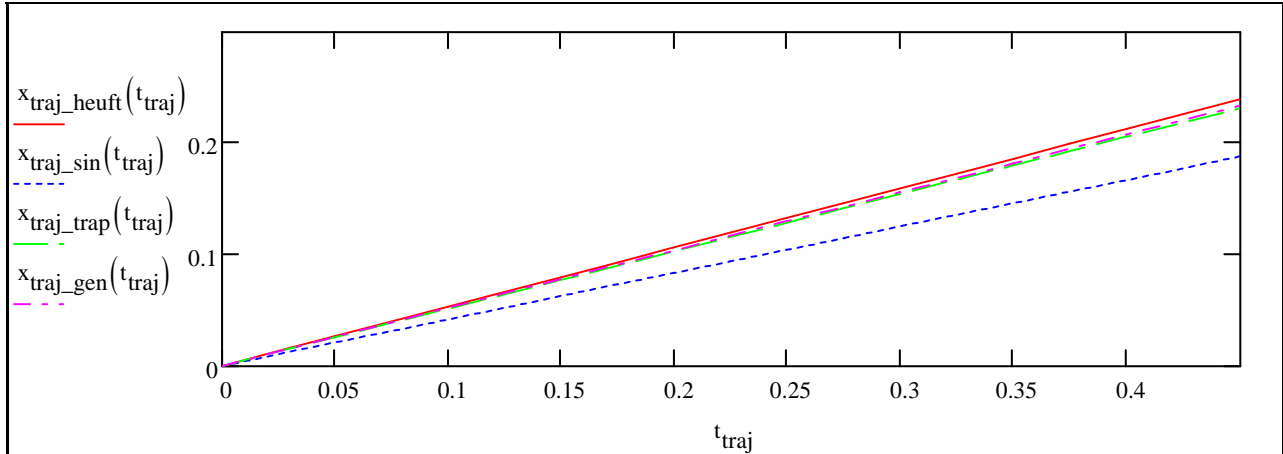
$$t_{\text{fin}} := \frac{L_{\text{glide}}}{v_{\text{line}}} \quad t_{\text{fin}} = 0.453 \text{ s}$$

Time of Trajectory

$$t_{\text{traj}} := 0 \cdot \text{s}, 0.025 \cdot \text{s}.. t_{\text{fin}}$$

X Displacement of Bottle of Trajectory (Downline)

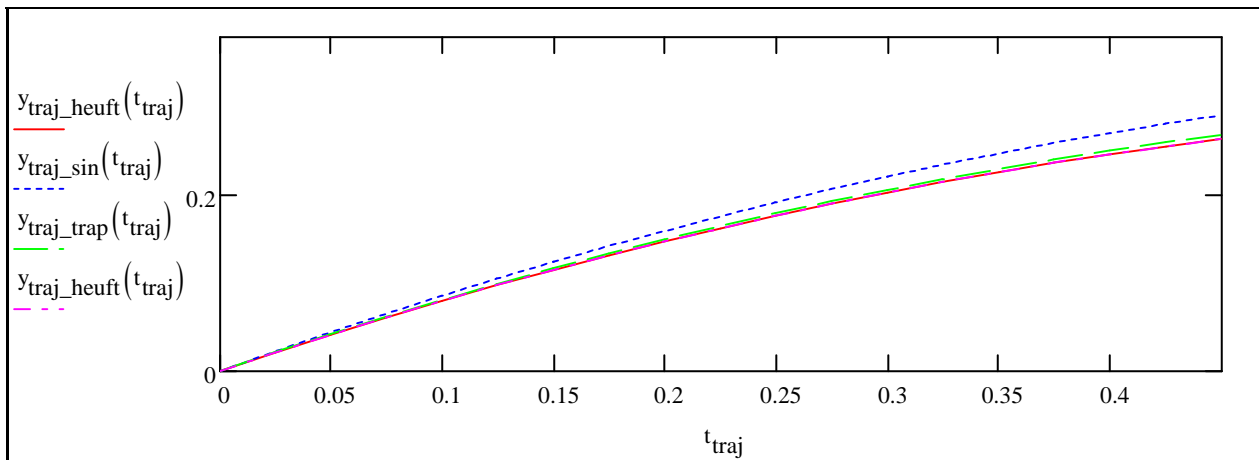
$$x_{\text{traj_heuft}}(t) := V_{x_0} \cdot t \quad x_{\text{traj_sin}}(t) := V_{x_1} \cdot t \quad x_{\text{traj_trap}}(t) := V_{x_2} \cdot t \quad x_{\text{traj_gen}}(t) := V_{x_3} \cdot t$$



Y Displacement of Bottle Trajectory (Across Conveyor)

$$y_{\text{traj_heuft}}(t) := V_{y_0} \cdot t - .5 \cdot a_{\text{friction}} \cdot t^2 \quad y_{\text{traj_trap}}(t) := V_{y_2} \cdot t - .5 \cdot a_{\text{friction}} \cdot t^2$$

$$y_{\text{traj_sin}}(t) := V_{y_1} \cdot t - .5 \cdot a_{\text{friction}} \cdot t^2 \quad y_{\text{traj_gen}}(t) := V_{y_3} \cdot t - .5 \cdot a_{\text{friction}} \cdot t^2$$



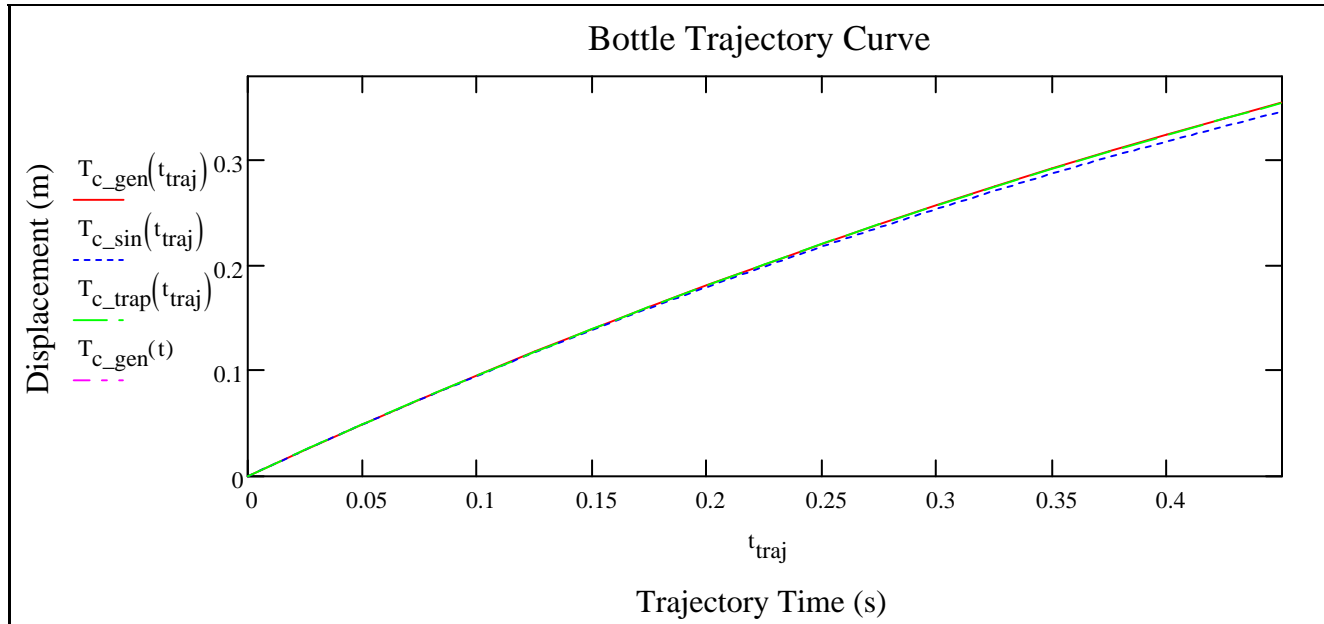
Trajectory Curve

$$T_{c_heuft}(t) := \sqrt{x_{\text{traj_heuft}}(t)^2 + y_{\text{traj_heuft}}(t)^2}$$

$$T_{c_trap}(t) := \sqrt{x_{\text{traj_trap}}(t)^2 + y_{\text{traj_trap}}(t)^2}$$

$$T_{c_sin}(t) := \sqrt{x_{\text{traj_sin}}(t)^2 + y_{\text{traj_sin}}(t)^2}$$

$$T_{c_gen}(t) := \sqrt{x_{\text{traj_gen}}(t)^2 + y_{\text{traj_gen}}(t)^2}$$



Notice that the trajectories of the proposed contours all produce similar trajectories to the Heuft model currently in place. This reduces any concern for the proposed contours' ability to produce a bottle trajectory that clears the dividing wedge.

Timing

The nature of the cam is such that one half revolution is a full rise cycle of the cam. The cam must complete a full rise at the same speed of the bottle. Thus the cam must make one half revolution in a minimum t_{final} .

$$t_{\text{final}} := \frac{L_{\text{split}}}{v_{\text{line}}}$$

$$t_{\text{final}} = 0.239 \text{ s}$$

$$\omega_{\text{op}} := \frac{140 \text{ deg}}{t_{\text{final}}}$$

$$\omega_{\text{op}} = 97.665 \text{ rpm}$$

Operating Angular Velocity

Angular Acceleration

The successful operation of this system is based upon the fact that the system must be binary, i.e. either on or off. Binary operation is only achieved when the system is at full operating speed during the cam rise actuation. In order to accomplish this, the cam design incorporates a buffer dwell angle to allow for servo acceleration. The buffer dwell angle is based on a spin up time specified. The specified spinup time has a definite range whose extremities are governed by several criteria. The lower extreme of spinup time is governed by servo torque. The upper extreme is governed by line speed, bottle spacing and cam geometry.

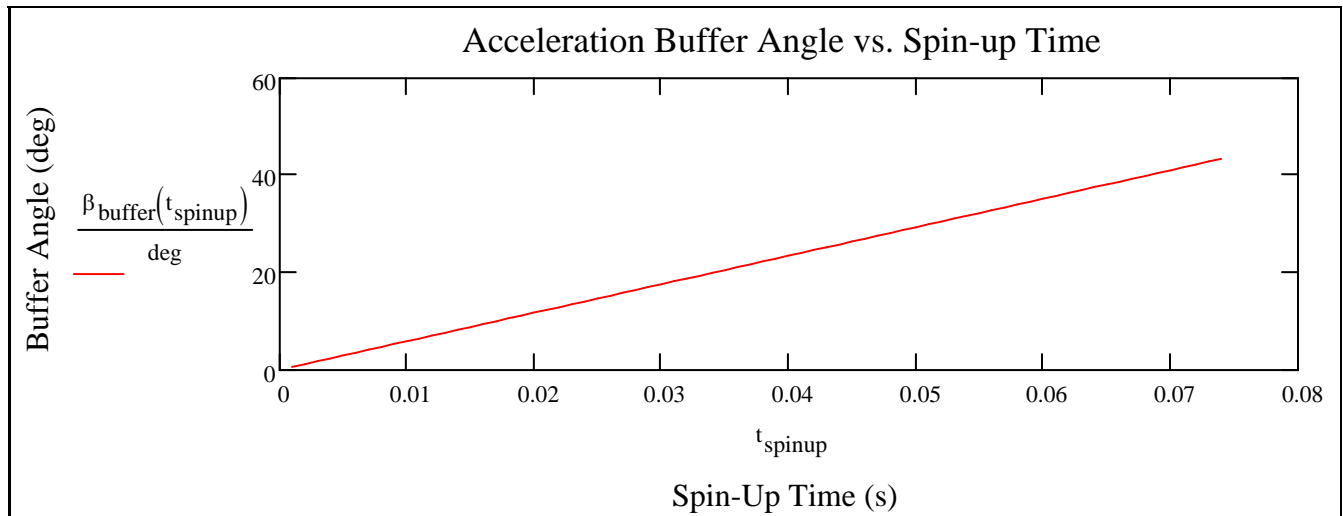
There is often a spacing between the bottles on the line, however it is not unusual for bottles to be directly adjacent to each other. In this case, the spacing between the bottles is a bottle diameter. The worst case time between the bottles is thus full line speed and one bottle diameter spacing.

$$t_{\text{worst}} := \frac{d_{\text{bottle}}}{v_{\text{line}}} \quad t_{\text{worst}} = 0.075 \text{ s} \quad \text{Worst Case Scenario Spin Up Time}$$

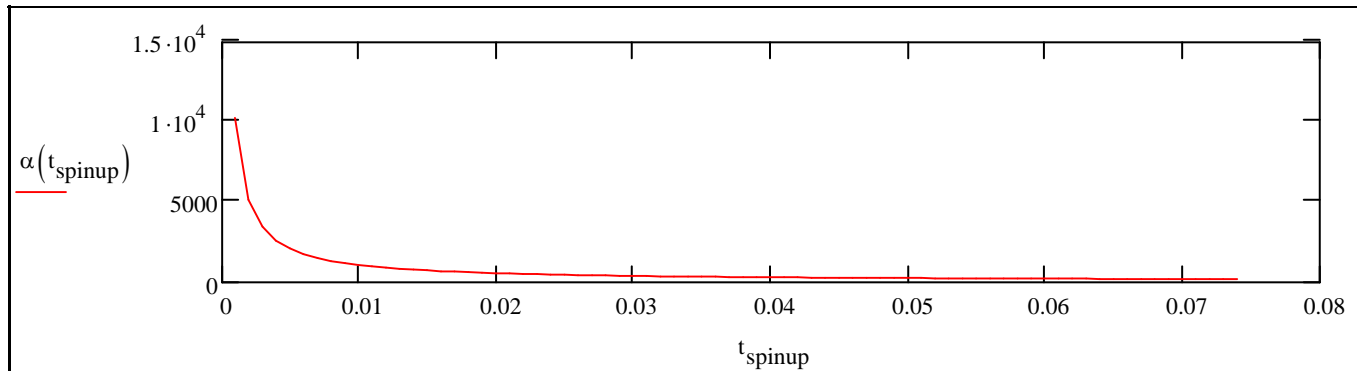
The fastest a servo can accelerate is based on its torque, motor inertia and inertia of the cam. We can specify an arbitrary lower time of 0 for spinup.

$$\omega_{\text{op}} = 97.665 \text{ rpm} \quad t_{\text{spinup}} := 0.001 \text{ s}, .002 \text{ s}.. t_{\text{worst}}$$

$$\beta_{\text{buffer}}(t_{\text{spinup}}) := t_{\text{spinup}} \cdot \omega_{\text{op}}$$



$$\alpha(t_{\text{spinup}}) := \frac{\omega_{\text{op}}}{t_{\text{spinup}}}$$



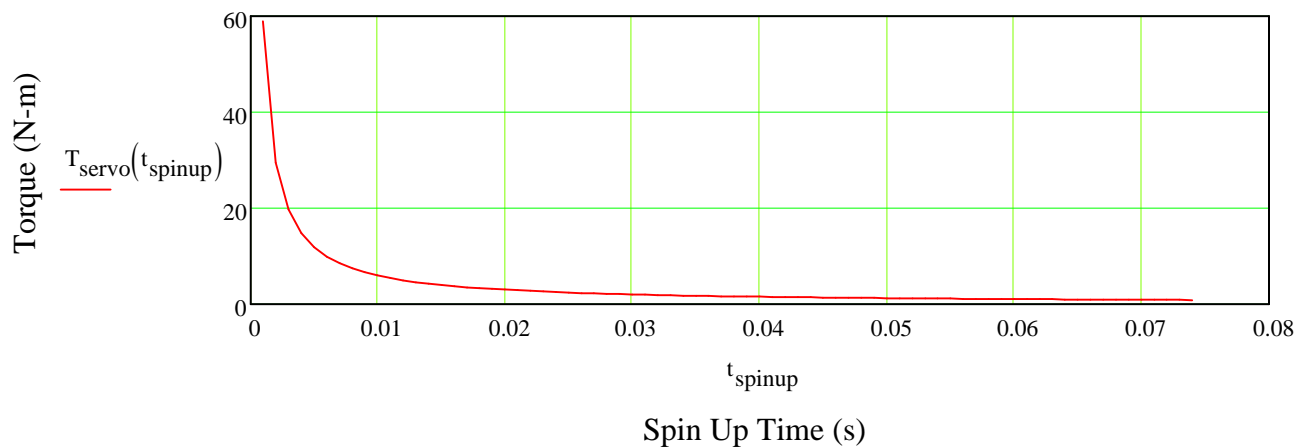
Torque

$$I_{zz_cam} := 18.64 \text{ lb} \cdot \text{in}^2 \quad I_{zz_cam} = 5.455 \times 10^{-3} \text{ s}^2 \cdot \text{mN} \quad \text{Cam Moment of Inertia}$$

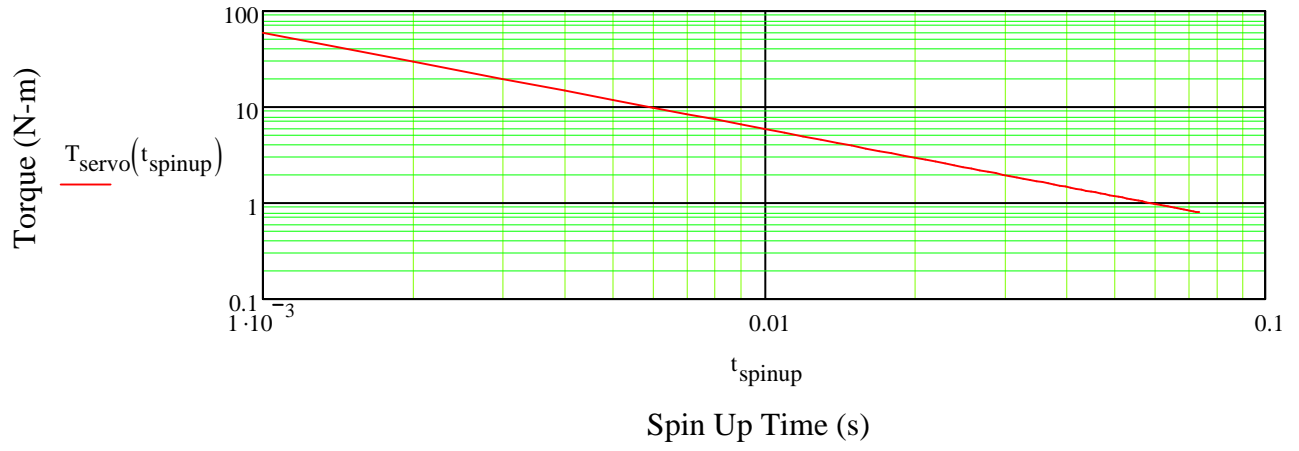
$$I_{zz_motor} := 3 \text{ kg} \cdot \text{cm}^2 \quad \text{Motor Moment of Inertia}$$

$$T_{\text{servo}}(t_{\text{spinup}}) := \alpha(t_{\text{spinup}}) \cdot (I_{zz_cam} + I_{zz_motor})$$

Servo Torque vs. Spin Up Time



Servo Torque vs. Spin Up Time



Cam Physical Properties

$$M_{\text{cam}} := 5.332 \text{ lb}$$

$$M_{\text{cam}} = 2.419 \text{ kg}$$

Mass of Cam

$$V_{\text{cam}} := 122.99 \text{ in}^3$$

$$V_{\text{cam}} = 2.015 \times 10^3 \text{ cm}^3$$

Volume of Cam

$$I_{zz_cam} = 18.64 \text{ lb}\cdot\text{in}^2$$

$$I_{zz_cam} = 5.455 \times 10^{-3} \text{ kg}\cdot\text{m}^2$$

Cam Moment of Inertia about Rotational Axis

Shaft Properties

$$\rho_{\text{steel}} := 7.8 \frac{\text{gm}}{\text{cm}^3}$$

Density of Steel

$$L_{\text{bearing}} := 1 \text{ in}$$

Bearing Length

$$W_{\text{gear}} := 2 \text{ in}$$

Gear Width

$$L_{\text{shaft}} := L_{\text{split}} + 2L_{\text{bearing}} + W_{\text{gear}} + 2.5 \text{ in} \quad L_{\text{shaft}} = 16 \text{ in}$$

Shaft Length

$$D_{\text{shaft}} := .75 \text{ in}$$

Shaft Diameter

$$I_{zz_shaft} := .25 \cdot \pi \cdot \left(\frac{D_{\text{shaft}}}{2} \right)^4$$

$$I_{zz_shaft} = 6.465 \times 10^{-9} \text{ m}^4$$

Moment of Inertia

$$J_{\text{shaft}} := \frac{\pi}{2} \cdot \left(\frac{D_{\text{shaft}}}{2} \right)^4$$

$$J_{\text{shaft}} = 1.293 \times 10^{-8} \text{ m}^4$$

Polar Moment of Inertia

$$V_{\text{shaft}} := \pi \cdot \left(\frac{D_{\text{shaft}}}{2} \right)^2 \cdot L_{\text{shaft}}$$

$$V_{\text{shaft}} = 115.833 \text{ cm}^3$$

Volume of Shaft

$$m_{\text{shaft}} := \rho_{\text{steel}} \cdot V_{\text{shaft}}$$

$$m_{\text{shaft}} = 0.903 \text{ kg}$$

Mass of Shaft

Keyway Analysis

$$W_{\text{key}} := \frac{3}{16} \text{ in}$$

Width of Key

$$L_{\text{key}} := 1.5 \text{ in}$$

Length of Key

$$D_{\text{key}} := \frac{3}{32} \text{ in}$$

Depth of Key

$$S_{\text{yt_ABS}} := 52 \text{ MPa}$$

Tensile Yield Strength of ABS Plastic

$$S_{\text{yt_A25}} := 38 \text{ MPa}$$

Tensile Yield Strength of Accura 25 Plastic

$$S_{\text{yt_steel}} := 250 \text{ MPa}$$

Tensile Yield Strength of Steel

Shear Stress Analysis

$$T_{\text{max}} := T_{\text{servo}}(0.01367 \text{ s})$$

$$T_{\text{max}} = 4.306 \text{ N}\cdot\text{m}$$

Maximum Torque Transmission

$$F_{\text{shear}} := \frac{T_{\text{max}}}{\frac{D_{\text{shaft}}}{2}}$$

$$F_{\text{shear}} = 452.029 \text{ N}$$

Shear Force

$$A_{\text{sec}} := W_{\text{key}} \cdot L_{\text{key}}$$

$$A_{\text{sec}} = 1.815 \times 10^{-4} \text{ m}^2$$

Cross Sectional Area of Key

$$\tau_{\text{ave}} := \frac{F_{\text{shear}}}{A_{\text{sec}}}$$

$$\tau_{\text{ave}} = 2.491 \text{ MPa}$$

Average Torsional Shear Stress

Safety Factor

$$S_{ys_ABS} := 0.5 \cdot S_{yt_ABS}$$

$$S_{ys_ABS} = 26 \text{ MPa}$$

Theoretical Yield Strength

$$S_{ys_A25} := 0.5 \cdot S_{yt_A25}$$

$$S_{ys_A25} = 19 \text{ MPa}$$

$$S_{ys_steel} := 0.5 \cdot S_{yt_steel}$$

$$S_{ys_steel} = 125 \text{ MPa}$$

$$\eta_{ABS} := \frac{S_{ys_ABS}}{\tau_{ave}}$$

$$\eta_{ABS} = 10.437$$

Safety Factor

$$\eta_{A25} := \frac{S_{ys_A25}}{\tau_{ave}}$$

$$\eta_{A25} = 7.627$$

$$\eta_{steel} := \frac{S_{ys_steel}}{\tau_{ave}}$$

$$\eta_{steel} = 50.177$$

Shaft Analysis

$$G_{steel} := 216 \text{ GPa}$$

Modulus of Elasticity

$$\delta_{\theta\text{shaft}} := \frac{T_{\max} \cdot L_{\text{shaft}}}{G_{\text{steel}} \cdot J_{\text{shaft}}}$$

$$\delta_{\theta\text{shaft}} = 0.036 \text{ deg}$$

Shaft Torsional Deflection

$$\tau_{\text{shaft}} := \frac{T_{\max} \cdot \frac{D_{\text{shaft}}}{2}}{J_{\text{shaft}}}$$

$$\tau_{\text{shaft}} = 3.172 \text{ MPa}$$

Torsion Stress in Shaft

Fatigue Failure Analysis

Torsional Fatigue

$$S_{ut} := 400 \text{ MPa} \quad S_{ut} = 400 \text{ MPa}$$

Ultimate Tensile Strength

$$S_e' := .5 \cdot S_{ut} \quad S_e' = 200 \text{ MPa}$$

Uncorrected Endurance Limit

$$C_{load} := 1$$

For Torsional Loading

$$C_{size} := 0.869 \cdot \left(\frac{D_{shaft}}{\text{in}} \right)^{-.097}$$

Size Correction

$$A := 4.51 \quad b := -.265$$

$$C_{surface} := A \cdot \left(\frac{S_{ut}}{\text{MPa}} \right)^b \quad C_{surface} = 0.922$$

Surface Finish Correction

$$C_{temperature} := 1.0$$

Ambient Temperature Correction

$$C_{reliability} := .753$$

Material Reliability Correction

$$S_e := C_{load} \cdot C_{size} \cdot C_{surface} \cdot C_{temperature} \cdot C_{reliability} \cdot S_e'$$

Corrected Fatigue Function

$$S_e = 124.049 \text{ MPa}$$

Safety Factor

$$\eta_{torsion} := \frac{S_e}{\tau_{shaft}}$$

$$\eta_{torsion} = 39.109$$

Keyway Stress Concentration Factors

$$\sqrt{a} := 0.039 \quad a := 0.039^2$$

$$r := .01$$

$$q := \frac{1}{1 + \frac{\sqrt{a}}{\sqrt{r}}}$$

$$K_t := 2.62$$

Neuber's Constant

Notch Radius

Notch Sensitivity Factor

Static Stress Concentration Factor

Peterson stress concentration factor for flat end mill. (furlong lecture 19, machine design 473)

$$K_{fs} := 1 + q \cdot (K_t - 1) \quad K_{fs} = 2.165$$

Fatigue Stress Concentration Factor

Shear Stress Concentration due to Torsion

$$\tau_{\text{concentration}} := K_{fs} \cdot \tau_{\text{shaft}}$$

$$\tau_{\text{concentration}} = 6.869 \text{ MPa}$$

Safety Factor

$$\eta_{\text{keyway}} := \frac{S_{\text{ys_steel}}}{\tau_{\text{concentration}}}$$

$$\eta_{\text{keyway}} = 18.199$$